1986

Olfactometric in Situ Soil Exploration: Development of the Electro-Odo-Cone.

Mohammad Mohammadi
Louisiana State University and Agricultural & Mechanical College

INFORMATION TO USERS

While the most advanced technology has been used to photograph and reproduce this manuscript, the quality of the reproduction is heavily dependent upon the quality of the material submitted. For example:

- Manuscript pages may have indistinct print. In such cases, the best available copy has been filmed.

- Manuscripts may not always be complete. In such cases, a note will indicate that it is not possible to obtain missing pages.

- Copyrighted material may have been removed from the manuscript. In such cases, a note will indicate the deletion.

Oversize materials (e.g., maps, drawings, and charts) are photographed by sectioning the original, beginning at the upper left-hand corner and continuing from left to right in equal sections with small overlaps. Each oversize page is also filmed as one exposure and is available, for an additional charge, as a standard 35mm slide or as a 17"x 23" black and white photographic print.

Most photographs reproduce acceptably on positive microfilm or microfiche but lack the clarity on xerographic copies made from the microfilm. For an additional charge, 35mm slides of 6"x 9" black and white photographic prints are available for any photographs or illustrations that cannot be reproduced satisfactorily by xerography.

Mohammadi, Mohammad

OLFACTOMETRIC IN SITU SOIL EXPLORATION: DEVELOPMENT OF THE ELECTRO-ODO-CONE

The Louisiana State University and Agricultural and Mechanical Col. PH.D. 1986

PLEASE NOTE:

In all cases this material has been filmed in the best possible way from the available copy. Problems encountered with this document have been identified here with a check mark ✓.

1. Glossy photographs or pages _____
2. Colored illustrations, paper or print _____
3. Photographs with dark background ✓
4. Illustrations are poor copy _____
5. Pages with black marks, not original copy _____
6. Print shows through as there is text on both sides of page _____
7. Indistinct, broken or small print on several pages ✓
8. Print exceeds margin requirements _____
9. Tightly bound copy with print lost in spine _____
10. Computer printout pages with indistinct print _____
11. Page(s) _____ lacking when material received, and not available from school or author.
12. Page(s) _____ seem to be missing in numbering only as text follows.
13. Two pages numbered _____. Text follows.
14. Curling and wrinkled pages _____
15. Dissertation contains pages with print at a slant, filmed as received ✓
16. Other _____

_____

_____

OLFACTOMETRIC IN SITU SOIL EXPLORATION: DEVELOPMENT OF THE ELECTRO-ODO-CONE

A Dissertation

Submitted to the Graduate Faculty of the
Louisiana State University and
Agricultural and Mechanical College
in partial fulfillment of the
requirements for the degree of
Doctor of Philosophy

in

The Department of Civil Engineering

by
Mohammad Mohammadi
B.S., University of North Carolina, 1980
M.S., Texas A & I University, 1982
December 1986

ACKNOWLEDGMENTS

Many people have knowingly or unknowingly contributed to this study. They include virtually all my professors, colleagues, and friends. I am most grateful to my major professor Dr Mehmet T. Tumay, who inspired this study and offered continuous direction, encouragement, assistance, and patience throughout the course of this research. Special thanks are due to my committee members, Professor Ara Arman, Drs. J.N Suhayda, D. Roy, N. Stoltzfus, and R. Ferrell for their suggestions, guidance, and support; assistance of Dr. John Carden (Georgia Institute of Technology) is also greatly appreciated. Special acknowledgments are due Prof. N.N. Tanyolac, Bogazici University, Istanbul, Turkey, for sharing his valuable experience in olfactometry and odor detection technology during the initial phase of this study. Mr. R. Vanauker of Feldspare Corporation, Edgar, Florida, made available the samples used in this study, his generous help is gratefully acknowledged. I am thankful to Messieurs Ray Gostowski and John Vincent for their help in fabrication of the various parts of the experimental setup and finalization of the EOC circuitry utilized in this work. Dr. Seals and the Department of Civil Engineering are gratefully acknowledged for providing valuable support for this study. Partial financial support provided by the Hazardous Waste Research Center of Louisiana State University is thankfully recognized. Special thanks are extended to G & E Engineering for their understanding and support during preparation of the manuscript. United Nations Development Program in Turkey is thankfully acknowledged for their provision of the assistance extended to this research under the realm of TOKTEN guidelines. Finally, my gratitude goes to Bonnie Grayson and Elizabeth Coleman for their patience and help in typing and preparing the manuscript.

TABLE OF CONTENTS

LIST OF TABLES

LIST OF FIGURES

LIST OF SYMBOLS

AA = acetic acid

A = acetone

ACP = acrylic copolymer

a = radius of a capillary

B = Brenner's number

BENZ = Benzene

C = solution concentration

CA = cellulose acetate

C/EOC = cone with electro-odo-cell (odor-cone)

CTA = cellulose triacetate

C_i^* = trace concentration in stagnant values

DCM = dichloromethane

DUR = polyvinylidene fluoride

D_o = molecular diffusion coefficient

D_t = transverse dispersion coefficient

D_L = longitudinal dispersion coefficient

D_m = dispersion coefficient for mechanical mixes

D_d = dispersion coefficient for diffusion flour

d_p = particle diameter

dv/dt = time rate of output voltage of electro-odo-cell and C/EOC

E = dielectric field

EG = ethylene glycol

EOC = electro-odo-cell

ETH = ethanol

E' = ability of a material to transmit electromagnetic energy

E'' = ability of a material to adsorb energy from an electromagnetic frequency

E_x = work due to adsorption forces in bringing an adsorbate to a distance x from the source

ΔE = energy of vaporization at zero pressure

e = charge of a molecule

F = Gibbs, free energy

f = stagnant fraction of cell volume

H_m = heat of mixing (in solubility)

I = ionization energy of a molecule

I_o = Bessel's function of the first kind

J_i = material flow across a membrane

J_e = electric current flow across a membrane

J_p = polarization flow across a membrane

J_a = advection solute flux

J_d = diffusion flux

J_m = mechanical mixing flux

K = kaolinite

K_o = specific electrolyte conductivity

K = dielectric constant

k = Boltzman's constant

k^* = complex conductivity

k_1 = adsorption rate

k_2 = desorption rate

k_3 = equilibrium constant (in adsorption)

K_1 = longitudinal dispersion coefficient

L = Onsager's proportionality coefficient between flour and force

LL = liquid limit

L_p = polarization constant

m = molecule weight

MT = methanol

N = Peclet's number

NC = nitro cellulose

n = conventional porosity

n^* = viscosity of a pure solvent

[n] = intrinsic viscosity

P_e = equilibrium pressure of an adsorbed film

p = electrical dipole moment of a molecule

P_x = pressure at adsorbed state

P_g = pressure at gaseous state

p = vapor pressure

P_i = initial pressure

PL = plastic limit

PTFE = polytetrafluroethylene

P_s = saturation pressure

PV = polyvinylidene

$\bar{q}$ = rate of loss or supply of solute per unit volume of soil

Q = heat of adsorption

q = Darcy's flux

r = pore radius

R = universal gas constant

RC = regenerated cellulose

S_t = sticking ability of a molecule

SL = shrinkage limit

S_1 = kinetic adsorption concentration

S_2 = equilibrium adsorption concentration

S_i = initial degree of saturation

S_s = sink/source rate constant

t = time

T = absolute temperature (°k)

u = pore fluid pressure

V = seepage velocity

V_c = steady state output voltage

V_i = ionic valance

V_m = volume of an adsorbed monolayer

V_o = initial velocity at the center of a capillary tube

$V(\xi)$ = displacement probability

W = wave frequency

w = angular velocity

α = polarizability factor

α_T = transverse dispersitivity

α_L = longitudinal dispersitivity

β = bulk density of porous median

β_t = wall effect coefficient

∂ = volumetric water content

γ = surface tension

γ = viscosity

μm = micrometers = 10^{-6}

μ = dipole moment

$\mu_{induced}$ = induced dipole moment

μ_j = chemical of component j

ε = dielectric constant on persistivity

ε' = complex dielectric constant

Ω = OHMS, measure of

ϕ = fractional pore value

ξ = displacement of a contaminant front

$(\xi)_{AV}$ = average displacement of a contaminant front

η_o = electrolyte concentration in clay double layer

δ = solubility factor

ABSTRACT

The suitability of the electro-odo-cell (EOC) for detection of organic chemical contaminants in ambient air and soil strata was investigated under laboratory conditions. The existing concept of the EOC was modified to incorporate the system into a state of the art subsurface soil investigation probe (electric cone penetrometer). Partial theoretical support for EOC operation was developed. The state of the art in reactive solute transport in soils was reviewed. From this review inferences were made about time of travel of a permeant in soil samples, which was consequently compared with time of initial response of the laboratory prototype cone penetrometer with EOC (C/EOC). Combinations of different membranes and contaminants were tested in ambient conditions. EOC responses to variations in temperature, pressure, cell-chamber geometry, membrane pore size, membrane composition, external ionic field, salt solutions, contaminant concentration, contaminant type and membrane solubility were investigated. Problems associated with simulated C/EOC operation under saturated conditions were addressed.

The results of adsorption/desorption were presented as plots of changes in C/EOC output voltage vs. time. Statistical analyses of the results provided good correlation between the output voltage and concentration, vapor pressure, surface tension, dipole moment of the organic permeant, solubility factor of membrane, and hydraulic conductivity of the soil. Based on the findings of this study, the following conclusions were reached:

1. EOC and C/EOC are capable of odorous contaminant detection in both gaseous and aqueous conditions.

2. Theories based on chemisorption are most suitable in explaining characteristic operation of the C/EOC in detection of contaminants.
3. Variations in temperature or the environment and pore size of the membrane have minimal effects on EOC output.
4. Each chemical and membrane combination has a unique output signal signature which is different from any other.
5. C/EOC response to sudden external pressure and application of ionic field is characteristically different from contaminant detection response.
6. It is envisioned that C/EOC can be used for either continuous or intermittent (multiple) contaminant monitoring in saturated porous media.
8. C/EOC has capabilities for selective detection of different contaminants and different concentrations.

This is an exploratory pilot study, recommendations for future research on the topic are also given.

CHAPTER 1

INTRODUCTION

Developing new and corrective designs for landfills for impounding both hazardous and nonhazardous waste has become an important concern of geotechnical engineers. Before any remedial design measures are taken, a reliable means of predicting and detecting failures (i.e., monitoring) must be available. Theoretical approaches in the field suffer from oversimplification, which is unavoidable when engineering science is applied to unpredictable media like soils. The probabilistic applications of monitoring theories (i.e., waste migration models) to soils-related problems leave much to be desired before a definite statement about extent of pollutant migration can be made.

The current most widely used practical monitoring technique is monitoring-well installation. These wells are installed around landfills, generally downstream to the direction of flow. Fluids discharged into these wells are collected for laboratory analysis. The reliability of this method depends on whether there is a mixing of leachates from different layers, and if such mixing has resulted in the formation of a new compound. A positive answer to either of these questions renders test results misleading.

It is the objective of this study to develop, test, and evaluate the reliability of a new in situ monitoring technique capable of indicating the presence of leachates around a landfill. Such a device is expected to be mobile, inexpensive, versatile and operational at any depth.

Table 1.1. Summary of monitoring techniques

	Technique	Principle of Operation	Used From	Range (m)	Extent of Anomaly	Estimated Cost for Monitoring
FIELD METHODS	Drilling-Sampling	Soil Samples Collected and analyzed in the lab	Borehole	70	Depth	High
	Monitoring Wells	Water samples are Collected from packers in the well	Wells	A few tens of METERS	Depth	High
	Pan & Suction Lysimeters	Quality of water samples from porcelain pans are tested for chemical detection	Borehole		Depth	Moderate
	Time-Domain Reflectometry Grid	Dielectric change due to leakage along transmission lines is detected direction	Parallel wires in direction	100 New sites	= spacing of the lines	High
	Acoustic Emission	Sound emitted from fluid flow in soils is measured	Borehole			Moderate
	Electrical Resistivity	Resistance over a length vs. horizontal and vertical position is measured	Surface Borehole	100 New sites	Depth	Low
LABORATORY METHODS	Soil Column Contact	Washing soil columns with stimulated or actual contaminant	Samples in the lab	Specula-tion on uniformity	Depth	Low
	Soil Thin Layer Chromatography	Retardation effect of soil on leachate samples is analyzed	Samples in the lab	Specula-tion on uniformity	Depth	Low
	Hydraulic Conductivity	Susceptibility of soil to leachate seepage	Samples in the lab	Specula-tion on uniformity	Depth	Low
ANALYTICAL METHODS	Lapidus-Amundson	Solve for infinite column with mobile and stagnant regions	$c = c_o e^{\frac{vz}{2D}} [f(t) + k_2 \int_0^t f(t)\,dt]/2D$ $f(t) = f$ (modified Bessel function of 1st kind)			
	Wilson & Miller	Uses principal of mass transport to express the extent and severity of waste migration	$c = (e^{x/B} W(u,r/B)/4\pi\sqrt{D_x D_y}$ f = mass rate of pollutant			
	Molecular Modeling	Uses TLC results to quantify organic mobility based on molecular fraction theory	$R_f = e \log s + p\partial + c$ R_f = molecular fragment mobility			

LIST OF SYMBOLS

x,y = COORDINATES WITH ORIGIN AT THE POLUUTANT SOURCE
D ,D = LONGITUDINAL AND TRANSVERSE DISPERSION COEFFICIENTS
n = POROSITY
B = 2D /V
V = INTERSTIAL VELOCITY
u,r = FUNCTIONS OF DISPERSION
P = A CONSTANT CHARACTERISTIC OF THE TYPE OF REACTION
∂ = A CONSTANT REFLECTING THE ABILITY OF THE FRAGMENT TO ATTRACT ELECTRONS
S = WATER SOLUBILITY OF FRAGMENT IN PPM
e & c = CONSTANTS
C_o = CONCENTRATION IN SOIL SOLUTION
C = INITIAL CONCENTRATION
V = CONVECTIVE PORE WATER VELOCITY
D = DIFFUSION COEFFICIENT
Z = VERTICAL DISTANCE
T = TIME
K = BACKWARD REACTION RATE

1.1 MONITORING TECHNIQUES

The physical movement of waste in landfills and possibly through clay liners has been analytically mapped and practically monitored by many engineers through different approaches. Monitoring techniques developed in recent years can be classified under three categories (Waller and Davis, 1982) which are summarized in Table 1.1:

A. Field techniques

B. Laboratory methods

C. Analytical approaches

Besides these methods, there are others such as hydraulic conductivity and chemical conductivity tests, which are used mainly for design rather than monitoring purposes, and thus are not directly evaluated here.

The majority of present monitoring techniques are handicapped by a variety of factors, including cost, oversimplified and unsubstantiated assumptions in formulation, sampling errors, cross contamination, poor correlation between laboratory and field data, limited use in relation to sites under construction, and insufficient data base for general conclusions. These problems call for a new, more reliable, and cost-effective technique (see Chapter 2).

CHAPTER 2

A NEW MONITORING TECHNIQUE

2.1 ELECTRO-ODO-CELL (EOC)

A new monitoring technique should provide fast, representative, repetitive, and economical in situ measurements of the parameters pertaining to the transport of chemical waste through soil liners. Since the majority of the toxic hydrocarbons present in contaminated leachates are volatile, their presence can be verified by either olfactometric means (i.e., as odors) or electro-chemical means (i.e., in solute state).

A new procedure for hazardous waste detection could be possible by modifying implementation of an Avant-Garde sounding technique such as the electric Piezo-Cone Penetration Test (PCPT) (Tumay et al., 1981) generally used in situ evaluation of the geomechanical properties of soil. PCPT will help determine the nonhomogeneity of the soil within a fraction of an inch, providing reliable identification of soil stratigraphy and zones of higher permeability.

For monitoring the amount and mode of hazardous waste transport in such permeable zones, the effectiveness of the cone-penetrometer will require a device capable of detecting the presence of pollutant chemicals to be implemented in the cone. Figure 2.1 presents a schematic diagram of the piezo-cone penetrometer. In a process of quasi-static penetration PCP takes continuous records of tip resistance, sleeve friction and excess pore pressure. From these measurements, soil stratigraphy and relative permeability are determined. A typical record of such measurements is provided in Figure 2.2.

The electro-odo-cell (EOC) has the capabilities for detection of presence of contaminants (Tanyolac, 1969). In the new design of the

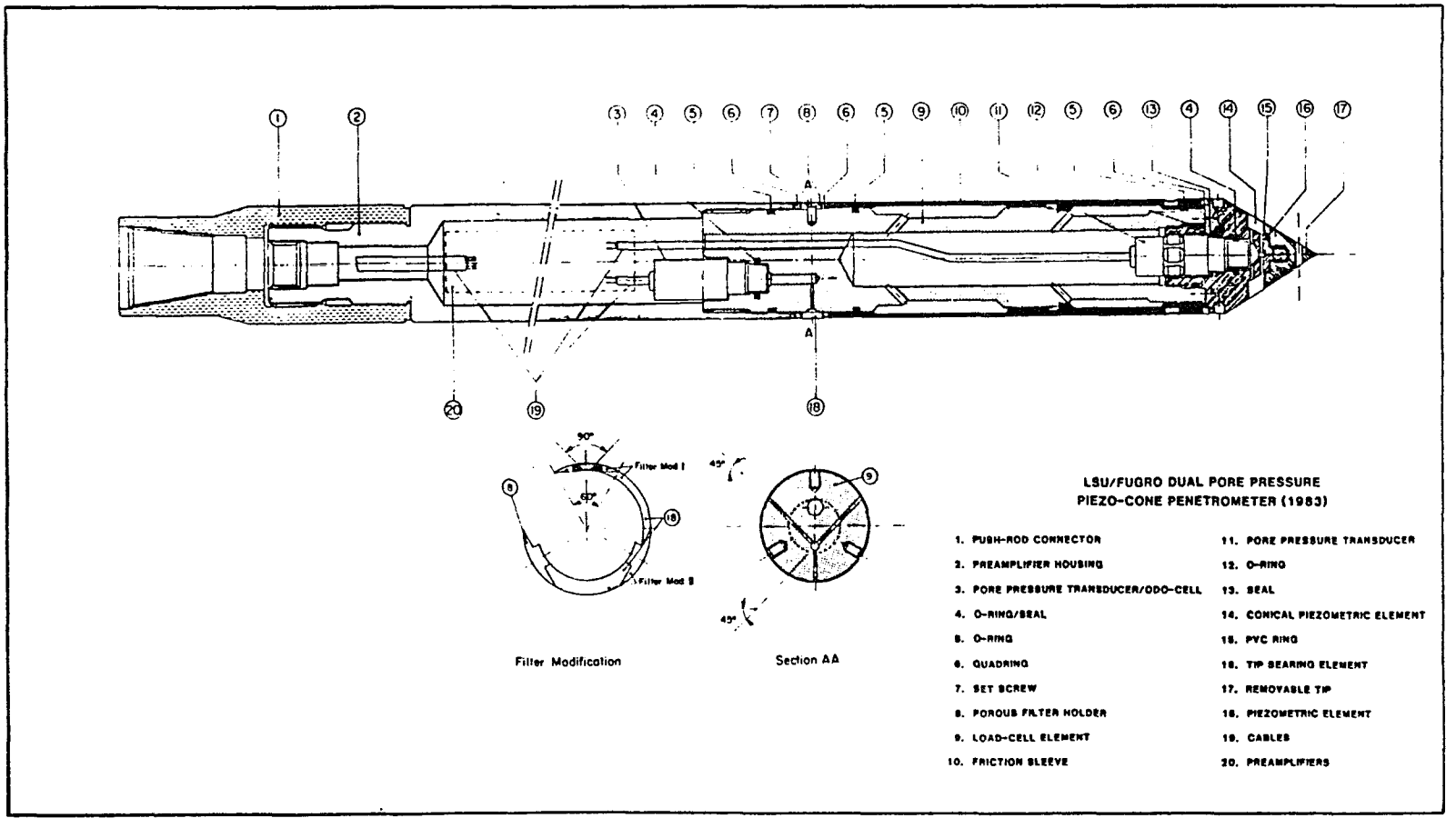

Figure 2.1. Schematic diagram of piezo-cone penetrometer.

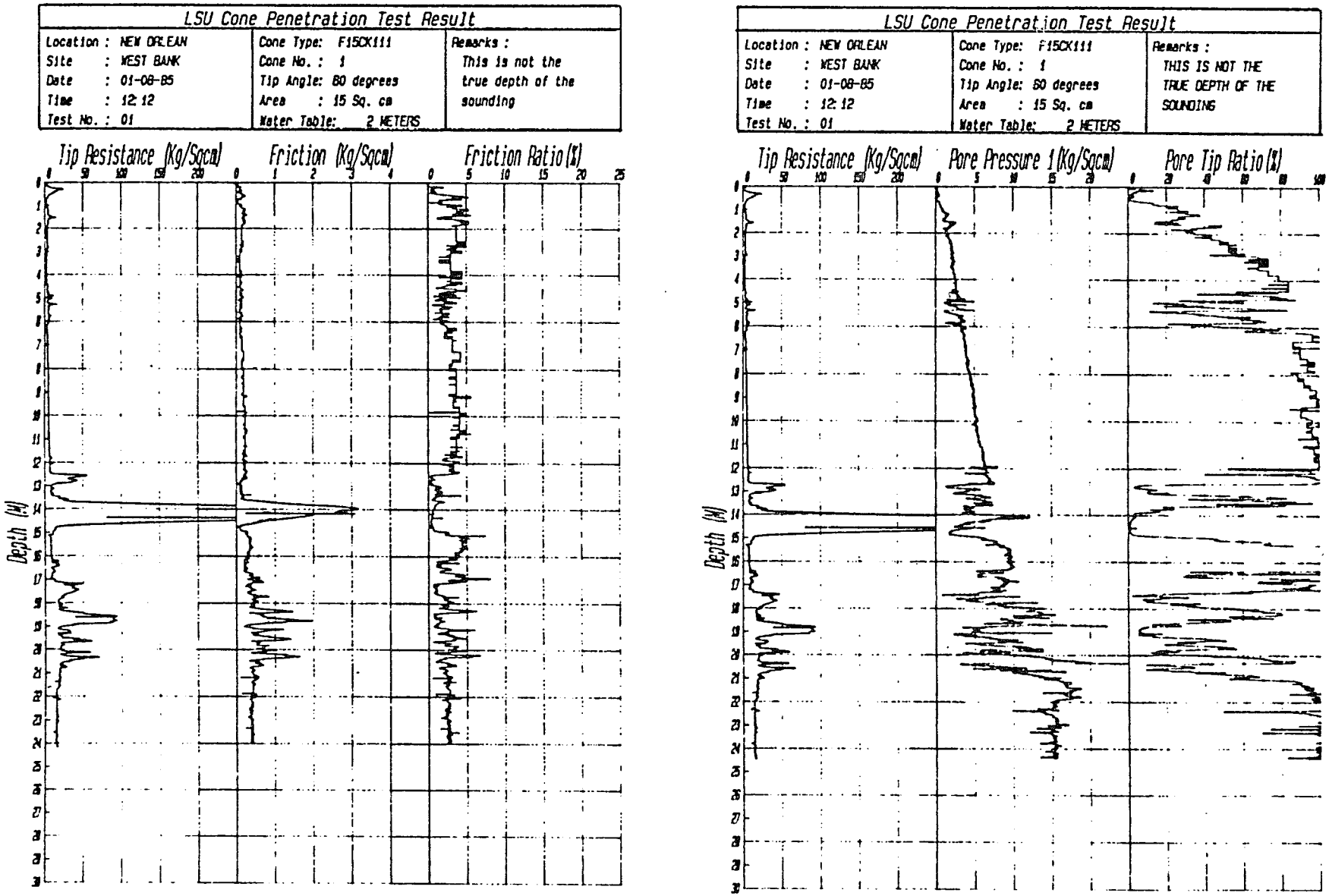

Figure 2.2. Typical output record of piezo-cone penetrometer output (after Tumay, 1985).

piezo-cone penetrometer provisions for incorporating such a device are provided. The new combination of the cone and the electro-odo-cell is referred to as C/EOC throughout this study. Figure 2.3 shows the basic components of the EOC.

Part 1 is a detector-transducer which has a surface sensitive to the molecules of adsorbed materials and produces a change in voltage or current on the detector, depending on the type and the amount of molecules adsorbed on this surface. The sensitive surface of the detector (a) is open to the odorant molecules and is made of di-electric materials. The conducting surface of the detector (b) is covered with a copper or silver plate which is connected to a cable (c) well-insulated from outside leakage and static charge; (d) is insulation between the metal plate and the ground.

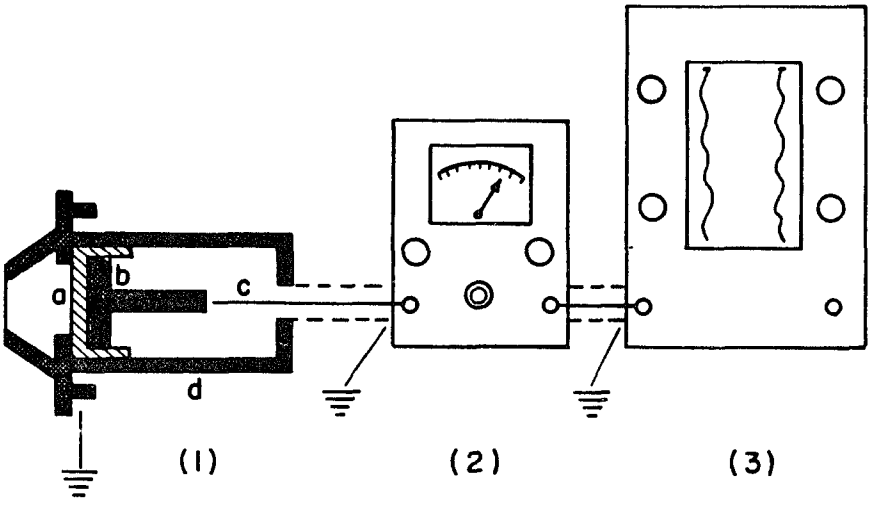

Figure 2.3. Components of the electro-odo-cell. (after Tanyolac, 1969)

Part 2 is a microvoltmeter which can retrieve the voltage changes in the detector.

Part 3 is an automatic recorder which records the indication of the microvoltmeter as microvolts--or microamps--versus time.

The EOC operates in a manner similar to the human nose, in that the incoming odor molecules are the source and their mobility resulting from any gradient is the vehicle of transmission.

Kinetics of odor molecules movement around the EOC creates currents. The intensity of which is a function of the type and number of odor molecules present on the dielectric membrane of the EOC. The stream of odor molecules are adsorbed on a sensitive dielectric membrane (analogous to the sensitive tissues of the human nose). The energetic quantities generated by the interaction between odor molecules and the membrane are converted to an electrical signal through a transducer, a process analogous to the excitation of the sensing cells in the human nose.

The electrical signals that are the signatures of specific odorants are then filtered, amplified, linearized, or otherwise conditioned before being sent to an objective evaluator (a recorder for the EOC analogous to the human brain).

An EOC circuit equivalent used in conjunction with a power supply source is shown in Figure 2.4.

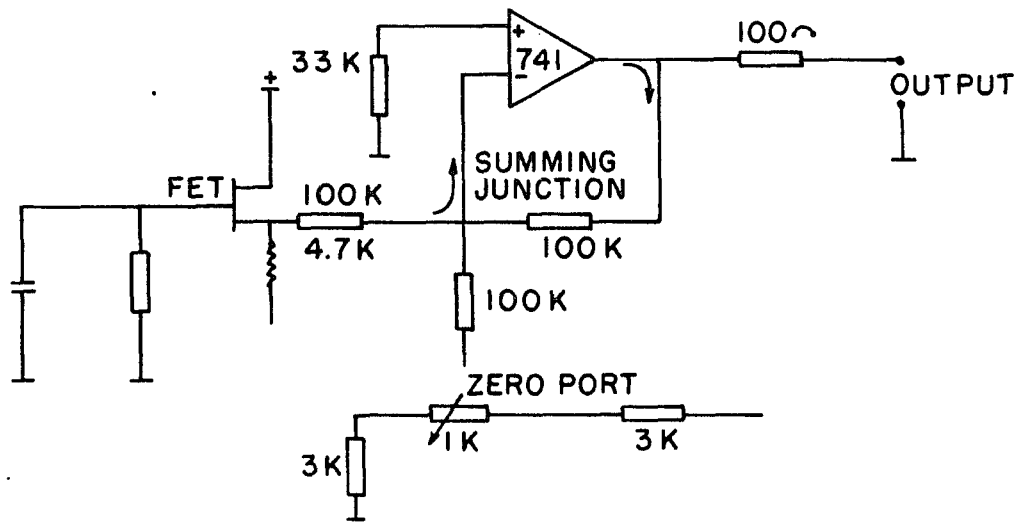

Figure 2.4. Actual circuit equivalent of EOC in conjunction with a power supply (after Tanyolac, 1964).

In earlier stages of this study the following attempts in modification, enhancement and redesigning of the EOC were made; these included the following: the popular 741 operation amplifier (op. amp) was replaced by an ultra-low input current bias op.amp (ICH 8500/A).

ICH 8500/A is unconditionally stable. The .01 picoamper input current bias of the op.amp is the same for both inverting and non-inverting input and it is constant over the operating temperature range of -25°C to +85°C.

ICH 8500/A has an output voltage swing of ±11 volts and an input capacity of 1.5 picofarads. The time constant (the time necessary for the input signal to stabilize) is about .5 seconds.

Pin configuration in the ICH 8500/A is such that any leakage in the flow of current between the case and the input, as well as any leakage that may exist between any of the pins and the input is intercepted and eliminated (Figure 2.5).

In the modification and redesign of the EOC, two main factors were considered: (1) The data acquisition was to be made by a computer, thus eliminating the need for a power supply and for interfacing of such with the EOC. (2) Signal manipulation and conditioning were also to be done through the data acquisition unit, thus eliminating the need for signal-conditioning. The final circuit is simpler with fewer parts and thus reduced possibility of experimental error.

The new version of the EOC transducer was designed as a capacitor in series with a voltage generator. A leakage resistance shunts this series combination as shown in Figure 2.6.

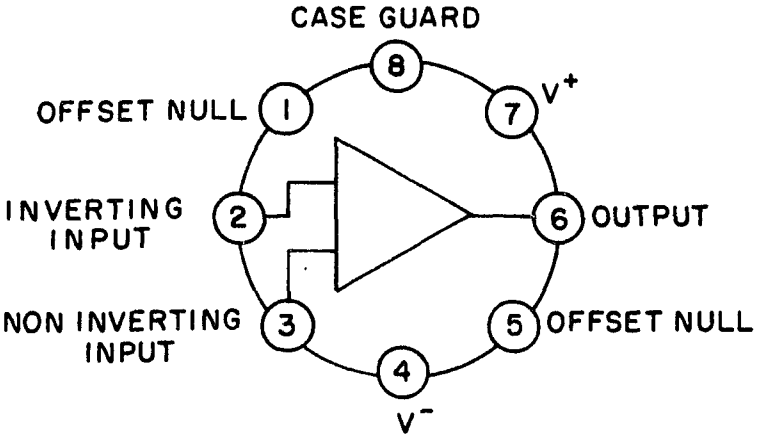

Figure 2.5. Pin configuration in ICH 8500/A operational amplifier.

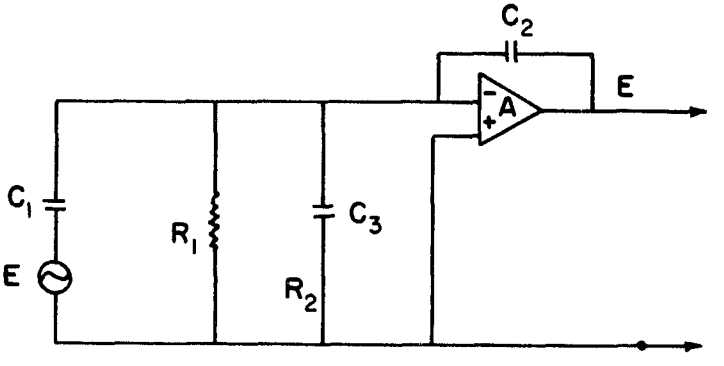

Figure 2.6. Simplified EOC circuit.

The steady-state dc output voltage in this system, in absence of any influencing force field, may be expressed as:

$$V = C_1 R_1 / (R_1 + R_2) \qquad (2.1)$$

where V = output voltage
C_1 = capacitance
R_1 and R_2 = resistance of resistors 1 and 2 respectively.

The introduction of a contaminant to the unit may trigger the release of energy based on adsorption of contaminant molecules on the

sensitive dielectric surface (E and C_1). Released energy will cause changes in the thermodynamic state of the dielectric surface, the conducting plate, and the resistors, resulting in changes in the value of the resistors from R_1 to R_{01} and from R_2 to R_{02}.

The output voltage of the unit is also influenced by the changes in the value of the internal capacitance in the following manner.

By definition

$$C = \frac{\text{Potential Difference in Coulombs) (Q)}}{\text{Voltage } (V_c)} = \frac{\int i_c dt}{V_c} \tag{2.2}$$

$$C = \frac{\int i_c dt}{V_c} = \frac{i_c}{dV_c/dt} \tag{2.3}$$

$$\frac{dv_c}{dt} = \frac{i_c}{C} \rightarrow V_c(t) = \frac{1}{C} \int i_c dt \tag{2.4}$$

where i_c = current passing through capacitor C

The value of the capacitance, C, also changes in accordance with Faraday's law, which states that when the plates of a capacitor are separated by dielectric material the value of the capacitance changes with changes in the dielectric constant of the material in the following manner:

$$C = KA \times 10^{-5}/36\pi d \tag{2.5}$$

where K = dielectric constant
A = cross-sectional area of the capacitor
d = separation distance between the plates of the capacitor.

The dielectric constant is the main variable in this equation. Its value changes with adsorption of odor molecules on the dielectric membrane material.

Due to variations in the capacitance and resistance, the value of the output voltage changes from that expressed by the equation (1) to:

$$V = C_{01} R_{01} / (R_{01} + R_{02}) \tag{2.6}$$

where R_{01} and R_{02} = final resistance value
C_{01} = final capacitance value

The loop equation for the circuit of Figure 2.7 is:

$$\frac{1}{C} \int ic\, dt + i\, R*C(t) = 0 \tag{2.7}$$

The quantity R*C is a characteristic of the instrument called the time constant, which is the time required for the input signal to stabilize and be reflected in the output. For the circuitry of simplified EOC, where a resistor, R, with a value of $5x10^9\Omega$, and a capacitance, C, of 10 pico Farads were used, the time constant is .5 seconds.

EOC operation may be summarized as follows: Referring to Figure 2.7 from t=0 to $t=T_1$ the output is a series of impulse increases in the voltage with time. The instantaneous impulse increases are represented by a step function approximated by $V_0 = V_C [1-\exp (-t/R*C)]$. For $T_1 \leqq t < T_2$ the membrane is saturated and the output is steady at the maximum level of V. During desorption $T_2 < t < T_3$ the output experiences the reversal of the adsorption process as expressed by

$$V_0 = V_C [1 - \exp (t/R*C)]. \tag{2.8}$$

EOC instrument characteristics such as selectivity, sensitivity, range, scale, and precision are discussed in Appendix A.

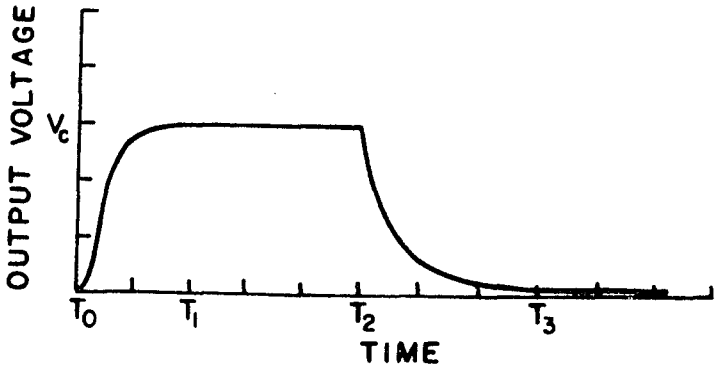

Figure 2.7. Idealized EOC response variation with respect to time.

2.2 THEORIES OF DETECTION

A literature review suggested that the basis for accepting or rejecting a single theory capable of fully explaining odor-detection phenomena is nonconclusive. In fact, it can be argued that because of the complexity and variability of the components involved, a singular theory may not exist. There may well be a series of complementary theories for odor-molecule detection. They may include:

I. Physical adsorption

II. Chemisorption

III. Ionic diffusion

IV. Dielectric changes

V. Volume filling of micropores

VI. Capillary condensation

2.3 PRIMARY FORCES IN ADSORPTION THEORY OF OLFACTION

The odor-cell detection system consists of wondering molecules in the vicinity of the sensitive dielectric membrane. Upon hitting the surface, some of these colliding molecules bounce back elastically, but the rest lose enough energy on collision to stick to the surface for a short time and then fly away.

If neither the surface nor the molecule experiences a permanent structural or crytalographic change, the adsorption is physical. If the electron shell of a molecule penetrates that of the surface, then weak chemisorption is present. If electrons from an admolecule are transferred to the surface, or vice versa, then ionic adsorption is the case (Chile, 1967; De Bore, 1950; Adamson, 1967; Mautland et al., 1981).

The adsorption or solid surface tension of the odor molecules can be gas-to-liquid contact (interfacial tension), liquid-to-solid contact, or gas-to-solid contact. The binding forces in any case are one or more of the following types:

(a) Van Der Waals forces, which are responsible for physical adsorption.

(b) Exchange or homopolar forces in which the electron shell of the contaminant molecule may penetrate that of the adsorbent membrane (weak chemisorption).

(c) Coulomb or heteropolar forces in which electrons from an admolecule are transferred to the adsorbent or vice versa (strong chemisorption or ionic adsorption).

The schematic diagram of three limiting cases of electronic interactions in the adsorption process is shown in Figure 2.8.

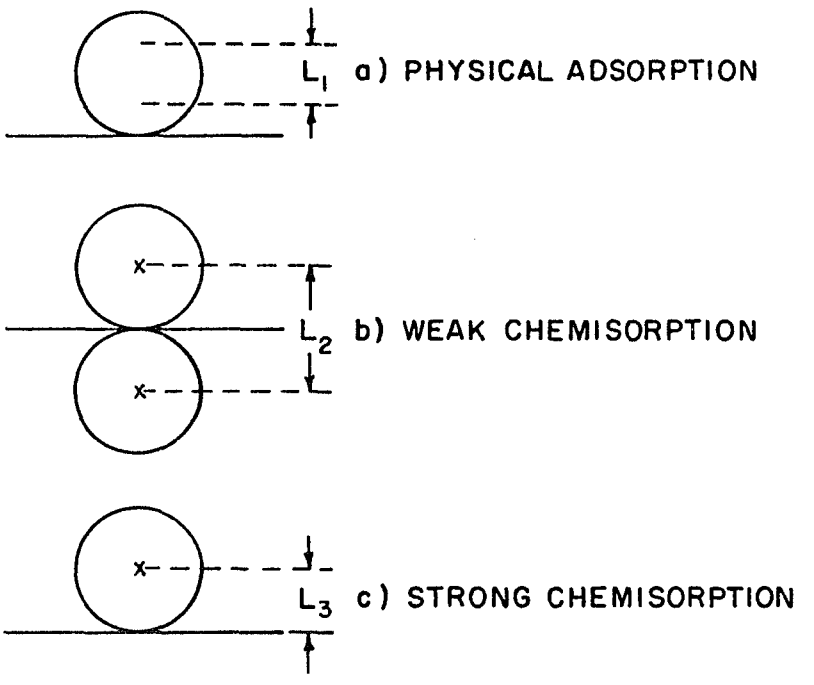

L = Distance between centers of adsorbent and adsorbing molecules

Figure 2.8. Schematic diagram of three limiting cases of electronic interactions in the adsorption process. (after Tanyolac, 1969)

2.3.I PHYSICAL ADSORPTION

Physical adsorption takes place on "inert" membrane surfaces where molecule-membrane interaction is limited to vibrational characteristics of the molecules without any changes in their structural configuration (Adamson, 1967; Atkins, 1976; Billmeyer, 1976; Conway, 1967).

Physical adsorption may result from one or more of the following molecular interactions:

(a) Dipole-dipole interactions: These forces arise between the molecules with permanent electric dipole moments. One of the molecules rotates through all angles relative to the others in such a fashion that attractive forces are cancelled by repulsive forces. The amount of exchange energy according to Debye (1954) is:

$$E = -\frac{2}{3}\frac{P_1^2 P_2^2}{R^6}\frac{1}{kT} \qquad (2.9)$$

where R = Distance between two molecules

E = Potential energy between two molecules when they touch

k = Boltzmann's Const. = 1.38×10^{-23} J/°K

P_1, P_2 = Electric dipole moments of molecules 1 and 2 respectively

T = Absolute temperature in degrees Kelvin

(b) Dipole-induced dipole interactions (forces that depend on electrostatic induction): A polar molecule present in the vicinity of another molecule (polar or nonpolar) will polarize the second molecule. The induced dipole then interacts with the dipole moment of the first molecule, and the two molecules are attracted to each other. The magnitude of the effect depends on both the size and permanent dipole moment of the polar molecule and the polarizability of the second molecule. The induced dipole moment, ($\mu_{induced}$) is proportional to the actual local electric field experienced by the molecule and can be expressed as:

$\mu_{induced}$ = (polarizability) [1/3 (K + 2)]

where Polarizability is $\simeq 10^{-24}$

K = Dielectric Constant

The average interaction energy, E, for two molecules under these conditions can be expressed as:

$$E = (2 \alpha P^2)/R^6 \qquad (2.10)$$

R = Distance between two molecules

P = Electric dipole moment

α = Polarizability factor

(c) Transient dipole (induced-dipole-induced-dipole interaction): Two nonpolar molecules "R" distance apart have no permanent moment but their electron clouds are fluctuating, and may be considered as having an instantaneous dipole moment which is constantly changing in magnitude and direction. If one molecule flickers into an electronic arrangement which gives it an instantaneous dipole, it can polarize the other molecule and induce in it an instantaneous dipole. The two molecules polarize and stick together.

The attraction between two uncharged molecules in the above configuration is expressed by London Forces [E(R)] as:

$$E(R) = \left(\frac{3\pi (I_1 + I_2)}{2\alpha_1 \alpha_2} \right) / R^6 = C R^{-6} \qquad (2.11)$$

where C = dispersion constant associated with instantaneous dipole-dipole

α_1^1, α_2^1 = polarizabilities of 1st & 2nd molecule

I_1, I_2 = Ionization energy of the molecule

R = Distance between two molecules

Physical adsorption is an exothermic process and if the energy of adsorption is big enough to activate the EOC, then a response will be registered. In principle, physical adsorption takes place without any activation energy, and its rate should always be proportional to the first order of pressure. Deviations from these rules mean that some mass transfer effects are taking place in the adsorbent pores (Debore, 1953).

Considering the kinetic theory of gases, it can be stated that from the odorant molecules striking the membrane surface, a number N is absorbed for a time t. Both N and t depend on the nature of the surface and of the molecules, the temperature of the surface, and the kinetic energy of the molecules (Kennard, 1938).

$$N = 3.52 \times 10^{22} \, (P/\sqrt{Mt}) \qquad (2.12)$$

$$t = t_o \exp (Q/RT) \qquad (2.13)$$

where P = Equilibrium pressure of the adsorbed film

M = Molecular weight

t = Absolute temperature

T_o = Time of oscillation of the molecule in the adsorbed state (10^{-12}--10^{-14} seconds)

R = Universal gas constant = 8.314 J/K/mol

Q = Heat of adsorption = the amount of heat that is liberated when the molecule is brought from a gaseous to an adsorbed state

N is also a factor of the sticking ability of the molecule, S_t. The proportion of collision with the surface that leads to adsorption is called sticking ability. When the odor molecules strike the membrane's surface, only the molecules that are able to dissipate their energy into thermal vibration of the membrane molecules before bouncing back are trapped.

The value of S_t (and consequently, N) depends on how much of the surface is uncovered. S_t drops as the membrane surface is covered.

Physical adsorption equilibrium is very rapid except when limited by

(a) Mass transport of the gas to the adsorbent surface (convection and external diffusion)

(b) Mass transport within pores in the adsorbent (internal diffusion)

(c) Surface migration

(d) The possibility that adsorption may change into a volume reaction

Upon adsorption to a solid surface, vapor molecules form one or more layers of adsorbate with characteristics different from those of the vapor and the solid. This interaction brings about changes in the thermodynamic properties of the solid surface to trigger the release of an existing energy in the interface which, if strong enough, can be detected by EOC.

2.3.II CHEMISORPTION

In chemisorption, electron transfer and sharing of electrons (the formation of a new molecular orbital) take place between the adsorbent and adsorbate as in the case of normal chemical compounds (Moore, 1956; Adamson, 1967).

The approach to the chemisorption bond can be described in terms of chemical state (molecular form, valency) of the constituents. Chemisorption may take one of the following forms:

1. The localized bond approach: This regards chemisorption as simply a bond formation between an atom of the adsorbate molecule and one of the adsorbent, obeying the same energetics as if the process was one of formation of a diatomic molecule.

2. Semiconductors: Some aspects of adsorption on oxides and other semiconductors can be treated in terms of the dielectric properties of the solid. Adsorption on semiconductor surfaces constitutes an important phenomenon since it can affect the performance of the semiconductor as an electrical component, usually adversely.
3. Acid-base systems: Here a proton transfer occurs between the adsorbent site and the adsorbate.

2.3.II ADSORPTION ISOTHERMS

Adsorption isotherms are plots of surface coverage vs. pressure at constant temperature for a specific adsorbate and adsorbent. Theoretical expressions exist for either monolayer or multilayer adsorption. Appendix B contains different approaches employed in deriving these expressions.

There are basically five types of vapor adsorption isotherms as shown in Figure 2.9 (Perry and Chilton, 1973). The applicability of each isotherm depends on the extent of relative pressure of the adsorbent. Normally as relative pressure increases so does the extent of adsorption and number of adsorbed layers.

Langmuir Type Monolayer | Mono and Multilayer Adsorption | Mono and Multilayer Plus Capillary Condensation

Figure 2.9. Vapor adsorption isotherms (after Perry and Chilton, 1973).

2.3.III ION CROSSING

In this approach, the interaction of ions with the membrane is examined as a problem in dielectrics. The membrane is treated as a region of low-polarizability acting as a barrier to the passage of molecules with specific resistance as high as $10^8 \Omega/cm^2$ as illustrated in Figure 2.10 (Parsegian, 1969).

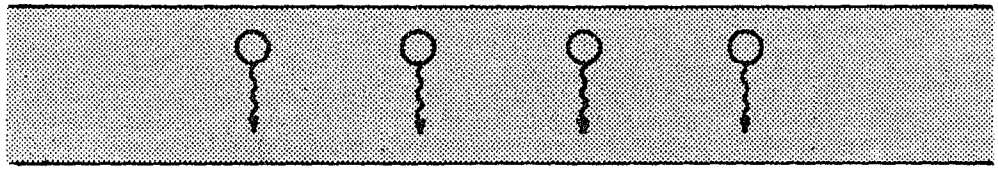

Figure 2.10. Ion crossing through the membrane (after Parsegian, 1969)

A conducting charge of radius, a, and charge magnitude, e, in an infinite medium of dielectric constant, ε, has an electrostatic self-energy (born charging energy) equal to $e^2/2\ \varepsilon a$. When this charged molecule attempts to penetrate or cross a low dielectric membrane, its self energy will be reduced because:

(a) "Charge-pairing" may occur between continuous-charge molecules.

(b) The membrane may have high dielectric "pores" through which the ion can pass.

(c) The ion may be wrapped in a neutral molecule or "carrier" of high polarizability which tends to solvate it (increase effective radius) in the low dielectric membranes.

For the same charged molecule trying to pass through a membrane of thickness, t, the following are true:

(a) The self-energy is lowered by an amount equal to

$$1.4 \times \frac{\text{Charge Radius}}{\text{Membrane Thickness}}$$

because of the finite thickness of the membrane. This effect is negligible for membranes 40-100A° in thickness.

(b) "Charge-pairing" does not appreciably reduce the self-energy so long as the interaction between positive and negative charges is ionic. Only if there is a covalent association between charged particles will the electric field around them be reduced sufficiently to be energetically important.

(c) "Pores" of high polarizability, filled with protein, can significantly lower the energy of a charge and possibly permit its passage through the membrane. In addition to direct interaction of the ion with the "pore" material, there is charge induced on the boundary between "pore" and membrane material which gives an additional, positive term to the self-energy.

(d) A "carrier" is simply a neutral molecule of high polarizability that can form a spherical complex with the ion inside. This local "solvation" of the charge is expected to lower its energy in the hydrocarbon region. Given an electrostatic self-energy gain of more than 8 k cal/mole by forming a pore, a membrane may well thin out at the point where an ion is forced across it by an applied electric field.

Under the combined effect of the above factors, a membrane may thin out at places or deform at points and even undergo structural changes.

In general, the permeability of EOC membrane to odor molecules is determined by both the diffusion coefficient D and the solubility coefficients, s, of the membrane. The diffusion coefficient decreases with increasing molecular weight of the odorant gas for a given membrane.

The solubility coefficients depend on interaction between the gas and the membrane materials. There is, however, no relation between the molecular weight of the gas and the permeability coefficient. The more flexible the chains of the membrane material, the less the activation energy needed for the diffusion, and the greater also will be the diffusion coefficient.

2.3.IV DIELECTRIC DIFFUSION

Dielectric diffusion is a consequence of the interaction of an electric field (DC or AC) with a medium in which there are gradients of the dielectric constant and conductivity. The phenomenon consists of a flow of material in the direction of increasing dielectric constant (Bruer and Robinson, 1969).

The phenomenon might play an important part in odor molecule transport processes through artificial membranes. Since membranes can be composed of regions of different dielectric constants, ionic mobilities into and on the membrane will be affected by their dielectric diffusion.

Upon application of an electric field, E, the membrane is polarized with subsequent dielectric losses. The phenomenological equations are described by Bruer and Robinson (1969). To obtain the following solution for changes in dielectric constant of the membrane:

$$D \left(\frac{d\mu_1}{dc_1}\right) \left(\frac{dc_1}{dx}\right)^2 - L_p \bar{I}^2 \left(\frac{1}{k_o} - \frac{1}{k}\right) + T \bar{I}^2 \left(\frac{k_o}{k^2} - K\right) = 0 \qquad (2.14)$$

Where

D = Diffusion coefficient of membrane (binary diffusion coefficient)

μ = Chemical potential

c = Concentration

L_p = Polarization constant

$\bar{I}$ = Time average of the electric current

k = Specific conductivity of the system = $k_o + \frac{w}{4\pi}\varepsilon$

k_o = Specific electrolyte concentration

T = Absolute temperature

w = Angular velocity

ε = Dielectric constant

From equation 2.14 changes in the k and consequently the dielectric constant ε can be measured. These changes are reflected in the output voltage of the EOC according to equations 2.4 and 2.5.

2.3.IV.1 DIELECTRIC CONSTANT AND THE SOLID GAS INTERFACE

The dielectric constant is a quantity that describes the response of a material to electromagnetic fluctuations. It has been expressed as

$$E(W) = E'(W) + iE''(W) \qquad (2.15)$$

where E' describes the ability of a material to transmit electromagnetic energy at a given frequency and E" describes the ability of the continume to absorb energy from an electromagnetic frequency, and i is the complex variable. A plot of E vs. frequency (W) for hypothetical material is presented in Figure 2.11.

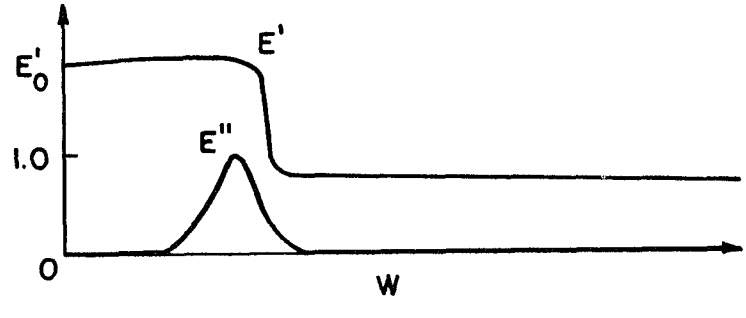

Figure 2.11. Changes in capacitance of a dielectric cell with adsorption (after Moore and Mitchell, 1974).

Changes in E" are reflections of the physical process of interaction of the material with the radiation in that frequency range. The phenomenon of peaking of E" at certain frequencies is termed adsorption (Moore and Mitchell, 1974).

In reversible adsorption, values of k may change according to equation 2.16:

$$k = k_{adsorbent} + V\,(k_{ads} - k_{des}) \qquad (2.16)$$

V = Surface Coverage

k = Electrical conductivity

Experimental data on changes in the value of capacitance of a dielectric cell upon adsorption (Figure 2.12) show a linear increase in cell capacity with the quantity adsorbed. The discontinuities in this trend were attributed to completion of monolayers of inception of capillary condensation (McIntosh, 1976).

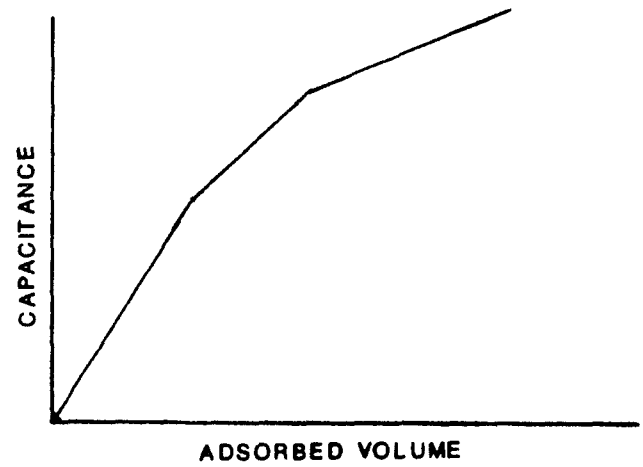

Figure 2.12. Changes in dielectric cell capacity vs. adsorption.

2.3.V VOLUME FILLING OF MICROPORES

When the adsorbent contains a large number of micropores, the dimensions of which are comparable with those of the molecules,

multimolecular gradual adsorption may not occur. The pores will be completely filled at very low pressures while only a small fraction of a layer would be formed on the smooth parts of the surface at the same pressure.

For the porous membranes, the amount of adsorbed odor molecules will rise very little with increased pressure after the micropores have been filled, and a flat plateau parallel to the pressure coordinate will appear on the adsorption isotherm.

If micropores are considered as a potential field into which the adsorbate molecules "fall," then the adsorbed layer resembles the atmosphere of a planet. It is most compressed at the surface of the solid and decreases in density outward. The surfaces of equipotentials can be represented as lines (in cross section). The space between such sets of equipotential surfaces corresponds to a finite volume and a finite energy level (Adamson, 1976). If E_x represents the work done by the adsorption forces when the adsorbate is brought up to a distance x from the surface, then $E_x = \int_{P_g}^{P_x} V dp$ and the work for the adsorbate, w, is given by

$$w = V \int_0^{\infty} (P_x - P_g)\, dx \qquad (2.17)$$

where V = Surface coverage

P_x = Pressure at adsorbed state

P_g = Pressure at gaseous state

For cellulose and protein membranes, the situation is different from gel systems and inert membranes, in that a strong interaction between the adsorbate and adsorbent is normally observed. The interaction is far

removed from that of physical adsorption for inert substances. Apparent molecular polarization in excess of that known for bulk matter is also reported for these systems. Volume filling of micropores thus does not apply to reactive membranes and is appropriate for inert membranes such as teflon.

2.3.VI CAPILLARY CONDENSATION

When the relative pressure of an organic vapor which comes in contact with the porous membrane adsorbent increases from zero to unity, several mechanisms for the filling of the adsorbent surface, or rather of the space within the pores of the adsorbent, participate successively.

With the lowest relative pressures, reversible volume filling of the narrowest micropores takes place. A monomolecular layer is formed on the surface of wider pores and on the nonporous part of the surface. When the relative pressure increases, polymolecular adsorption starts. With relative pressures of roughly 0.2 - 0.3 the amount adsorbed starts to increase more rapidly than that corresponding to polymolecular adsorption if the adsorbent contains pores of a width equal to several times the diameter of the molecules being adsorbed. This is caused by the so-called capillary condensation of the organic vapor on the membrane surface.

The principle of capillary condensation can be explained as follows: The increase in the thickness of the multimolecular adsorbed layer, on reaching a certain relative pressure, may cause the layers on opposite sides of the narrowest part of the pore to join together, forming a concave meniscus. Thus, owing to the influence of the number of surrounding molecules, adsorbate molecules in the meniscus surface are

attracted into the adsorbed phase with an intermolecular force greater than into the plane surface of the membrane as illustrated in Figure 2.13.

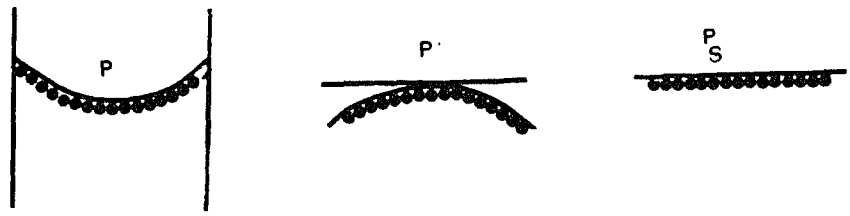

Figure 2.13. Volume filling of micropores.

The vapor pressure above this surface will then be less than the vapor pressure over a plane surface at the same temperature. Therefore, vapor condensation takes place on this meniscus and the entire volume of the pore is gradually filled with the condensed adsorbate (condensate). Even wider pores are filled when the pressure rises.

The quantitative relationship between the vapor pressure and the radius of curvature, r, of the meniscus in a pore filled with condensed vapor is defined by the following equation (Crowell, 1967):

For a spherical convex meniscus:

$$R\ T\ \ln(P_s/p) = 2\ \gamma\ V_m/(r - t) \qquad (2.18)$$

For a cylindrical meniscus:

$$R\ T\ \ln(P_s/p) = \gamma\ V_m/(r - t) \qquad (2.19)$$

where r = pore radius

P_s = saturation vapor pressure

p = existing vapor pressure

γ = surface tension

V_m = molar volume of the condensate

T = temperature (°k)

t = thickness of adsorption layer

R = universal gas contact = 8.314 J/°k/mol

Capillary condensation is frequently manifested by hysteresis (Appendix A) on the adsorption isotherm; that is, from a certain pressure upward, the value of the equilibrium amount of condensate adsorbed is greater when a specific pressure value was achieved by lowering the pressure than when the same value was achieved by increasing the pressure.

The experiments were designed to compare the output for physical adsorption cases (non-reactive membranes) vs. chemisorption (reactive membranes) in detection of odor molecules. Dielectric diffusion effects were examined through application of external ionic fields and volume filling of micropres was examined by comparison of the output for different pore sizes of the same membrane (see Chapters 5 and 7).

CHAPTER 3

WASTE MIGRATION

Soil and waste components, both separately and in conjunction with each other, are dynamic systems. Both of these constituents of a waste disposal site may have unsatisfied force fields. These force fields are either based on the physicochemical nature of soils and/or organics and associated with atomic-molecular, electrical, and thermodynamic forces or produced by geogravitational forces resulting from the weight of the overburden material, hydrodynamics of the ground water, etc.

Because of these factors, some organic chemical wastes react with and move within the soil mass. The potential for and extent of such migrations depend among other factors upon the hydrogeological setting, the concentration and characteristics of chemical waste, the miscibility of the waste in pore fluid, the interaction between liquid and solid phases, energy potentials in the direction of flow, the cross-sectional area, and the time (Gilham and Cherry, 1982).

The migration process may take place through advection and/or dispersion.

1. Advection, which is attributed to the average motion of the fluid, is the mechanism of migration in deposits with hydraulic conductivities greater than 10^{-6}cm/sec. or in cracks of finer deposits. Advection is mainly controlled by hydraulic gradients within the boundaries of a porous body.
2. Dispersion may result from two processes:
   a. Molecular diffusion, resulting from the thermal kinetic energy of a molecule (or chemical gradient) which, in the

presence of concentration gradients, results in the net flux of solute towards the low-concentration zone.

b. Mechanical mixing, resulting from velocity variations within the porous media because of the velocity distribution associated with the flow of viscous fluid through a pore; the variation in velocity as a result of pore geometry; and the fluctuation in the stream lines with respect to the mean flow direction.

In the face of these generalities, it must be noted that for unfractured silty or clayey deposits, diffusion generally controls the migration of waste. In the presence of fractures, however, advective transport may occur along the fractures. In this case, molecular diffusion acts as an attenuating factor, causing the transfer of the contaminant from fractures to the relatively impervious matrix. This reduces the concentration in the main zones of advection and increases the concentration in the zones of lower flow (Gilham and Cherry, 1982).

At high gradients, rapid migration by advection along permeable zones or smooth surfaces causes irregular contaminant flow within fingers containing undispersed contaminant concentration.

If the contaminant is reactive then such reactions might either retard or enhance the pattern and extent of migration.

The physical movements of waste through soils can be mathematically expressed in the following manner (Van Genuchter et al., 1976; Gilham and Cherry, 1982):

Let $J_a = qc$	Express advective solute flux	(3.1)
$J_d = -n D_d \text{ grad } (c)$	Is modified Fick's Law for diffusion flux, and	(3.2)
$J_m = -n D_m \text{ grad } (c)$	Express mechanical mixing	(3.3)

Where

n = volumetric water content

q = Darcy's flux (LT^{-1})

c = concentration of the solute

D_m,D_d: dispersion coefficients for mechanical mixing and diffusion flow respectively

The general differential equation describing simultaneous diffusion and convection for steady flow in x-direction with dispersion in x and y directions for an isotropic homogeneous media is expressed as (Feda, J., 1982):

$$\frac{\partial c}{\partial t} = D_L \frac{D^2 c}{Dx^2} + D_T \frac{\partial^2 c}{\partial y^2} - \bar{V} \frac{\partial c}{\partial x} \qquad (3.4)$$

With

$D_t = D_d + \alpha_T |\bar{V}|^m$ = Dispersion coefficient in Y direction

$D_L = D_d = \alpha_L |\bar{V}|^n$ = Dispersion coefficient in X direction

Where

n,m = experimental constants

α_T = transverse dispersivity

α_L = longitudinal dispersivity

$\bar{V}$ = Velocity

Except for small values of V/D, all solutions to (3.4) are symmetric (saturated flow only). Under unsaturated conditions, the larger pores are eliminated for transport and the proportions of fluid which does not readily move within the soil is increased (dead or stagnant fluid) leading to deviations from symmetry in solutions to (3.4) (Cameron and Klute, 1977; Selim, et al., 1976).

A more frequently used formula for expressing 1-D advective-dispersive flow of solute in porous media at steady hydraulic flow with constant water content is:

$$\frac{\partial c}{\partial t} = D \frac{\partial^2 c}{\partial x^2} - V \frac{\partial c}{\partial x} - \frac{\beta}{\theta} \frac{\partial s}{\partial t} - q \qquad (3.5)$$

where

c = concentration of the mobile fluid (mass/volume of solution)

s = absorbed phase concentration in units of mass of absorbed chemical per mass of porous media

D = hydraulic dispersion coefficient which is equal to $0.5\ V\delta dp$ for a nonhomogeneous unconsolidated pack

V = seepage (Darcian) velocity

β = bulk density of porous medium

θ = volumetric water content of soil

$\bar{q}$ = rate of loss or supply of solute per unit volume of soil

$$\bar{q} = S_s\ c/c_o \qquad (3.6)$$

c_o = concentration of applied solute

S_s = sink/source rate constant

3.1 DISPERSION IN MIGRATION

In homogeneous media, contaminants injected continuously as a plane source would move forward in the direction of flow at a velocity V. The concentration distribution at the front, at a sufficient distance from the source, is usually assumed to be Gaussian (Perkins and Johnston, 1963; Gilham and Cherry, 1982).

In heterogeneous deposits, however, the contaminants move in complex patterns. In the more permeable zones, diffusion causes contaminants to migrate from heterogeneities into the adjacent heterogeneities of lesser permeability. The net result is a reduction in concentration and flux in the permeable zone and an increase in concentration in less permeable zones. Over time, the diffusion tends to generate increasing uniformity of concentration distribution in the front.

Dispersion in macroscopic and larger scales within a system is accomplished primarily by molecular diffusion, which acquires its driving force from transient local concentration gradients imposed on the macroscopic system by preferential advection transport in more permeable layers or lenses.

The moving front at moderate flow rates will create a slightly asymmetrical mix zone (tailing edge stretched out), with the longitudinal dispersion coefficient approximately equal to the first power of the average fluid velocity. If the velocity in interstices is large enough, there will be sufficient time for diffusion to equalize concentration within pore spaces. In these regions, longitudinal dispersion increases more rapidly than fluid velocity.

At low velocities in interstices, transverse dispersion is characterized by a region in which transverse diffusion dominates. If the fluid velocity is high enough, there will be a transition into regions where there is stream splitting with mass transfer. Insufficient residence time in these regions prevents complete damp-out of concentration variations within pore spaces. For this range the longitudinal dispersion, K_1, is expressed as (Dean, 1963):

$$K_\ell = \frac{D_o}{F\phi} + 0.5\ V\ \delta\ d_p \qquad (3.7)$$

where

D_o = molecular diffusion coefficient

v = seepage velocity

d_p = particle diameter

δ = nonhomogeneity factor or number of particles in a mixing cell

F = formation electrical resistivity factor

ϕ = fractional pore volume

In general, longitudinal dispersion is caused by (Green, Lee, and Jones, 1980):

1. Molecular diffusion in the flow direction
2. Turbulent (cell) mixing
3. Lateral transport process coupled with velocity or residence time distribution including:
   a. "Taylor diffusion" caused by the interaction of velocity profiles in individual voids with lateral molecular diffusion
   b. Separation and remixing or interdiffusion of streams having different velocities around particles
   c. The coupling of gross velocity profiles caused by inhomogeneous porosity with lateral dispersion
4. Finite mass-transfer rate between a porous matrix and flowing phase, and a finite diffusion rate inside elements of the porous matrix.

The final expression for laminar flow conditions in a typical unconsolidated, random pack may be given by (Perkins and Johnson, 1963):

$$K_t = \frac{D_o}{F\phi} + 0.0157\ V\ \delta\ dp \qquad \text{for } \frac{V\delta dp}{D_o} < 10^4 \tag{3.8}$$

[see equation (3.7) for the legend]

There are several factors that must be considered and controlled to get consistent longitudinal and transverse dispersion results; among them are porosity, particle size and distribution, particle shape, packing or permeability heterogeneities, viscosity ratio, gravity ratio, edge effect (wall effect) in packed tubes, amount of turbulence, effect of immobile phase, the ratio of the interface pore in a sample to the volume of the sample, and the degree of consolidation (Dunn and Mitchell, 1982).

3.2 MIGRATION MODELS

Literature review reveals a vast number of modeling techniques and approaches applied to the study of solute migration through porous material. Prominent among these models are:

1. Statistical-geometrical model: In this model a process of spatial averaging is used to replace the microscopic scale of description with a conceptual macroscopic scale. In the macroscopic description, quantities defined as a point represent the average or microscopic effects in the vicinity of the point (Scheidegger, 1953).

2. Completely disordered capillary model (Scheidegger, 1953): Here the medium is assumed as a "one piece" ensemble of similar pieces with identical properties and dimensions. The fluid is also considered as a continuous medium. Then the fluid "particle" displacement is treated by the integral probability approach; i.e., if a particle of fluid undergoes a displacement ξ ($\xi = \xi\ \hat{i} + \Psi\ \hat{j} + \mu\ \hat{k}$) in every interval of time, τ, then the probability of such displacement occurring is denoted by $v\ (\xi)$ for

$\int v\ (\xi, \Psi, \mu)\ d\ \xi\ d\ n\ d\ \mu = 1$. The average displacement is $\langle \xi \rangle_{av} = (\bar{\xi}, \bar{\Psi}, \bar{\mu})$.

3. The mixing cell model (Dean, 1963) is based on equivalence between the diffusion in series of perfectly mixed cells, the i^{th} cell in the series is governed by the simple material balance $c_{i-1} - c_i = dc_i/d\tau$, $i=1 \rightarrow N$, where c_i is the concentration of a trace component in the flowing stream and τ is the dimensionless time based on the mean residence time in the mixing cell. If the medium is composed of flowing and nonflowing volumes, then the above expression becomes

$$c_{i-1} - c_i = (1-f) \frac{dc_i}{d\tau} + f \frac{dc_i^*}{d\tau} = - \frac{\partial c}{\partial x} \tag{3.9}$$

$$f \frac{dc_i}{d\tau} = a\ (c_i - c_i^*) \tag{3.10}$$

where f is the fraction of cell volume which is nonflowing (stagnant)

c_i^* is the trace concentration in the fraction

a is a dimensionless mass-transfer modulus

4. Taylor's model (Pettyjohn, 1981; Roberts et al., 1981; Nielsen and Biggar, 1962) for solute movement through a single capillary tube of constant radius, transport is expressed as

$$V = 2V_o\ (1 - \frac{r^2}{a^2}) \tag{3.11}$$

where V = velocity at a radial distance r from the center of the capillary tube of radius "a". V_o = initial velocity at the center of the tube. The expression which combines dispersion owing to the above velocity distribution and to molecular diffusion when the diffusion coefficient D is assumed constant is:

$$D\left[\frac{\partial^2 c}{\partial x^2} + \frac{1}{r}\frac{\partial c}{\partial x} + \frac{\partial^2 c}{\partial r^2}\right] = \frac{\partial c}{\partial t} + 2V_o\left(1 - \frac{2}{a^2}\right)\frac{\partial c}{\partial x} \qquad (3.12)$$

x = distance along the capillary tube

c = concentration of fluid

If the displacement is taken as a "random walk" process, consisting of successive statistically independent straight steps taken in equal small time intervals, then using the central limit theorem the probability function of the displacement will be Gaussian (normal) with a variance proportional to time. Upon integrating the solute concentration distribution, c, in the effluent (breakthrough curves) resulting from continued displacement of the original fluid (c = o) by a solution, (c = c_o) is given by:

$$c/c_o = \tfrac{1}{2}\ \mathrm{erfc}\ [(x-Vt)/\sqrt{4Dt}] \qquad (3.13)$$

x = distance

V = average velocity (flux divided by proportion of soil volume occupied by water)

D = factor of dispersion (not equal to molecular diffusion coefficient)

t = time of travel

3.3 THE LIQUID PHASE AND MISCIBLE DISPLACEMENT

In addition to migration by diffusion through the solid phase, organic waste migrates within and reacts with both the liquid and gaseous phases of soil ensembles. Water is usually the major component of the liquid phase in natural soils. Water structure may be considered as a giant polymer of hydrogen-bonded molecules. It forms a monolayer on surfaces or soil at a relative humidity of 20% and 20°C temperature. The

first layer of water adsorbed on clays exhibits high viscosity and has been described as immobile and ice-like. Adsorbed water dissolves organic and inorganic compounds and permits their diffusion but at rates much lower than in the bulk solution.

A major factor in waste migration is the condition of saturation prevailing in the soil environment. In unsaturated zones diffusivity and capillary action govern the flow and might lead to partial saturation. Mathematical expressions for such movements are not well defined. For saturated flow, however, there are a number of expressions for the flow of liquid phase (Pettyjohn, 1981; Young and Warkentin, 1966; Ali and Moore, 1981). These include:

a. Flow dominated by infiltration where capillary forces draw liquid into partially saturated, finely grained material
b. Flow in large openings where inertia terms predominate
c. Darcian flow where gravitational forces predominate
d. Modification to Darcian flow such as Kozeny-Carmann's equation
e. Statistical treatments and probabilistic modeling.

A fluid waste usually migrates through a porous media which is partially or fully saturated by other fluids. The waste may or may not be miscible with the existing fluid in the pores, and even if two fluids are miscible, their mixing in the porous media is not the same as diffusion mixing of two fluids in contact. In porous media, additional mixing may be caused by uneven flow or by concentration gradients resulting from fluid flow. Miscible displacement of a fluid by another is affected by several factors, among them:

1. Viscosity: If the displacing fluid is less viscous than the displaced fluid, viscous fingering may occur. When the displacing fluid is more viscous (favorable viscosity ratio), the usual dispersion mechanism will continue to operate.

A favorable viscosity ratio will tend to suppress the effects of packing or permeability heterogeneities and will reduce the distance between moving parallel interfaces. Suppression of the dispersion coefficient, therefore, depends upon the degree of inhomogeneity in the pack, perhaps the length of the mixed zone, and the relative amount of diffusion within the pore spaces.

2. Density: If the fluids of different density are used during miscible displacement, gravity forces may influence dispersion. In vertical displacement, if the dense fluid is placed above the less-dense fluid, then gravity will usually cause distribution or gravity fingering. However, if the denser fluid is on the bottom (favorable gravity forces), then a stable displacement will usually occur.

Favorable gravity forces will suppress dispersion in two ways. First, any unevenness of the front caused by packing or permeability heterogeneities will tend to be reduced by a factor which might be as large as δ (δ=heterogeneity factor). Secondly, if there is not a complete equalization of composition within each pore space by diffusion, then gravity can cause further reduction of dispersion within pore spaces.

Several conceptual and empirical models are currently used for expressing miscible displacement within porous media. The most widely recognized of these models are:

A. Capacitance model: Capacitance or stagnant pore-volume effects are most apparent when a concentration step-change miscible displacement is taking place. This is a model where a continuous solvent bank is injected beginning at time t_o, to displace the in situ fluid from a core. The concentration profile predicted by this equation is nearly symmetrical around one pore volume, but in the presence of the capacitance effect, there is an asymmetry which is attributed to a hold up of in situ fluid in regions of stagnant or nearly slow flow, with subsequent bleeding out of the in situ fluid as the mixing zone passes through. Capacitance effect and asymmetric mixing zones are more pronounced for short cores but are minimized for longer cores.

B. Stochastic model (Mitchell and Hooper, 1965): Here it is assumed that the fluid is a continuous medium of which each point has a flow path. The fluid moves as piston flow through small regions, and displacement is divided into a motion phase and a rest phase. A Galton probability is applied for the variation of the solute concentration in the time and space. The concentration distribution is given by

$$c/c_o = \tfrac{1}{2}\ [1+\mathrm{erfc}\ (V\sqrt{\frac{t}{D}} - \sqrt{\frac{xv}{D}}\ - \frac{1}{8V}\sqrt{\frac{D}{t}}\ - \frac{1}{8}\sqrt{\frac{D}{xV}})] \qquad (3.14)$$

where
- c = permeant concentration
- c_o = initial concentration
- D^o = dispersitivity
- V = pore fluid velocity
- I_o = Bessels function of the first kind
- t^o = time
- x = distance
- erfc= error function

C. Capillary tube model (Perkins and Johnson, 1963): In this model, the tube is filled with one fluid and a second fluid is injected at one end of the tube. If the two fluids are of the same viscosity, if

diffusion effects are of no significant value, and if flow is laminar, then the concentration of the displacing fluid in the effluent stream is determined by integrating the flow equation for laminar conditions. There will be no injected fluid appearing in the effluent stream until one half of the tube volume has been injected.

For continuous injection, the effluent concentration is given by:

$$x = 1 - (\frac{V_p}{2V})^2 \tag{3.15}$$

For $V > \frac{V_p}{2}$ where V = volume injected, V_p = total volume of the tube and x = volume fraction of injected fluid in the effluent. In the actual case, molecular diffusion will cause mixing along the interface. The net result will be a mixed zone growing at a more rapid rate than would be obtained from diffusion alone, but less than that predicted by the above equation.

If the fluids were displaced by another fluid under the conditions where diffusion could nearly damp-out radial concentration variations, then a symmetrical-longitudinal mixed zone could be established. The mixed zone would travel with the mean speed of the injected fluid and would be dispersed if there were a constant dispersion coefficient given by:

$$K_\ell = D_o + (V^2 a^2)/48D_o \tag{3.16}$$

where

K_ℓ = longitudinal dispersion coefficient

V = average velocity

a = radius of the capillary

D_o = molecular diffusion coefficient

The value of dispersion coefficient indicates the extent of miscibility of two fluids. Perfect mixing is assumed for a dispersion coefficient of infinity. The effluent concentration, c, for the capillary tube is given by the diffusion equation as (Perkins and Johnson, 1963):

$$c = \tfrac{1}{2} \left[1 \pm \operatorname{erfc} \left(\frac{0.5}{\sqrt{K_{\ell}/VL}} \right) \left(\frac{1-V/Vp}{\sqrt{V/Vp}} \right) \right. \tag{3.17}$$

The empirical data indicate that a greater volume of solution is required to achieve displacement of a miscible fluid than can be theoretically justified. The discrepancies may be explained on the basis of the stagnant liquid zone concept as discussed before.

Dispersion coefficient in miscible migration is also a function of interfacial boundary conditions of soil and the apparatus. In solving the general miscible migration equations the soil and apparatus may be taken as two different layers with diffusion coefficients D_1 and D_2.

Analytical results (Gilham and Cherry, 1982) indicate that the effect of the apparatus on the dispersion coefficient is not significant in short-column experiments. One can also expect apparatus-induced dispersion to become more significant as the water content of the porous material decreases, because the relative magnitude of the dispersion depends in part on the ratio of the residence time of the solution in layer two to that in layer one in a two-layer treatment. This ratio is inversely proportional to the water content of layer one.

Another factor of importance in determining the diffusion coefficient of a sample is the wall effect in a permeameter. Experiments with spherical particles packed into a cylinder indicated that there were packing irregularies near the container walls (Perkins and Johnson, 1963),

and zones of high porosity may extend two to three particle diameters from the container walls. The interface (to regular packing) caused by the container wall is not limited to the immediately adjacent region but is propagated through the entire area. Packing irregularities of this type have an effect on both longitudinal and transverse dispersion. These effects may be included in expression of transverse dispersion coefficient as empirical constant β_t

then

$$K_t = \frac{D_o}{F\phi} + 0.0157\ V\ \delta\ d_p\ \beta_t \qquad (3.18)$$

where K_t = transverse dispersion coefficient
D^t = molecular diffusion coefficient
F^o = formation electrical resistivity factor
ϕ = fractional pore volume
V = velocity
δ = nonhomogeneity factor
d_p = particle diameter

3.4 LEACHATE

Organic waste is usually present in soils in the form of leachate. Leachate is defined as liquid that has contacted solid material and has extracted and/or suspended constituents from it. Leachate is generated by either gravity water washing through hazardous material or by the movement of liquids contained within a disposal impoundment through soil beneath the disposal area.

Leachate generation and quality depends upon a number of factors, including pH, temperature, buffer capacity of the system, complexation capacity, dielectric constant, contact time, water availability, and, more importantly, solubility of the constituents in pore fluid (Garret et al., 1981).

Solubility is a function of the chemical composition of the liquid phase and the solid medium, contact time, pH, and temperature of the system. Because dissolution is directly proportional to the surface area, small particles permit increased contact and a corresponding increase in leaching.

Porosity affects solubility by influencing the flow rate and thus the contact time between liquids and solids. As contact time increases (low porosity), dissolution increases to the maximum soluble concentration of the constituent in the liquid. Lower porosity, on the other hand, allows more complete chemical reactions between the liquid and the solid.

pH affects solubility in two principal ways: either by alteration of solution equilibria or by direct participation in redox reactions. The presence of acids of low molecular weight and carbon dioxide reduces the pH and contributes to changes in solubility.

Temperature changes within the system caused by the temperature of the material added, redistribution of heat, and the heat generated by waste decomposition influence solubility rates. Solubility rates generally increases with increases in temperature of the environment.

For ease of analysis, leachate wastes have been grouped into the following classes:

1. Aqueous-inorganic: here, water is the dominant fluid (solvent) and the solutes are mostly inorganic.
2. Aqueous-organic: the solutes are organic chemicals that are polar or charged as inferred by their water solubility.
3. Sludges: are generated when a waste stream is dewatered, filtered, or treated for solute recovery.

The organic substances present in the leachate may be classified as (Garret et al., 1981):

1. Organic acid is any organic fluid that has acid-functional groups. These can be very reactive with and mobile in clay liners. Organic acids like benzoic acid and acetic acid are readily adsorbed on clays. The hydroxyl group of the acid interacts either directly with the interlayer or by forming a hydrogen bond with the water molecules coordinated to exchangeable cations on the clay surfaces. Organic acids can also be absorbed by forming salts with the exchangeable cation.
2. Organic bases are organic fluids capable of accepting a proton to become an ionized cation. These potentially charged fluids are absorbed strongly by clay surfaces, and, thus, have the potential for changing clay interlayer spacings.
3. Neutral nonpolar compounds are organic fluids that have no charge and a small dipole moment. These chemicals have the ability to move through clay liners rapidly and erode the pores through which they pass. They can also displace water from the clay liners and cause shrinkage. These compounds include aromatic compounds such as benzene which can interact with clay surfaces. In the case of tolulene, and xylene, both coordination and physical absorption by the clay surfaces are possible. Phenols are absorbed by way of proton transfer.
4. Neutral polar compounds have no charge but exhibit strong dipole moments. This class contains alcohols, aldehydes, glycols, and ketons. They effect the permeability of the clay liners by changing the interlayer spacing of the clay and changing the surface tension of the pore water.

3.5 REACTIVE SOLUTE MIGRATION

Soils and organics are dynamic systems. In their migration through soils, organic leachates may also react with the soil mass. The potential for reactive migration depends, among other factors, upon the hydrogeological setting, the concentration and properties of the chemical leachate, the miscibility of waste in existing pore fluid, the interaction potential between soil and the waste, the energy potential in the direction of flow, and time.

It is generally expected that the concentration and, thus, the toxicity of leachates will attenuate as they move within the soil (Miller and Benson, 1983).

Foppe and Chain (1981) reported that for extractable volatile organics show a 90% concentration reduction for every 200 meters (600 feet) from the source in clayey material. The attenuations, they reported, tend to decrease with decreasing molecular weight, possibly because of the decreasing absorption capacity of compounds with low molecular weight.

Ehrlich et al. (1982) reports that over 95% of phenolic compounds are removed within 300 meters (1000 m) of the contamination source. This was attributed to anaerobic bacterial conversion of phenolic compounds to methane and CO_2 as well as processes discussed below.

Reactive processes affecting the fate of chemicals in clay soils may include sorption, ion pairing, co-precipitation-dissolution, complexing, redox, and biodegradation. Since clay liners are composed of colloidal components, any interaction will have to obey colloidal system interaction properties. The behavior of the colloidal systems is governed primarily by their large interfacial area, and physico-chemical and thermodynamic properties of the interface.

At the soil-waste interface, there is a segregation of positive and negative charges in a direction normal to the phase boundary. These charges are in form of ions, electrons, dielectric molecules, and polarized atoms attached to the particles. Charge concentrations have a tendency to diffuse away from the surface towards the bulk of the solution where their concentration is low. This diffused and active layer may extend several molecular diameters in thickness.

The sequence of the kinetics of a soil-waste reaction, in a general way, can be supposed to consist of the following steps:

1. Macrotransport (diffusion of reactants to the soil surface)
2. Microtransport (movement through micropores to absorption sites)
3. Absorption of the reactant by soil
    a. Physisorption (rapid initial association)
    b. Chemisorption (slower increases in sorption because of the formation of a strong chemical bond)
4. Desorption (partial and slow) of products of the third step
5. Diffusion of the product away from the soil surface

The presence of the nucleophobic (electron donor) and electrophobic (electron donor) sites on the surface of clay minerals and the electric charge of the unit layer (diffuse layer of Helmholtz, Gouy-Chapman) enables these minerals to adsorb polar organic compounds and ions.

If, the clay surface is considered to be flat with uniform charges, and the organic ions are considered to consist of two distinct moieties, a hydrophilic head (where electron charge is concentrated) and a hydrophobic tail (a straight or branched structured hydrocarbon chain that is organophilic). In the double layer, organic ions are arranged

so as to accommodate their long-range electrostatic attraction by the following mechanisms:

1. The organic ions in the bulk solution must dissociate before they can enter the double layer.
2. Hydrophilic heads of organic ions must be dehydrated before penetrating the inner Helholtz layer.
3. Polarized water molecules are repelled from the double layer to the bulk solution by the penetrating organic ions. There are additional repulsive forces resulting from the self-atmosphere potential of the ions present in the double layer and also from the electric field induced by the clay surface. Clay-organic interactions at the adsorbed layer are different from bulk interactions. Within the absorbed film, surface geometry seems to affect the activation energies and strengths of adsorption and desorption and thus control the concentration and mobility of surface species. When organic substances penetrate into the inner Helmholtz layer, the short-range forces (chemisorption) begin to operate.

Sorption is considered to be a fundamental and at times the only reaction between clay soils and organic waste. The extent of sorption in a heterogeneous soil system depends on the following factors:

1. The absorption capacity of soil having the order: organic matter>vermiculite>montmorollonite>illite>chloride>kaolinite.
2. Soil structure, which through its relation to the exposed surface, affects the process of sorption. In general, absorption increases with an increase in the number of bonds in a

molecule; number of orientation possible for absorption symmetry number; molecular size; and pore size; coagulation.

3. Solute characteristics such as solubility, molecular weight, functional group, charge distribution, polarity, and molecular configuration. Sorption is believed to decrease as the solubility in the solvent liquid increases.

4. Properties of organics at the interface which affect their reactivity with soils (Gillham and Cherry, 1982).

   a. Surface concentration or surface excess: positive values of this factor indicate positive sorption and negative values indicate negative sorption capacity. Negative values indicate that the concentration of the component is smaller in the interface than in the bulk. For absorption from the gaseous phase, surface excess increases with an increase in the partial pressure of the absorbate.

   b. Chemical potential is a quantity expressing the tendency of a component to change its concentration either by reacting chemically with another component in the same phase, or by migration to another phase.

   c. Surface tension or free surface energy: This is equal to mechanical work expended in changes that are necessary for a new interphase to come about. The absorption of liquids and gases to soil surfaces translates into minimizing the free surface energy which is established by a change in the composition of the phases to make the unbalanced force-field assume minimum intensity per unit area.

d. Surface activity, which is a function of interface component properties, grain size, surface area of the soil, and water content.

5. Temperature: The effect of temperature is directly related to the strength of absorption. The weaker the bond, the lower the effect of temperature, and the higher the temperature, the lower the absorption. Diffusion-controlled absorption's response to temperature takes place through changes in molecular velocity, which varies with the square root of the absolute temperature.

6. Water content: When normal water is associated with a metal cation, H^+ is often produced, resulting in an acidic condtition that can readily donate protons to bases such as amines and amides. Also in dilute modes (high effective water content), more surface area is exposed resulting in higher absorption.

7. pH of the soil has a remarkable effect in absorption, particularly for weak acids and weak bases. The weak acids are free in areas of low pH and are more highly absorbed in this form than as anions. Polar organics are capable of hydrogen bonding and, as such, will show somewhat different absorption with changes in pH values. The correlation of pH with absorption in soils has proven to be poor with soil organic matter, because the properties of soils [pH, organic matter, cation exchange capacity (CEC)] are interdependent and interrelated and this tends to obscure any conclusive inference with respect to pH only. When clay minerals are in environments where the pH is neutral to alkaline, hydrolysis reactions can result in the

precipitate of metals as the respective hydroxides. In weakly acid media, chemisorption of partially hydrolyzed hydrocarbons onto clay has been observed by Miller and Benson (1983). The exchangeable cation apparently polarizes water molecules and generates protons on the edge surface of the clay mineral. The polymer is then absorbed into these protonated sites.

3.6 SORPTION MECHANISMS IN SOILS

Sorption can take place in one or more of the following ways:

1. Ion exchange: In this process, one type of ion is taken from a solution in exchange for another type contained in or absorbed by the soil. The extent of this process depends on the concentration of the ion in the aqueous phase relative to the concentration of other sorbable ions, the exchange capacity of the absorbent, and its selectivity for the particular ion (Miller and Benson, 1983). Ion exchange in soil-waste reactions can be either cationic or anionic.
   a. Cation exchange: The replacement process in which organic molecules, positively charged by protonation, are absorbed by clay is referred to as cation exchange. In salt-affected soils, ions may be attached to soils by a combination of forces ranging from electrostatic to covalent, with corresponding increases in bonding energy. Small organic cations are absorbed by soil up to CEC. At low concentrations the organic cations are absorbed by clay as individual counter ions, but at higher concentrations they associate through interfacial interaction of the hydrophobic moieties of the ions with the soil. These

interactions result in the formation of "hemimicelles". Through formation of these hemimicelles, the system reaches stability.

Smectite and vermiculite absorb cations in their interlayer spaces to satisfy their negative charges. But kaolinite and, to a lesser extent, illite interact through their broken bonds around the edges of silica-alumina units and exposed hydroxyls. In many cases the exchangeable cation will affect the magnitude of clay absorption and the mechanisms by which the molecule is absorbed. In addition, the saturating cations, through steric effects on the absorbed molecule, can change the degradation rate of organics.

b. Anion exchange: Even though it is not the dominant mode of ionic exchange for clay soils, anion exchange may take place either electrostatically or with a degree of chemical bonding for a wide range of soil materials. It seems that organic cations may act as bridges between the organic anion and the clay surfaces, thus enabling the sorption of anions.

2. Charge transfer complexes involve a partial exchange of electron density and the formation of resonance structures involving ionic forms of donor and acceptor molecules. Such structures may form between molecules containing bonds or loose pair electrons.

Electron-rich organics, such as aromatics, and lone pair donors, such as alcohols and amines, may interact with basic

sites in the oxygen plane and/or negative poles of water molecules in the hydration sphere of a cation. A direct interaction of organic protons with the oxygen, forming hydrogen bonds, requires a low surface charge density at the clay surface and a low hydration energy for the inorganic exchangeable cations on the clay surface.

3. Polar nonionic compounds: These compounds can be bound to clay by strong ion-dipole attractions; hydrogen bonding, coordination, Van der Waals forces, and ion-exchange. The extent of absorption seems to depend heavily on the exchangeable cation. Sorption takes place as a result of specific interaction between small exchangeable cations and electronegative oxygen atom possessing loose electron pairs in the clay soil. The specific interaction is that of solvation of the cation by polar molecules, similar to the hydration of cations in aqueous solutions.

4. Complexation: Aromatic molecules are sorbed onto the interlayer of smectite by complex formation with the metal ions. Organics such as benzene and phenol form complex organic radical cations by oxidizing the metallic cation and being oxidized or by donation of electrons.

   Chelation is a form of complexation and occurs when an equilibrium reaction between a metal ion and an organic ligand results in more than one bond between the metal and a molecule of the complexing agent through the formation of a heterocyclic ring that includes the metal ion.

   Chelates have the potential for forming complexes of greater stability than analogous complexes in the metal if coordinated

in a noncyclic fashion with water, other organic ligands, or both.

5. Redox: Clays, when dried to low water content, behave as acids. The reactive proton originates from the dissociation of residual water molecules due to polarization by exchangeable cations and from dissociation of the functional groups in organic matter. These protons provide a reaction pathway of low energy in acid-catalyzed hydrolysis by withdrawing electrons and weakening the molecular bond so that it can be broken.

   Fe and Al trace metals within layer silicates and adsorbed oxygen have been identified as catalysts promoting free radicals.

   Oxidation for organic chemicals in soil environment takes two different forms. In the heterolytic or polar oxidation, an electrophobic agent attacks an organic molecule and abstracts an electron pair. In the homolytic or free-radical reaction pathway, an agent abstracts an electron pair.

   The intensity of oxidation-reduction reactions in both cases is a function of the electrical potentials in the reacting systems. For oxidation to occur, the potential of the soil must be greater than that of the organic chemicals present in the pore fluid. Water solubility is another factor of importance. Affinity for oxidation increases as the water solubility of an organic passes a lower limit.

6. Polymerization: Clays are able to influence polymerization reactions. The initiation of organic polymers by clays involves

the conversion of the appropriate monomer to a reaction intermediate. Polymer formation appears to increase with the increasing surface activity of the clay. It is considerably enhanced by prolonged contact with an excess amino acid solution and by heating.

7. Clay dissolution: Either organic acid or organic bases may solubilize portions of the clay structure. Acids have been reported to solubilize aluminum, iron, alkali metals, and alkaline earths, while bases dissolve silica. Because clay minerals contain both silica and aluminum in large quantities, they are susceptible to partial dissolution by either acids or bases.

3.7 MATHEMATICAL FORMULATION OF REACTIVE SOLUTE TRANSPORT

The one-dimensional form of the advective-dispersive equation of waste-transporting homogeneous media modified to account for the combined effect of chemical reactions can be expressed as (Gupta and Greenkorn, 1973; Cameron and Klute, 1977):

$$\frac{\partial C_S}{\partial t} = D \frac{\partial^2 C_S}{\partial x^2} - V \frac{\partial C_S}{\partial x} - G \qquad (3.19)$$

Where

C_S = concentration of the mobile solute (mass/volume of solution)

S = adsorbed phase concentration in units of mass of adsorbed chemical per mass of porous medium

D = hydraulic dispersion

V = seepage velocity

where G is the rate at which dissolved species are removed from the solution and its expressions vary depending on the type of absorption-desorption model used to express chemical behavior in the soil environment. Since pore surfaces may be composed of organic molecules, clays, aluminum, iron compounds, and other constituents in mixed and varied proportions, a chemical (organic) moving through ensembles of pores may react with different constituents at different rates. At selective reactive sites there may occur rapid interaction (inducing an instantaneous equilibrium) or a slow absorption of solute. These conditions will determine the specified expressions of G. For sorption, however, the general expression may resemble

$$G = \frac{\beta}{\theta} \frac{\partial S}{\partial t} \tag{3.20}$$

where β = Bulk density of porous medium

θ = Volumetric water content

S = Concentration of the soluble solute (mass/volume of solution) expressions of which depends on the adsorption-desorption model in the event that local adsorption equilibrium prevails. $\partial S/\partial t$ may be expressed as

$$\frac{dS}{dC_S} \frac{dC_s}{dt}.$$

S may be obtained by $S = S_1 + S_2$ where S_1 = absorbed concentration due to kinetic absorption and S_2 = that due to equilibrium absorption.

Consequently, for a model with first-order linear reversible kinetic adsorption, the transport model can be expressed (Cameron and Klute, 1977) by:

$$\frac{\beta}{\theta} \frac{\partial S_1}{\partial t} + (1-k_3) \frac{\partial C_S}{\partial t} = D \frac{\partial^2 C_S}{\partial X^2} - V \frac{\partial C_S}{\partial X} \tag{3.21}$$

$$\frac{\partial S}{\partial t} = k_1 \frac{\partial}{\beta} C_S - k_2 C_S + k_3 \frac{\partial}{\beta} \frac{\partial C_S}{\partial t} \tag{3.22}$$

where

k_1 = absorption rate

k_2 = desorption rate

k_3 = equilibrium constant

Normalizing the parameters as

$T = vt/L$ = # of pore volumes paned through a column with length L (3.23a)

$C = C_S/C_o$ (3.23b)

$K_1 = \frac{L\ k_1}{v}$, $K_2 = \frac{L\ k_2}{v}$, $K_3 = k_3$ (3.23c)

$B = vL/4D$ is Brener's number (3.23d)

B = o For Diffusion Flow; B = ∞ for Piston Flow

$N = B_S/\theta C_o$ is Peclet's number (3.23e)

$\xi = x/L$ (3.23f)

3.21, 3.22, and 3.23 combine to yield:

$$(1+k_3) \frac{\partial C}{\partial t} = \frac{1}{4B} \frac{\partial^2 C}{\partial \xi^2} = \frac{\partial C}{\partial \xi} - \frac{\partial N_1}{\partial T} \tag{3.24a}$$

and

$$\frac{\partial N_1}{\partial T} = K_1 C - K_2 N_1 \tag{3.24b}$$

with B.C. & I.C. as

$C(0,T) = 1 \qquad T>0$ (3.25a)

$C(\xi,0) = 0 \qquad \xi>0$ (3.25b)

$N(\xi,0) = 0$ (3.25c)

Applying Laplace transform to 3.24

$$S\ (1-K_3)\ \bar{C} = \frac{1}{4B} \frac{d^2\bar{C}}{d\xi^2} - \frac{d\bar{C}}{d\xi} - S\ \bar{N}_1 \tag{3.26}$$

$$S\bar{N}_1 = K_1 \bar{C} - k_2 \bar{N}_1 \quad \dashrightarrow \bar{N}_1 = K_1 \bar{C}/(S + K_2) \tag{3.27}$$

then

$$\frac{1}{4B} \frac{d^2\bar{C}}{d\xi^2} - \frac{d\bar{C}}{d\xi} = S \left(1 + K_2 + \frac{K_1}{S+K_2}\right) \bar{C} \tag{3.28}$$

for which

$$C(\xi,T) = \frac{2}{\sqrt{\pi}} (e^{2\beta\xi}) \int_w^\infty \exp[-h^2 - B^2 \xi^2/h^2]J \, dh \tag{3.29}$$

where

$$w = \sqrt{B\xi^2 (h\, k_3/T)} \tag{3.30a}$$

$$x = K_1 B \xi^2/h^2 \tag{3.30b}$$

$$y = k_2 [T-B \xi^2(1+K_3)h^2] \tag{3.30c}$$

$$J = \text{A characteristic function of the media} \tag{3.30d}$$

With a similar approach Lapidus and Amudson (1952) arrived at a solution to a conceptualized model where the organic adsorption on soils was linear and irreversible. Their solution has the form

$$C/C_o = \tfrac{1}{2} \left[\exp \left(\frac{1-\delta}{2\xi}\right) \operatorname{erfc} \left(\frac{1-\delta T}{2\sqrt{\xi T}}\right) + \exp \left(\frac{1+\delta}{2\xi}\right) \operatorname{erfc} \left(\frac{1+\delta}{2\sqrt{\xi T}}\right) \right] \tag{3.31}$$

where

$$\delta = \sqrt{1 + 4D\, k_1/\phi V^2}$$

ϕ = fraction pore volume of the soil
C_o = initial concentration of the reactive solute

And the remaining parameters are as defined before.

Similar solutions are also formulated by Wilson and Miller (1978). All of these solutions, however, are variations to (36) and differ in details that are actually overshadowed by empirical parameter measurement.

3.8 CASE STUDIES

To study the interaction between soils and organic chemicals, Law and Kunze (1966) examined the reactions between kaolinite and montmorolinite clays with three classes of organics: anionic (A), cationic (C), and nonionic or polar (N). Their observations indicated that, for kaolinite, absorption increased almost linearly with the amount of chemicals added to the soil. Kaolinite absorption was highest for "C" and lowest for "A" groups. X-ray diffraction did not indicate any lattice expansion for kaolinite. The presence of absorbed compounds in these tests was detected as exothermic peaks in differential thermograms, with the exothermic area under the curve representing the amount of organics present.

For montmorillonite soils, however, one or two layers of organic compounds were retained on the lattice depending on treatment rate. Both "C" and "A" groups were absorbed but no absorption with the "N" group was detected.

Law and Kunze (1966) conclude that

1. Anions are not strongly absorbed by soils. The absorbed part is released to the liquid phase upon wetting. The magnitude of absorption depends on the rate of treatment.
2. Cations are strongly absorbed by the soil exchange complex and not readily released upon rewetting. Soil hydrophobicity is increased by increasing the amounts of cationic substances added to the soil.
3. Nonionics are absorbed by hydrogen bonding, with their absorption energy being somewhat greater than that of water.

In another experiment, Doner and Mortland (1969) studied benzene-soil interactions. The results of their experiment indicated that a reaction was detected when Cu (II) montmorolinite through the electrons in orbitals of benzene which are capable of reacting with Cu (II) in Cu (II) montmorolinite.

Tests with tolulene, xylene, and chlorobenzene gave the same results; i.e., reaction with Cu (II) montmorolinite and no reaction with other cation montmorolinites.

3.9 BIODEGRADATION IN SOILS

Biodegradation is an important factor affecting the fate of organic waste in soil landfills. Microbial analysis has revealed that hydrocarbon-utilizing bacteria and fungi are present in unamended soil, making it a biochemically active body.

Biodegradation rates were determined in respirators in which soils were incubated at constant temperature. A continuous stream of Co free air was passed over the soil in the incubation flasks, and the evolved Co was collected from the air leaving each flask. The results indicated that the maximum rate was found for clay soils (Donelly and Brown, 1981).

Microorganisms were observed to be active in both aerobic and anaerobic conditions in solubilizing and oxidizing organic waste constituents. Usually aerobic microorganisms give way to anaerobics as oxygen is depleted (usually by increased depth). Anaerobic microorganisms may then generate significant amounts of gases, such as methane, hydrogen sulfide, and ammonia, that can cause odor and explosions (Overcash, 1982).

Studies with aromatic compounds in soils show that specific organisms that degrade benzene are present in soil in slight numbers and degradation in such cases takes place after a period of time when aromatics are added to soils.

The ability to degrade aromatic substances is not limited completely to benzene or to those compounds resulting from the degradation sequence, such as phenols. Rather, chlorinated derivatives of these compounds are more or less rapidly degraded by ring divisions.

The rate of biochemical degradation in soils has been suggested to depend upon the following factors:

1. Chemical composition of the membrane
2. Organic matter content of the soil
3. pH of the environment
4. Concentration of added compounds and previous application
5. Make-up: amount and type of clay, silt, sand, etc.
6. Moisture, pressure, and temperature environments
7. Structure, mineralogy, bulk density, and surface area of the solid part

An understanding of reactive chemicals migration in soils and the concept of biodegradation are important in this study from

1. Since the C/EOC essentially measures the presence of an organic in a soil matrix in a given space and time. It is essential to know what has happened to reactive organic chemical which was introduced to soils hydrogeological system at point x and time t. These questions may be partially explained by the material presented in Chapter 3.

2. The process of reaction between clay and the organic chemical constituents of its pore fluid may culminate in production of new odors which may mask, retard or enhance the monitoring capabilities of C/EOC. The same arguments hold for biodegradation in soils.

CHAPTER 4

HYDRAULIC CONDUCTIVITY

Hydraulic conductivity of a soil has been considered as a strong indication, and at times the sole factor, in predicting waste migration through soils. Measurement of this parameter is affected by several factors (Dunn and Mitchell, 1984), including:

1. Compaction method:
    a. Impact
    b. Kneading
    c. Static compaction

Tests (Dunn and Mitchell, 1984) show that at dry densities (both greater than and less than ASTM standards), the static compaction method produces samples with higher hydraulic conductivity than either kneading or impact method. On the wet of optimum, the degree of soil particle dispersion increases with level of shear strain induced by the compaction method. Static compaction induced the lowest level of shear strain (thus, higher isotropic hydraulic conductivity) than the other two methods.

2. Hydraulic gradient: In spite of Darcian flow laws which state that flow is independent of the hydraulic gradient, high gradients have been shown to induce migration of soil particles, resulting in clogging of the pore space and changing the hydraulic conductivity of the soil. Recent studies (Dunn and Mitchell, 1984; Hamidon, 1984; Forman and Daniel, 1986) indicate that hydraulic conductivity decreased with decreasing hydraulic gradients; such decreases were less in samples compacted to 95% of max dry density than those of 90% max dry density, because

the denser the sample, the fewer the number of particles available for migration. Additionally, the higher density soils would have less pore space available for particles to migrate through. Even though growth of microorganisms (pore blockage), dispersion of soil fabric by tap water are contributing factors to reductions of soil hydraulic conductivity, consolidation caused by changes in effective stress brought about by changes in the hydraulic gradient seems to be a strong influencing factor. Studies by Foreman and Daniel (1986) show the effect of hydraulic gradient on hydraulic conductivity to be dependent on type of permeant. Type of permeameter (rigid wall or flexible wall) type of soil, and the range of hydraulic gradients applied.

3. Saturation procedure: Back pressure and possibly vacuum application may lead to over-consolidation and change in hydraulic conductivity (Lee and Morrison, 1970).
4. Sample consolidation: If back pressure is applied too rapidly, or too large increments of it are applied, parts of the sample may be over-consolidated. If the sample is not later consolidated to an effective stress higher than that felt by any part of the sample during back pressure, measurements of hydraulic conductivity are in error.
5. Thixothropic effects: Increasing curing time between sample preparation and the start of test results in higher hydraulic conductivity (Dunn and Mitchell, 1984). Apparently with time, the fabric tends toward an increased degree of flocculation than that created by compaction, and thus the effective pore

diameter increases in size. Failure to cure test samples for sufficient periods could result in lower values of hydraulic conductivity being measured in the lab than in the field.

6. Type of permeameter (Daniel, 1984): Hydraulic conductivity was measured in compaction mold, a fixed-wall (cell) permeameter, and a flexible wall permeameter. Test results show:

   a. At hydraulic gradients greater than 150, kaolinite has a higher hydraulic conductivity to methanol than to water (roughly twice) for both flexible-wall and fixed-wall permeameters, results of tests from flexible and rigid-wall permeameters were similar for methanol and water.

   b. On the average, compaction-mold devices showed kaolinite to be approximately 10 times more permeable to methanol than to water. Side leakage might have contributed to high values of hydraulic conductivity.

   c. With flexible permeameters, hydraulic gradients appear to have little effect on hydraulic conductivity for gradients between 50-300.

   d. With a fixed-wall (consolidation cell) permeameter, hydraulic gradient appears to have a very substantial effect on hydraulic conductivity, k. At a gradient of 50, $k_{methanol} = \frac{1}{2}k_{water}$, but at gradient of 200-300, $k_{methanol} = 2k_{water}$. One possible explanation for low values of k at low gradients for methanol is that the pressure head at these gradients is not large enough to cause full saturation of the soil. As methanol flows through soil, the pressure drops and any gas dissolved in

methanol beyond the solubility limit at the reduced pressure would be released because the solubility of air in methanol is approximately 10 times the solubility of air in water. The opportunity for release of gas from solution is much greater with methanol than with water.

e. The high back pressure used with the flexible-wall permeameter probably prevents the formation of any significant volume of gas and the phenomenon in (d) will not take place.

f. A compaction mold permeameter seems to indicate an increasing hydraulic gradient, causing an increase in the hydraulic conductivity of kaolinite to both water and methanol.

7. Type of permeant fluid: If the permeability of a soil to water is known, the viscosity to density ratio (μ/γ), of a permeant usually indicates the percent of increase in permeability over values obtained for water (Anderson and Brown, 1982). With reactive permeants, however, this did not hold. With acetone (μ/γ=2.4), for example, increases as much as 1000% in permeability over that of water were observed. This deviation may be explained in the following manner. The high dipole moment of acetone (2.74 debys) may cause initial increases in interlayer spacing between adjacent clay particles as compared with water alone. As more acetone is passed through the soil cores, however, more water layers are removed from clay surfaces, resulting in gaps not completely filled by absorbed acetone layer, making more pore space available for fluid flow. The

inability of acetone to form as many absorbed fluid layers on soil as water comes from its lower dielectric constant (D = 21.4).

For acetone concentrations greater than 75%, an increase in hydraulic conductivity was observed. The lower concentrations (12.5% and 25%) of acetone apparently have a lower k than water, suggesting that low concentrations of acetone may cause dispersion and swelling while high concentrations may result in flocculation and shrinkage. In addition there may be an interaction between low concentrations of acetone and the water layers on mineral surfaces, resulting in an alignment of carboxyl groups towards the mineral surface and the methyl groups (hydrophobic in nature) towards the pore wall. This alignment could result in a decrease in effective pore diameter at low concentrations of acetone.

The higher hydraulic conductivity of soil (clay) to polar organics generally diminishes as the organics are diluted with water, such that mixtures of over 50% water behave like water. The higher hydraulic conductivity to polar organics may be the result of organic moving through preferential channels. The channels are probably created when chemicals displace water and dessicate the clays, thus causing them to shrink and crack. Cracks, however, may also result from syneresis. Syneresis is a chemical reaction that causes shrinkage and dewatering in a colloidal material due to the aggregation of particles by physicochemical attraction. Syneresis cracks are formed as the samples shrink.

Testing for acetic acid has indicated (Brown et al., 1984) an initial decrease in hydraulic conductivity, which may be due to partial dissolution and subsequent migration and settling in the pores of soil particles. But, generally, soil-dissolving agents eventually cause an increase in permeability by eating soil away, so that piping becomes the predominant factor in permeability changes (Brown et al, 1984).

When montmorolinite was solvated with water-organic mixtures from 0-100%, several distinct types of behavior were observed as the proportions of organics increased (Griffin et al., 1984):

I. Osmotic swelling and dispersion

II. Swelling to a greater degree with water

III. Little or no change in swelling for parts of the mixture range

IV. Progressive collapse to about d-spacing with pure organics (acetone and ethanol)

V. Development of mixed-layer or poorly defined complexes

Also at low applied back pressure, there was an increase in void ratio with increasing dielectric constant of the permeating fluid for montmorolinite, whereas the opposite effect was observed for kaolinite. Also, the equilibrium void ratio at a particular pressure decreased as the dielectric constant of the pore fluid increased for kaolinite. The opposite behavior was observed for montmorolinite.

At low values of dielectric constant for the pore fluid both montmorolinite and kaolinite had nearly the same magnitude of

rebound. The results revealed that the rebound behavior was primarily controlled by the double layer repulsive forces for montmorolinite and elastic rebound and hydrostatic pressure deficiency for kaolinite.

Acetone and ethanol caused relative expansion of montmorolinite, followed by a step-wise collapse to a spacing less than that for water (19A). Methanol addition, however, led to a stable spacing of about 19A up to about 50% mole, followed by a sudden collapse to about 17A from 50-100% mole. Griffin et al. (1989) report that acetone and ethanol caused relative expansion of the clay, followed by a progressive stepwise collapse to a spacing of about 19A up to about 50% mole, followed by a sudden collapse to 17A from 50-100% mole.

Permeability is influenced by the thickness of the double layer as expressed by (Mitchell, J.K., 1976):

$$1/k = \sqrt{\frac{DkT}{8\pi\eta_o\varepsilon^2 r^2}} \qquad (4.1)$$

Where η_o = Ion Concentration

V_i = Ionic Valance

D = Dielectric Constant of the Medium

ε = Unit Electrical Charge

k = Boltzman's constant

Organics with high dipole moments (acetone for example), which can easily displace water, cannot form as many layers of adsorbed fluid on soil (double layer) as water can (due to the low dielectric constant of acetone). Thus, the permeability of clay to acetone will be affected in two different directions.

In addition, soil dissolution and subsequent migration and setting in the pores of soil particles by organic acids (like acitic acid) may result in initial increases in permeability, but such permeants finally render the soil more permeable than "neutral" permeants like water.

Volume change, void ratio, and hydraulic conductivity: volume changes brought about by either external forces (changes in water table and leaching action) or by expansion or contraction of interlayer water when replaced by a fluid of different dipole. The surface-bond layers of water are held strongly by clay. They, however, represent only a part of the interlayer water. The water layers farther from the clay surfaces are held in place by hydrogen bonds. The hydrogen bonded water extends back to the structured water layers anchored to the clay surfaces. These outer layers of water would easily be displaced by an intruding fluid. If the replacing fluid lacks water's large dipole moment or its ability to form a hydrogen bond, a decrease in interlaying spacing would probably result, as fewer layers of organic molecules would be retained.

If the intruding fluid has a higher affinity for the clay surface then the structured surface layers of water, large decreases in interlayer spacing would be possible.

When permeating kaolinite with a host of organics of varying dipole moment and dielectric constant, Sridharan and Rao (1973) observed that:

1. With the exception of acetone, the e - p curve for fluids with low dielectric constant shows higher equilibrium void ratios. When compared with other fluids, acetone has a relatively higher dipole moment and this may be the reason for the deviation of e - p curves of acetone from the observed norm.

2. At low applied external pressures, there was a decrease in void ratio with increasing dielectric constant. The reverse effect was observed for higher external pressures.
3. In one dimensional consolidation test, the equilibrium void ratio at a particular pressure decreased as the dielectric constant of the pore medium increased.
4. The interaction between low concentrations of polar organics and water layers of the clay mineral surfaces may result in an alignment of the carboxyl group towards the mineral surface and the hydrophobic methyl groups towards the pore wall. This alignment could result in a decrease in effective pore diameter and a subsequent decrease in hydraulic conductivity of the soil (Brown, Thomas, and Green, 1984).

A note on variations of γ/d ratio during permeation: The viscosity-to-density ratio of a nonpolar permeant is presumed to provide reasonable approximations of the hydraulic conductivity increases over those due to water.

An important fact which is usually overlooked is that in migration through soils, the guest permeant finds it easier to mix with the free water than to replace the adsorbed water of the double layer. This mixing results in a weak permeating front whose density and viscosity are variables in time and space and consequently should not be treated as constant values. This translates to fluctuations in the viscosity to density (γ/D ratios due to dilution that may not be monotonic with dilution, but may provide an explanation for the variation of hydraulic conductivity above and below those values due to water.

CHAPTER 5

LABORATORY TESTING: PHASE I

5.1 INTRODUCTION

Laboratory experiments were designed to verify the ability of EOC as a hazardous waste monitoring device. This verification followed the steps outlined in the flow chart diagram of Figure 5.1.

The laboratory experiments were carried out in two phases. Phase one was the broad testing of all the chemicals of interest and all the available types of membranes. The objectives of this phase were:

a. To understand the factors affecting the EOC response (and to estimate the magnitude of influence of each factor on EOC response)

b. To support theoretical predictions of EOC response to contaminants

c. To detect any design deficiencies of the EOC and modify the design to remedy such deficiencies.

d. To select the membranes most responsive to a chemical or a host of chemicals

e. To understand selective detection, where a membrane responds to only one chemical from among a group

Phase I was conducted in ambient conditions, where the EOC was exposed to organic vapor, and the response was monitored and recorded.

The data acquisition/control/reduction system consists of an HP data acquisition, an HP-85 computer, an HP open plotter. Software was developed such that data was collected on specified time intervals,

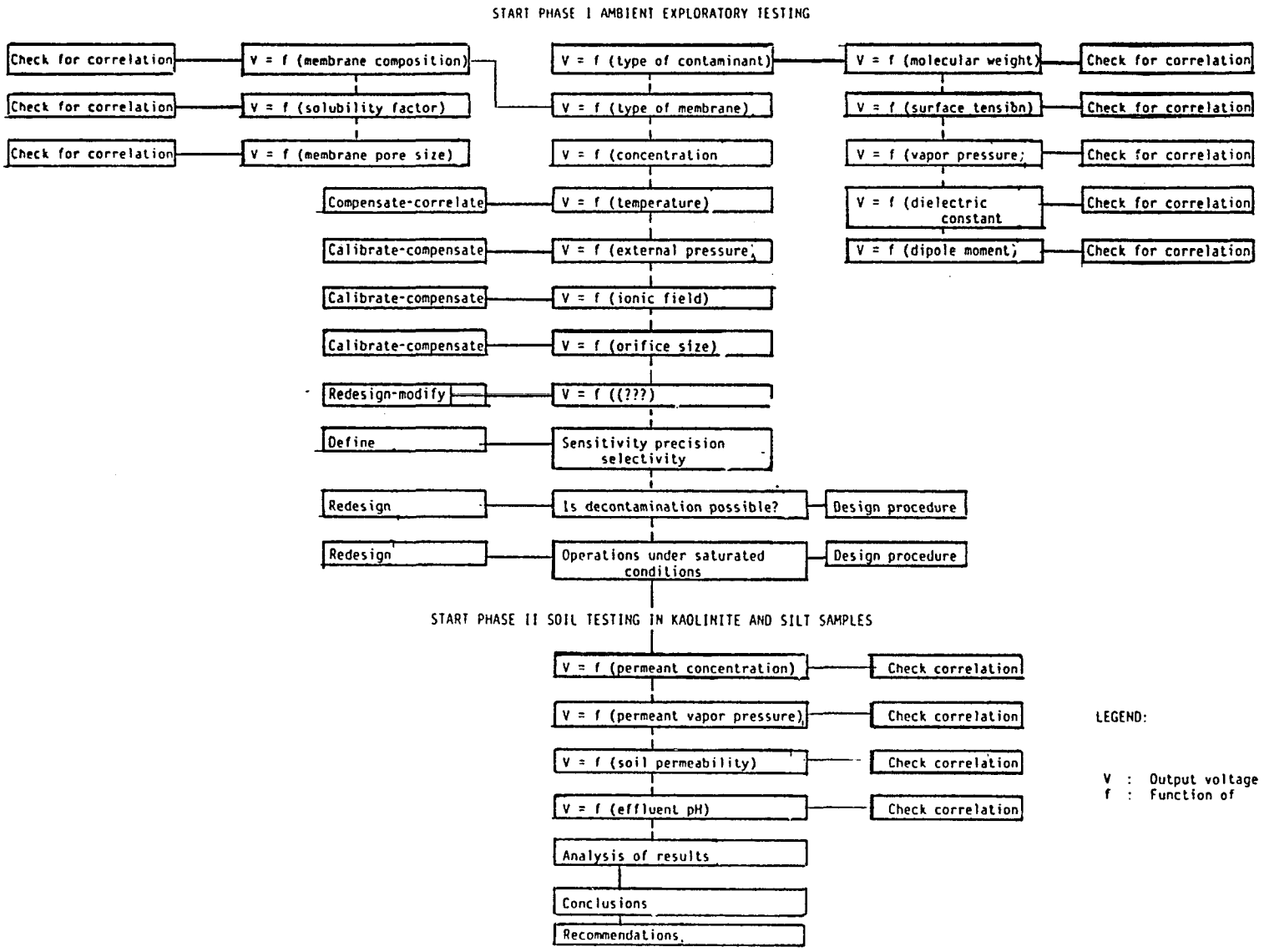

Figure 5.1. Methodological flow chart diagram.

recorded into a permanent file (disk), for later reduction (plotting, correlation, and manipulation).

In the second phase, or soil testing phase, the design replicated the field condition in which the cone is pushed into a soil layer permeated with organic contaminants. A special triaxial testing apparatus with a hollow inside cylinder was designed. The C/EOC was placed in this cavity. After saturation with water, the soil sample was permeated with desired organics. The organic chemicals migrated through the soil and reached the C/EOC through the inlets at the lower half of the cylindrical cavity.

The C/EOC output voltage was monitored throughout the permeation period. Tests were repeated for selected organics and soils at different concentration levels. The detailed procedures and results follow.

5.2 MEMBRANES

As mentioned in Chapter 2, membranes form the reactive component of EOC. Membranes are restrictive barriers which influence the transport and exchange of matter by diffusion, osmosis, or otherwise of various molecular and ionic species contained in the two compartments separated by the membrane. By virtue of being barriers, the membranes act as physicochemical machines which regulate the flow of the energetic processes that occur across their thickness. In doing so, they transform various forms of energy into others; for instance, osmotic energy into mechanical work or into electrical energy.

The membranes used in these tests were porous by virtue of their functional expectation. They acted as sieves that screened out the various species of solute particles according to their different size, and in the case of ions, according to the sign and magnitude of their

charge. They also acted as collection surfaces for contaminant molecules.

Polymer membranes are inherently insulators. Their composition, however, is adjusted to permit some conductivity. This conductivity does not arise from the polymer per se, but results from the inclusion of a second conducting phase. These can be in the form of atomic nuclei, electrons, and polar groups.

The charges that form the movable part of the electric double layer at the pore wall/solution interface are attached firmly to the membrane's pore walls. They are unable to move and thus do not participate in the transportation of electricity. The counter ions of the fixed-wall charges are dissociated off into the liquid in the pores. They are freely movable and therefore able to participate in the transportation of electricity, the current being transported across the membrane by these ions and whatever other electrolytes that may be present in the pores. Therefore movable counter ions of the fixed-wall charges are the vehicle for a larger and larger fraction of the virtual transportation of electricity in the membrane as it decreases in porosity.

Membrane filters can be classified as a function of their surface energy as either hydrophobic or hydrophilic. Hydrophilic membranes are thought to be wettable spontaneously with pure water (surface tension approximately 72 dynes/cm^2 at ambient conditions).

Hydrophobic membranes require some elevated pressure to allow water to intrude into the pores of the structure. Solvents, or mixtures which possess a relatively low surface tension, can wet hydrophobic membranes spontaneously. Hydrophobic membranes allow the passage of vapors but prevent the passage of aqueous solutions below the intrusion pressure of the membrane.

Membranes can also be classified according to the following parameters:

1. Pore size: ranges from 0.025 to 10 μm
2. Porosity: most of the membranes have a porosity of about 70%
3. Absolute surface retention: When liquids or gases are passed through the membrane filters, all particles larger than membrane pore size are retained on the surface. When dry gases are passed through a membrane, particles of smaller diameter than the rated pore size are retained due to the high electrostatic charge built up on the filter surface.
4. Thickness: may vary between 170 to 190 μm.
5. Solubility and chemical resistance: The membranes are chemically resistant to some organic chemical and chemically reactive with others; more on this subject follows. charts provide such information as whether a membrane is reactive with a certain chemical.
6. Surface chemistry: the matter from which a membrane is made has an effect on its participation in chemisorption reactions with the organic chemicals. The following section provides more information on membrane composition.

5.2.I MEMBRANE TYPES: Membranes in this experiment are presented below identified by their trade name, chemical composition, and physico-chemical characteristics:

1. Durapore: Polyvinylidene fluride

   Pore size 0.2 and 0.45 μm

   Maximum operating temperature 126°C

   Chemical resistance similar to teflon

2. Mf-Millipore: Composed of pure biologically inert mixtures of cellulose acetate and cellulose nitrate

   Hydrophilic

   Pore size 0.22 μm

   Compatible with dilute acids and bases, aliphatic and aromatic hydrocarbons, and nonpolar liquids

   Maximum operating temperature 75°C

3. Celotate: Made of pure acetate

   Hydrophilic

   Pore size 0.2 μm

   Breakable

   Compatible with dilute acids and alkalines, aliphatic and aromatic hydrocarbons, nonpolar liquids, and lower molecular weight alcohols such as ethanol and methanol

4. AE-91 & AE95/7: Made of nitrocellulose

   Has very high wet strength (800 bars/cm)

   Hydrophilic

   Pore size 0.45 μm

   Maximum operating temperature 125

   The relative quantities of the elements found in the membrane are:

   Na>Ca>Mg>Si>Al>Cu>Zn>Fe>Mn

5. TE 30, 35, 36, 37: Made of polytetrafluorethylene which is laminated to inert, nonwoven polyprolene

   Hydrophilic

   Pore size 30 (.02 μm), 35 (.2 μm), 36 (.5 μm), 37 (1.0 μm)

   Compatible to all the chemicals used

6. GA-Metricel: Composed of cellulose triacetate

   Hydrophilic and hydrophobic

   Pore size .2 μm (GA-8), .8 μm (GA-1)

7. TCM-Metricel: Is identical to type GA except it is made without the wetting agent

   Hydrophobic

   Pore size .2 μm

   Chemical resistance similar to GA-Metricel

8. Versapore: Is a highly microporous membrane composed of an acrylic copolymer cast in a nonwoven nylon sulfate

   Hydrophobic and hydrophilic

   Pore size V200 (0.2 μm), V450 (.45 μm), V800 (.8 μm)

   Maximum operating temperature 88°C

   Resistant to most of the organic chemicals, resistant to low concentration of acetic acid, and nonresistant to acetone and phenol

9. RC-59: Regenerated cellulose

10. Teflon-200: Polytetra flueoroethylene (PTFE)

11. MITEX.10μ: PTFE

12. HT-200: Aromatic polymer

13. ST-68: Cellulose acetote

14. Nuclepore:

Membranes 1-6 are from Millipore Co., Bedford, Mass.; and 7-13 are from Gelman Co., Ann Arbor, Mich.

5.2.II MEMBRANE MATERIAL

The membranes used in this experiment were made of one or more of the following polymers:

1. Cellulose Acetate (ST-58 Membranes)

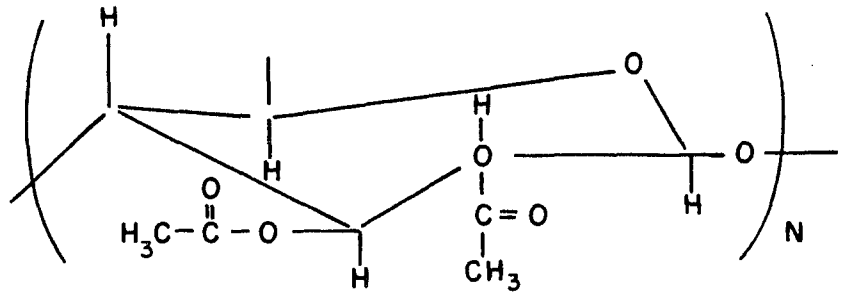

This is the ester of cellulose and acetic acid. A cellulose acetate-acetone system is characterized by an endothermic dilution when the polymer content is low, while the dilution of concentrated solution is highly exothermic. This behavior may be related to the tendency of cellulose acetate to form a molecular complex with acetone, which has been observed as a distinct crystalline phase (Katz and Weidinger, 1932).

2. Cellulose Triacetate (GA & TCM Membranes): This polymer is prepared by the reaction of cellulose with acetic acid and acetic anhydride in the presence of sulfuric acid and basically reacts like cellulose acetate. Acetic acid reacts with this polymer to provide cellulose; acetone, however, attacks the polymer structure with a subsequent swelling or dissolvation.

3. Cellulose Nitrate (AE & BA Membranes)

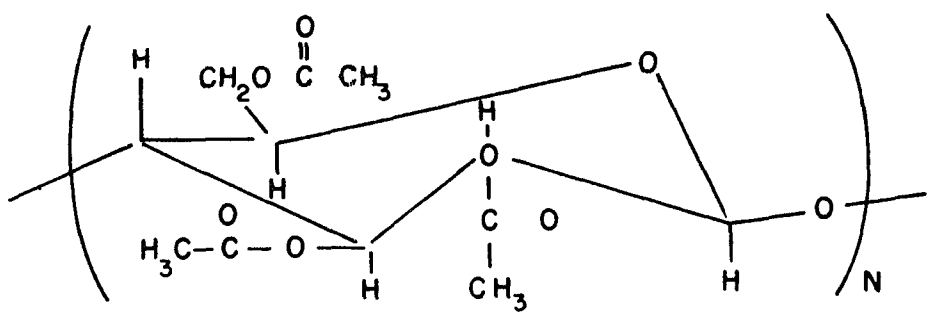

This polymer is obtained by the reaction of nitric acid and sulfuric acid with cellulose. The product is certified as primary, secondary, or tertiary according to how many groups in each repeating anhydroglucose unit in cellulose are nitrated. Type of hydrogen bonding (strong -- poor) is important in determining a usable value for studying the solubility of nitro-cellulose in organic solvents. It may be soluble in glacial acetic acid and alcohol. The solubility varies according to the percent of nitrogen in the polymer. The higher N% the more insoluble the polymer.

Table 5.1 provides the properties of the membranes used in the preliminary experiments. This table is extracted from membrane manufacturers' technical data and literature. The membranes selection lends itself to a factorial design of the experiment with factors of variation being membrane pore size, membrane composition, and membrane reactivity, with a particular organic chemical.

5.3 CHEMICAL SELECTION

Organic chemicals tested in this experiment were selected from the list of organics most frequently used by researchers studying leachate migration through landfills and those studying the effects of different chemicals on hydraulic conductivity of clay liners. Chemicals were selected to cover a range of physical and chemical properties. The initial list included acetone, acetic acid, benzene, dichloromethane, ethanol, ethylene glycol, n-hexane, methanol, phenol, and xylene.

Preliminary testing revealed that low vapor pressure chemicals including xylene, phenol, n-hexane, ethylene glycol, and benzene, did not indicate significant output with most membranes and were not used in later testing.

Detailed experimentation was conducted with the chemicals listed in Table 5.1.

TABLE 5.1. PROPERTIES OF CHEMICALS USED IN PRELIMINARY EXPERIMENTS

COMPOUND	FORMULA	DIELECTRIC CONSTANT	DIPOLE MOMENT (DEBYES)	VAPOR PRESSURE (mmHg)	SURFACE TENSION (Dyne/cm^2)	SOLUBILITY (gr/e)		
						WATER	ALCOHOL	ACETONE
WATER	H_2O	80.4	1.83	28	72.7	∞	∞	∞
ACETONE	C_3H_6O	20.7	2.90	184.8	23.7	∞	∞	∞
METHANOL	CH_4O	33.62	1.66	96	22.6	∞	∞	∞
ETHANOL	C_2H_6O	24.3	1.69	66	22.3	∞	∞	∞
DICHLOROMETHANE	CH_2cl_2	6.1	1.74	11.8	26.5	8.08	∞	∞
ETHYLENE GLYCOL	$C_2H_6O_2$	38.66	2.28	1	47.7	∞	∞	∞

These chemicals cover

(A) A range of vapor pressure from 2 to 400

(B) A range of surface tension from 22.3 to 47.7 Dyne/cm

(C) A range of dielectric constants from 6.1 to 38.7

(D) A range of dipole moments from 1.66 to 2.28 Debyes

(E) With the exception of Dichloromethane the rest of the chemicals are infinitely soluble in water, alcohol and acetone.

The experiment was a factorial experiment with factors M and D representing membrane type and organic chemical, respectively. The experimental sample space included M_i D_j samples (tests) for i is the number of membranes equal to 117 and j=number of organic chemicals used. Under this design a total of 114 test were considered.

Every membrane was exposed to an organic chemical contaminant in a set-up similar to that of Figure 5.2. The output voltage was continuously

monitored for 180 seconds. At this time the source of contamination was discontinued and the EOC was left in ambient conditions to desorb. During desorption the output voltage normally reversed itself from previously increasing trend (adsorption) and occasionally it was stabilized at the starting value of zero within 220 seconds after the source of contamination was removed.

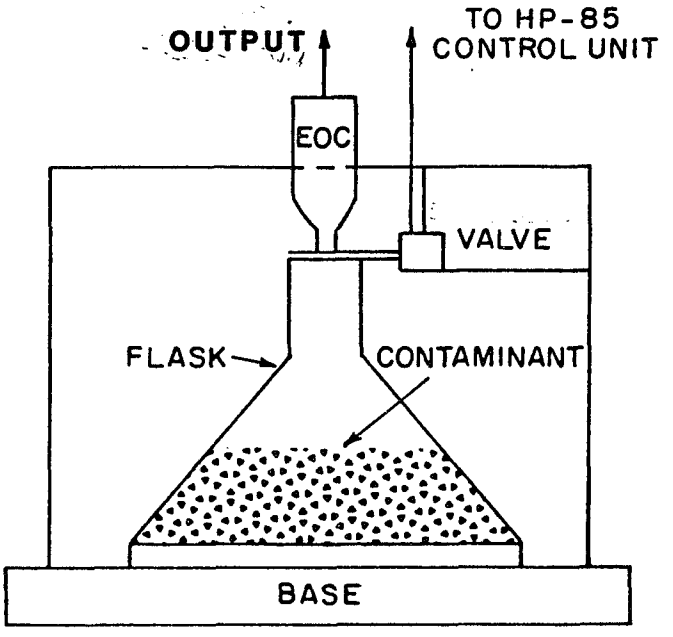

Figure 5.2. Test set up for preliminary laboratory experiments.

For the cases where voltage dissipation was slow and complete desorption could not be achieved within 220 seconds after removal of source of contamination, EOC was purged with an inert decontaminant such as freon-12. Once a stable zero voltage (datum) was established the same procedure was repeated for each organic chemical. All membranes

were tested in the same manner. Most experiments were conducted at least twice to check the repeatability of EOC response.

Table 5.2 provides a summary of the test results. Shown in this table are time rates of change of voltage for both adsorption (dv/dt) and desorption (-dv/dt) process.

These numbers are direct measurements from output voltage vs. time plots for each organic chemical-membrane combination. These plots are shown in Figures 5.3a through 5.3p. Each figure includes the voltage vs. time plots for a specific membrane and six organic chemicals. Visual inspection of these figures provides an indication of membranes best suited for detection of an organic. It is the membrane that yields high dv/dt during adsorption and its voltage dissipates rapidly during "desorption" with a given contaminant, with the emphasis being on the adsorption response of the membrane.

Table 5.3 provides a summary for such cases where the output is significant (i.e., dv/dt > 10 m volts/sec). These combinations will produce better detection limits and are recommended for use in EOC. Detail analysis of these results is forthcoming.

5.4 SOLUBILITY TESTING

Most polymers occurring in nature or synthesized in the laboratory are soluble under some conditions. Insoluble polymers are cross-linked structures and a few highly crystalline materials such as teflon.

Membrane manufacturers provide a chart of chemical compatibility (similar to Table 5.2) with their product. These charts can provide an idea about the solubility of a membrane in a certain chemical.

TABLE 5.2. SUMMARY OF TEST RESULTS

	ACETONE			METHANOL			ETHANOL			D.C.M.			ACETIC ACID			ETHELYENE GLYCOL		
CHEMICAL MEMBRANE	dv/dt	-dv/dt	max	dv/dt	-dv/dt	max	dv/dt	-dv/dt	max	dv/dt	-dv/dt	max	dv/dt	-dv/dt	max	dv/dt	-dv/dt	max
NUCLEPORE-1.0	0.48	-0.1	0.08	27	17	4.1	0.8	0.5	0.14	0.47	0.05	0	8.2	6.1	1.4	0.04	-0.2	0.05
NUCLEPORE-8.0	0.2	-0.01	0.04	1.5	0.3	0.11	0.09	-0.09	0.021	0.05	-0.07	0.03	0.07	-0.11	0.06	0.44	0.08	0.04
MF-MILLIPORE	26.3	18.3	4.34	19.2	13.2	3.1	0.02	0.15	0.03	43.4	34	7.5	-0.1	-0.5	0.15	-0.4	-0.07	0.44
MITEX, 10μ	0	0.2	-.1	1.4	0.8	0.24	0.12	0.1	0.06	2.1	2.7	0.4	0	0	0	0.4	-0.8	0.17
CELOTATE, 0.2μ	0.6	0.3	0.13	2.9	1.8	0.5	3.7	0.2	0.1	0.43	-0.3	0.14	1.2	0.8	0.2	0.1	-0.02	0.02
DURAPORE, 0.45μ	0.2	0.3	0.08	30.5	22.3	5.2	0.3	0.2	0.1	1.5	1.1	0.3	0.5	0.14	0.11	-0.01	0.2	0.06
BA85/7, 0.45μ	54.0	36.3	8.14	9.98	6.8	1.7	2.3	1.1	0.4	47.3	22	6.0	-0.5	-0.06	0	-0.9	-0.07	0
PN20 (NPLC)	33.4	14.0	5.5	47.5	10.2	8.1	1.6	-9.5	2.4	26.4	14.4	3.09	+0.09	-0.06	0.6	0.09	-1.2	0.3
ST68, 0.8μ	0.09	0.02	0.04	2.5	1.2	0.46	0.05	0	0.03	3.5	2.0	0.6	0.03	0.02	0.03	0	-0.2	0.09
RC59, 0.6μ	2.34	0.42	0.34	23.6	27.8	3.8	8.6	1.6	1.4	-0.8	-0.7	0.03	7.2	-12.5	4.01	1.8	-2.3	0.6
AE-91	48.8	10.9	8.03	27.7	23.6	5.1	27	26.7	5.3	1.9	1.2	0.32	1.8	-0.6	0.45	0	0	0
AE9517,1.2μ	16.3	12	2.7	15.9	10.9	2.5	0.33	0.36	0.06	10.6	7.5	1.7	1.09	0.8	0.24	-0.31	-0.31	0
TE 30	-0.7	0.4	0.37	5.5	3.8	0.91	-0.11	0.1	0.02	-0.7	0.3	0.1	0.08	-0.1	0.05	-0.75	-0.4	0.03
TEFLON-200	1.5	0.9	0.23	0.38	0.2	0.1	0	0	0	0.3	0.2	0.09	0	0	0.05	0	0	0
GA-8	28.1	24.4	5.8	-0.8	0.7	0.33	-0.15	0.9	0.3	45	17	7.1	-1.3	1.7	0.2	0.3	-2.5	0.6
VERSAPORE-800	49.6	18	8.07	49.8	17.6	8.1	45.4	16.5	7.8	51.0	9.8	8.3	45.8	6.0	7.5	2.2	-14.4	3.7
VERSAPORE-200	46.7	24.7	7.8	45.9	19	7.5	39.0	16.8	6.4	51	14	8.3	39	5.2	6.4	1.45	-8.2	2.2
HT-200	49.9	7.4	8.2	51.8	7.4	8.3	38.5	-2.3	6.3	50.7	8.3	8.1	1.2	-15.8	3.9	0.46	-7.9	1.95
TCM-200	18	13.3	3.1	26	19.6	4.5	1.3	0.9	0.23	11.72	8.2	1.9	-0.05	-0.03	0.02	-0.18	-0.13	0.07

$\frac{dv}{dt}$ = rate of absorption (mv/sec)

$-\frac{dv}{dt}$ = rate of desorption (mv/sec)

max = maximum output voltage (volts)

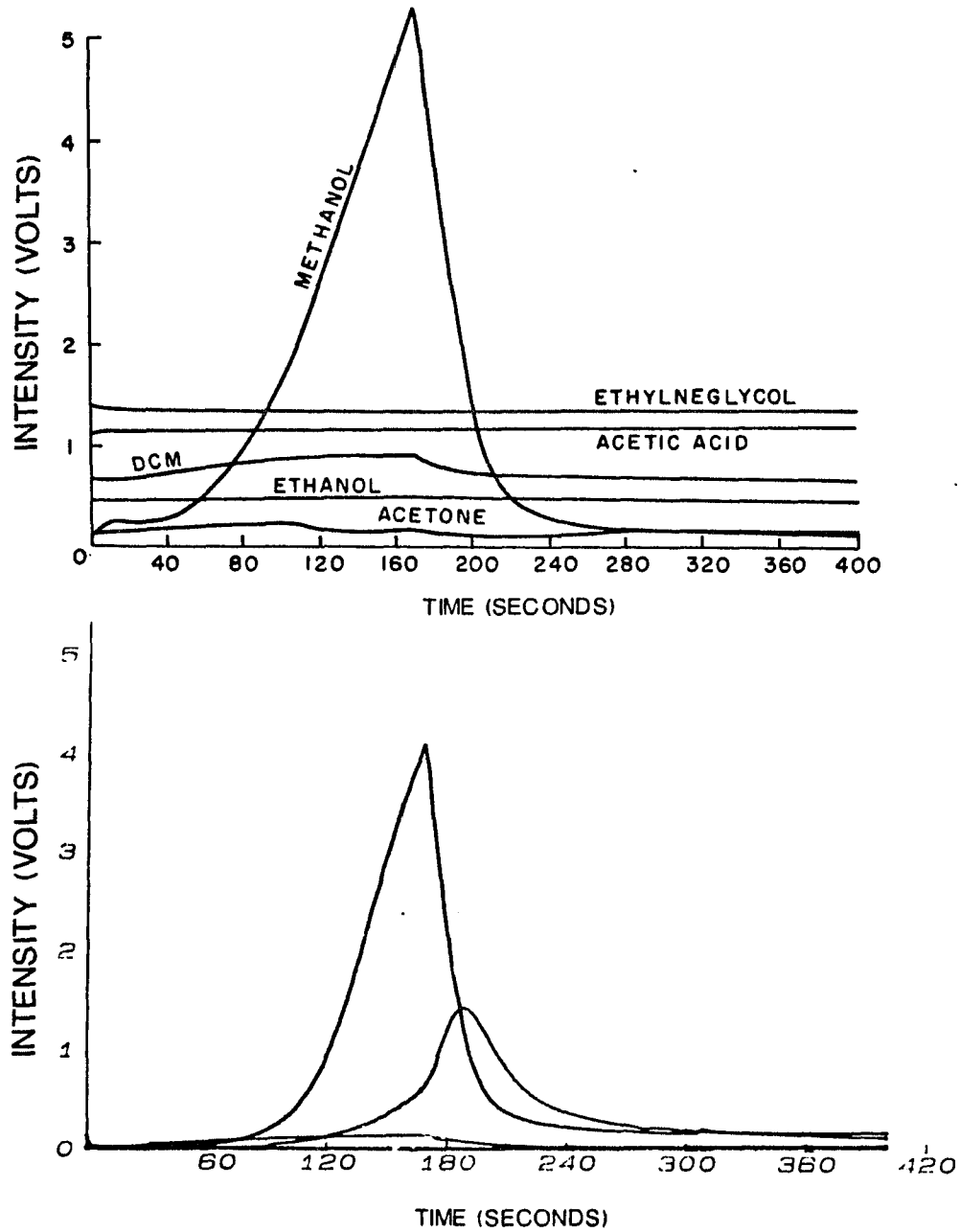

Figure 5.3. Plots of voltage vs. time for preliminary EOC testing.

a. Membrane is durapore 0.45

b. Membrane is nuclepore 1.0

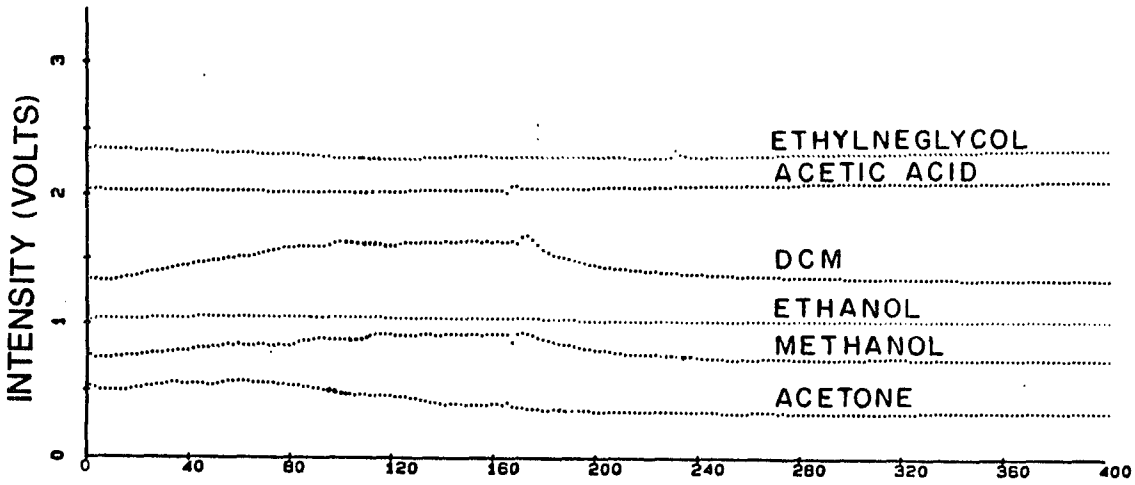

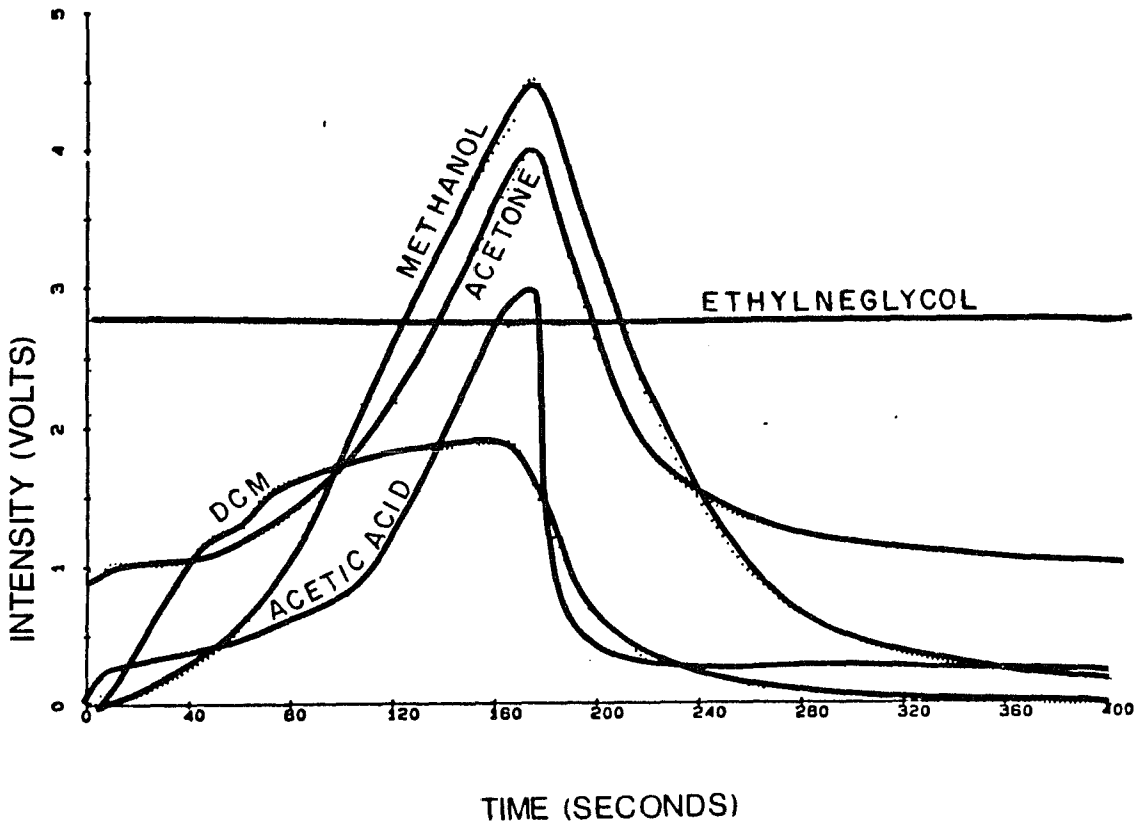

Figure 5.3.c. Membrane is mitex-10.

Figure 5.3.d. Membrane is GA-8.

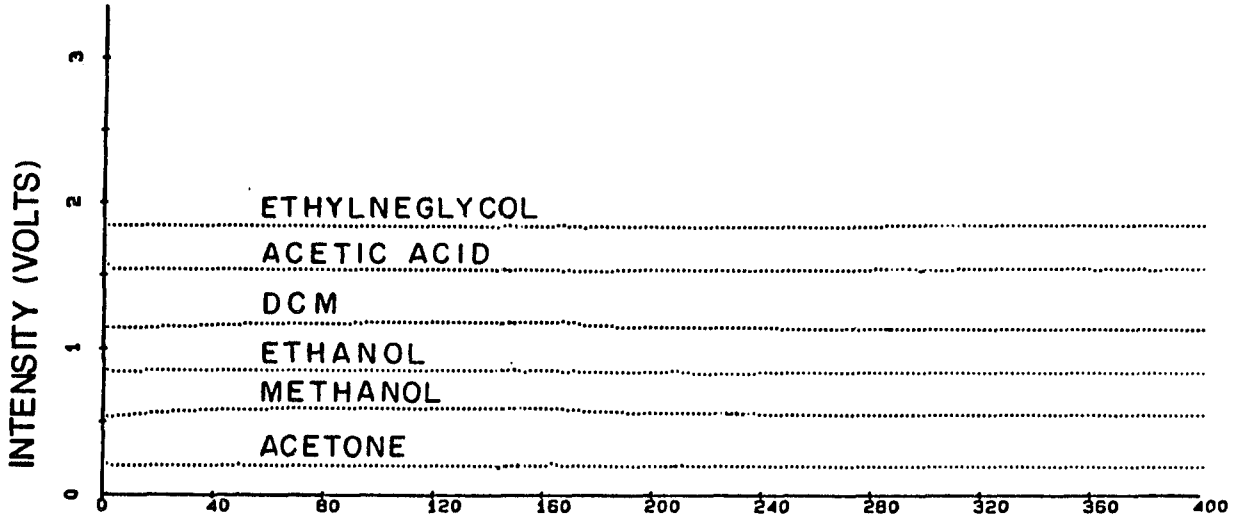

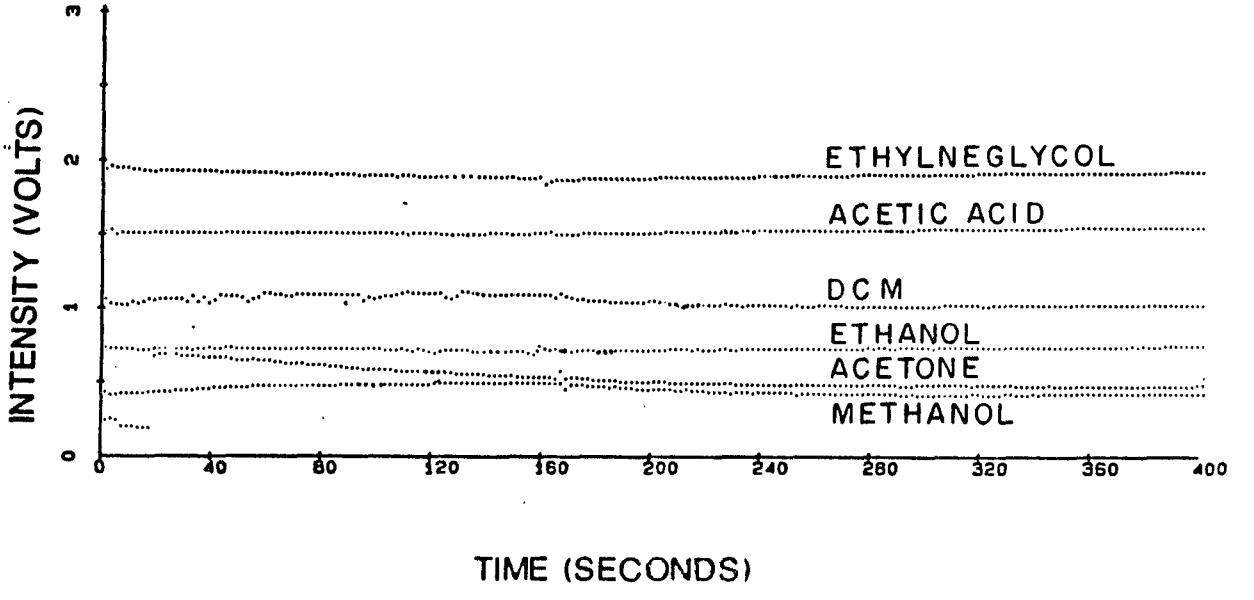

Figure 5.3.e. Membrane is teflon-200.

Figure 5.3.f. Membrane is TE-30.

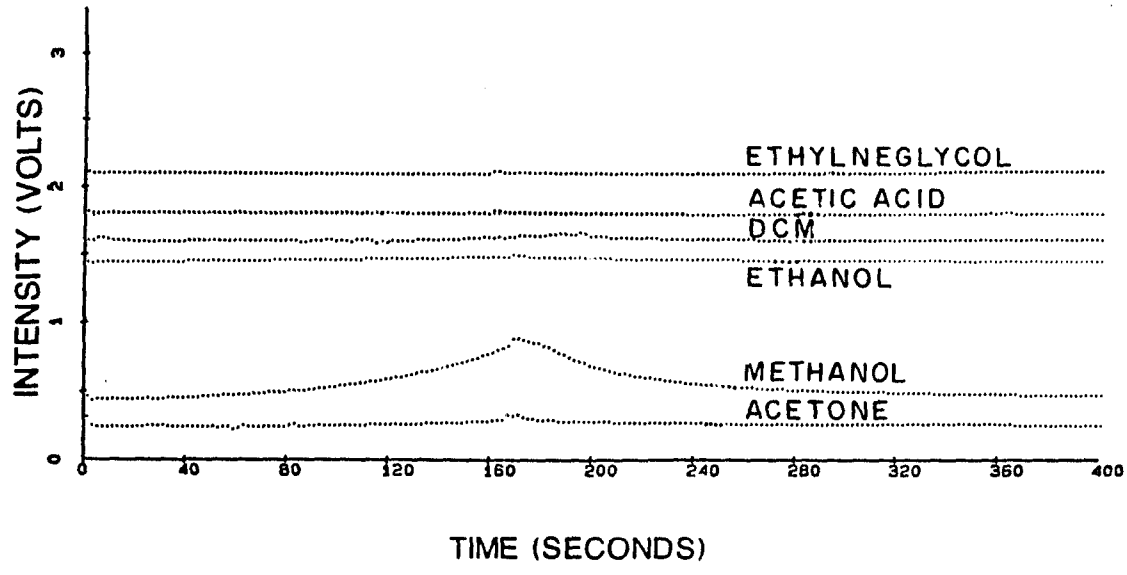

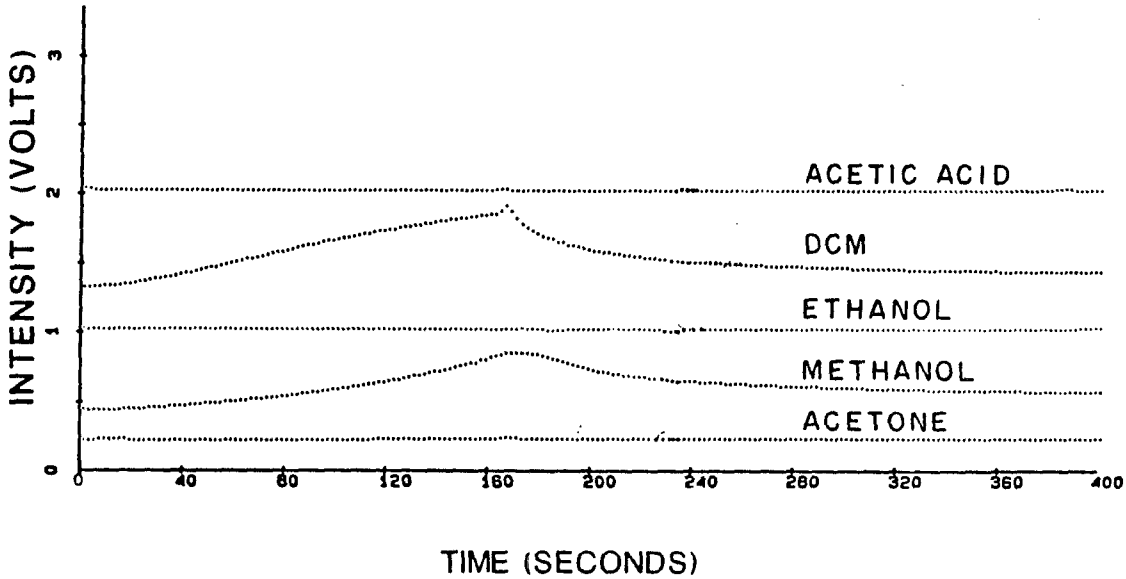

Figure 5.3.g. Membrane is celotate - 0.2.

Figure 5.3.h. Membrane is 51-68 - 0.8.

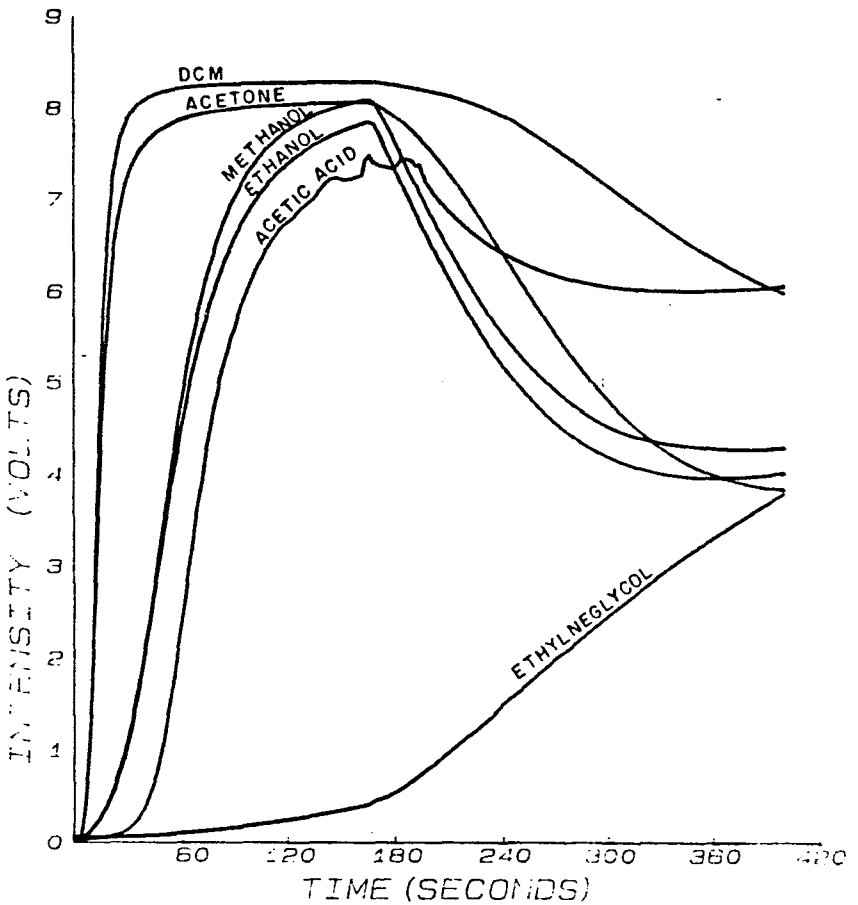

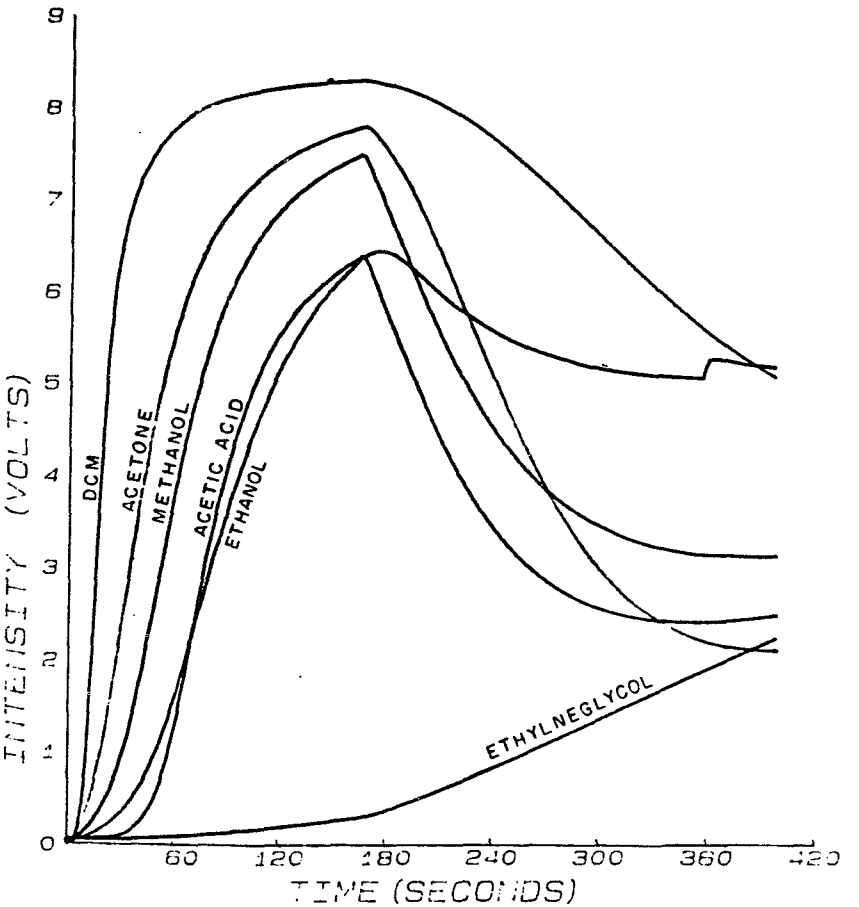

Figure 5.3.i. Membrane is versapore 800.

Figure 5.3.j. Membrane is versapore 200.

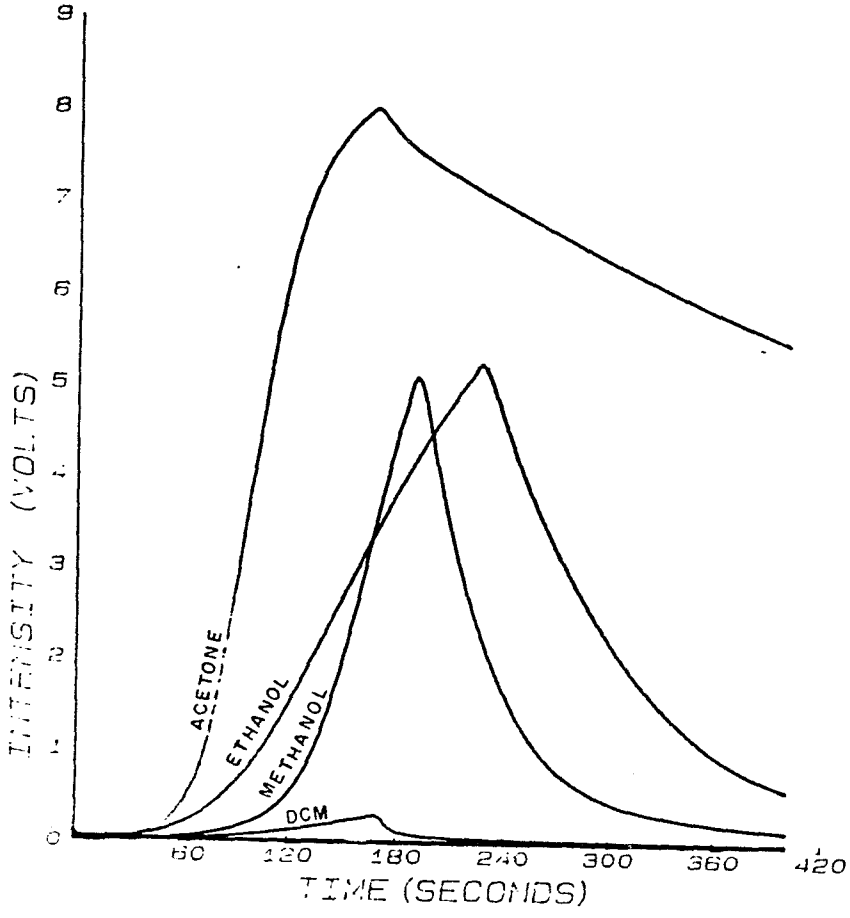

Figure 5.3.k. Membrane is AE-95.

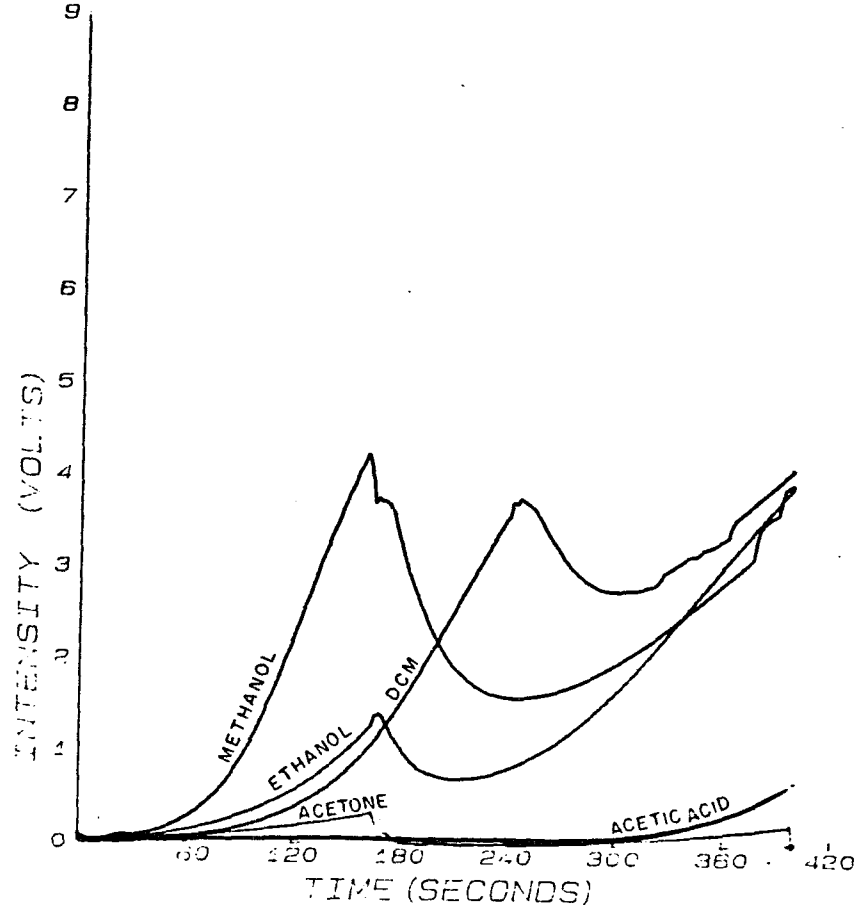

Figure 5.3.l. Membrane is RC69 - 0.6.

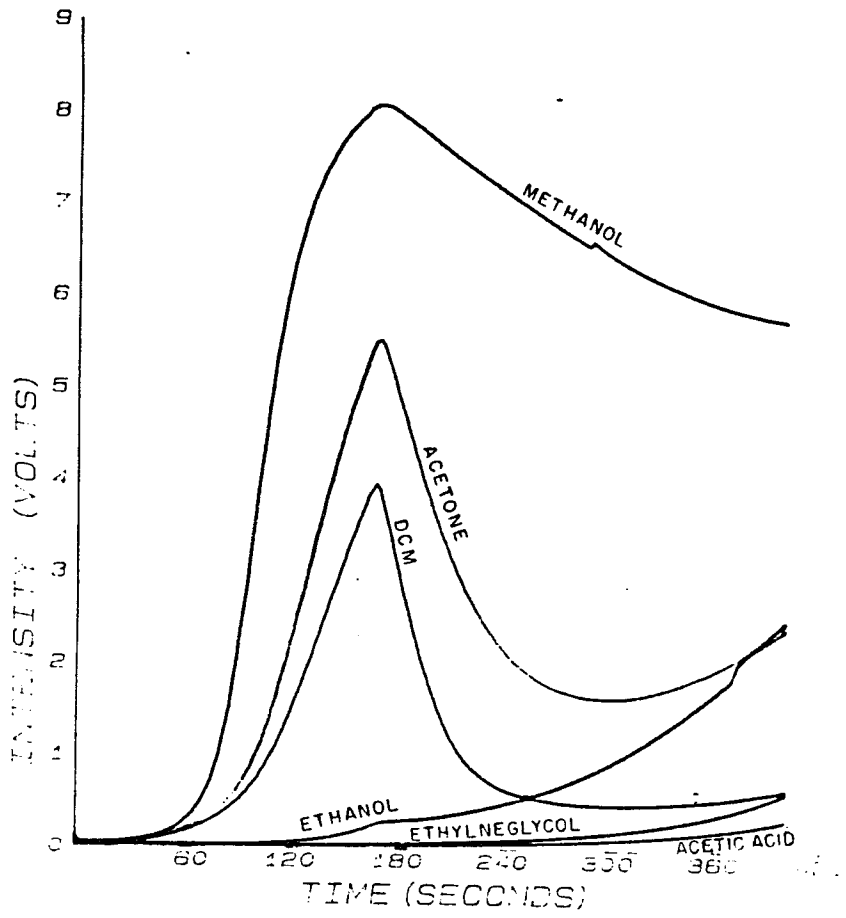

Figure 5.3.m. Membrane is HT-200.

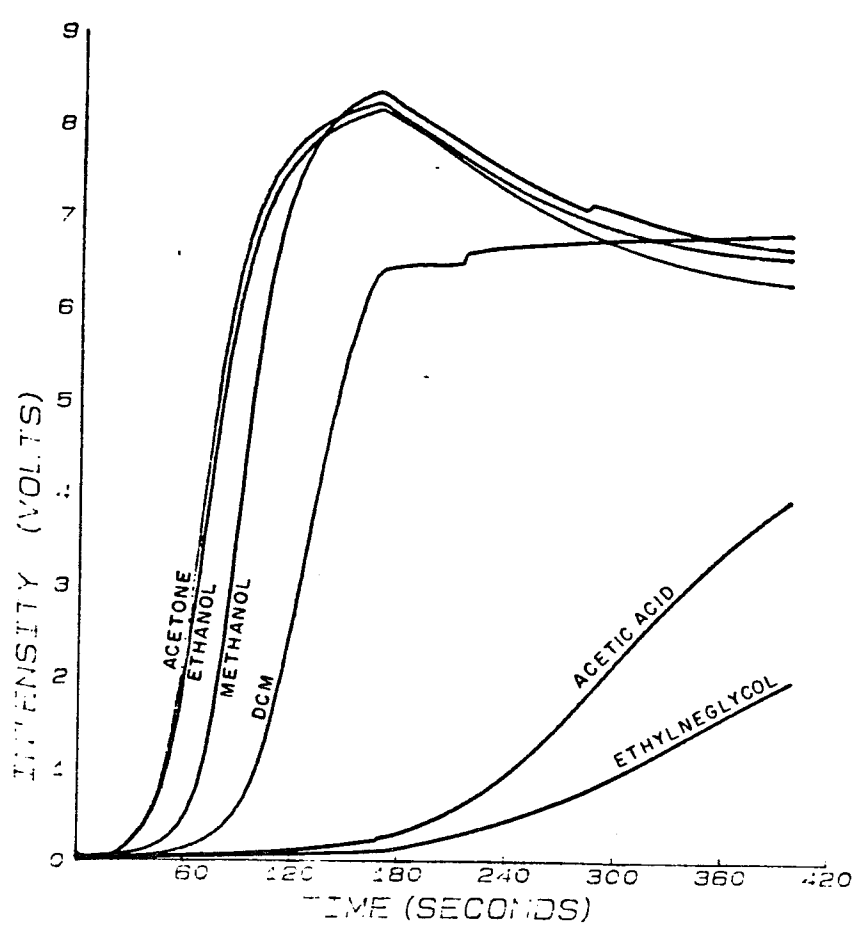

Figure 5.3.n. Membrane is TCM-200.

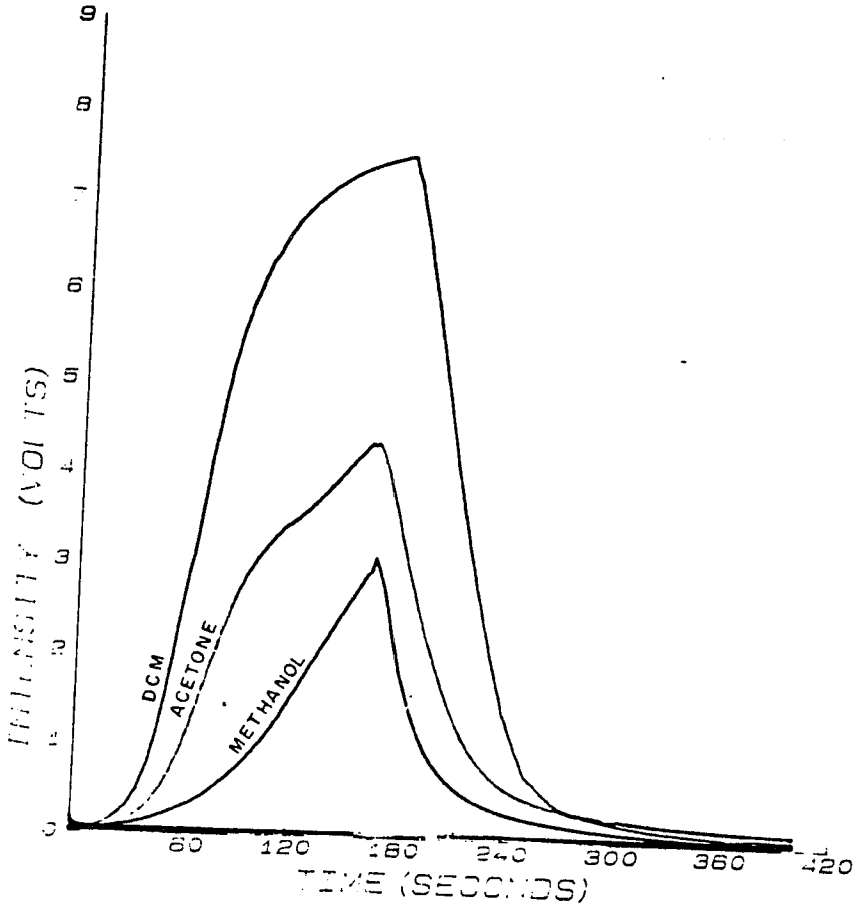

Figure 5.3.o. Membrane is MF-millipore.

TABLE 5.3. SUMMARY OF TEST RESULTS FOR SIGNIFICANT OUTPUT (dv/dt > 9 mv/sec)

CHEMICAL MEMBRANE	ACETONE			METHANOL			ETHANOL			D.C.M.			ACETIC ACID			ETHELYENE GLYCOL		
	dv/dt	-dv/dt	max	dv/dt	-dv/dt	max	dv/dt	-dv/dt	max	dv/dt	-dv/dt	max	dv/dt	-dv/dt	max	dv/dt	-dv/dt	max
NUCLEPORE-1.0					27	17	4.1											
NUCLEPORE-8.0																		
MF-MILLIPORE	26.3	18.3	4.34		19.2	13.2	3.1			43.4	34	7.5						
MITEX, 10μ																		
CELOTATE, 0.2μ																		
DURAPORE, 0.45μ					30.5	22.3	5.2											
BA85/7, 0.45μ	54.0	36.3	8.14	9.98	6.8	1.7				47.3	22	6.0						
PN20 (NPLC)	33.4	14.0	5.5	47.5	10.2	8.1				26.4	14.4	3.09						
ST68, 0.8μ																		
RC59, 0.6μ				23.6	27.8	3.8	8.6	1.6	1.4									
AE-91	48.8	10.9	8.03	27.7	23.6	5.1	27	26.7	5.3									
AE9517,1.2μ	16.3	12	2.7	15.9	10.9	2.5				10.6	7.5	1.7						
TE 30																		
TEFLON-200																		
GA-8	28.1	24.4	5.8							45	17	7.1						
VERSAPORE-800	49.6	18	8.07	49.8	17.6	8.1	45.4	16.5	7.8	51.0	9.8	8.3	45.8	6.0	7.5			
VERSAPORE-200	46.7	24.7	7.8	45.9	19	7.5	39.0	16.8	6.4	51	14	8.3	39	5.2	6.4			
HT-200	49.9	7.4	8.2	51.8	7.4	8.3	38.5	-2.3	6.3	50.7	8.3	8.1						
TCM-200	18	13.3	3.1	26	19.6	4.5				11.72	8.2	1.9						

TABLE 5.4. PROPERTIES OF MEMBRANES SELECTED FOR PRELIMINARY EXPERIMENTS

MEMBRANE	COMPOSITION	SIZE μm	THICKNESS μm	AC	AA	DCM	ETH	MT	EG	BENZ
GA-8	CELLULOSE TRIACETATE	0.2	130	NR	LR	LR	NR	LR	R	R
TCM-200	CELLULOSE TRIACETATE	0.2	150	NR	LR	LR	NR	LR	R	R
TEFLON-200	POLYTETRAFLUEORO-ETHYLENE (PTFE)	0.2	175	R	R	R	R	R	R	R
TE-30	PTFE	0.02		R	R	R	R		R	R
HT-200	AROMATIC POLYMER	0.2	165	NR	R	R	R	R	R	R
VERSAPORE-800	ACRYLIC COPOLYMER W/ NON-WOVEN NYLON	0.8		NR	R	R	LR	R	R	R
AE-95, 91	NITRO-CELLULOSE	0.2 0.8		NR	NR	NR	NR	NR	R	R
BA-85	NITRO-CELLULOSE	0.45		NR	NR	NR	NR	NR	R	R
ST-68	CELLULOSE ACETATE	0.8	140	NR	R	R	NR	R	LR	R
RC-59	REGENERATED CELLULOSE	0.6	120	R	R	R	NR	R	LR	R
DURAPORE	FLUORO CARBON POLYMER	0.22	100 - 150	R	R	R	R	R	R	R

Chemical compatibility is determined by "Dynamic or Static Flow Tests" at 25°C after 48-hour exposure and then checked for swelling and deterioration.

R: Resistant, no significant changes are observed in flow rate of the membrane

LR: Limited resistance, moderate changes in physical properties or dimensions of the membrane were observed. The membrane may be suitable for short term non-critical use.

NR: The membrane is basically unstable. In most cases, extensive shrinkage or swelling occurs. The membrane may gradually or partially weaken or partially dissolve after extensive exposure.

Generally dissolving a polymer in a solvent is governed by free energy equation:

$$\Delta F = \Delta H - T\Delta S \qquad (5.1)$$

where

ΔF = change in Gibb's free energy

ΔH = heat of mixing

T = the absolute temperature

ΔS = entropy of mixing

A negative ΔF predicts that a process will occur spontaneously (Burrel, 1976), as the dissolution of a polymer is always connected with a large increase in entropy. The magnitude of the heat of mixing, ΔH, is the deciding factor in determining the sign of the free energy change.

Hildebrand and Scott (1949) proposed that,

$$\Delta H_m = V_m \left[\sqrt{\Delta E_1/V_1} - \sqrt{\Delta E_2/V_2} \right]^2 \phi_1 \phi_2 \qquad (5.2)$$

where

ΔH_m = overall heat of mixing

V_m = total volume of the mixture

ΔE = energy of vaporization of component 1 or 2 to a gas at zero pressure

V = molar volume of component 1 or 2

ϕ = fractional volume of component 1 or 2

$\Delta E/V$ is the energy of vaporization per cubic centimeter, also described as the solubility parameter and denoted by δ.

$\Delta E/V = \delta$ = solubility has the dimensions of $\sqrt{CAL/cm^3}$ or $45.23 \sqrt{J/m^3}$

The Hildebrand-Scott equation then may be rewritten as

$$(\Delta H_m/V_m \phi_1 \phi_2) = (\delta_1 - \delta_2)^2 \qquad (5.3)$$

where the left-hand side is the heat of mixing per cubic centimeter at a given concentration. If the heat of mixing is not to be so large as to prevent mixing, then $(\delta_1 - \delta_2)^2$ has to be relatively small. In fact if $(\delta_1 - \delta_2)^2 = 0$, then the solution is assured by the entropy factor.

As $\delta_1 \rightarrow \delta_2$ two substances will be miscible. The solubility parameter (δ) governs only the heat of mixing of liquids or amorphous polymers. A noncrystalline polymer will, according to this theory, dissolve in a solvent of similar δ without the necessity of solvation, chemical similarity, association, or any specially directed intermolecular force. The high entropy change made possible with polymers is sufficient reason for solution to occur.

Table 5.5 provides the solubility parameter for polymers and organic chemicals used in this experiment.

TABLE 5.5. SOLUBILITY PARAMETER FOR POLYMERS AND ORGANIC CHEMICALS OF PRELIMINARY EXPERIMENT

Substance	$\delta(\sqrt{cal/m^3})$	Hydrogen Bonding
Acetic Acid	10.1	Strong
Acetone	9	Moderate
Ethanol	12.7	Strong
Methanol	14.5	Strong
Methyle Chloride (DCM)	9.7	Moderate
Ethylene Glycol	19.6	Strong
Freon 12	5.5	Poor
Water	23.4	Strong
Cellulose Acetate	11.12.7	Poor
	9.9 - 14.7	Moderate
	0	Strong
Nitrocellulose	11.1 - 12.7	Poor
	7.8 - 14.7	Moderate
	12.7 - 14.5	Strong
Poly Vinylchloride	10.6 - 11.1	Poor
	9.3 - 9.9	Moderate
	0	Strong
Poly Vinylidenechloride	9.5 - 11.1	Poor
	10.8 - 14.7	Moderate
	0	Strong
Poly Tetracludroethylene	6.2	Strong

Solubility of a polymer in an organic can also be inferred from viscosity measurements (Billmeyer, 1974). Measurements of solution viscosity are usually made by comparing the flux time, t, required for a specified volume of polymer solution to flow through a capillary tube, with the corresponding flux time, t_o, for the solvent. At a low concentration of solute, the viscosity of the solution is expected to be related to the viscosity of the pure solvent by $n = n^* + AC_p$ (Atkins (1976) where A is a constant, n^*: the viscosity of the pure solvent and C_p: polymer concentration. The constant A is normally written as

$$A = n^* [n] \tag{5.4}$$

where

[n] is the intrinsic viscosity and has the dimensions of inverse concentration (cm^3/gr).

Most of the polymer molecules in this experiment are macromolecules (high molecular weight) when most of the organics are of low molecular weight. In binary systems of this format, the general theory of phase equilibrium is rather complex, and it is questionable whether a theoretical model lending itself to mathematical analysis can take account of all the factors involved. It is much simpler to consider the limiting case of a two-component system in which the mutual solubility of the components is very low, in that each phase contains one component in highly dilute solution, while the other component is virtually in its standard state.

Gases above a critical temperature may also provide a solvent medium for polymeric solutes. In this case the cohesive energy density is very sensitive to pressure. The model for calculating such critical temperatures may be viewed as follows. Considering the vapor-membrane or

fluid-membrane solution to consist of a number of cells or sites, each site may be occupied by a solvent molecule or by one link or monomer unit of the polymer. The requirement for complete solution is that successive links occupy adjacent sites.

The polymer solution can then be treated as a regular solution with the added aspect that the entropy of the links is reduced because of their having to remain connected. The entropy effect is complicated by the distortion of the solution's behavior in making intermediate compositions less probable than for an ordinary regular solution. As a consequence, the dilute solutions tend to be very dilute and the concentrated solutions tend to be very concentrated, corresponding to slightly solvated polymers in equilibrium with a dilute solution.

The critical temperature at which this phenomenon takes place is expressed (Elias, 1976) as $T_c = w/_{2k}$: where w = interaction energy and k is boltman's constant. Below this temperature, a polymer will not be very soluble, whereas above this temperature, it is almost completely miscible with the solvent.

In equation 5.2 the term E/V is the energy of vaporization per unit volume of a liquid or the cohesive energy density. This term can be used for estimating the heat evolved from solution of nonpolar polymers with nonpolar solvents.

Exothermic solutions of polar polymers accompanied by a negative excess entropy leads in some cases to polymer precipitation when the system is heated to moderate temperatures. The nature of the interaction leading to exothermic interactions is sometimes quite obscure. No correlations between heat of mixing and output levels from EOC are established. This may require an extensive research program in itself.

In order to address the relation between empirical solubility of a polymer and an organic chemical and the EOC output voltage a solubility test was conducted for all membrane-chemical combinations of this experiment.

The solubility testing was a static dissolution test in which a 50cc flask was filled with an organic chemical. The membrane disk was then dropped in the flask and the flask was sealed. Physical changes of the membrane disks were monitored over a period of 48 hours.

Test results are presented in Table 5.6.

Because of its high exothermic energy, membrane solubility is expected to contribute appreciably to EOC output.

Comparison of results in Tables 5.3 and 5.6 indicated that, with a few exceptions, this expectation is supported.

5.5 MEMBRANE SATURATION

It may be required to operate the odo-cell under saturated or partially saturated conditions with the present configuration. This will present two problems:

(a) Not only the membrane, but the whole odo-cell, is contaminated and to decontaminate the whole cell (if possible), several hours are required.

(b) The electrical circuit of the cell, when exposed to a liquid, might develop a "short," rendering the system nonoperational.

The solution to problem (b) calls for a material or technique capable of letting the vapor molecules pass to the olfactory region of the cell without letting the liquid reach the cell. An extensive search indicated that there are commercially available prous liquid barriers. They are either hydrophobic in nature or have very high liquid entry

TABLE 5.6. RESULTS OF SOLUBILITY TESTING

CHEMICAL MEMBRANE	ACETONE	DICHLOROMETHANE	METHANOL	ETHANOL	ACETIC ACID	TIME
	D	D	NC	NC	D	0 Hours
TCM-200	D	D	PD	NC	D	24 Hours
	D	D	PD	NC	D	48 Hours
	S	D	NC	NC	NC	0 Hours
HT-200	PD	D	NC	NC	NC	24 Hours
	D	D	NC	NC	NC	48 Hours
	PD	PD	PD	PD	D	0 Hours
VERSAPORE	PD	D	PD	PD	D	24 Hours
	D	D	D	PD	D	48 Hours
	D	D	NC	NC	D	0 Hours
GA-8	D	D	NC	NC	D	24 Hours
	D	D	NC	NC	D	48 Hours
	NC	NC	NC	NC	NC	0 Hours
TEFLON	NC	NC	NC	NC	NC	24 Hours
	NC	NC	NC	NC	NC	48 Hours
	PD	NC	NC	NC	PD	0 Hours
AE-95	PD	S	NC	NC	PD	24 Hours
	PD	PD	PD	NC	PD	48 Hours
	D	PD	NC	NC	PD	0 Hours
ST-68	D	PD	NC	NC	PD	24 Hours
	D	PD	NC	NC	D	48 Hours
	NC	NC	NC	NC	NC	0 Hours
RC-59	NC	NC	NC	NC	NC	24 Hours
	NC	NC	NC	NC	NC	48 Hours
	NC	NC	NC	NC	NC	0 Hours
PN-20	NC	NC	NC	NC	NC	24 Hours
	NC	NC	NC	NC	NC	48 Hours
	E	E	NC	NC	PD	0 Hours
BA-85	E	E	NC	NC	PD	24 Hours
	PD	PD	NC	NC	PD/S	48 Hours
	NC	PD	NC	NC	PD	0 Hours
NUCLEPORE	PD	D	PD	PD	PD	24 Hours
	PD	D	PD	PD	PD	48 Hours
	D	NC	NC	NC	D	0 Hours
MF-MILLIPORE	D	PD	NC	NC	D	24 Hours
	D	PD	NC	NC	D	48 Hours
	NC	NC	NC	NC	NC	0 Hours
MITEX	PD	NC	NC	NC	NC	24 Hours
	PD	NC	NC	NC	NC	48 Hours
	D	PD	NC	NC	PD	0 Hours
CELOTATE	D	PD	NC	NC	PD	24 Hours
	D	D	NC	NC	PD	48 Hours
DURAPORE	PD	NC	NC	NC	NC	

LEGEND
PD - PARTIALLY DISSOLVED
D - DISSOLVED
S - SHRUNK
E - EXPANDED
NC - NO CHANGE

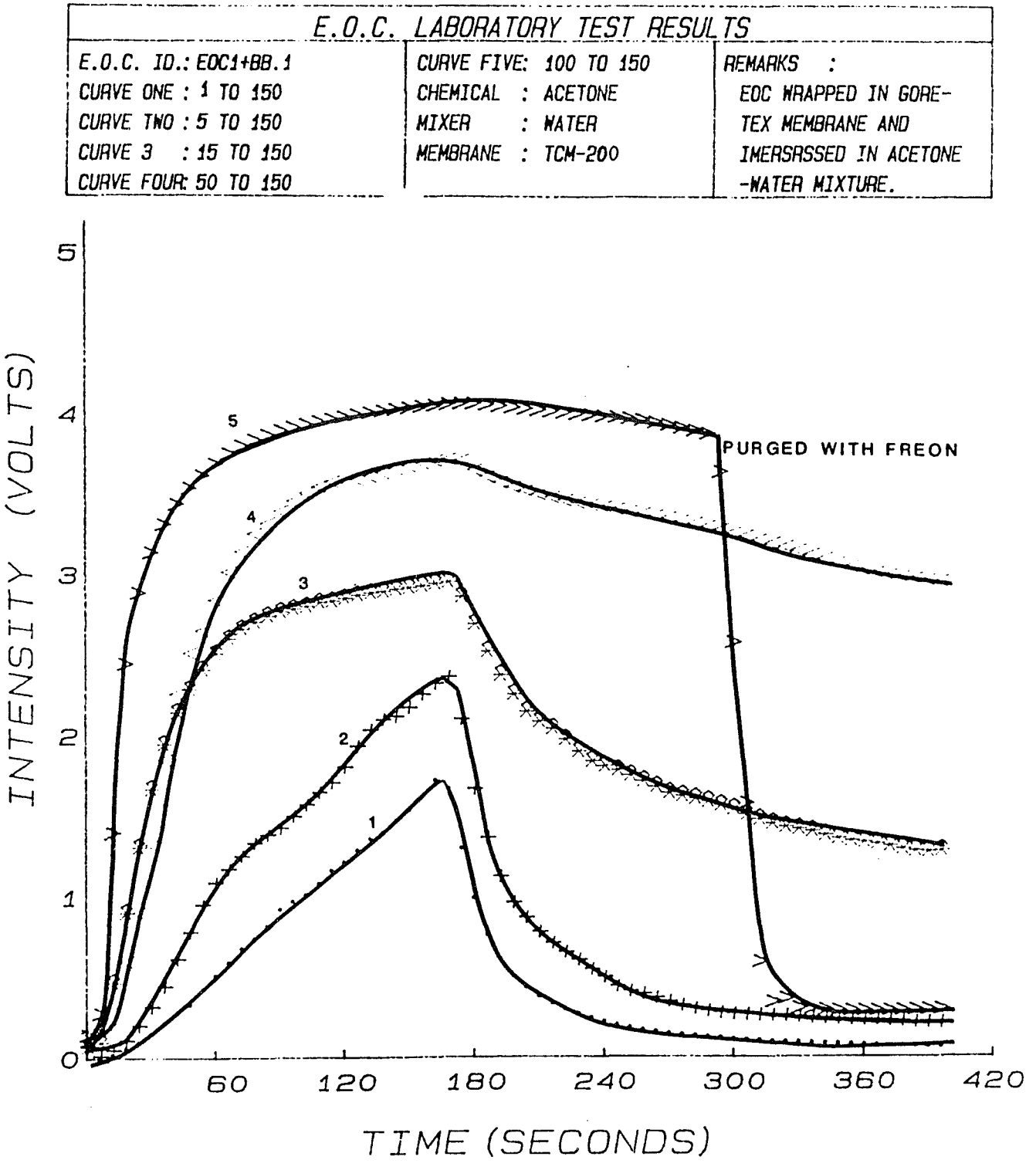

Figure 5.4. Results of immersion tests with EOC and Gore-tex membrane.

points, making liquid intrusion practically impossible. Gore-tex (Atlanta, Georgia) manufactures a product which is extensively used in ski clothings and specialty shoe manufacturing. The Gore-tex laminated vent membranes are made of nonreactive PTFE (polytetrafluoroethylene) and will not let any liquid with surface tension greater than 30 dynes/cm pass through, but the vapor will pass through its pores. Experiments indicate (see Figure 5.4) that when the cell is placed in a pouch made of Gore-tex membrane it is basically operational under water (surface tension 72) and under most water-chemical mixtures.

5.6 DESORPTION AGENTS

Once the EOC is exposed to a contaminant, molecules are absorbed and partially desorbed on the membrane, leaving a residual contaminant charge on the exposed (to the organic) parts of the EOC.

In order to render the EOC operational for multiple testing without having to wait for long periods of time for "natural desorption" or charge dissipation, it was desired to find a process of speeding up the desorption process. For this purpose, several gases were applied to an already contaminated EOC. These gases were applied at temperatures ranging from -5°C to 45°C (Figure 5.5a through j). The figures depict results of each desorption agent being applied to three different sections of the EOC (back panel, inlet, and sides). The experiment was conducted for desorption agents: freon-12, nitrogen, and carbon dioxide. Test results indicate:

1. Self dissipation (dissipation in ambient air) is slower than forced dissipation with CO_2 when CO_2 is applied to the inlet or sides of EOC and it is faster than forced CO_2 dissipation when CO_2 is applied at the back panel of EOC. Forced desorption

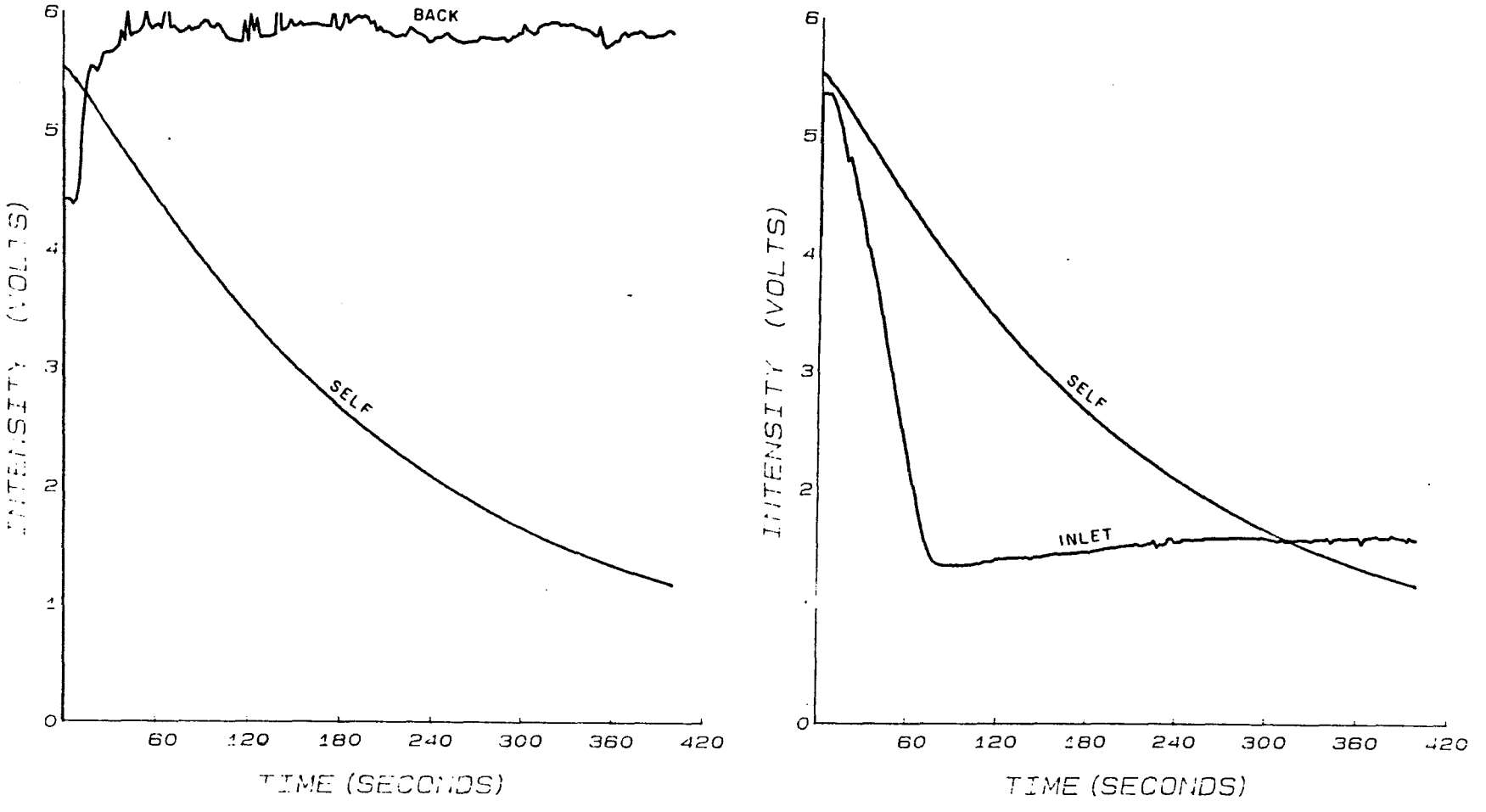

Figure 5.5. Plots of voltage dissipation vs. time with application of desorption agents.

a. CO_2 applied at the back panel of EOC vs. self dissipation.

b. CO_2 applied at the inlet of EOC vs. self dissipation.

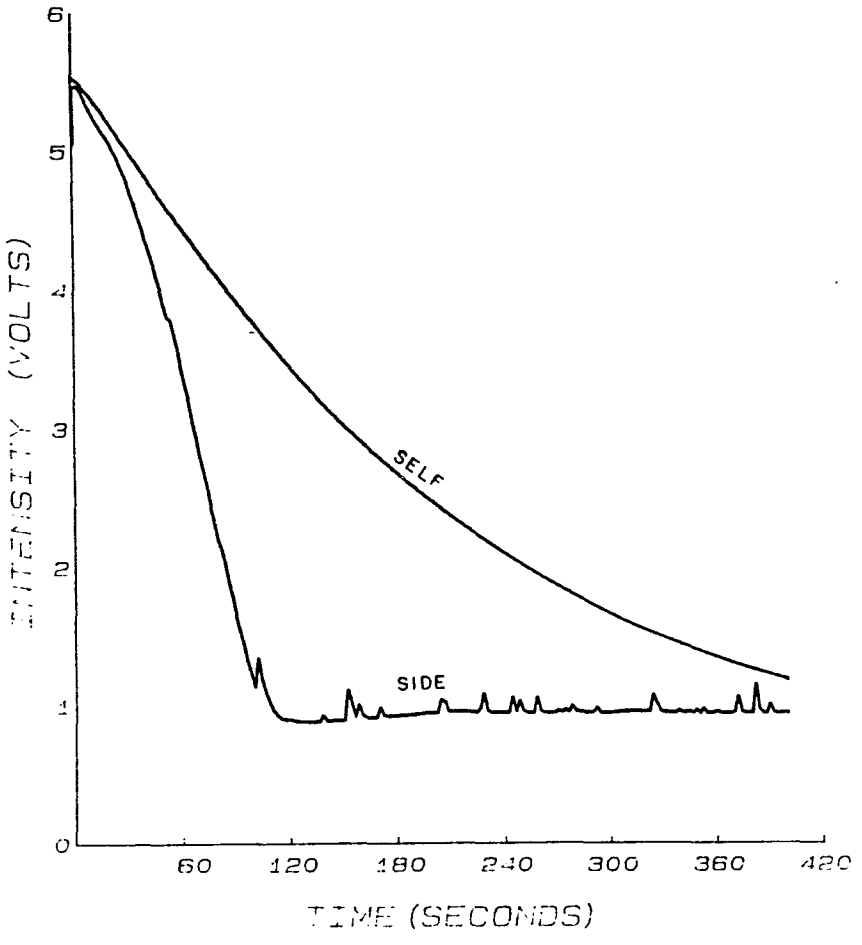

Figure 5.5.c. CO_2 applied at the side of EOC and self dissipation.

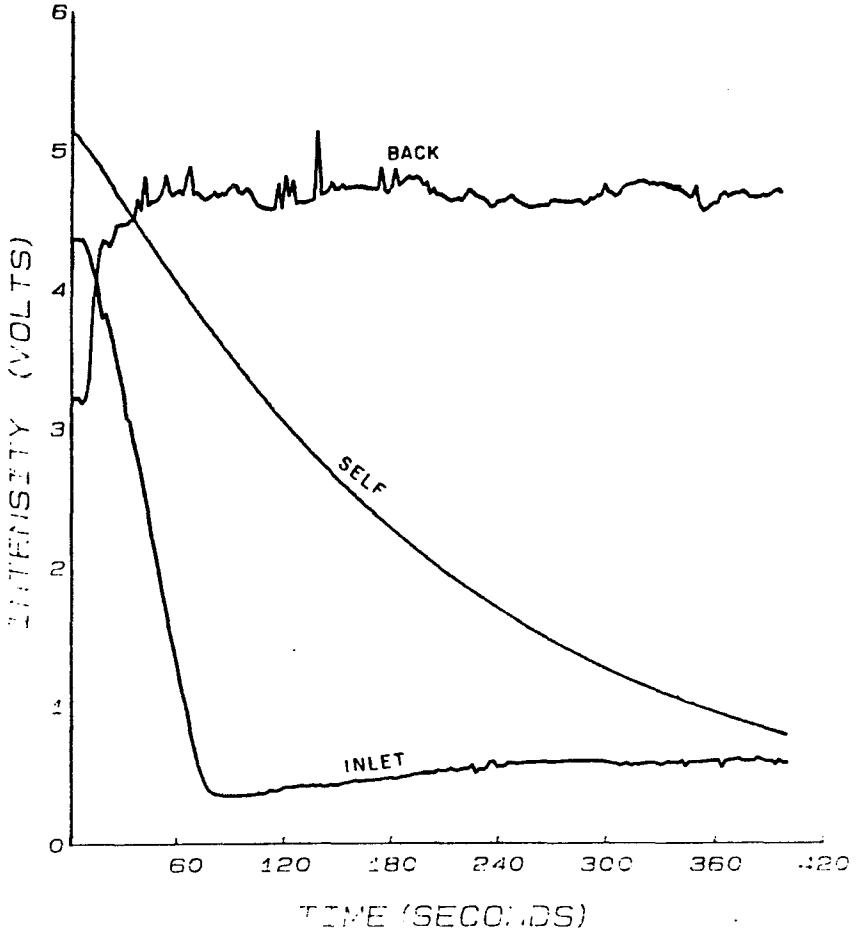

Figure 5.5.d. Comparison between three purging schemes.

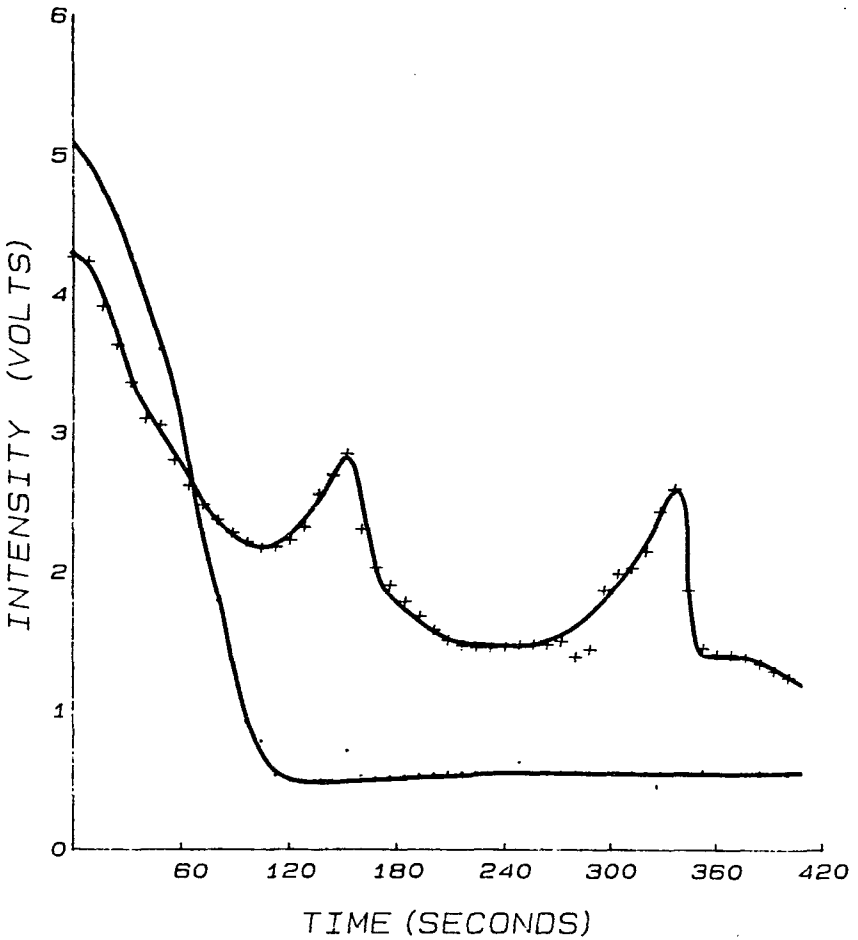

Figure 5.5.e. Effect of temperature on inlet dissipation.

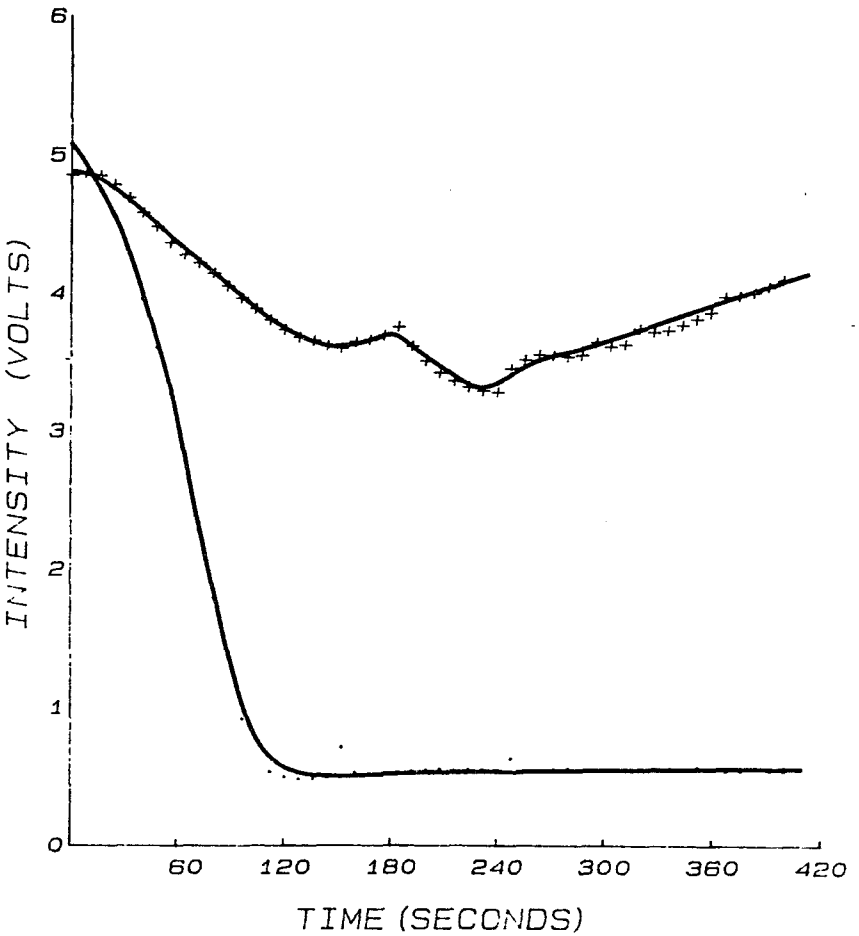

Figure 5.5.f. Effect of temperature on back dissipation.

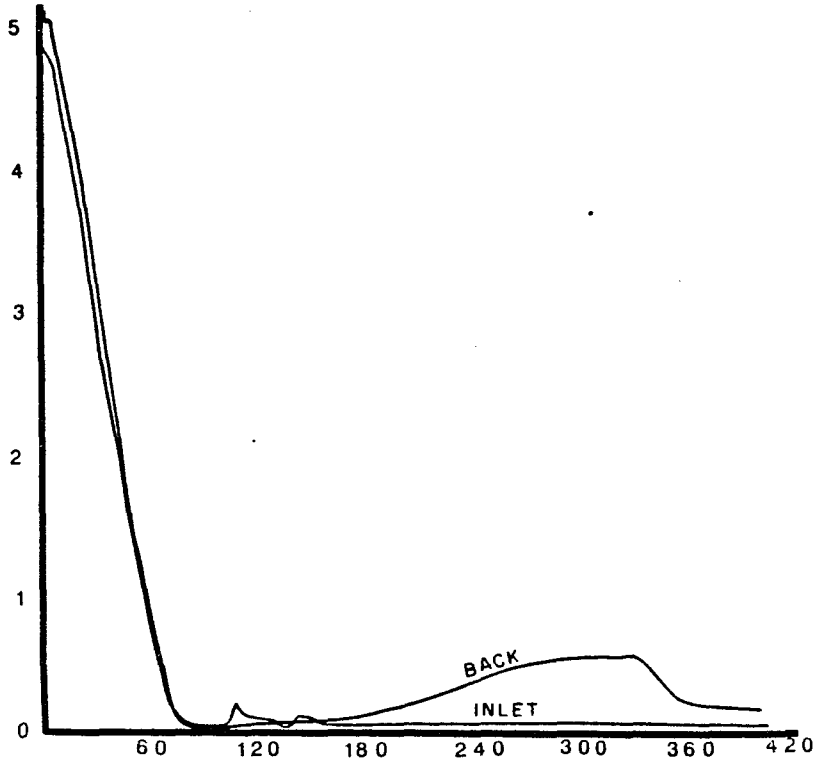

Figure 5.5.g. Dissipation due to Freon application at back, inlet, and sides at 20°C.

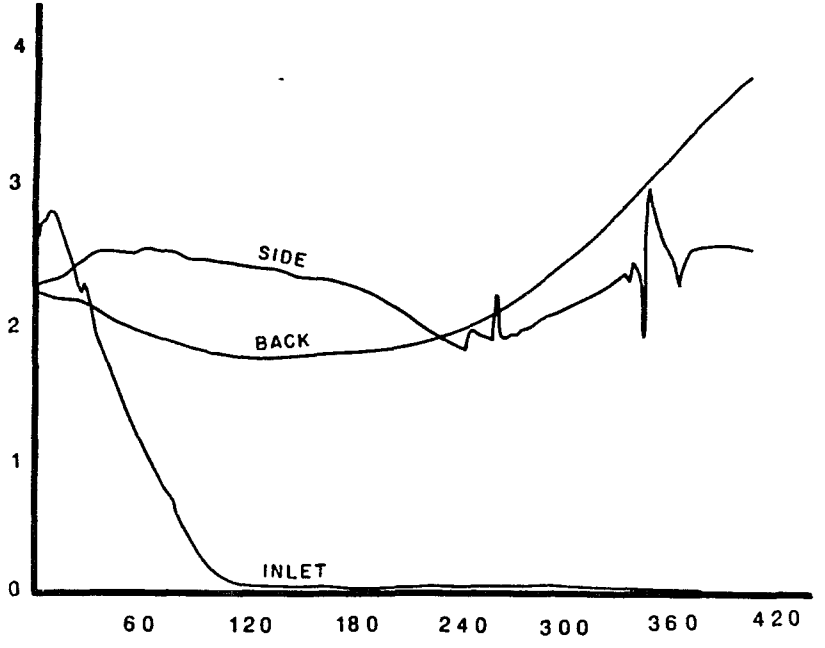

Figure 5.5.h. Dissipation due to Freon application at back, inlet, and sides at 0°C.

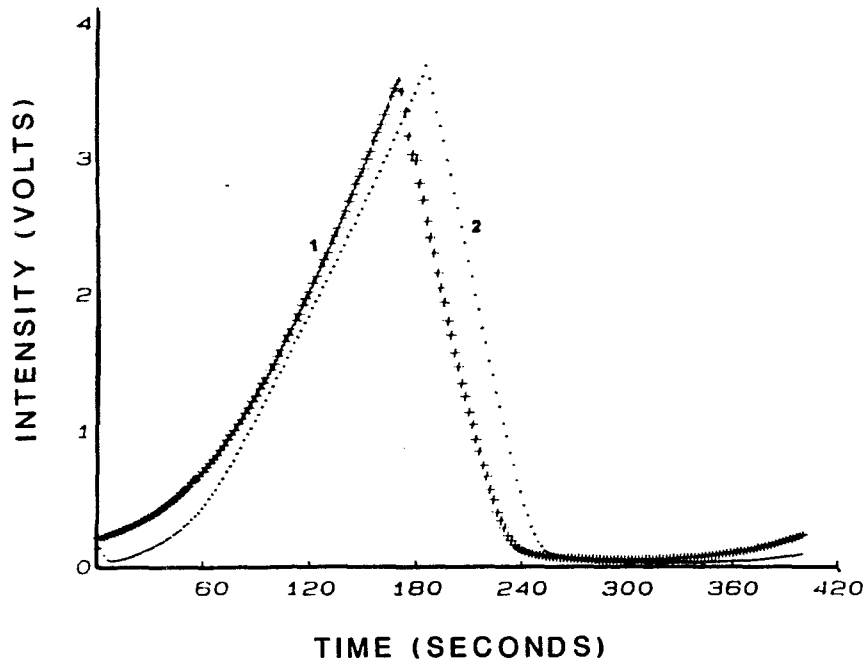

Figure 5.5.i. Dissipation due to Freon application during adsorption.

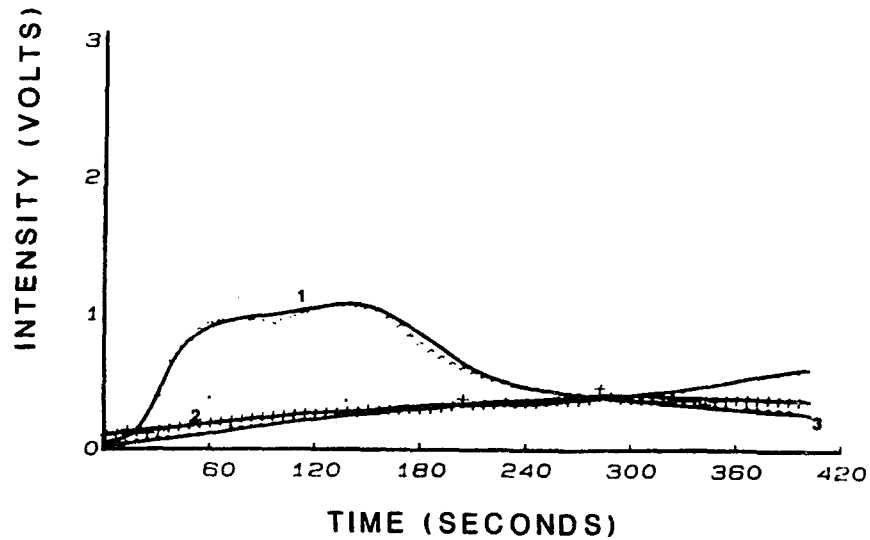

Figure 5.5.j. Dissipation due to nitrogen application at back, inlet, and sides of EOC.

with CO_2 is most effective with application of gas to the back or inlet of EOC and not effective when applied to the sides. The reason for this is that in the first case the purging gas (CO_2) comes in direct contact with the contaminated parts of EOC, i.e., the membrane and the inlet. And finally, CO_2 is a better desorption agent at higher temperatures when compared with Co_2 applied at the same position but at lower temperature.

2. Nitrogen did not prove to be an effective desorption agent regardless of position on EOC at which it is applied or the temperature of the gas.
3. The most effective desorption agent which could produce reliable, fast deionization-decontamination was shown to be freon-12. A noncontaminating gas, Freon forces residual molecules out of the system (when ventilation is provided) or purges the system by solvating the contaminant molecule and removing them. Figure 5.5 shows desorption effect of freon on EOC when freon is applied to a flask containing acetone. It can be seen that after about 300 seconds the voltage (and thus the charges absorbed on the membrane) are forced to zero and can be maintained at that level). Freon was used, successfully, as the purging gas in this study.

5.7 ADSORPTION OF MIXTURES

The mixing of two components with vapor pressures P_1^o and P_2^o according to Dalton's law of partial pressures results in a solution with a total pressure of $P = P_1^o + (P_2^o - P_1^o)\, x_2$; where x_2 is the mole fraction of a highly miscible second constituent. Since EOC responds directly to the

vapor pressure of the mixture, the extent of adsorption will be determined by the equilibrium vapor pressure.

Denoting the part of surface occupied, in equilibrium, by the molecules of the first component by θ_1, and the part occupied by molecules of the second component by θ_2 the rate of adsorption of the components may be expressed as:

$$r_{ads\ 1} = k_{ads\ 1}\ P_1^o\ (1-\theta_1-\theta_2) \tag{5.5}$$

$$r_{des\ 1} = k_{des\ 1}\ \theta_1 \tag{5.6}$$

$$r_{ads\ 2} = k_{ads\ 2}\ P_2^o\ (1-\theta_1-\theta_2) \tag{5.7}$$

$$r_{des\ 2} = k_{des\ 2}\ \theta_2 \tag{5.8}$$

At equilibrium

$$r_{ads\ i} = r_{des\ i} \tag{5.9}$$

Then for

$$a_i = k_{ads\ i}/k_{des\ i} \tag{5.10}$$

$$\theta_1 = (a_1P_1^o)/(1+a_1P_1^o+a_2P_2^o) \tag{5.11}$$

$$\theta_2 = (a_2P_2^o)/(1+a_1P_1^o+a_2P_2^o) \tag{5.12}$$

$$(\theta_1/\theta_2) = (a_1P_1^o)/(a_2P_2^o) \tag{5.13}$$

This ratio gives an indication of contribution of each component to the EOC output.

In an experiment designed to monitor EOC response to a mixture of contaminants. EOC response in a flask containing acetone was monitored To this flask dichloromethame was added such as to give solution ratios of 1 to 5, 3 to 5, 5 to 5, and 5 to 1. EOC output for all these cases is presented in Figure 5.6. They indicate that introduction of a host chemical will gradually change the characteristics of the output from

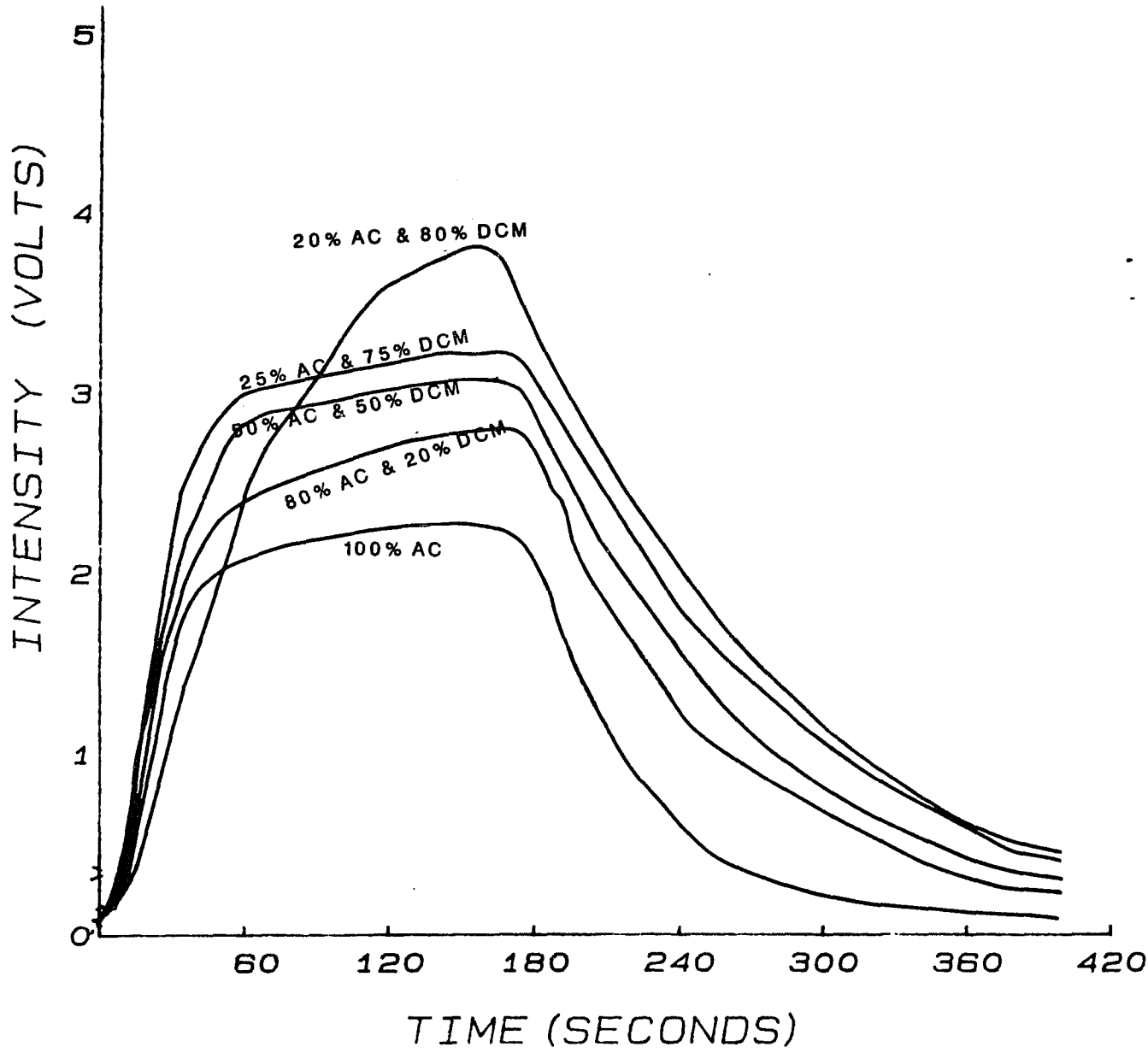

Figure 5.6. EOC response in monitoring mixture of acetone and dichloromethane.

that for the guest chemical to that of the host chemical. This change is a function of the ratio of the most chemical present in the final solution. The final output curve is the characteristic curve of the dichloromethane, which has become the dominant fraction of the solution, but it also reflects presence of acetone by a higher than normal (for dichloromethane) peak in the output curve.

5.8 EOC RESPONSE TO SALT SOLUTIONS

In leachate migration around a landfill, the migration front may contain, in addition to pollutants, a variety of salt solutions. A test was conducted to determine the EOC response to such electrolyte solutions, with the possibility of differentiation between response to salts and response to organic chemicals.

Also because of the low vapor pressure of the salt solutions, it is expected that these compounds will not be available for interaction with the membrane. The combination of these factors indicates that salt solutions will not produce significant output for EOC.

In exposing EOC to 3%, 5%, and 10% solutions of KCl, $MgCl_2$, and NaCl the responses as shown in Figure 5.7 were observed. A comparison will support the hypothesis that the contribution of salt solution in a leachate front to EOC output is small when compared with the response generated by the organics in the same front. The rate of change of voltage with time for 10% acetone solution is between 3 to 8 orders of magnitude higher than those due to salt solutions of the same concentration.

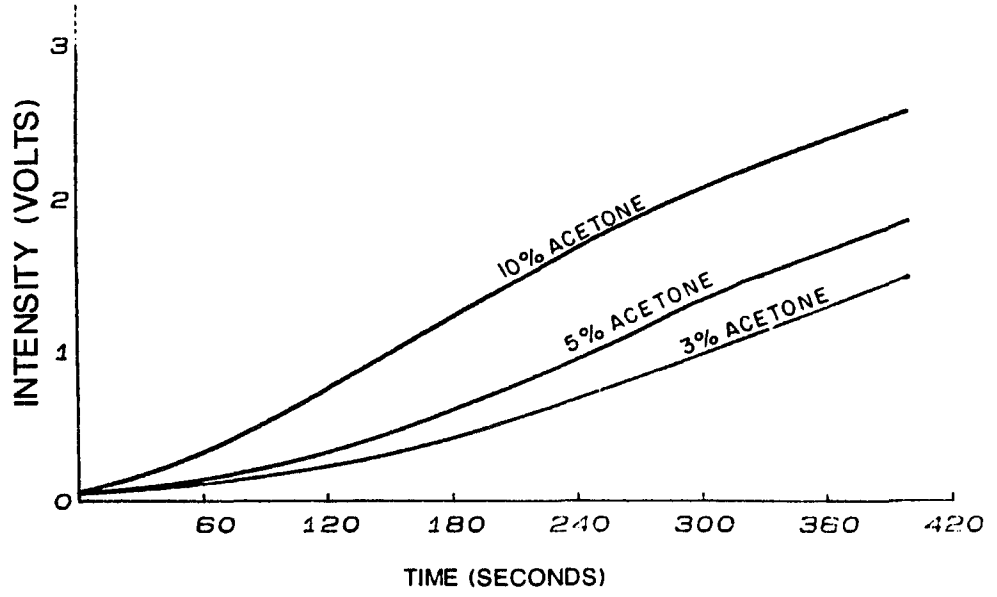

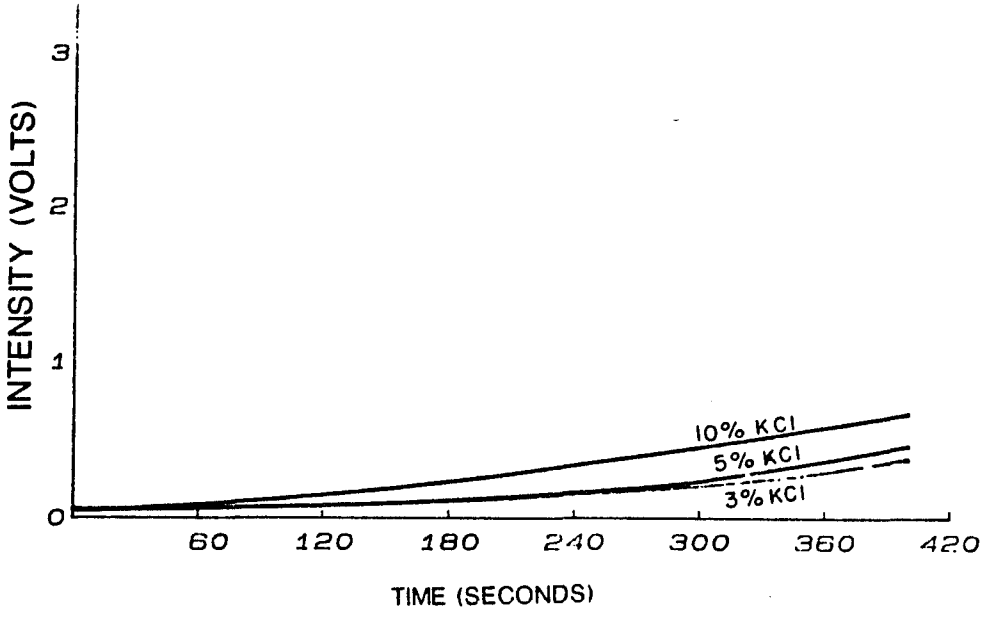

Figure 5.7. EOC response to salt solutions.

a. Response to NaCl.

b. Response to $MgCl_2$.

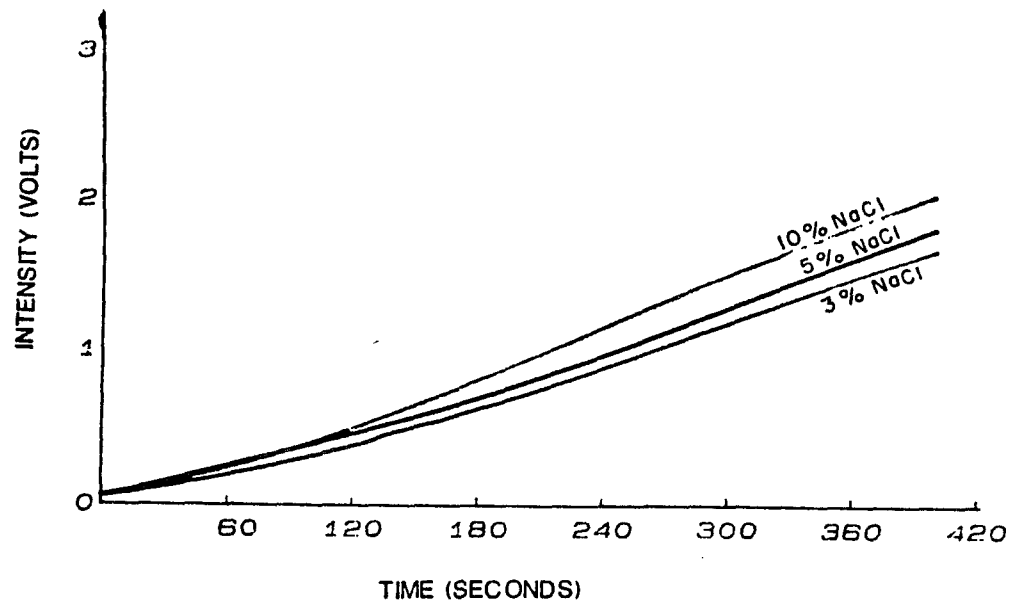

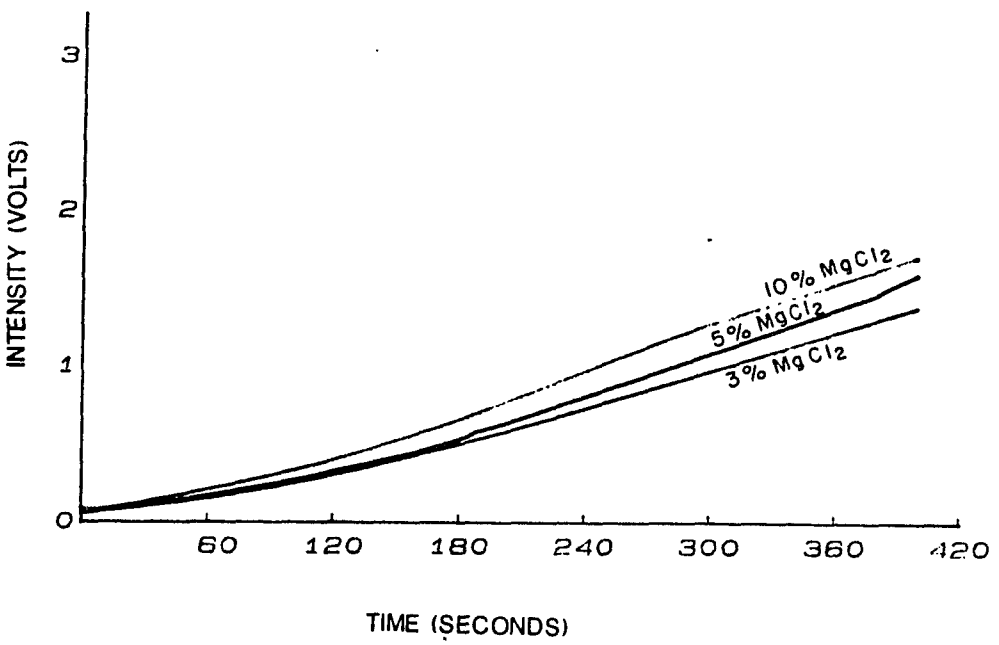

Figure 5.7.c. EOC response to three different concentrations of acetone.

Figure 5.7.d. EOC response to three different concentrations of Kcl.

CHAPTER 6

LABORATORY TESTING: PHASE II

6.1 EOC RESPONSE IN SOIL SAMPLES

The objective of this phase was to investigate the response of EOC in detecting organic chemicals permeated or leached through soils. This simulates the ground conditions in and around a landfill. The flow diagram of Figure 6.1 shows the methodology and logic of testing. The design of the experiment was such that it covered a range of soil permeability, a number of organic chemicals, and a range of concentrations for the organic chemicals.

The testing program that has proved most reliable and is in wide use in testing the hydraulic conductivity of hazardous organics is the triaxial set-ups with flexible wall permeameters. The conventional triaxial set-up, however, would not have accommodated the model of leachate flow around the C/EOC, so a special triaxial chamber was designed and fabricated (see Appendix B) to accommodate such requirements. The testing set-up and soil selection and testing procedures follow.

6.2 SOIL SELECTION

Due to the limitations on the number of test setups and time, it was decided to conduct the laboratory soil testing with soils most frequently used in studying the hydraulic conductivity of samples to organic permeants (Hamidon, 1985; Anderson et al., 1982). The soils best meeting these criteria were Georgia kaolinite clay furnished by Thiele Kaolin Company and silt furnished by Feldspar Corporation of Edgar, Florida.

The kaolinite used in this experiment was Georgia kaolinite. The generic mineral is basically a two-layered unit (1:1) formed by stacking a gibsite sheet on a silica sheet (Figure 6.1).

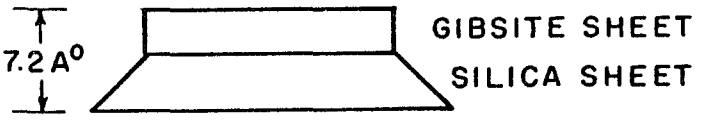

Figure 6.1. Typical kaolinite mineral arrangement.

The bonding between successive layers is both Van der Waals forces and hydrogen bonds. The bonding is of sufficient strength that there is no interlayer swelling.

Kaolinite posses a net negative charge on the order of 3-15 mega equivalents per 100 gram of soil. Evidence exists that kaolinite particles are charged positively on their edges in a low pH (acid) environment, and negatively in a high pH (basic) environment. Low exchange capacity is measured for high pH.

Well-crystallized particles of kaolinite occur as well-formed, six-sided plates. The lateral dimensions of these plates range from 0.1 to 4μ cm and their thickness may range from about 0.05 to 2μ cm. Poorly crystallized kaolinite generally occurs as less distinct hexagonal plates, and the particle size is usually smaller than for the well crystallized varieties.

The specific surface area of kaolinite ranges from 10 to 30 m^2/gram of dry clay with a specific gravity of 2.60--2.68. Breakdown of constituents in Georgia kaolinite are presented in Table 6.1.

The low activity of kaolinite means that the diffused double layer around the mineral is not fully developed and the fabric is nondispersed (or aggregated), leading to possibilities of higher hydraulic conductivity. Low-activity kaolinite also provides higher resistance to volume change when permeated with low dielectric fluids.

The silt samples were selected to study odor-cone detection capabilities in nonreactive and highly permeable porous media. The silt used in this study was in the particle size range of 100 to 150 micrometers and consisted of basically quartz material. It is considered to be nonreactive with the permeants used in this experiment.

6.3 SAMPLE PREPARATION

A preweighted amount of kaolinite was placed in a mechanical drum mixer and distilled water was added to it in 50 ml increments and mixed. From 15 to 20 minutes were allowed mixing each increment of water with low cycle rpm, stopping when it became necessary to scrape off the clay adhering to the sides of the mixer. This procedure was continued to produce a water content of about 27%. Past this limit, the rotary drum may cause smearing and shear-disaggregation of the mix, which may result in precompaction and alteration of hydraulic conductivity. To increase the water content to optimum level, additional moisture was added by spraying water on the soil manually, in an effort to avoid precompaction.

Once enough water was added to the sample to achieve 32% moisture, the soil was placed in polyethylene bags and cured for two to three days to insure uniform water content. A sample was taken for measurement of actual water content (to be compared with the calculated or expected value). Following this step, the soil was compacted.

6.3.I COMPACTION

Classical experimental testing evaluations have indicated that mechanical variables such as compaction effort, compaction scheme, clod size, changes in macrofabric caused by shrinkage, desiccation, and tension cracks might overshadow any anticipated microfabric changes due to the transport of organic fluid through compacted clay liners or soil samples used in experiments such as this one.

Figure 6.2 shows the effect of compaction on clay structure. It indicates that increasing the compaction effort on the dry side of the optimum decreases the total porosity and diminishes the fraction of large pores. Increasing the compactive effort on the wet side of the optimum has little effect on either the pore distribution or total porosity.

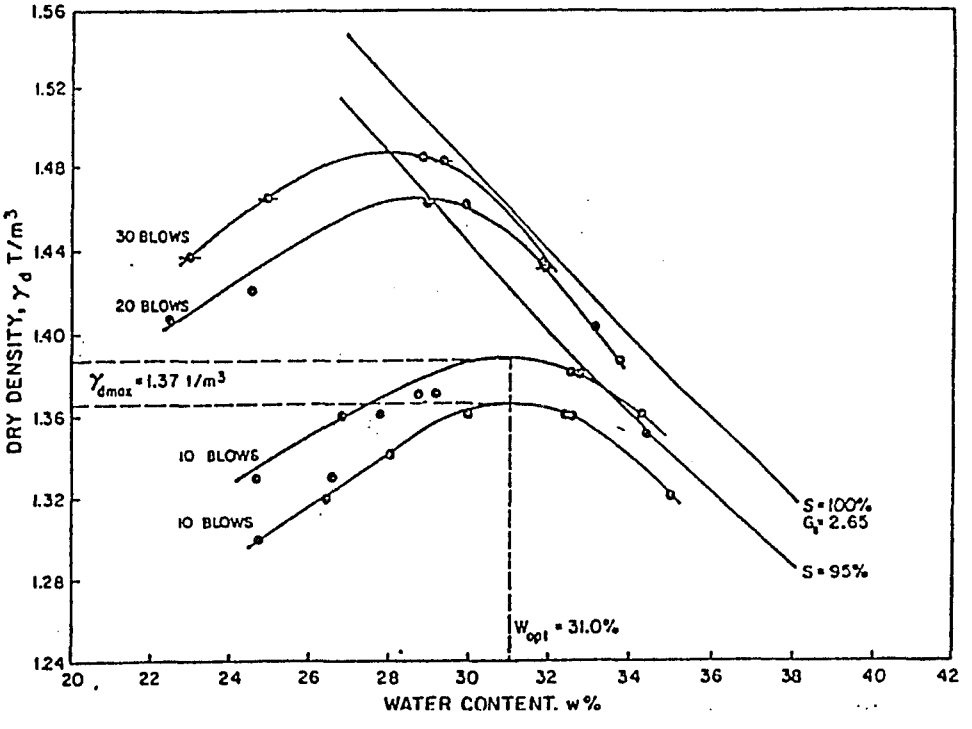

Figure 6.2. Effect of compaction on clay structure (after Hamidon, 1984).

Table 6.1
Chemical composition and geotechnical properties
of kaolinite (Hamidon, 1984)

Chemical Composition

(dry weight basis)

SiO_2	46.5 %
Al_2O_3	37.62 %
Fe_2O_3	0.51 %
TiO_2	0.36 %
P_2O_5	0.19 %
CaO	0.25 %
MgO	0.16 %
Na_2O	0.02 %
K_2O	0.40 %
SO_3	0.21 %
Loss on Ignition	13.77 %
Free Moisture	1.43 %

Particle Size Distribution:

Particle Size (microns)	Cumulative % Undersize
40	100
10	90
5	78
3	68
1	49
.5	40
.2	20

Liquid Limit in Water	64
Plastic Limit in Water	34
P.I.	30
Specific Gravity	2.65
Activity	0.32
Max Dry Density	1.37 T/m^3
Optimum Moisture Content	32 %

Figure 6.3 indicates that a decrease of 20% in the intended compacted dry density leads to an increase of about one order of magnitude in the hydraulic conductivity of the compacted soil.

In this experiment, following curing, kaolinite was compacted in the annular ring around the prototype C/EOC at an energy level slightly more than standard proctor compaction to insure wet of optimum compaction.

Compaction procedure details are outlined in Appendix B.

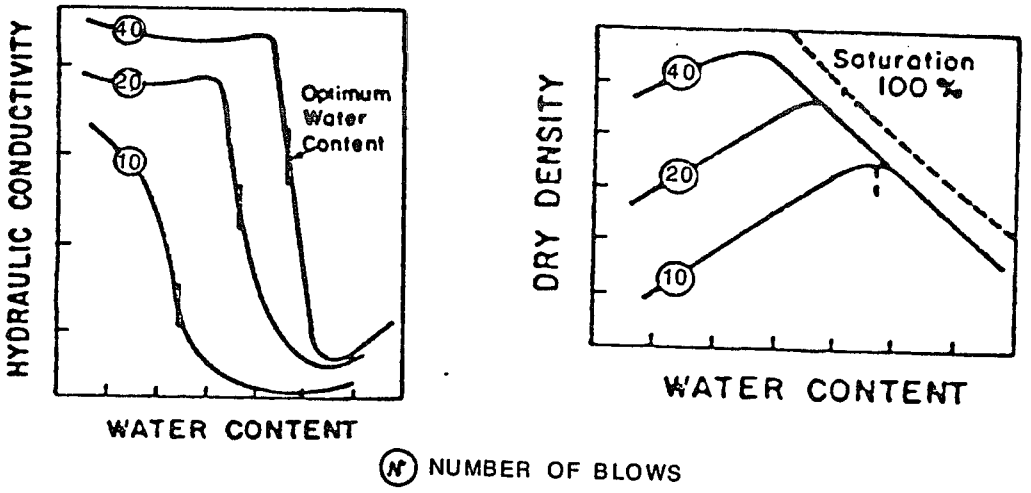

Figure 6.3. The effect of molding water content on hydraulic conductivity (after Mitchell, 1976).

6.4 SAMPLE SATURATION

Using an elevated back pressure to produce complete saturation in various laboratory test specimens has been well described and widely used for some time (Bishop and Henkel, 1962; Low and Johnson, 1960; Row and Barden, 1966; Mitchell et al., 1965; and Wissa, 1969).

The objective is to apply a sufficient back pressure of water to the sample to cause the pore air to dissolve completely into the surrounding pore water.

Low and Johnson (1960) have shown that the practical back pressure required to bring a sample from an initial degree of saturation, S_i, to a final degree of saturation, S_t, by both compression and solution of the pore air is:

$$P_{100\%} = 49\ (P_i \cdot (1-S_i) \qquad (6.1)$$

P_i = initial absolute pressure corresponding to S_1

S_i = initial degree of saturation

Lee and Morrison (1969) have indicated that a back pressure of 60 - 70 PSI is sufficient to achieve full saturation. The literature, however, is not clear on the duration of application of the back pressure. Duration may be verified through monitoring of the B valve. $B = \Delta\delta_3/\Delta u$ (where δ_3 = effective stress and u = pore fluid pressure) is the ratio of an increase in back pressure and the corresponding average increase in generated pore pressure under constant effective stress conditions.

When the B valve is sufficiently close to unity, and when its value does not change with further increases in δ_3, it is assumed that complete saturation is reached.

Full saturation may also be assumed when the volume or the inflow and outflow are equal (Daniel et al., 1984).

Since in this experiment the samples were identically prepared B values were measured only for three samples (one in each group) and saturation was checked by back pressuring one day past the time when volume of inflow and outflow ere equal.

6.4.I HYDRAULIC GRADIENTS

For the benefit of time, hydraulic gradients in laboratory tests are usually much higher than those existing in the field. These elevated

gradients become the major source of discrepancy between laboratory-measured and field value of hydraulic conductivity.

Figure 6.4 shows the effect of the gradient on the hydraulic conductivity. The data shows minimal nonlinearity and hysteresis for gradients of up to 150. This is because lower hydraulic gradients would minimize the particle migration effect. Foreman and Daniel (1986), however, demonstrate the variations in hydraulic conductivity of kaolinite with respect to the hydraulic gradient to be minimal for the range of 70-180 when the permeating fluid was methanol (Figure 6.4a). Similar results were also obtained for water (Figure 6.4b). In spite of these somewhat contradicting observations and considering lack of information on the effect of other permeants used in this experiment, the hydraulic gradient was kept under 150. This allowed for the tests to be conducted in a practical span of time without adverse effects on the hydraulic conductivity or the samples. In the case of dichloromethane, however, because of the extremely low permeability of kaolinite to the nonwater soluble corrosive organic, the hydraulic gradient was raised to 300. Due to their higher hydraulic conductivity value, hydraulic gradients in silt samples were kept around 50. Dichloromethane was not used in permeation through silt samples.

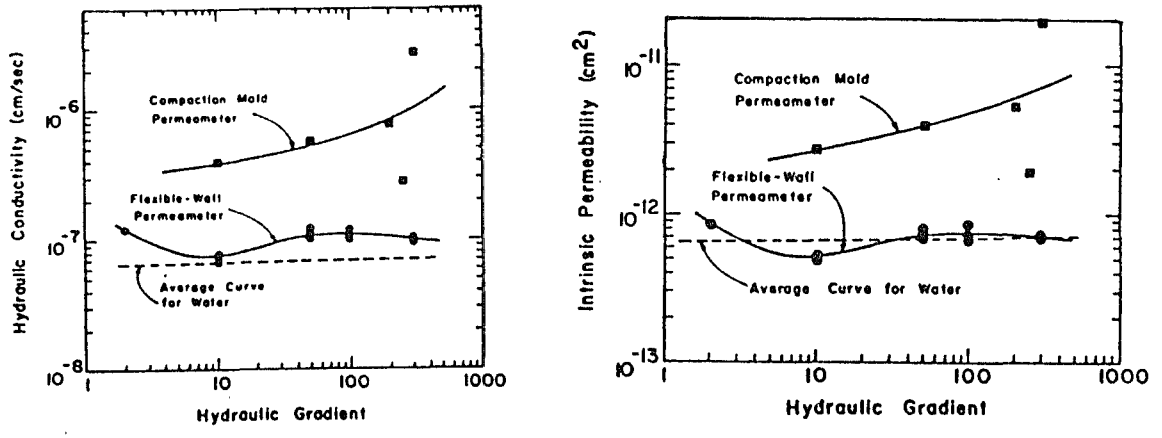

Figure 6.4. Effect of variation of hydraulic gradient on hydraulic conductivity for permeant a) methanol, b) water (after Foreman and Daniel, 1986).

6.5 PERMEANT SELECTION

Organic chemical permeants were chosen from the same group of organics that were tested in ambient conditions. They were selected to cover a range of parameters including vapor pressure (11.8—→400mmHg), dielectric constant (6.1—→33.62), polarity (1.66—→2.28 Debys), solubility in water (8.08 gr/lit—→∞) and viscosity (0.33 to 1.24 Centipoise).

These organics were also highly reactive with an appropriate membrane and produced appreciable response in EOC testing in ambient conditions. Table 6.2 presents properties of permeants used in this experiment:

TABLE 6.2. PROPERTIES OF CHEMICALS USED IN PRELIMINARY EXPERIMENTS

COMPOUND	FORMULA	DIELECTRIC CONSTANT	DIPOLE MOMENT (DEBYES)	VAPOR PRESSURE (mmHg)	SURFACE TENSION (Dyne/cm^2)	SOLUBILITY (gr/ℓ)		
						WATER	ALCOHOL	ACETONE
WATER	H_2O	80.4	1.83	28	72.7	∞	∞	∞
ACETONE	C_3H_6O	20.7	2.90	184.8	23.7	∞	∞	∞
METHANOL	CH_4O	33.62	1.66	96	22.6	∞	∞	∞
ETHANOL	C_2H_6O	24.3	1.69	66	22.3	∞	∞	∞
DICHLOROMETHANE	CH_2cl_2	6.1	1.74	11.8	26.5	8.08	∞	∞
ETHYLENE GLYCOL	$C_2H_6O_2$	38.66	2.28	1	47.7	∞	∞	∞

6.5.I ORGANIC PERMEATION

Permeating any fluid other than the molding fluid through a sample is expected to change the forces of repulsion and redistribute the net forces of interaction in the soil, leading to changes in microfabric and macrofabric engineering behavior.

As dictated by the physics of the clay-water-electrolyte system, the thickness of the diffused double layer is sensitive to variations in

surface charge density, δ, electrolyte concentration, η_o, cation valance V, dielectric constant of the medium D, and temperature T, in the following fashion:

$$\text{Diffused Double Layer Thickness} = \sqrt{\frac{DkT}{8\pi\eta_o E^2 V^2}} \qquad (6.2)$$

Where k = Boltzman's Constant

E = Electric Charge

Interaction repulsion due to double-layer interactions increases monotonically with the increasing dielectric constant, and thenet forces of interaction may vary in the manner of Figure 6.5 (Moore and Mitchell, 1974).

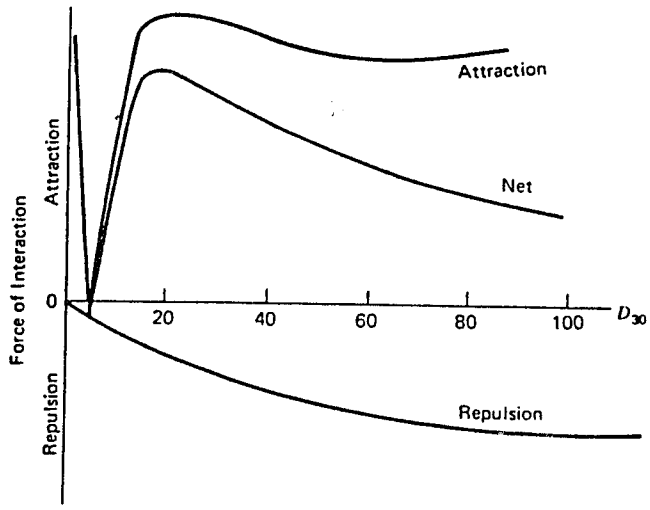

Figure 6.5. Combined forces of interaction in clay (after Mitchell, 1976).

This figure suggests that higher attractive values and thus thinner double layers with all the organic permeants when compared with those for water as pore fluid. This is especially true for acetone with a dielectric constant of 21 (maximum attractive force).

Doner and Mortland (1969) indicates that the effect of both cation valency and hydrated ion size can be overshadowed by the effects of the pH of the environment. This is because the exposed hydroxyl (OH) of clay may dissociate as

$$\text{Si OH} \xrightarrow{H_2O} \text{Si O}^- + H^+ \qquad (6.2)$$

The dissociation is strongly influenced by the pH. The higher the pH, the greater the tendency for the H^+ to go into solution and the greater the effective negative charge of the particle.

Acidic pH environment promotes development of the positive double layer. This is because exposed alumina is amphoteric and ionizes positively at low pH and negatively at high pH. Thus a low pH promotes a positive edge to negative surface interaction, leading to flocculation, where a high pH environment promotes dispersion of clay particles (Lamb, 1958).

The pH of the solution has been demonstrated to correlate well with the free swell and Atterburg limit of clay, as shown in Figure 6.6.

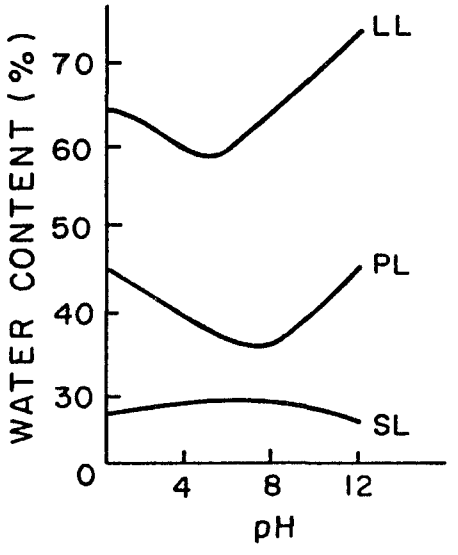

Figure 6.6. Relationship between Atterburg limits and solution's pH (Lamb, 1958).

Mitchell and Lin (1954) have indicated that permeability at a constant void ratio decreases with increasing dielectric constant of the permeant. On the other hand, reductions in the dielectric constant result in higher equilibrium void ratio (Sridharn and Rao, 1973).

Green et al. (1983) reports that there is a direct correlation between dielectric constant and free swell of clay soils as shown in Figure 6.7.

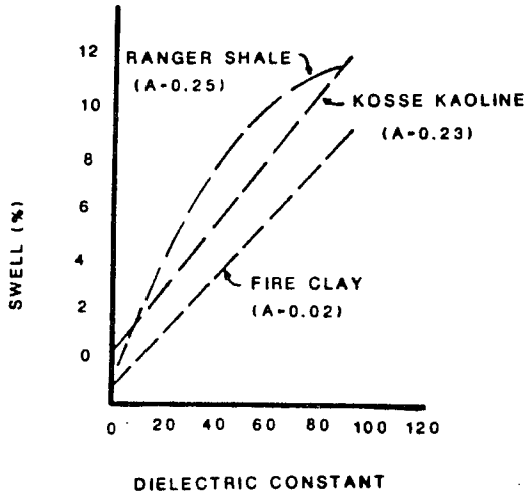

Figure 6.7. Effect of dielectric constant on swell behavior of compacted clay (after Green et al., 1983).

In general, low dielectric constant permeants seem to promote increased particle contact and increase attractive forces among particles. Reduction in the double layer brought about by replacing water with lower dielectric constant permeants results in volume reduction and increases in effective stress. Clay-pore water interaction may cause formation of wormholes through preferential flow of reactive fluid in large pores. But since kaolinite is a nonexpansive mineral such interactions are largely confined to the external crystal surfaces.

Polarity of the permeating fluid affects the fabric of clay in the sense that for higher polarity, permeants reduction in attractive forces will dominate the fabric and a more dispersed structure will be formed. Less polar fluids generate a flocculated structure and may cause shrinkage of the clay and open up flow channels, increasing the final hydraulic conductivity. Reorientation of particles in both cases may lead to a new stabilized fabric and a stable hydraulic conductivity value.

The polar organic permeants in this experiment are possibly adsorbed on the clay mineral surfaces and probably also on the edges of the mineral in competition with water. Through such adsorption they will change the capacity of the Stern layer, the zero point of the charges on the mineral, and possibly the Van Der Waals forces, consequently changing the double-layer constitution and particle interaction energy. These will, in turn, result in changes in the volume of the samples.

In light of the above considerations, states that mechanical variables such as compaction effort, clod size, compaction scheme, changes in the macrofabric caused by shrinkage, desiccation, and tension cracks might overshadow any anticipated microfabric changes due to transport of organic fluid through the sample.

Furthermore, microfabric changes due to changes in pore fluid chemistry of compacted soils confined to effective stresses of 10 psi are not expected to lead to dramatic increases in hydraulic conductivity. This is especially true for low-activity soils such as kaolinite. At higher confining pressures, microfabric reorientation and redistribution of pore size is restricted. For example, a twofold increase takes place from 10 psi to 2 psi in kaolinite hydraulic conductivity to acetone.

The miscibility of the replacing pore fluid in the molding fluid is an important factor affecting hydraulic conductivity of the soil samples.

The hydraulic conductivity of compacted soils decreases with low-solubility organic fluids. This is explained by decreases in flow volume due to the higher flow initiation pressure required to overcome the surface tension at the interface of the two fluids trapped in the smaller pores. This was experienced for slightly water-miscible dichloromethane, which required hydraulic gradients in excess of 300 for permeation. Permeation with dichloromethane resulted in a highly nonplastic and highly permeable soil once the permeation was complete. With silt, however, there were no complications in process of permeating the organics through the soil samples. This indicates that once the uncertainty associated with permeant-soil interaction is eliminated, the hydraulic conductivity of a soil and consequently the time of initial response of the C/EOC in the soil will become a relatively well defined parameter.

The selected organic chemicals were permeated through the samples following completion of saturation. To minimize diffusion through the latex membrane all samples were wrapped in teflon tape after compaction. Comparative experiments by Daniel et al. (1984) indicated that teflon tape rigidity causes only minor differences in measured hydraulic conductivity of the samples and its use is recommended. The permeants were introduced to the samples at concentrations of 10, 25, and 50%. Dichloromethane was applied commercial concentration (99.9%). Simultaneous with the introduction of the organic permeant, the C/EOC was placed in the cylindrical cavity of the triaxial chamber. The C/EOC response was monitored through an HP 973 data acquisition system throughout the

experiment. At the first stages of the experiment, sparse readings were taken, but upon the arrival of odor molecules within the olfactometric reach of the C/EOC, the data were collected at shorter intervals. The experiment was terminated when one of the following took place.

a. Fluid saturation: The organic fluid penetrated the protective Gore-tex breathing membrane through imperfections in the sealing between the membrane and the inside cylinder. Once in contact with the C/EOC, the fluid could either have penetrated the circuitry and created a short or it could have been adsorbed on the defective membrane disk and resulted in a sudden increase in activation energy that would have overflowed the range of the C/EOC output.

b. Vapor saturation: The organic odor molecules penetrated the membrane disk, occupying all available adsorption and solvation sites on the membrane and generating activation energies equivalent to the maximum range of the C/EOC. Past this point (11 volts) no variation in output voltage could be monitored.

c. Equilibrium state: Upon complete monolayer or multiple adsorption, the membrane was saturated and would not adsorb any incoming molecules unless it could have desorbed some adsorbed species. This may have been less than the maximum range of the output voltage.

After completion of this step the testing was stopped. The C/EOC was pulled out and purged with freon-12, forcing its complete decontamination. Subsequently, the C/EOC was placed back in the cylinder and a second set of data was taken. As expected, it was not necessary to

wait long for the volatile organic vapor to arrive at the olfactory reach of the C/EOC for repeat testing. The data monitoring started at short time intervals and continued to saturation of the membrane.

6.6 CONTROLLING SIDE LEAKAGE IN ANNULAR SAMPLES

As mentioned previously, the flexible wall in a permeameter provides great advantages over a rigid wall. In this experiment, however, the sample was annular and thus constrained by two boundaries, inner and outer. The outer boundary was chosen to be a flexible membrane in a triaxial set-up. The inner boundary, i.e., the cylindrical housing of the C/EOC was rigid and side leakage along the smooth surfaces of this portion of the boundary was an ever-present possibility.

In order to rectify this problem, two steps were taken. First, the outer surface area of the brass tube was covered with a waterproof epoxy and rolled in a clay bed. This gave the surface a nonsmoothness and provided for better packing uniformity with the rest of the sample. This procedure can also help to prevent formation of continuous fingering flow channels by obstructing the path of such formations. The second step was to apply an effective stress of 10 psi to the sample, expecting that the stress would be transmitted without much damping to the inner boundary, thus providing for a continuous firm and nonyielding (to the flow channels) interface between the sample and the brass tube. The results of this second step were checked by x-ray films of the sample to check (visually) for discontinuities along the sample brass interface. As shown in Figure 6.8, such discontinuities did not exist meaning that application of 10 psi confining pressure has precluded the presence of such "air gaps" and flow channels.

6.7 TEST RESULTS FOR PHASE II

Figures 6.9 through 6.15 present plots of output voltage vs. time for C/EOC response in kaolinite and silt samples. The C/EOC was placed in annules of the triaxial testing apparatus at the start of permeation and the output voltage was automatically monitored for 3 concentrations of the permeant simultaneously. The data acquisition unit was programmed to record data for shorter time intervals if the time rate of change of voltage between two successive readings exceed a limit value of 0.2 millivolts for 10,000 seconds. This was done to enhance monitoring of the C/EOC response during times of actual organic adsorption. Data were collected for 60,000 seconds past the time of initial responses, after which the test was stopped, the cone was purged with freon and checked for complete decontamination by letting it maintain zero output voltage for 10 minutes. Immediately following this step the C/EOC was placed back in the cylindrical cavity of the triaxial chamber and the output voltage was monitored for about 60,000 seconds. The second set of tests is a repetition of the first response monitoring and serves as an indication for reproducibility of C/EOC response in contaminant monitoring in soil environment. The time of initial response for repeat tests is practically zero. This is due to the fact that the contaminant is already available within the olfactory reach of the EOC.

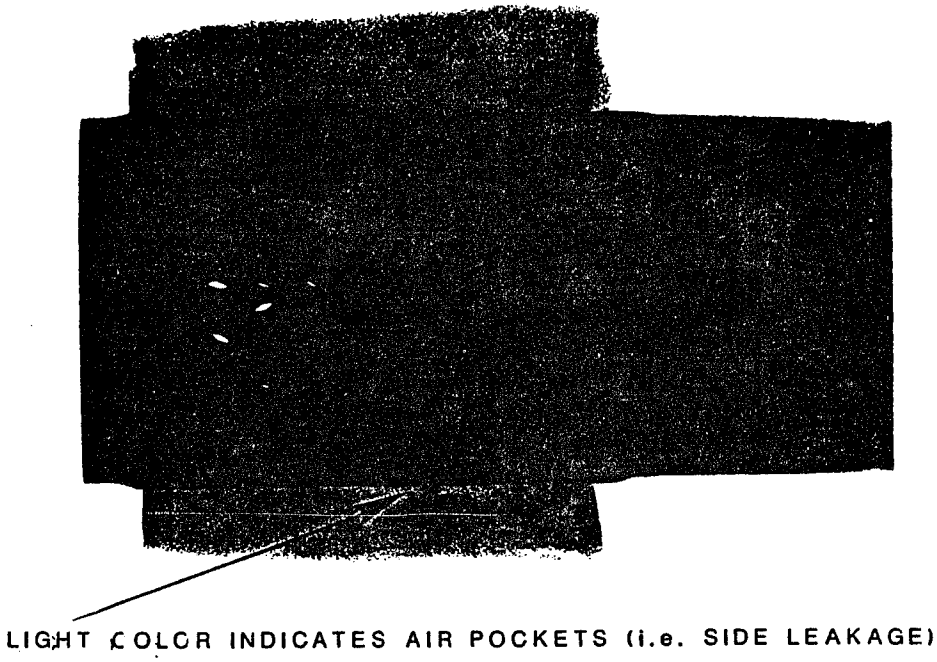

Figure 6.8 X-ray detection of side leakage.

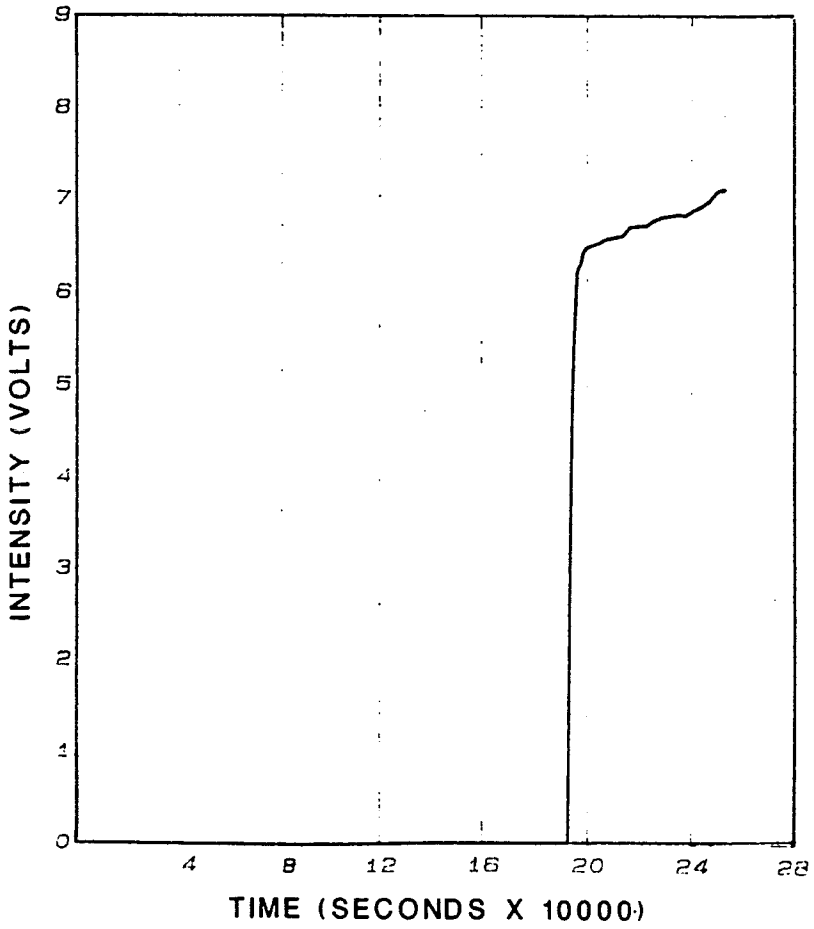

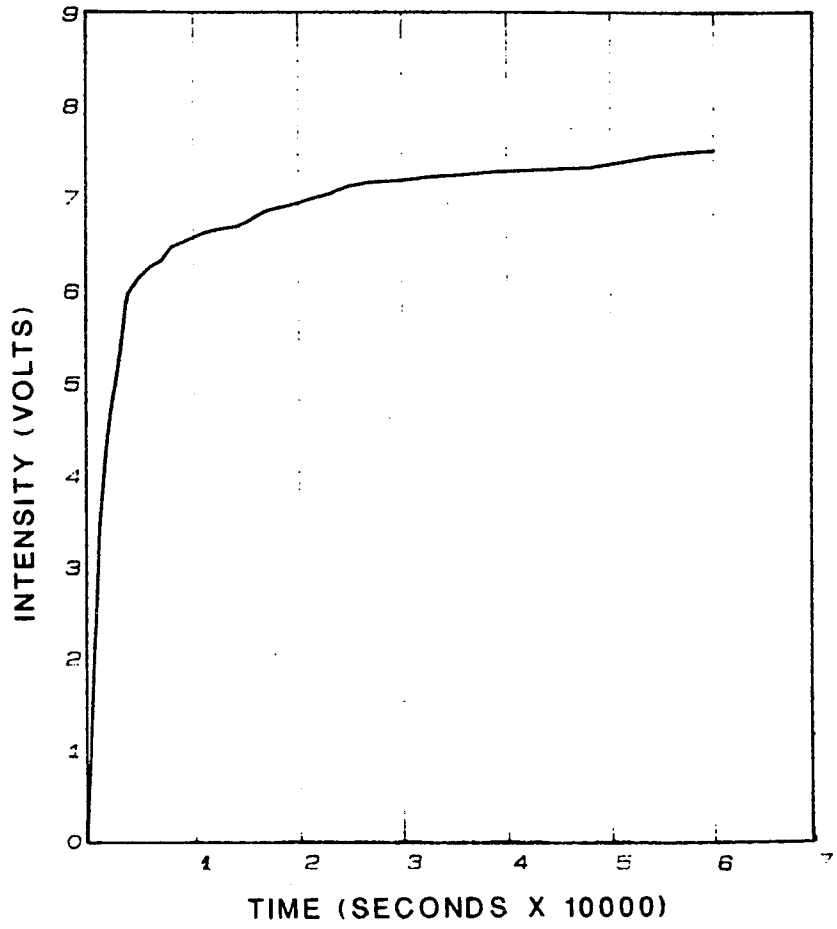

Figure 6.9. C/EOC output voltage vs. time for acetone permeated through compacted kaolinite samples.

6.9.a. 50% acetone permeation (first test).
6.9.b. 50% acetone permeation (second test).

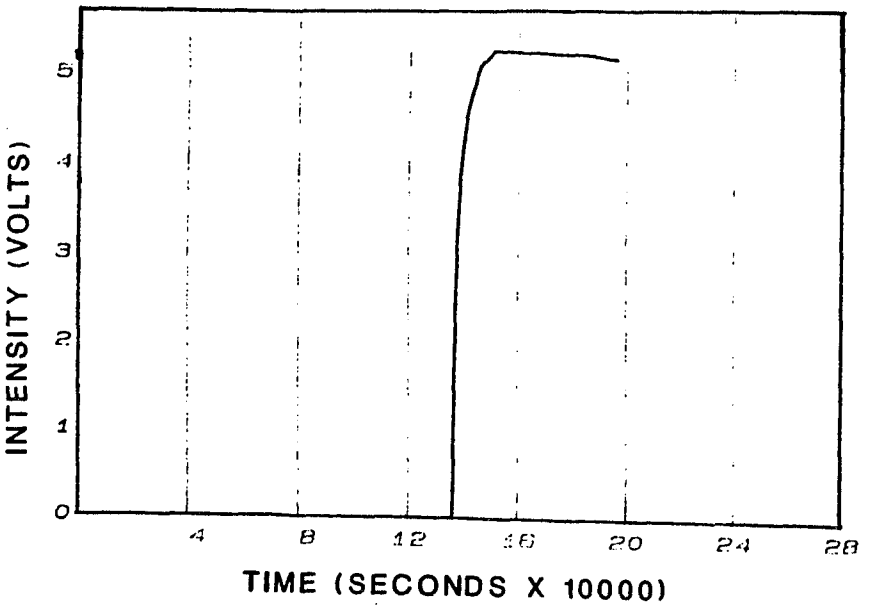

Figure 6.9.c. 25% acetone permeation (first test).

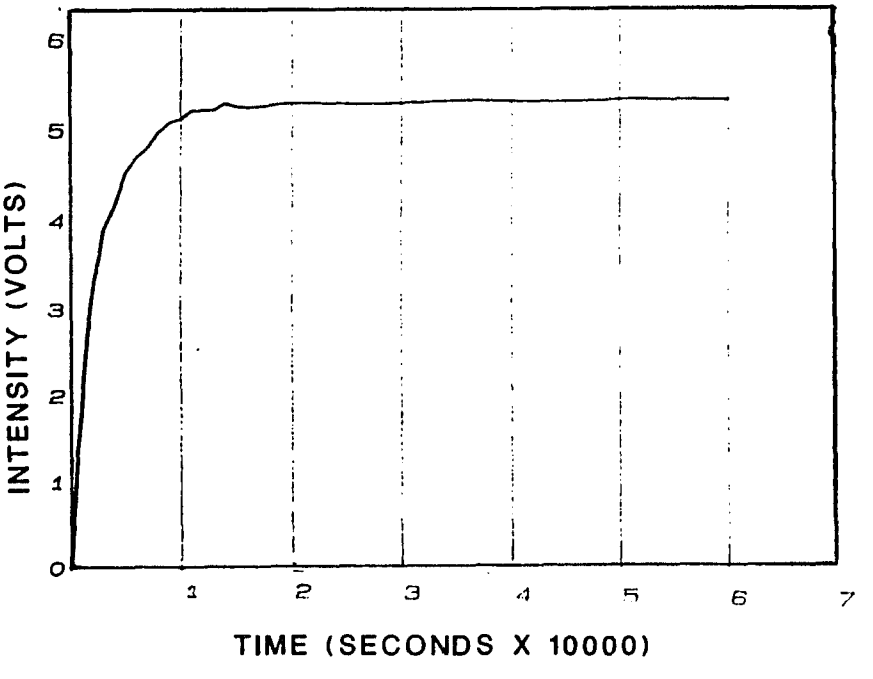

Figure 6.9.d. 25% acetone permeation (second test).

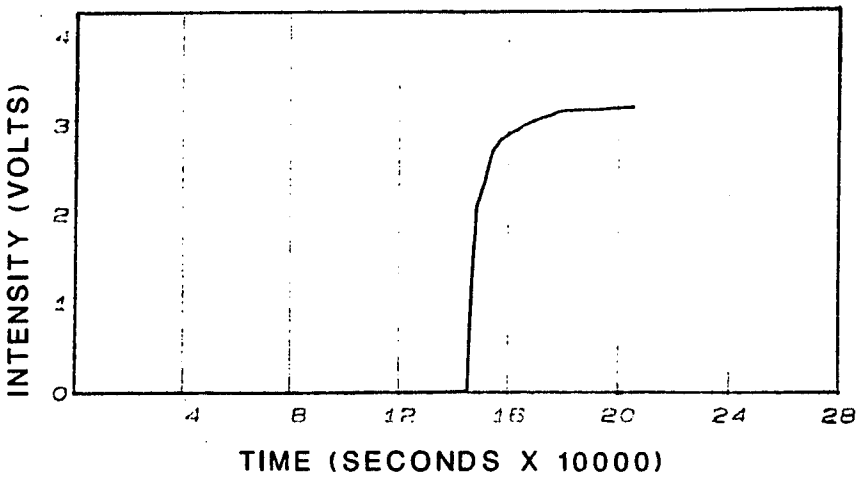

Figure 6.9.e. 10% acetone permeation (first test).

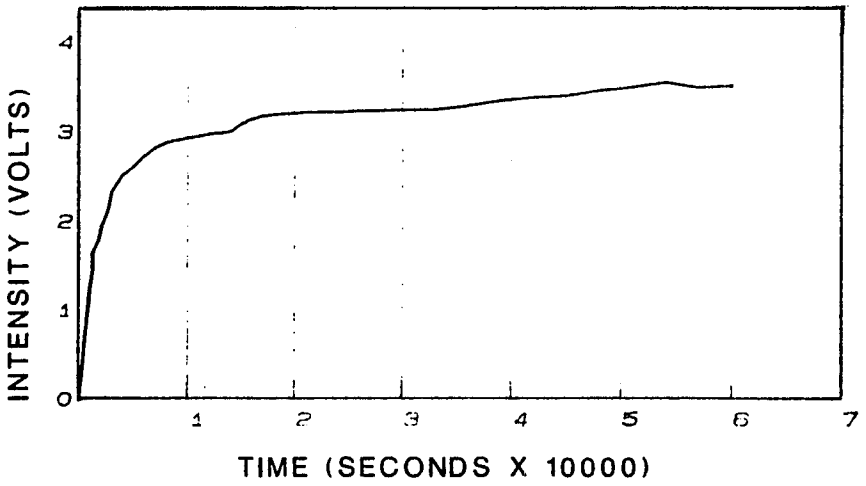

Figure 6.9.f. 10% acetone permeation (second test).

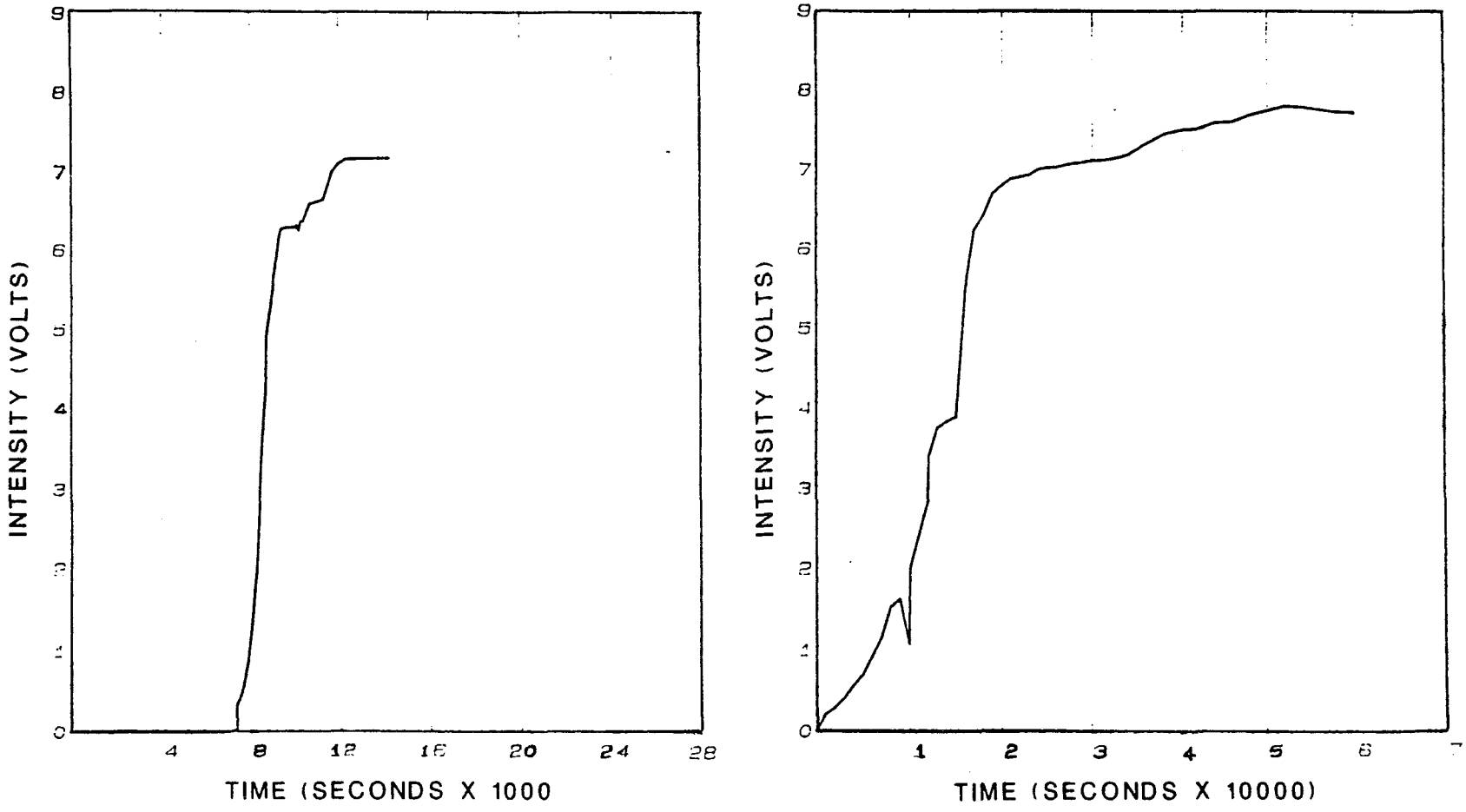

Figure 6.10. C/EOC output voltage vs. time for methanol permeated through compacted kaolinite samples.

6.10.a. 50% methanol permeation (first test).
6.10.b. 50% methanol permeation (second test).

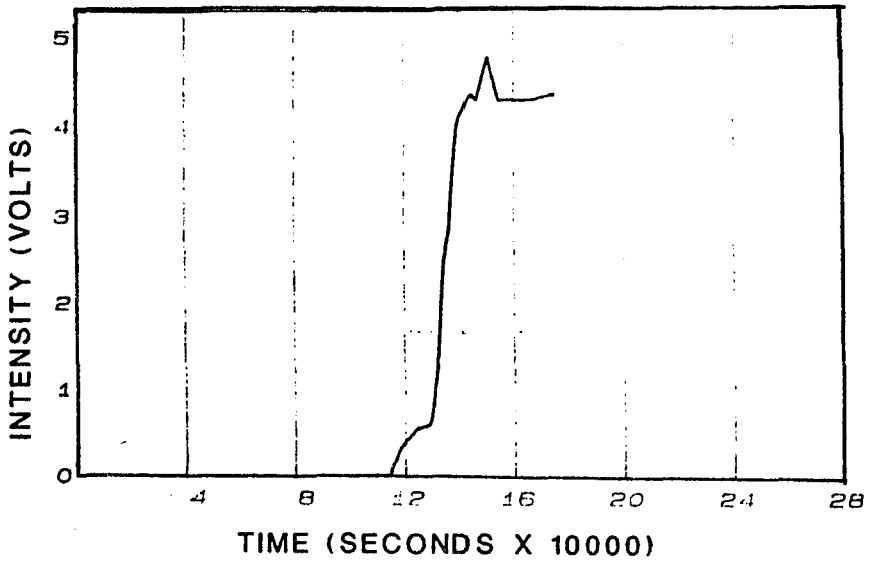

Figure 6.10.c. 25% methanol permeation (first test).

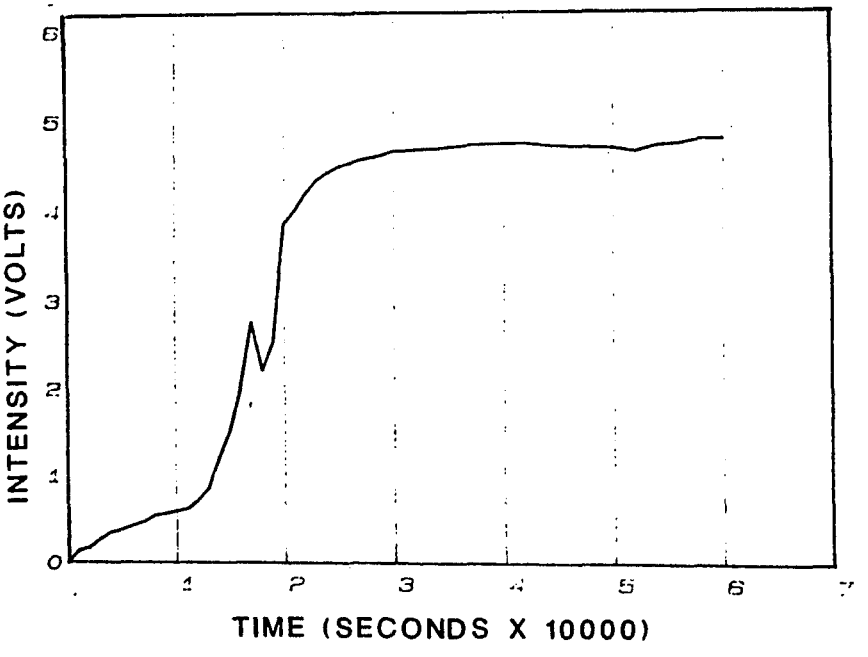

Figure 6.10.d. 25% methanol permeation (second test).

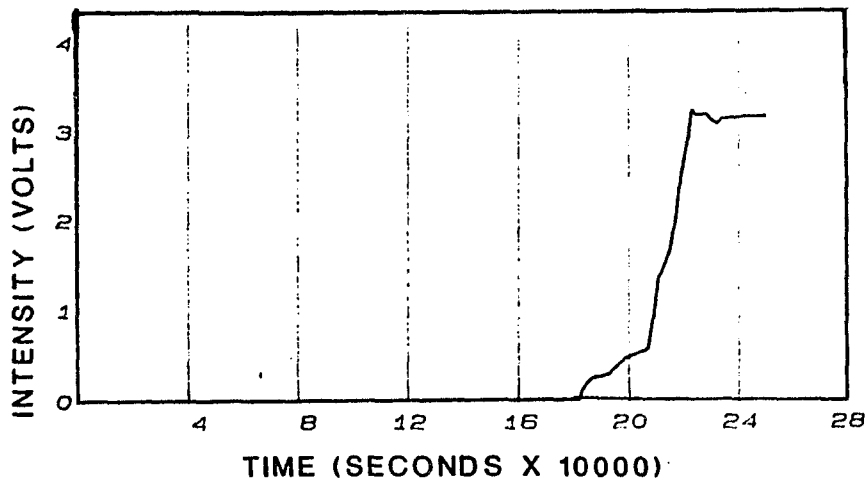

Figure 6.10.e. 10% methanol permeation (first test).

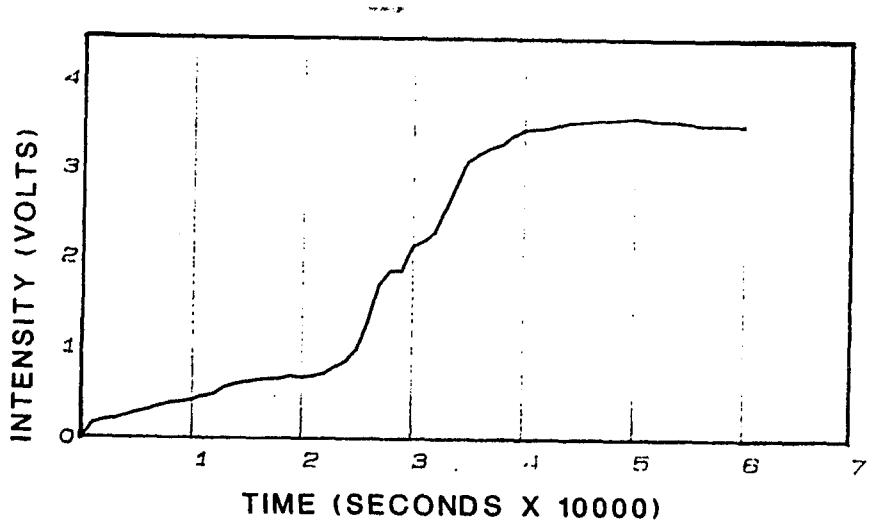

Figure 6.10.f. 10% methanol permeation (second test).

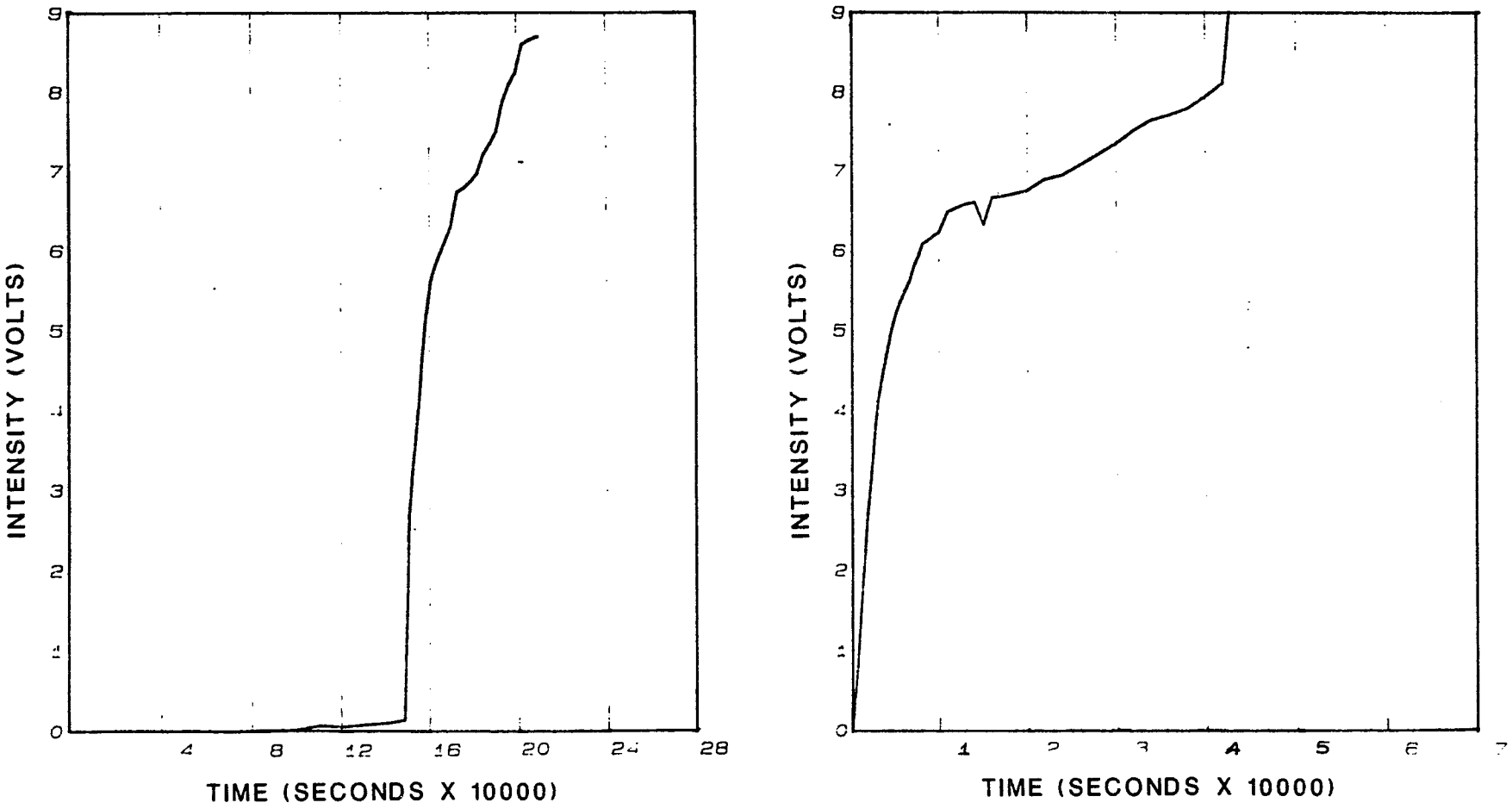

Figure 6.11. C/EOC output voltage vs. time for acetic acid permeated through compacted kaolinite samples.

6.11.a. 50% acetic acid permeation (first test).
6.11.b. 50% acetic acid permeation (second test).

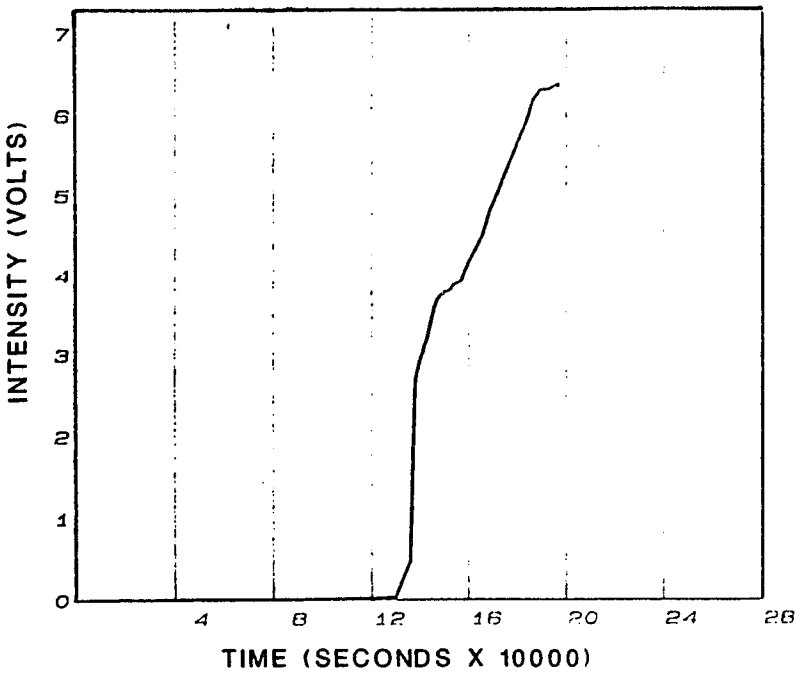

Figure 6.11.c. 25% acetic acid permeation (first test).

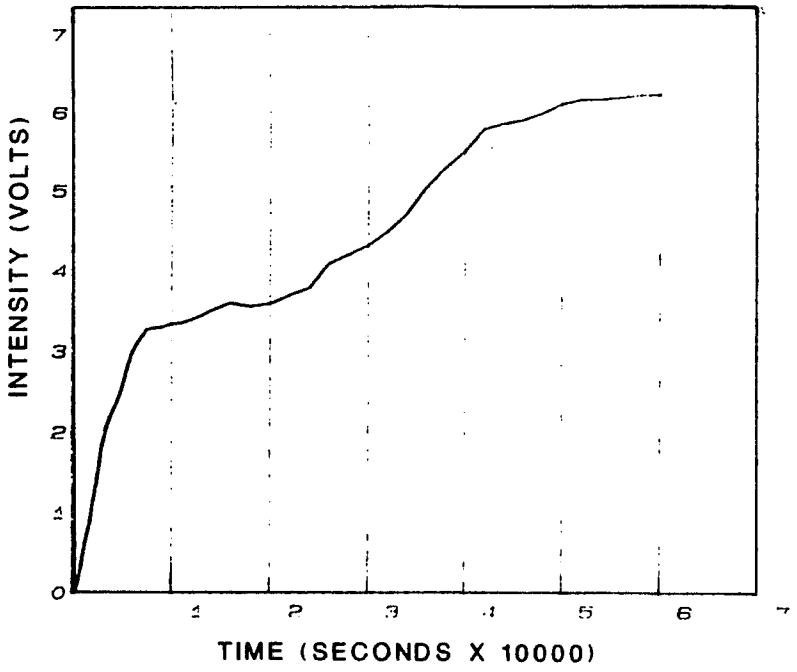

Figure 6.11.d. 25% acetic acid permeation (second test).

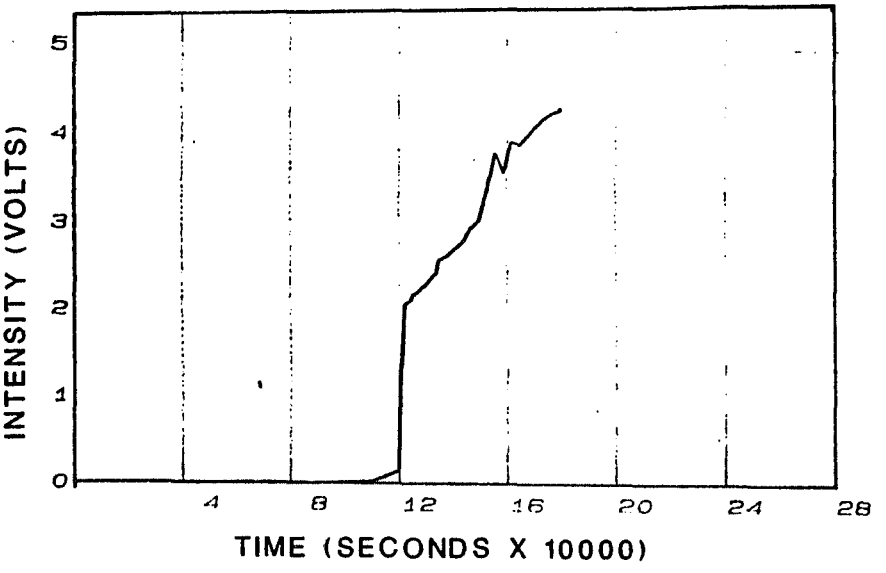

Figure 6.11.e. 10% acetic acid permeation (first test).

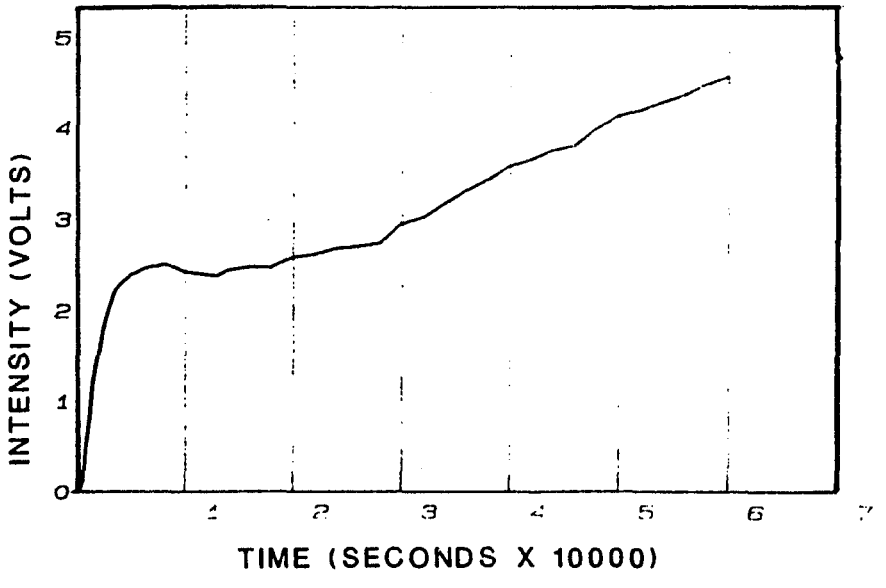

Figure 6.11.f. 10% acetic acid permeation (second test).

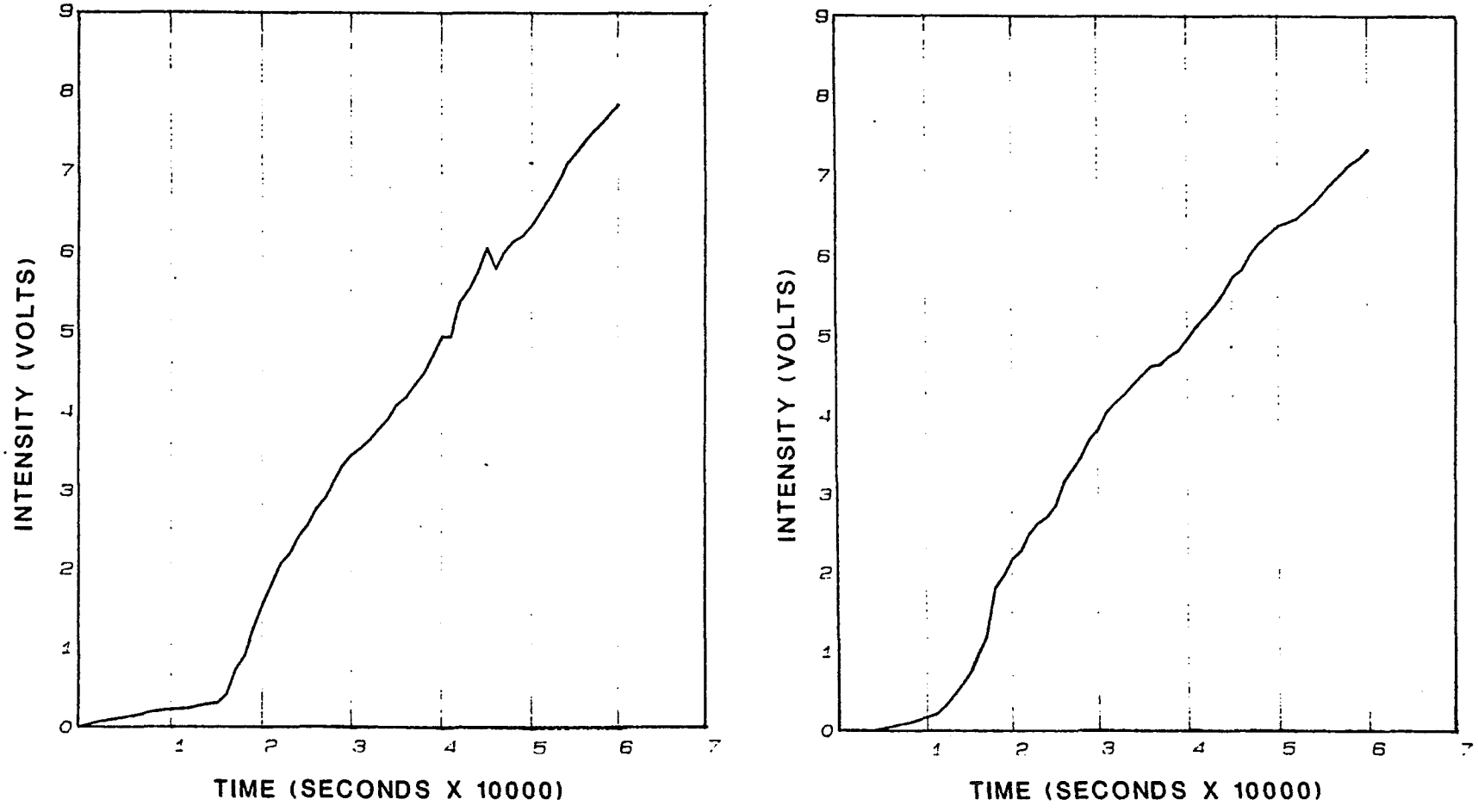

Figure 6.12. C/EOC output voltage vs. time for dichloromethane permeated through compacted kaolinite samples.

6.12.a. 100% dichloromethane permeation (sample one).
6.12.b. 100% dichloromethane permeation (sample two).

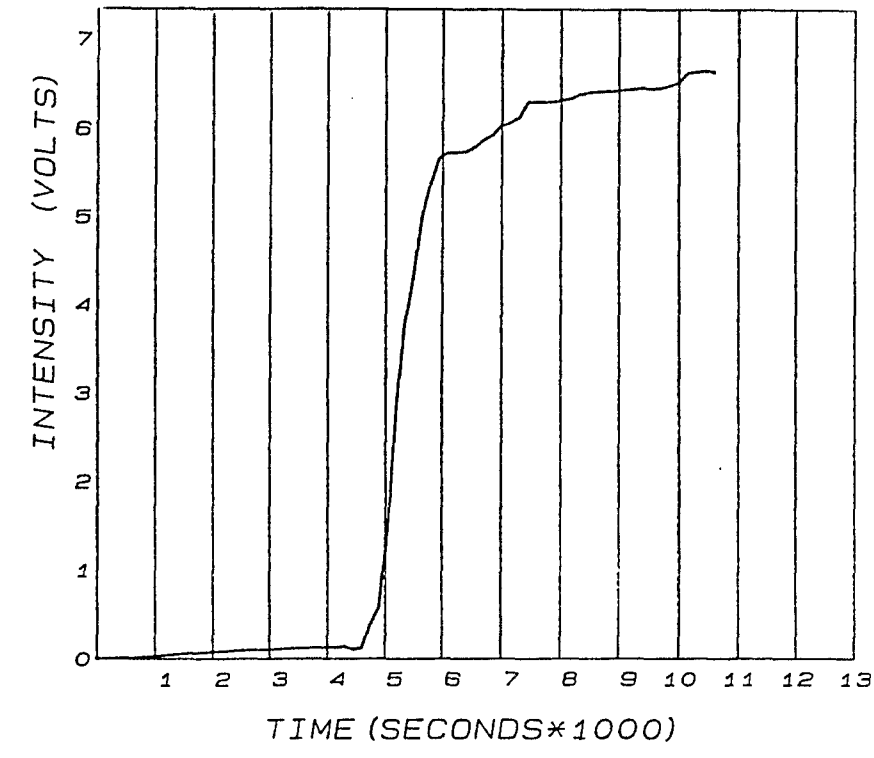

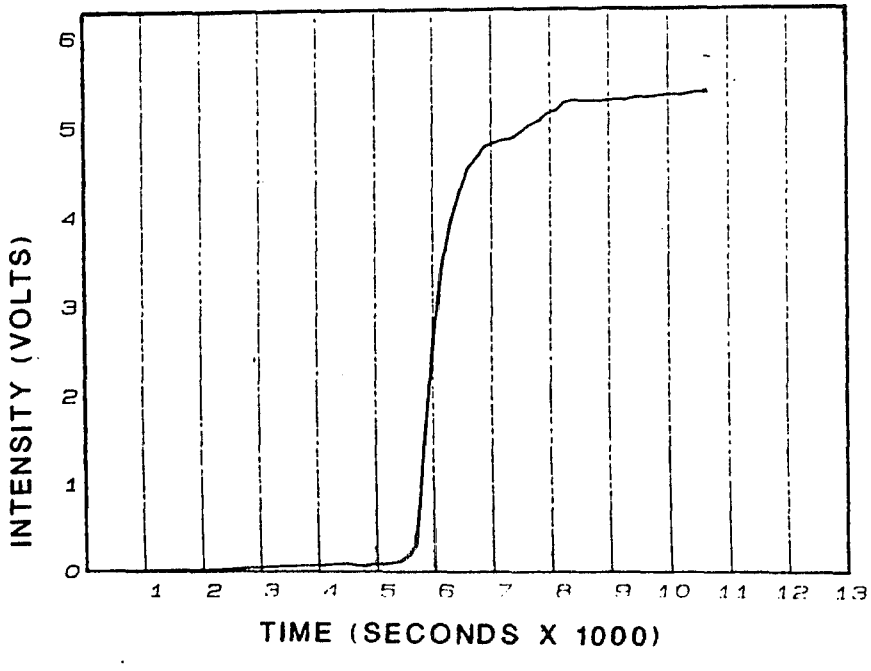

Figure 6.13. C/EOC output voltage vs. time for acetone permeated through compacted silt samples.

6.13.a. 50% acetone permeation.
6.13.b. 25% acetone permeation.

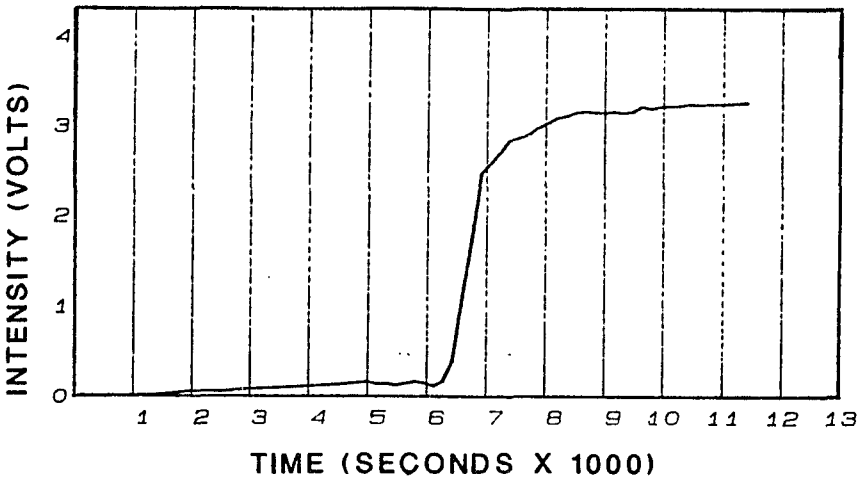

Figure 6.13.c. 10% acetone permeation.

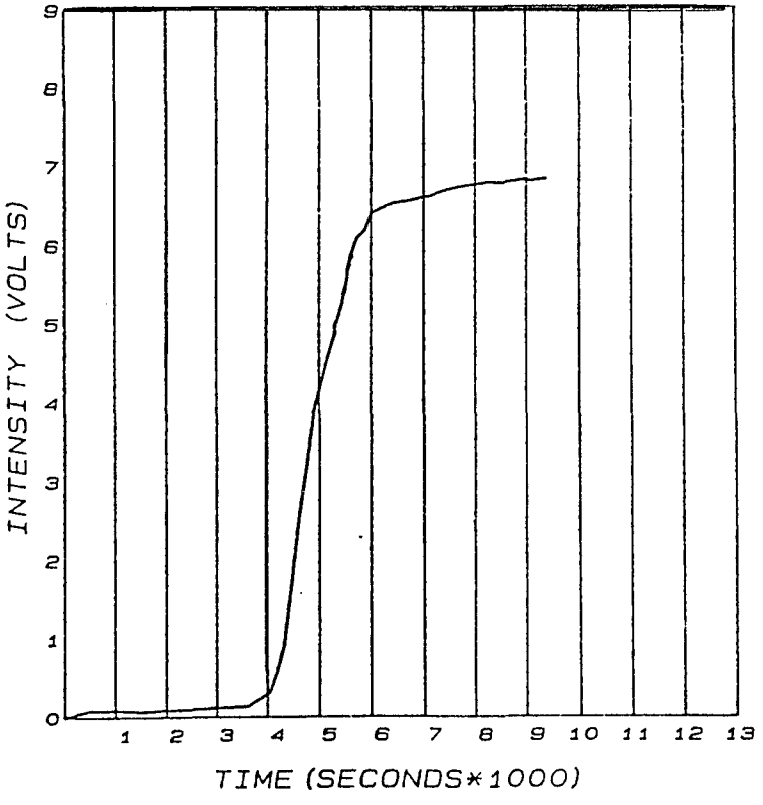

Figure 6.14. C/EOC output voltage vs. time for methanol permeated through silt samples.

6.14.a. 50% methanol permeation.

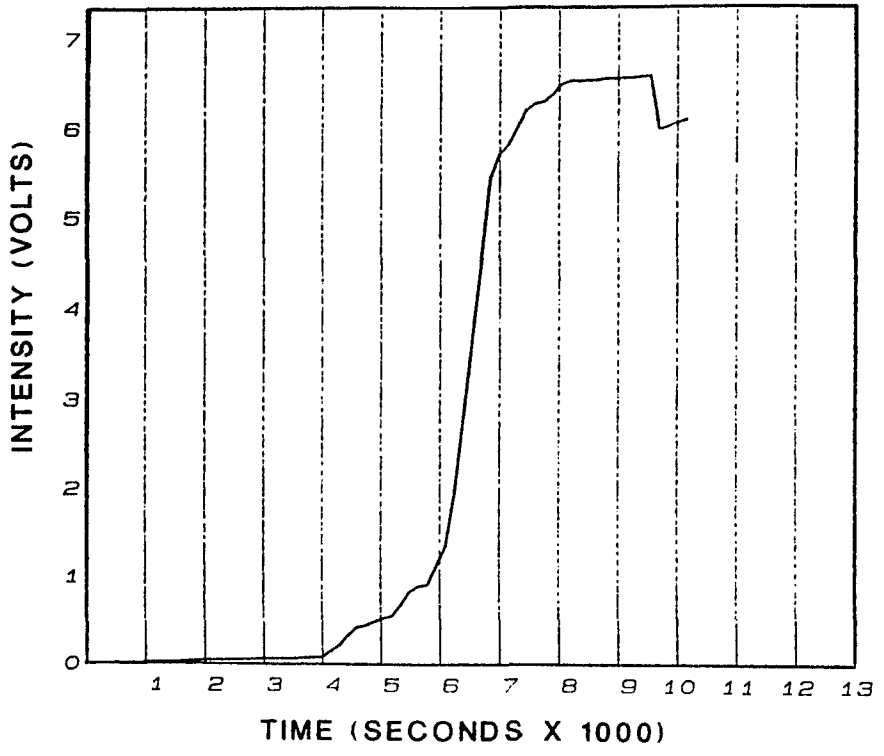

Figure 6.14.b. 25% methanol permeation.

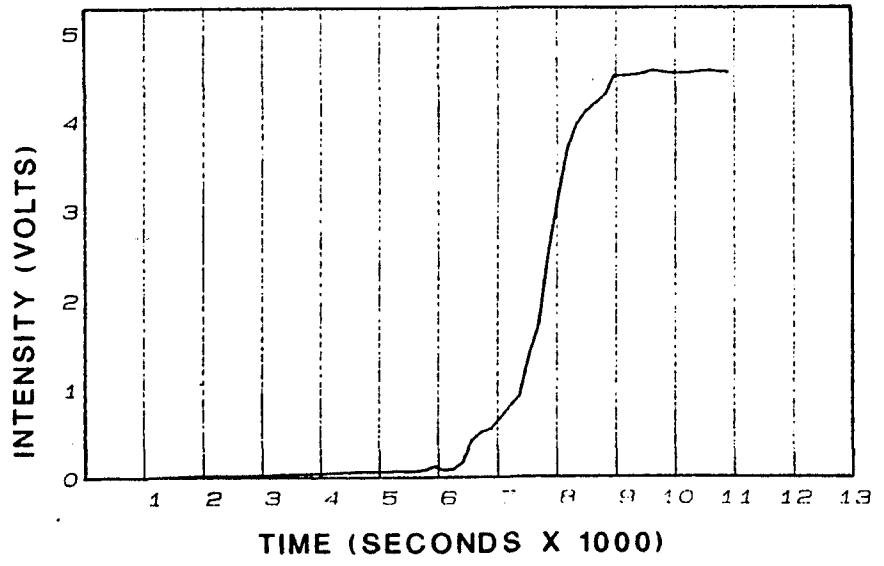

Figure 6.14.c. 10% methanol permeation.

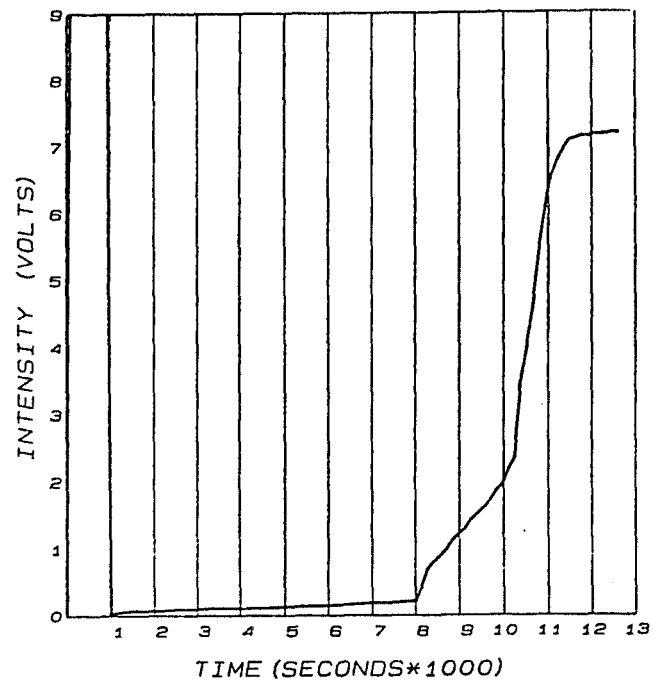

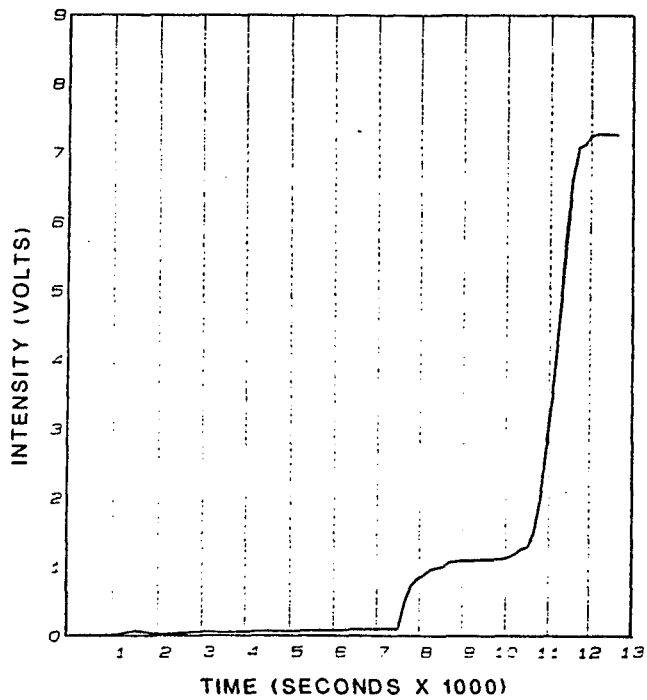

Figure 6.15. C/EOC output voltage vs. time for acetic acid permeated through silt samples.

6.15.a. 50% acetic acid permeation.

6.15.b. 25% acetic acid permeation.

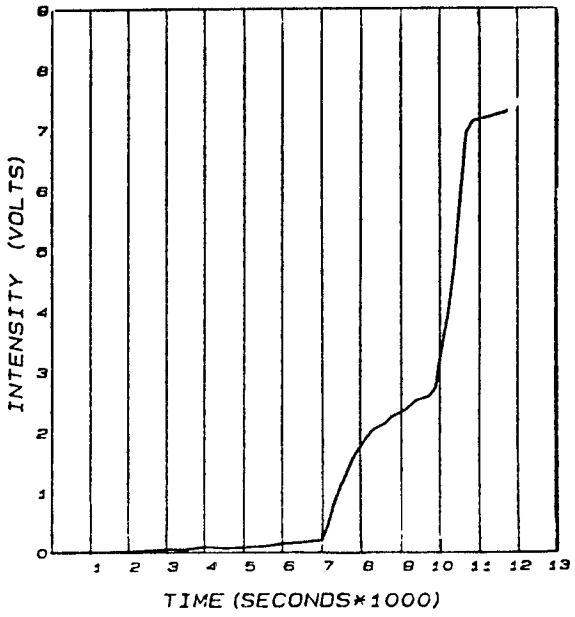

Figure 6.15.c. 10% acetic acid permeation.

CHAPTER 7

ANALYSIS OF RESULTS

7.1 INTRODUCTION

This chapter presents the results of the study for olfactometric contaminant detection in soils. This investigation was initiated for testing the reliability of an olfactometric device in ambient conditions. Tests with a host of organic and membranes were conducted to determine the membrane most suitable for use in contaminant detection in soils.

7.2 AMBIENT TESTING

The first phase of this study addressed factors influencing EOC output, including temperature and pressure of the testing environment, externally applied ionic fields, membrane pore size, membrane composition, vapor pressure, surface tension, and molecular weight of the contaminant. The variables of significant contribution were related to the EOC output voltage in a regressional model.

7.2.I EFFECTS OF TEMPERATURE ON EOC OUTPUT

When EOC is used for in situ monitoring of the contaminants, it may be exposed to severe changes in temperatures. In order to monitor and if necessary calibrate the effects of temperature fluctuations on EOC response, experiments were conducted in the following laboratory set-up:

The constant temperature bath was kept at -5°C and the experiment was conducted as explained in Chapter 6. The same procedure was repeated for bath temperature of 24°C.

The experimental results of the output voltage vs. time are shown in Figures 7.2 (a-e). The general conclusions from these figures show that

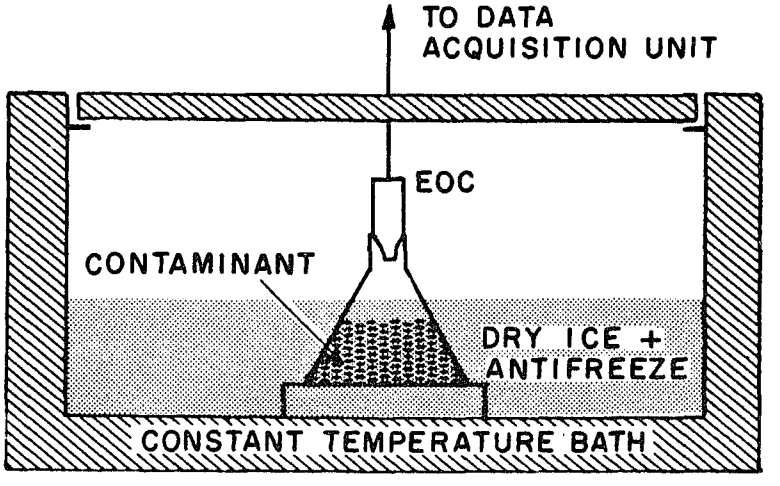

Figure 7.1. Laboratory set-up to examine effects of temperature on EOC response.

lower temperatures induce an instability in output voltage and that the effect of temperature on the EOC output is not significant. However, there exists a small decrease in the output levels at lower temperatures which can basically be attributed to the reductions of the mobility (i.e., lower vapor pressure of the contaminants in the lower temperature environment as expressed by the ideal gas law ($PV=n\bar{R}T$).

7.2.II EFFECT OF PRESSURE

Adsorption of odor molecules on the membrane surface is a pressure and temperature dependent process. Higher vapor pressure is normally demonstrated as larger fractions of the surface being covered with the guest molecule. It is for that reason that organic chemicals with higher vapor pressures demonstrate better detectability. Subjecting the EOC to externally applied pressure is expected to enhance the response of EOC to a given organic chemical, thus making chemical detection in environments where the pore pressure is high more reliable. To verify this fact and

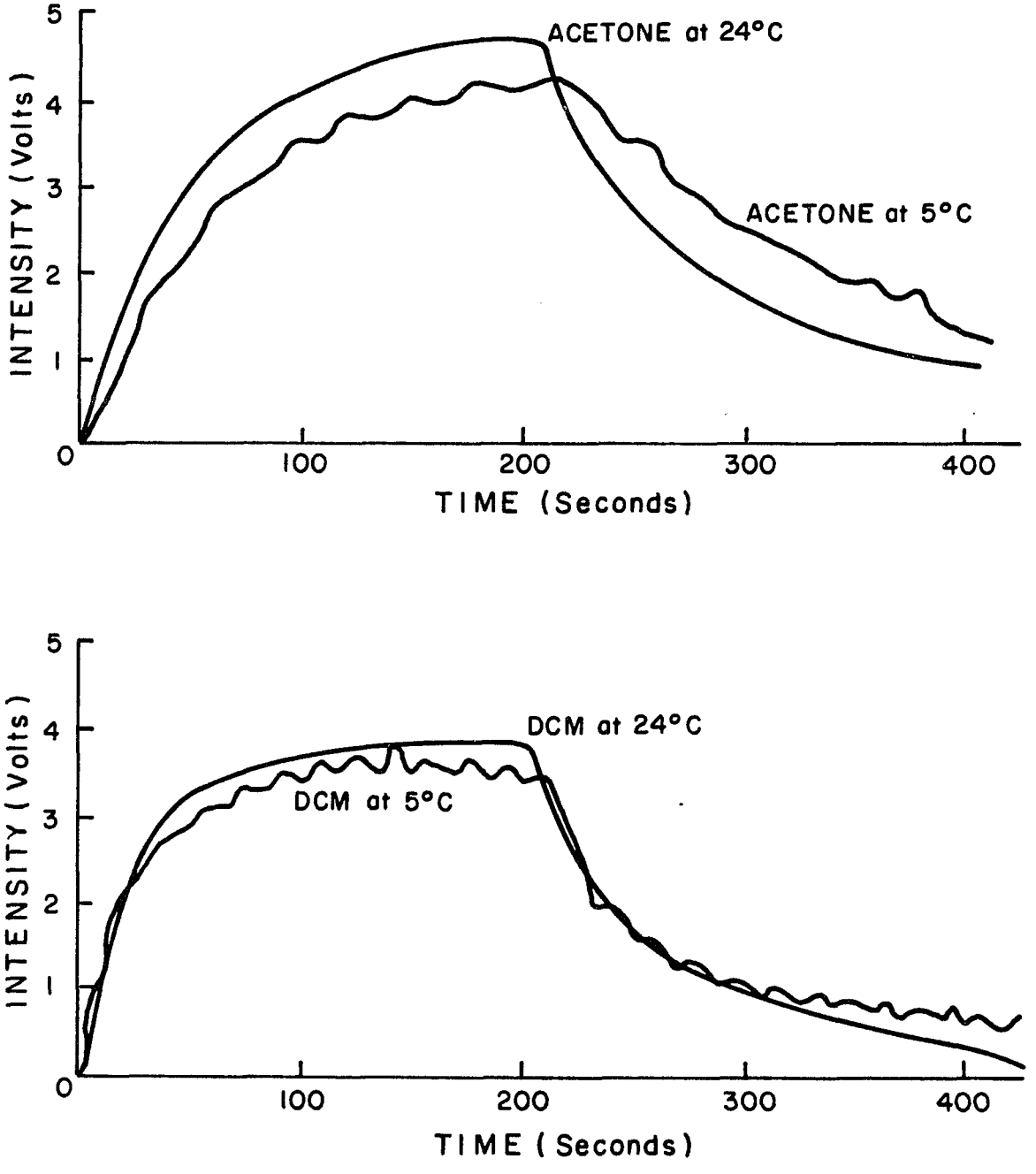

Figure 7.2. Effect of temperature on EOC response.

a. Acetone.

b. Dichloromethane.

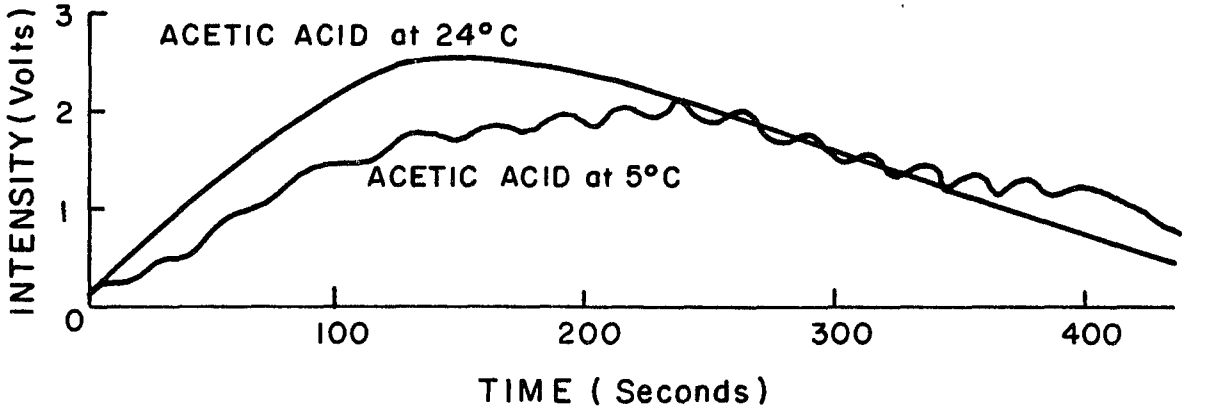

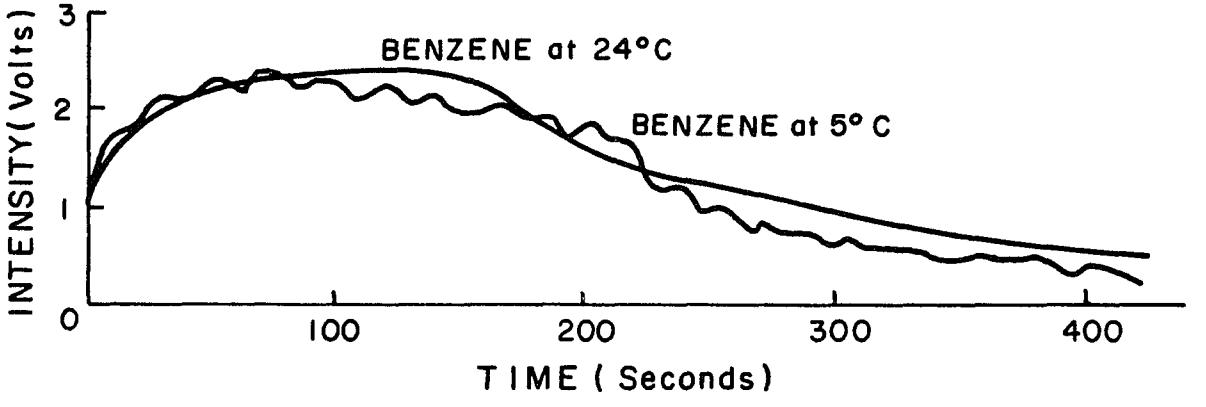

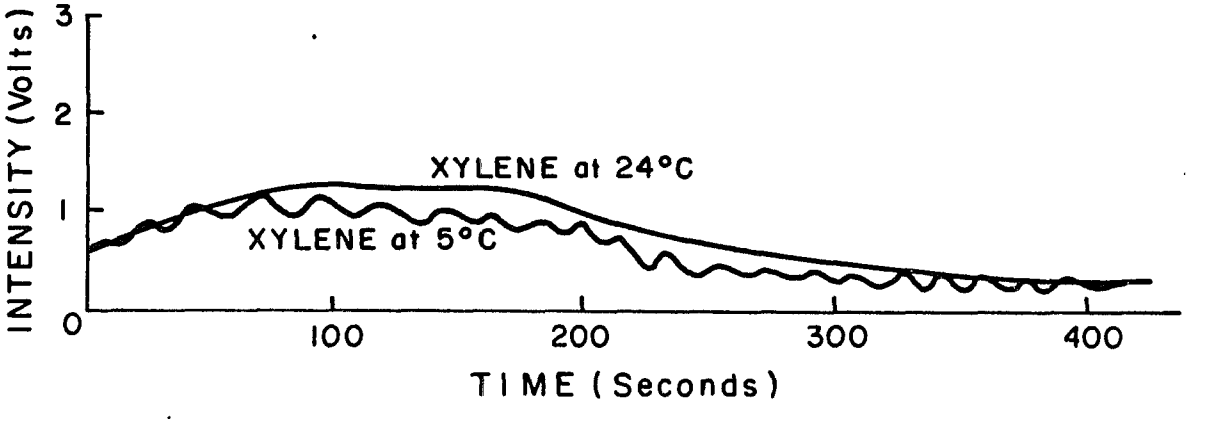

Figure 7.2.c. Acetic acid.

Figure 7.3.d. Phenol.

Figure 7.3.e. Xylene.

also check on the effects of sudden increases in pressure around EOC the following experiment was initiated.

In a specially designed triaxial cell, (Figure 7.3), the EOC was immersed in an acetone-water mixture. At time zero, the pressure valve was opened at once and the response was monitored. Figure 7.4 shows the test results when EOC is subjected to ambient, 1 PSI and 2 PSI pressure. The effect of pressure on EOC response is similar to that of the application of an ionic field, the exception being the residual voltage. In application of an ionic field, there was no residual voltage, whereas in elevated pressures the residual voltage is present.

The sudden rise in response voltage in this experiment was due to a sudden increase in partial pressure of the vapor present in the chamber. Once the pressure is stabilized and the differential pressure between the vapor and EOC opening is eliminated, the output voltage achieves a steady state response.

The test results support the hypothesis that the sudden triggering mechanisms have only short-lived effects on EOC response.

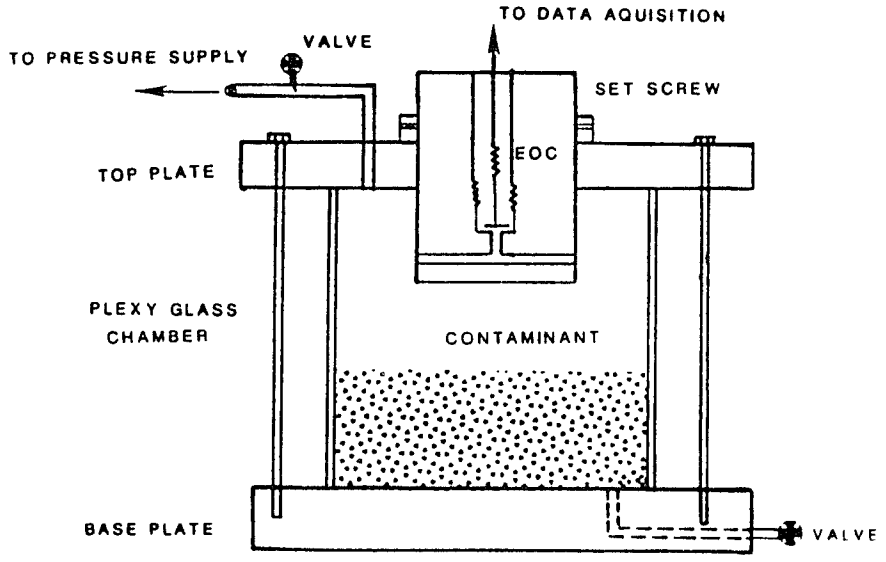

Figure 7.3. Triaxial set-up for pressure testing of odor cone.

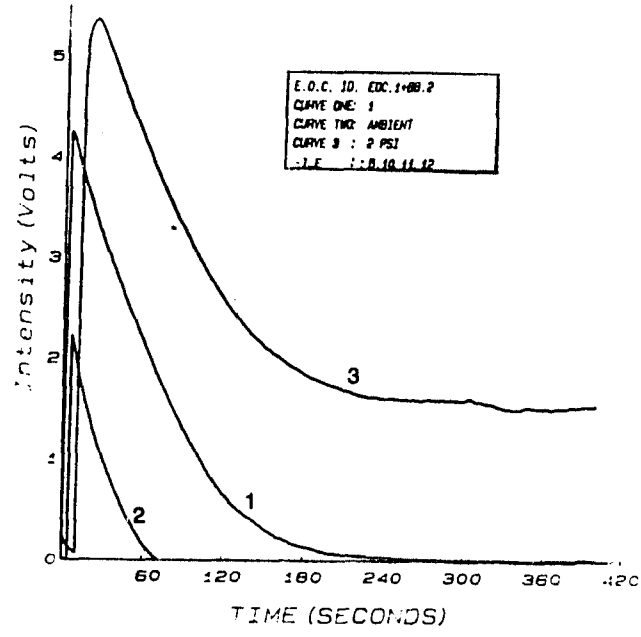

Figure 7.4. Results of pressure testing with the odor cone.

7.2.III EFFECTS OF EXTERNALLY APPLIED IONIC FIELD

Membrane polymers contain electrical charges in the form of atomic nuclei, electron and polar groups. Although they cannot leave their parent molecules, electrons will shift their center of motion a distance, d, in the positive direction of an electric field. The proton of hydrogen atoms shift their center of vibration toward the negative electrode. Polar groups and polar molecules align themselves with the electric field.

Under the application of an ionic source an ionic atmosphere will be generated whose coulomb potential at a distance r from an ion of charge $Z_i e$ is

$$\phi_i(r) = \frac{Z_i e}{4\pi\varepsilon_o\varepsilon_r r} \qquad (7.1)$$

where ε_r = relative dielectric constant of the medium

$\phi_i(r)$ = Coulomb potential

ε_o = vacuum dielectric constant

Polarization is brought about electronically (arising from an electron displacement within the atom), ionically (from comparable displacement of ions and atoms), orientationally (from preferential orientation of permanent dipole due to application of an electric field), and space charge polarization (due to pressure of lower resistivity materials within the dielectric).

The inclusion of conductive phases in the membrane will make the membrane, and thus EOC, responsive to the application of electric fields through polarization of membrane molecules.

Polarization is a thermodynamically reversible behavior of the polymer within an electric field involving no dielectric loss. Its reversibility, however, depends on whether there is sufficient time available for the necessary electronic, atomic, and dipole moments.

The polarization does not disappear immediately when the field is removed; rather, the electronic and ionic polarizations are relaxed and a residual, polarization P_n, persists. An opposing coercive field, $-E_c$, is required to balance the domain and reduce the net polarization to zero.

The instantaneous value of polarization is $P = (E-1)k_o$ where E is the dielectric constant and k_o is the specific electrolyte concentration. In a binary system, such as the one existing in the EOC, polarization causes changes in the dielectric constant (see 2.3.IV).

In subjecting the EOC to an electric field for response monitoring a "zerostat" (MFG. by Jensen, Columbia, MD) gun was used. Zerostat gun operates by utilizing two powerful piezo electric crystals and a compression trigger. A slow squeeze of the trigger emits a stream of positive ionized air over a surface. As the trigger is released, a negative shower of air particles is produced. The end result is complete reversal and neutralization.

EOC response to zerostat was prompt in both gain and dissipation with zero residual charge (Figure 7.5). The magnitude of the peak voltage depends on the intensity of the electric field and duration of its application. The peaks in Figure 7.5 correspond to single trigger and multiple triggers as identified in the graph.

The outstanding character of the response of EOC to application of ionic fields is that upon removal of the cause (zerostat ionic field generator) the effect (voltage output) immediately disappears without leaving any residual charges on the system. This phenomenon is different from EOC response to reactive organics which leaves a residual charge on the system.

The implications of these experiments are that if during its monitoring of a contaminant C/EOC is subjected to a sudden electric or ionic field the reflections of the intruding electrical or ionic factors can be differentiated from normal contaminant monitoring response and consequently can be filtered in data manipulation process.

7.2.IV EFFECT OF MEMBRANE PORE SIZE ON EOC RESPONSE

Membranes are basically very porous. Their porosity ranges from 70% to 80%. Membrane pores take different shapes, arrangements, and sizes. The pores are intended to entrap contaminant molecules when membranes are used as molecular sieves.

When odor molecules come in contact with the micropores of the membrane, they are adsorbed onto the walls of the micropores, leading to volume filling of the micropores. In this sense, micropores are potential fields into which contaminant molecules "fall." The speed and extent of adsorption and the response then may depend on the size and frequency of pores.

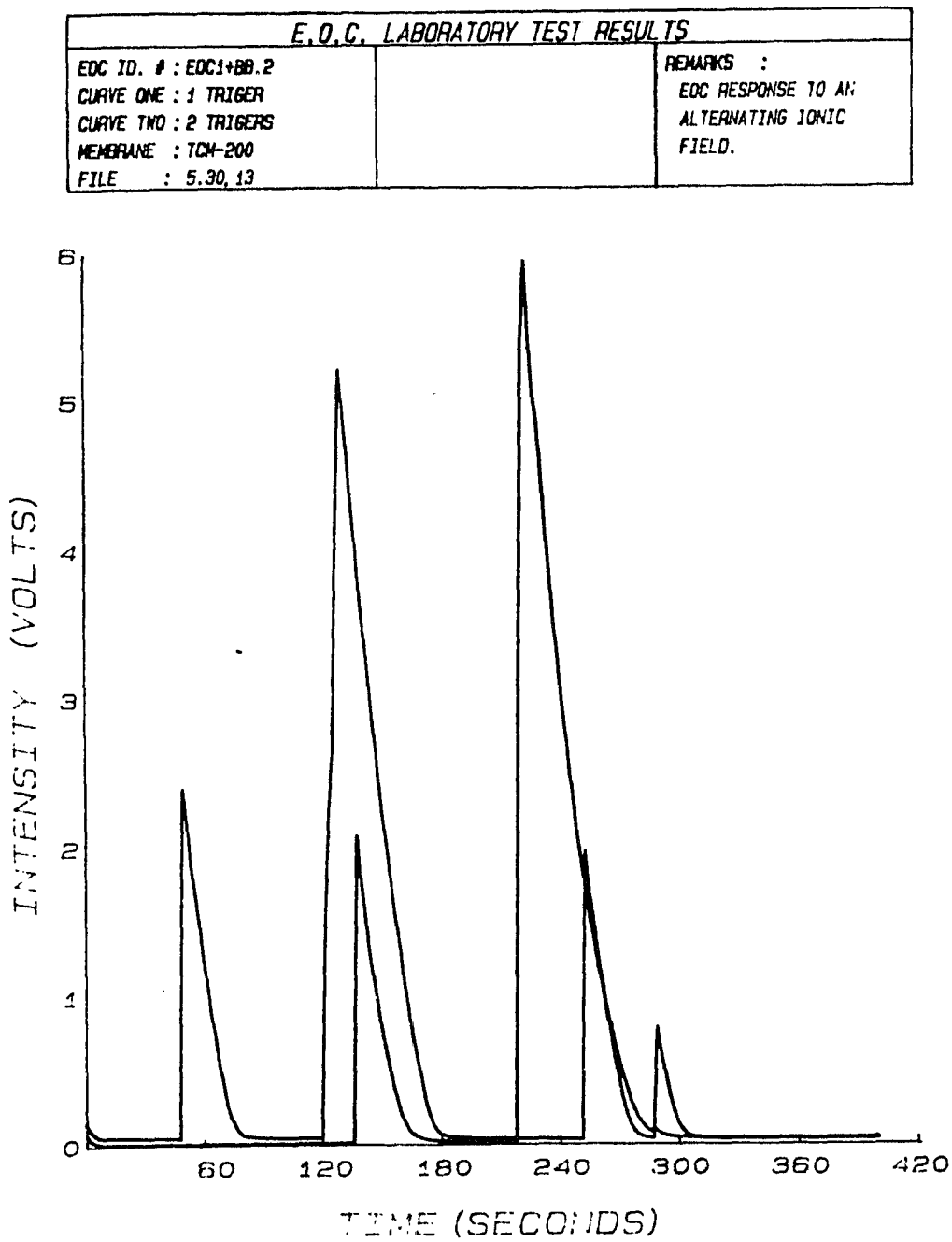

Figure 7.5. EOC response to externally applied ionic field.

In laboratory experiments, different pore sizes of the same membrane were exposed to different contaminants. Figure 7.6 shows the test results. The variation in response for the most part falls within the margin of repeatability. This suggests that the response is independent of the pore size of the membrane. The figures, however, can reinforce a previous statement that the pore size effect is different for different membrane-contaminants groups. That is, a membrane with a .8μ pore size may yield a higher output than with a .2μ pore size for one contaminant but a lower output for another. This is due to the different size compatibility between the contaminant molecule and the membrane pores. Regression analyses of the results (section 7.5) indicate a poor correlation between the output voltage and the membrane pore size.

7.2.V EFFECTS OF MEMBRANE COMPOSITION ON EOC OUTPUT

The effects of membrane composition on EOC output have been discussed in terms of the correlation between the solubility of a membrane in a contaminant and the output voltage. To study the effects of membrane material on the EOC output, the membranes were grouped according to their composition. The average response of each group to each contaminant was calculated and tabulated as shown in Table 7.1.

Table 7.1. Average response (millivolts/sec) of each contaminant to a membrane group.

Membrane composition	Membranes included in the group	Contaminants AC	MT	ET	DCM	AA	EG
PTFE	: TE30,Teflon,Mitex	.27	2.4	0	.63	0	0
RC	: RC-59	2.4	23.7	8.6	-.8	7.2	1.8
CTA	: GA-8,TCM	23.3	12.6	.6	28.4	.7	.06
CA	: Acetate,ST-68	.35	2.7	1.9	2.0	.6	.05
NC	: BA85,AE95,AE70	32.6	21.8	.6	28.4	.7	-.16
MEC	: MF-millipore	26.3	19.2	.02	43.4	-.1	-.4
ACP	: Versapore	48.1	47.8	42.2	51	42	1.9
PVD	: Durapore	54	10	2.3	47	-.5	-.9

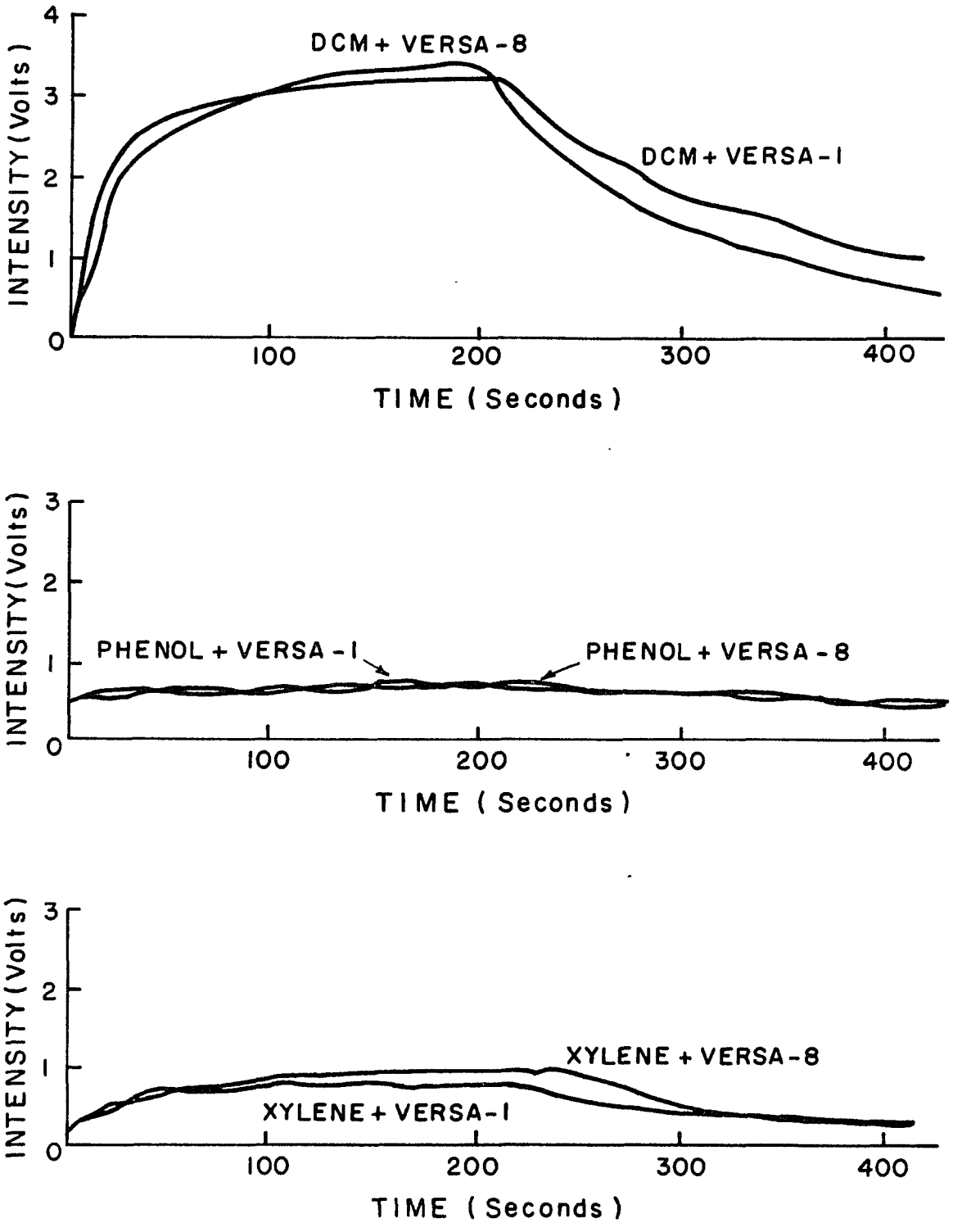

Figure 7.6. Effect of membrane pore size on EOC response membrane is versapore with pore sizes of .8μ and 0.2μ.

a. Acetone.

b. Acetic acid.

c. Benzene.

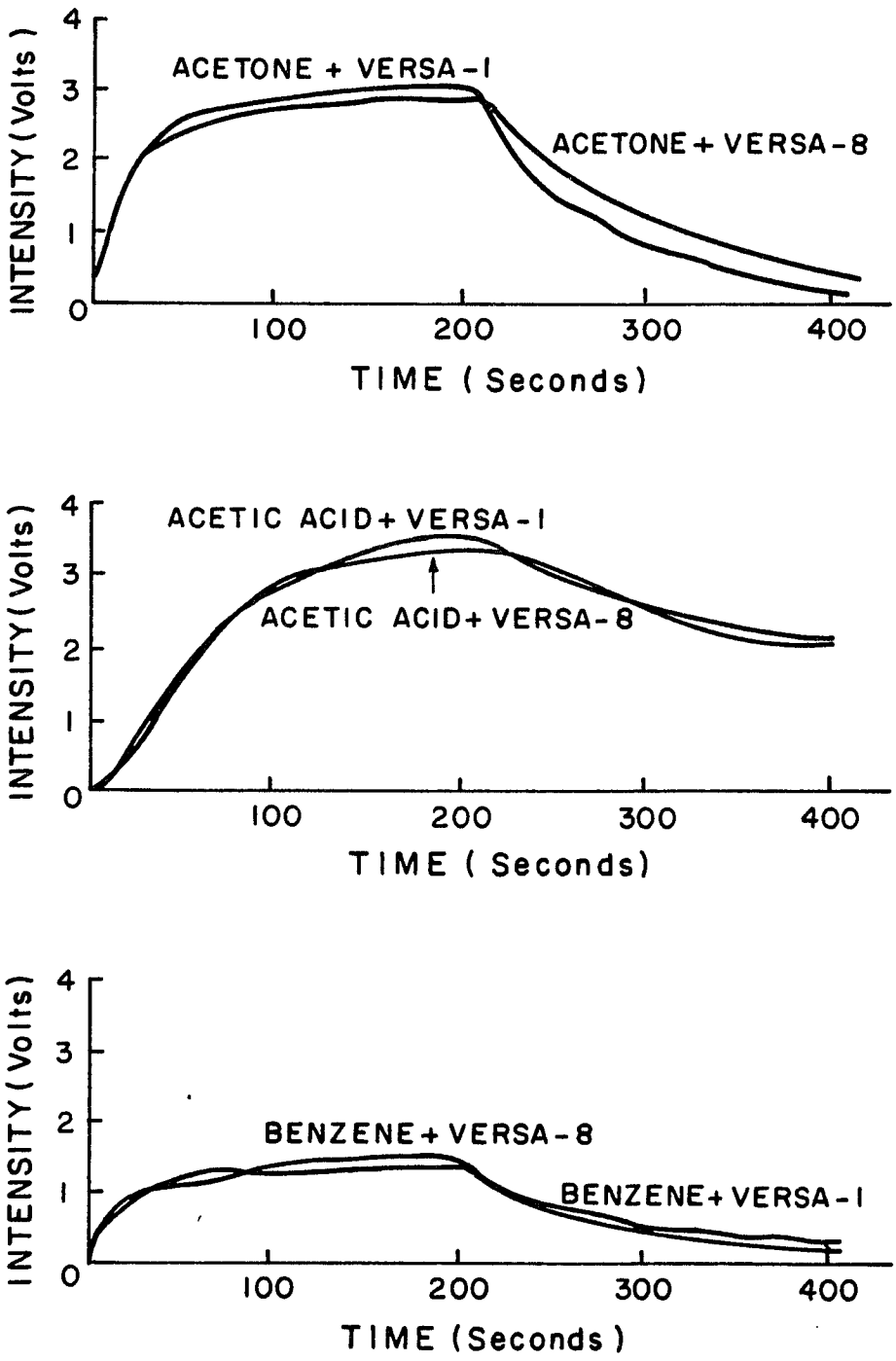

Figure 7.6.d. Dichloromethane.

Figure 7.6.e. Phenol.

Figure 7.6.f. Xylene.

Figure 7.7 presents a bar chart for average response of each compositional group of membranes to all contaminants. Examination of this figure suggests that:

(1) PTFE membranes are inert membranes that do not yield a significant response to any of the contaminants in this study. Their negligible output voltage makes them in appropriate for use as sensitive membrane surfaces in EOC.

(2) Acrylic copolymer (ACP) membranes, on the other hand, yield a significant level of response to all the contaminants regardless of their properties (with the exception of ethylene glycole). The high output levels of these membranes can provide the misleading impression that at all times a contaminant is being detected and thus there use is not recommended.

(3) Cellulose acetate (CA) membranes behaved similarly to the PTFE group, and are subjected to the same recommendations for use in the EOC.

(4) Polyvinilidene (PVD) membrane output is proportional to the vapor pressure of the contaminant. Even though the response for contaminants with lower vapor pressure is minute, the use of this membrane in general monitoring with EOC is appropriate.

(5) Mixed esters of cellulose (MEC) membranes behave similarly to the polyvinilidene group, with a better-defined relationship between the output levels and the vapor pressure of the membrane.

(6) Cellulose acetate (CA) membranes behave similarly to PVD and MEC groups, and they are subject to the same recommendations.

(7) Regenerated cellulose (RC) membranes behave similarly to the last three groups of the membranes for the contaminants with vapor pressures of up to 100 mmHg. After this point, however, they behave in

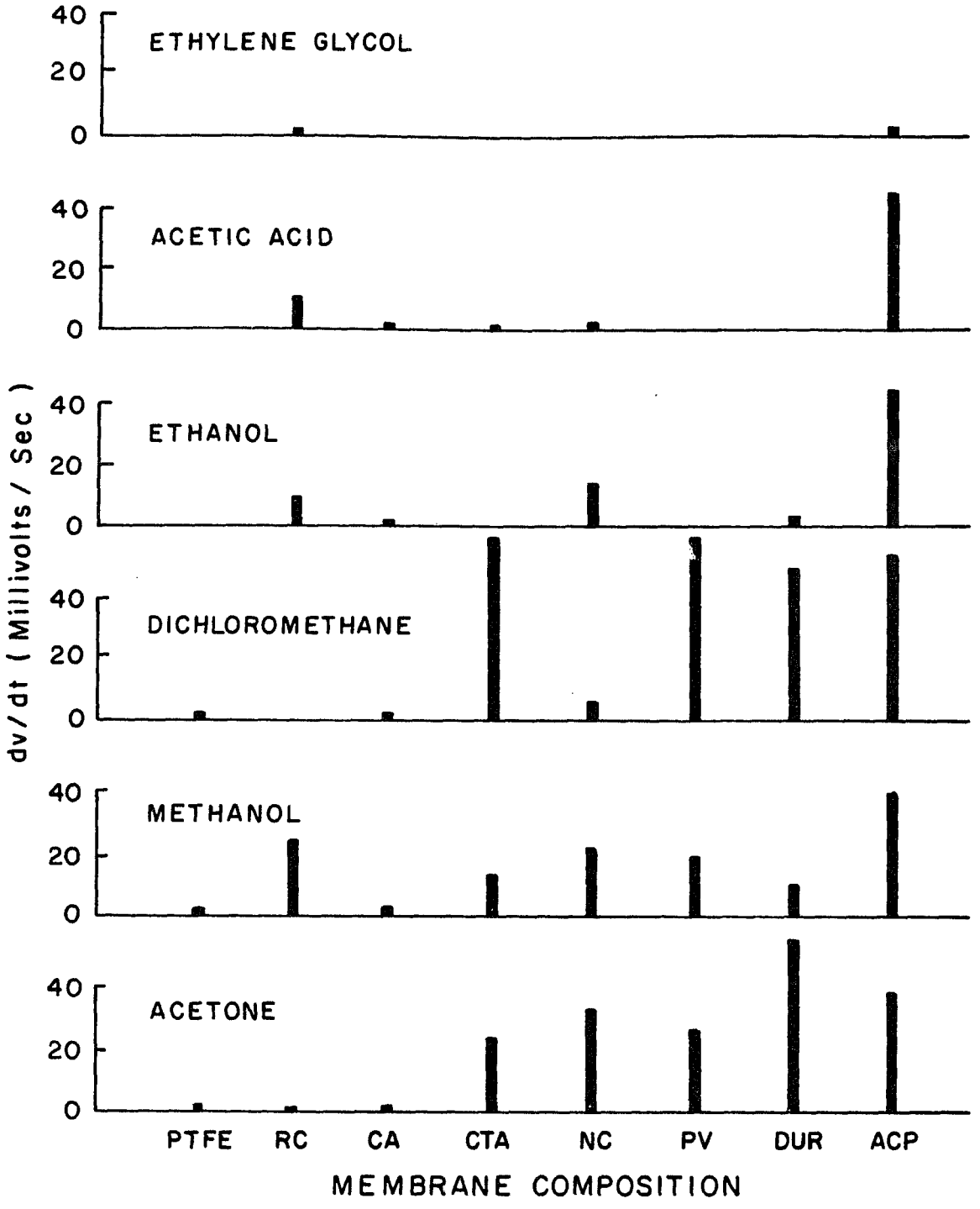

Figure 7.7. Effect of membrane composition grouping on EOC output.

an exactly opposite manner to the earlier groups. This group of membranes is especially suitable in the detection of lower vapor pressure contaminants.

(8) Nitrocellulose (NC) membranes behave similarly to the RC membranes, with the exception that the reversal in dv/dt takes place for contaminants with vapor pressures more than 200 mmHg. The same recommendations apply as the ones for RC membranes.

(9) Cellulose triacetate (CTA) membranes yield a significant output for most contaminants. The correlation between dv/dt and the vapor pressure of the contaminant is more uniform than the rest of the membranes in this experiment. This group of membranes seems to be suited best for the monitoring of the contaminants used in this experiment. These membranes were later used for detecting and monitoring the contaminants permeated through laboratory soil samples.

7.2.VI EFFECT OF SOLUBILITY FACTOR ON EOC RESPONSE

Solubility factor provides a measure of intensity of chemical interactions between the membrane contaminant (both in gaseous and liquid form). Results of solubility testing (see Table 5.6) were used to assign solubility factor to the membranes in the following manner:

Solubility Factor	Description
S_1	Membrane does not dissolve in contaminant
S_2	Membrane partially dissolves in contaminant
S_3	Membrane dissolves complete in contaminant

Based on preliminary test results presented in Figure 5.3, average dv/dt values were calculated for each case and were plotted against the solubility factor (Figure 7.8).

This plot presents a definite trend of increasing dv/dt with increasing solubility factor (i.e., increasing membrane dissolution in an organic chemical). This result is anticipated, since chemisorption is believed to play a major role in olfactometric contaminant detection. The same data indicates solubulity factor to be the governing factor on EOC output regardless of other variables (i.e., if the membrane does not yield a high solubility factor it will not yield a high output). It is for this reason that insoluble membranes such as teflon are not suitable for detection and consequently the theory of physical adsorption (mechanism of adsorption for nonreactive membranes) solely is inadequate in explaining the phenomenon of olfactometric detection.

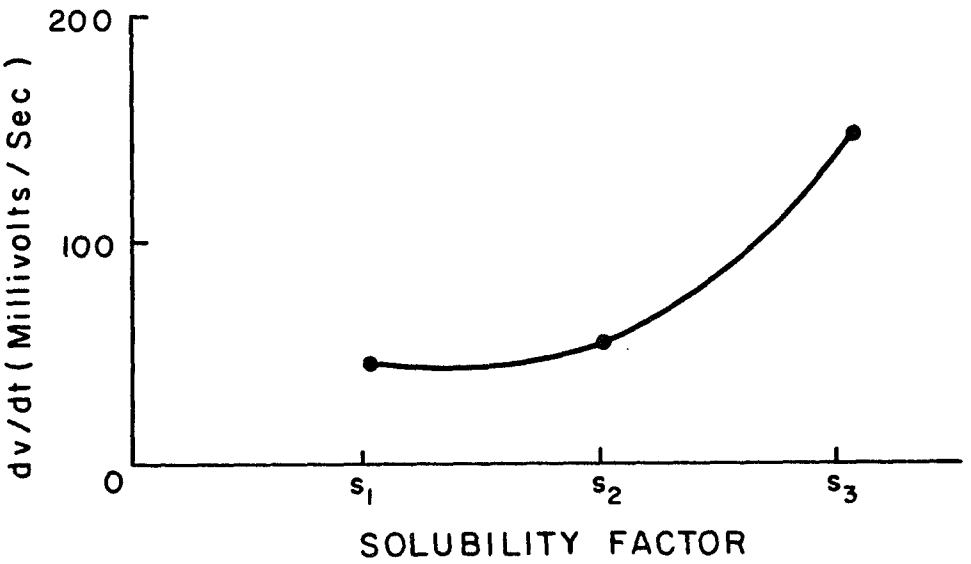

Figure 7.8. Effects of solubility factor on EOC response.

7.3 SOIL TESTING

The second phase of the study examined olfactometric contaminant detection in soil samples permeated by organic chemicals. In phase two, C/EOC output was correlated with influencing factors such as hydraulic

conductivity of the soil, pH of the effluent, concentration of the permeant, etc. Theoretical models were used along with experimental data of the other researchers to predict a time of initial C/EOC response and it was compared with actual observations. Time of initial response was also correlated with the concentration levels of the permeating organics.

7.3.I CONCENTRATION DIFFERENTIATION IN SOIL SAMPLES

EOC responds differently to varying concentrations of contaminants in ambient test (see Appendix A - The Instrument). Similar results were expected in monitoring different concentrations of the organic permeants in the soil samples. All permeants used in this study were permeated through identically prepared samples at three different concentrations of 10%, 25%, and 50% by volume.

Theoretical considerations suggest that in permeating a reactive fluid through porous media, the concentration of the permeant at a given point in time and space is a function of the medium's density, porosity, dispersion coefficient, and adsorption characteristics, as well as the initial concentration of the permeant. This was mathematically expressed for a conceptual model in equation 3.31 as:

$$C/C_o = \tfrac{1}{2}\left[\exp\left(\frac{1-\delta}{2\xi}\right)\operatorname{erfc}\left(\frac{1-\delta T}{2\sqrt{T\xi}}\right) + \exp\left(\frac{1+\delta}{2\xi}\right)\operatorname{erfc}\left(\frac{1+\delta T}{2\sqrt{T\xi}}\right)\right. \qquad (7.2)$$

In spite of the highly advanced mathematical modeling techniques that led to the development of conceptual models such as the one presented in equation 7.2 numerous handicaps persist when one is confronted with practical situations. Possible sources of error associated with

equation 7.2 include variations in kinetic rate of adsorption (a supposed empirical constant), impracticality of measuring dispersion coefficient of a sample, etc.

It seems that the efficiency offered by advancing a conceptual model is counter-balanced by the uncertainty in the measurement of factors introduced by the model and that only a combination of basic mathematical logic and dependable parameter measurements (either in situ or in the laboratory) can provide a realistic picture of the fate of the permeant in a reactive soil environment.

Experimental data from experiments conducted on similar soils by other researchers (Brown and Anderson, 1982; Acar, 1983; Daniel, 1984) served as the basis for comparative analysis of the EOC concentration differentiation in contaminant monitoring in soil samples.

It is indicated that the detection of concentrations of the permeant in the effluent is only possible after about .5 pore volumes of the replacing permeant is passed through the sample (Nielson and Biggar, 1962; Daniel, 1984). This is so because permeants mix with, move through, and replace the existing pore fluid, and thus the volume of the permeation required for first detection is less than one pore volume.

Figure 7.9 indicates that for all chemical permeants and all soil types, the time rate of change of output voltage increases with increasing concentration of the permeant. The exception to this is 50% methanol solution permeated through kaolinite. This deviation may be caused by either preferential flow channels that make portions of permeant unavailable to C/EOC or by the possibility that higher concentrations of methanol have a higher fixing ability with kaolinite thus causing a reduction in the number of sorbable (i.e., detectable)

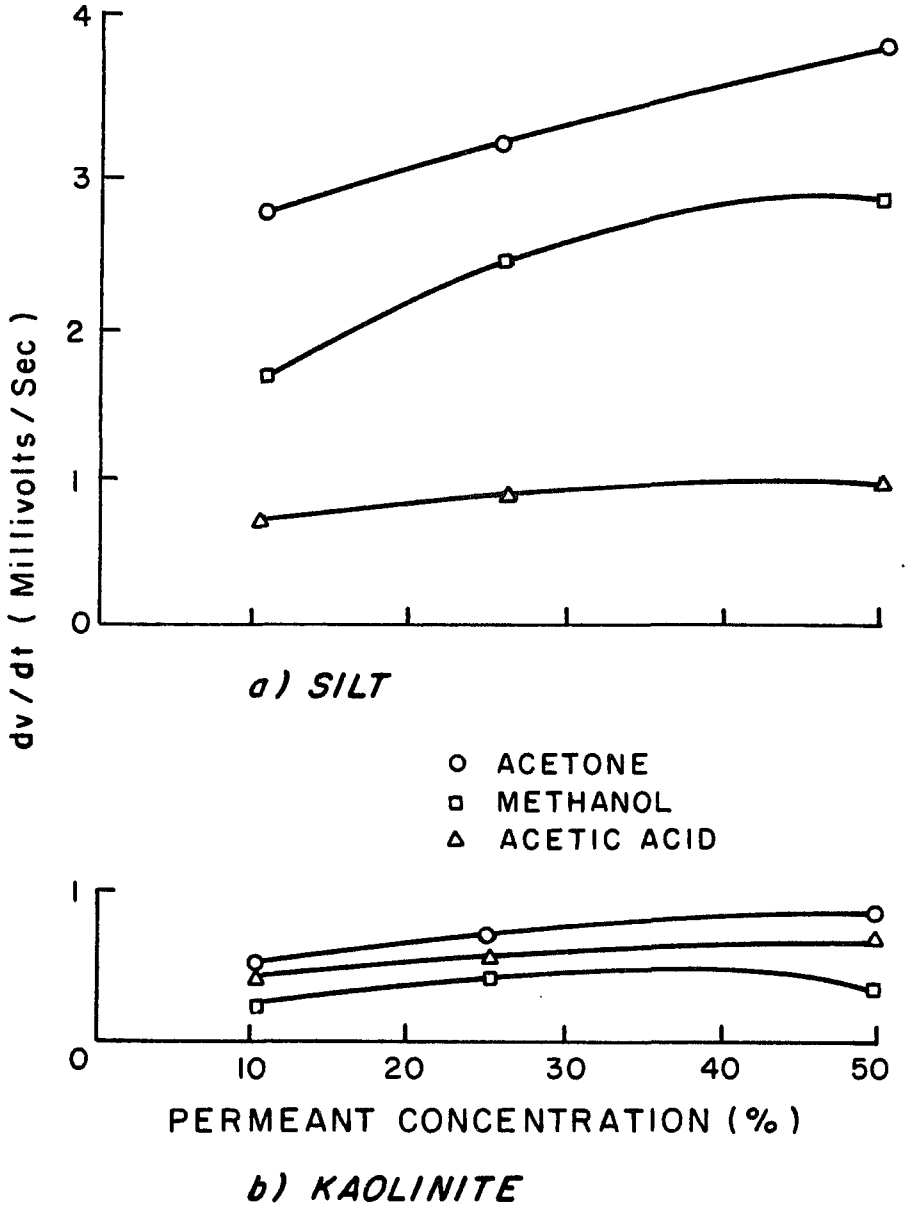

Figure 7.9. Time rate of change of voltage of odor cone in soils vs. concentration of the permeant.

methanol molecules. The first hypothesis is further supported by a relatively short time of initial response for the sample (see 7.3.II).

7.3.II TIME OF INITIAL RESPONSE

The C/EOC responds to the presence of organic contaminants in its olfactory reach. Contaminants can be present either in the form of volatalized odor molecules or in liquid form.

The contaminant front in porous media can advance both as a gas and as a liquid. The gaseous phase migration is produced by a gradient in gas partial pressure or a gradient in total gas pressure. In the event that a gradient in both partial and total pressure is present, a combination of diffusion and pressure flow will occur. The magnitude and direction of the combined flow will depend upon the magnitude and direction of the total and partial pressure gradients.

Collision with water or soil particles impedes the flow of volatile contaminant molecules. The flow of odor molecules is thus controlled by gas porosity of a medium, expressed as:

$$n' = (n/100) \times (1-S/100) \qquad (7.3)$$

where n' = gas porosity

n = conventional porosity

S = degree of saturation

It is obvious that for a saturated sample (i.e., S=100) gas porosity is almost zero and there is no differential odor front movement in the sample.

In saturated samples, the migration of the odor and leachate front are integrated and, for all practical purposes, identical. Once the leachate front arrives at the inlet port of the C/EOC, the liquid comes in contact with the Gore-Tex membrane, which restricts the flow of liquids and allows the passage of gaseous (odor) molecules. Odor molecules diffuse through the Gore-Tex membrane and in a strictly gaseous phase, migration advances toward the sensitive dielectric membrane of the C/EOC. The EOC responds immediately.

The initial time of response of the C/EOC, then, is equal to the time of migration of the leachate front from the top platten to the inlet port of the C/EOC. Consequently, the hydraulic conductivity of the sample is related to a specific contaminant.

Theoretical considerations suggest that a reliable analytical prediction of hydraulic conductivity of soil samples to a reactive permeant is almost impossible. A major task of researchers in the field of landfill design and behavior has been to explain the vast and nonconforming variations between theoretical predictions and experimental observations.

In comparing the initial time of C/EOC response with the theoretical predictor of such an observation, Darcian flow equation was used to calculate a predictor time of initial response. Hydraulic conductivity, k, values used in this equation were average experimental values reported by Brown et al. (1982) and Bakar (1984) which were corrected for the effect of viscosity to density ratio. Average estimated k values used were corrected for the effects of viscosity and density according to $k=K(\gamma/d)$, where γ is viscosity, d is density, and K is specific permeability of the sample to water. Table 7.2 presents variations in γ/d ratio with dilution. These values were used in estimating hydraulic conductivity.

Table 7.2

Permeant	Density (gr/cm)	Viscosity (centipois)	γ/d
100% AC	.33	.79	2.39
50% AC	.78	.895	1.15
25% AC	.87	.947	1.08
10% AC	.896	.98	1.09
100% AA	1.28	1.05	.82
50% AA	1.00	1.025	1.03
25% AA	.95	1.013	1.07
10% AA	.93	1.005	1.08
100% MT	.54	.79	1.46
50% MT	.72	.895	1.24
25% MT	.82	.947	1.155
10% MT	.897	.979	1.091

Table 7.3 provides values of measured and predicted time of initial response of the C/EOC.

A generic conclusion relating predicted and calculated time of initial response from Table 7.2 data may lack the accuracy needed for a scientific conclusion. General trends, however, may be observed from the existing data in Table 7.3. These are:

1. t_p/t_m ratio (where t_p and t_m are predicted and measured time of initial response, respectively) for kaolinite is about 65% with 50% acetone and 50% methanol being the extreme exceptions. Partial reasoning for 50% methanol's deviation were discussed in 7.2.I. For 50% acetone it is probable that initial hydraulic conductivity retaration effects of acetone (Anderson et al., 1982).
2. t_p/t_m for silt samples were about 90%. The deviations from norm were pronounced for acetic acid (all concentrations) and 10% methanol solution. In case of acetic acid and 10% methanol the initial stage output voltage (see figures 6.18

Table 7.3. Comparison of measured and predicted time of initial response of C/EOC.

Permeant	Measured t (seconds)	t_p/t_m	Predicted t (seconds)
10% AC+K	146000	0.63	91807
25% AC+K	135000	0.69	92827
50% AC+K	193000	0.45	87023
10% AA+K	120000	0.77	92827
25% AA+K	130000	0.72	94223
50% AA+K	148000	0.66	97904
10% MT+K	183000	0.50	91807
25% MT+K	116000	0.75	86725
50% MT+K	73800	1.1	80850
10% AC+S	6280	0.85	5319
25% AC+S	5700	0.94	5376
50% AC+S	4900	1.03	5027
10% AA+S	7160	0.75	5376
25% AA+S	7650	0.67	5108
50% AA+S	8140	0.69	5676
10% MT+S	3920	1.36	5322
25% MT+S	4300	1.17	5027
50% MT+S	6420	0.73	4683

AA: Acetic Acid
AC: Acetone
MT: Methanol
K: Kaolinite
S: Silt

and 6.19) is low. This will cause the point of initial response to be a nondiscrete entity thus making an experimental error in judgment of such point highly probable. Other experimental errors associated with organic permeation (such as organic permeants leakage to the chamber fluid) may be other possible sources of explaining the observed deviations.

3. Comparing t_p/t_m values for kaolinite and silt samples, it may be concluded that there is better correlation between measured and predicted time of initial response for silt samples than there are for kaolinite samples. This is mainly due to the fact that there are fewer reactions (if

any) between silt and the permeating organic than between kaolinite and the permeating organic. Consequently, there are less sources of variation and better correlation.

7.3.III CORRELATION BETWEEN pH OF THE EFFLUENT AND dV/dt

During permeation, the pH of the effluent was intermittently monitored. The average values of the pH corresponding to each soil type, permeant type, and concentration are tabulated in Table 7.4:

These observations do not provide a general definite trend of correlation between the pH of the effluent and the voltage output of C/EOC. The effluent pH seems to be a function and consequently an indicator of soil-permeant interaction as much as it involves permeant pH modifications.

Table 7.4

Permeant and soil	dv/dt	Average pH
10% AC+K	0.36	3.50
25% AC+K	0.63	3.60
50% AC+K	0.81	3.75
10% AA+K	0.32	2.70
25% AA+K	0.44	2.65
50% AA+K	0.59	2.55
10% MT+K	0.17	4.20
25% MT+K	0.34	4.10
50% MT+K	0.36	4.10
10% AA+S	2.6	7.70
25% AC+S	3.1	7.60
50% AC+S	3.7	7.25
10% AA+S	0.65	2.75
25% AA+S	0.80	2.60
50% AA+S	0.95	2.45
10% MT+S	1.60	8.35
25% MT+S	2.3	8.40
50% MT+S	2.8	8.55

7.3.IV EFFECT OF VAPOR PRESSURE ON dv/dt

Plots of vapor pressure of the permeating contaminant vs. dv/dt (Figure 7.10) serve to reinforce the conclusions of the ambient testing

with EOC, which indicated that dv/dt for the most parts increases with increases in vapor pressure of the contaminant. This indication was most pronounced in the case of ambient testing. It is more pronounced for the highly permeable silt samples than for low-permeability kaolinite samples. This may be expected since the lower hydraulic conductivity of reactive kaolinite may serve to dampen the high vapor pressure, whereas in ambient conditions there is no restrictive barrier to the advance of high vapor pressure contaminants to the olfactory reach of the EOC.

Comparison of Figures 7.10.a and 7.10.b shows that for kaolinite dv/dt actually decreases when vapor pressure increases from 11 to 96 mmHg. The reasoning behind this is the interactions of kaolinite soil with the permeating organic. Such interactions may serve to retard or enhance vapor pressure gradients in soil samples and consequently affect the C/EOC output. It is therefore important not to take vapor pressure at face value as it relates to C/EOC output. Vapor pressure effect on C/EOC output is best understood when it is examined as the product that reaches the olfactory reach of C/EOC and not as the undefined nominal value associated with a permeant organic.

7.4 STATISTICAL ANALYSES OF THE RESULTS

Phase I. Phase one was the exploratory phase of laboratory testing. Its intentions were to provide experimental substantiation or rejection bases for the hypothesized theories of olfactometric detection. The experiment was designed and analyzed as a factorial experiment with the independent factors being organic chemicals (at five levels) and membranes (at 19 levels). There were no intractive tests and no interaction statics.

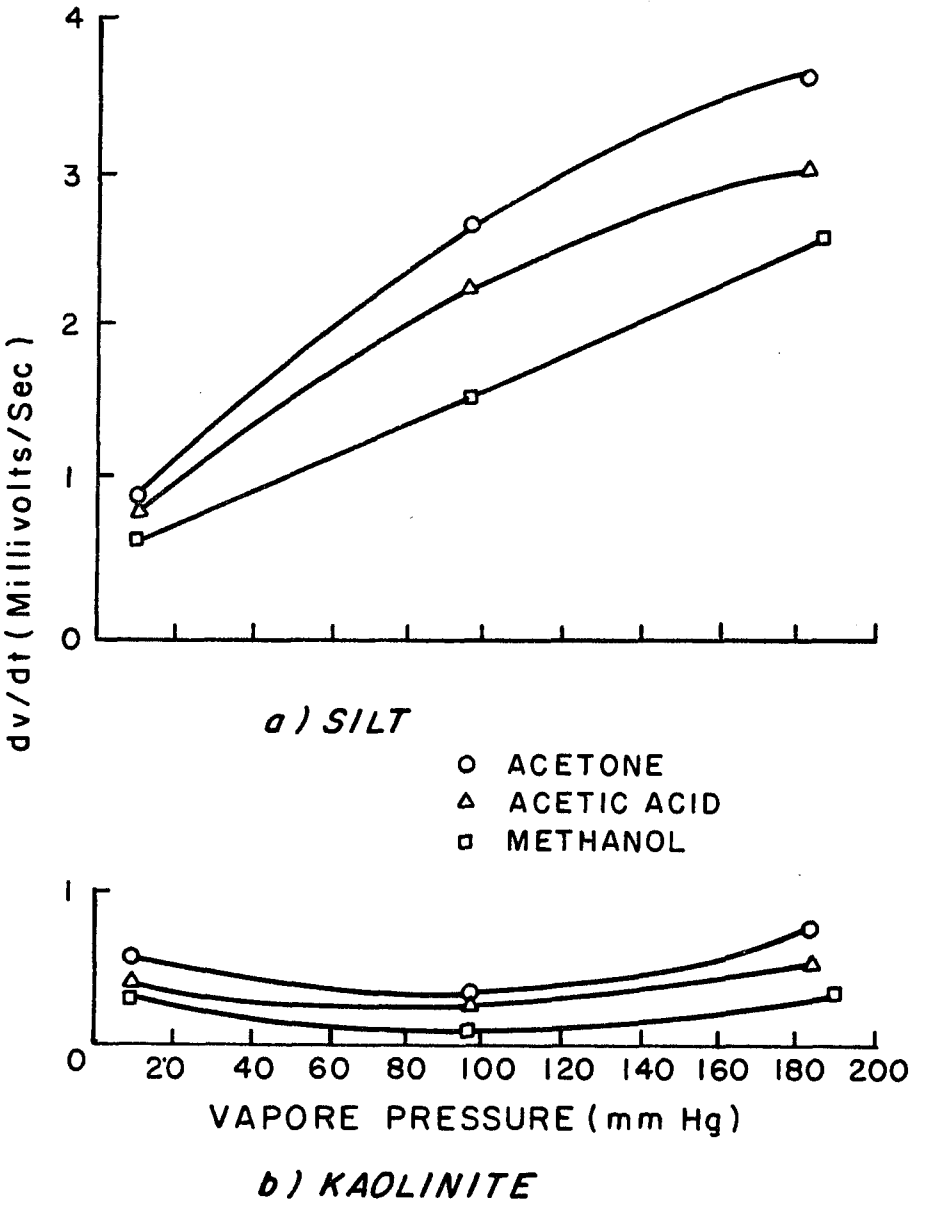

Figure 7.10. Time rate of change of voltage vs. vapor pressure of the permeant fluid.

Membranes were grouped in two categories: (a) according to their adsorption characteristics as represented by solubility testing and representing the combined result of all factors involved in EOC response, and (b) according to their pore sizes. Organic chemicals were grouped according to their (a) vapor pressure, (b) dipole moment, (c) dielectric constant, and (d) surface tension.

For analytical purposes and also by design, the experimental data were treated as independent observations because the factorial treatment levels applied to nested blocks of experimental units. Block one was the pore size block, with subblocks as shown below. Block two was the solubility block, with three subblocks as shown later.

Table 7.5. Pore size grouping of the membranes.

Subblock notation	Pore size	Membranes included in the subblock
P_1:	0.02 μm	(TE 30)
P_2:	0.2 μm	(TCM/HT/Versa 200/GA-8)
P_3:	0.22 μm	(MF-Millipore)
P_4:	0.45 μm	(Durapore, AE91, BA85)
P_5:	0.6 μm	(RC59)
P_6:	0.8 μm	(Versa 800)
P_7:	1.2 μm	(AE-95)

Solubility subblock for each contaminant	Membranes included in each subblock
$(S_1)_{AC}$	TCM/HT/GA-8/ST-68/MF-Millipore/Celotate/Versapore
$(S_2)_{AC}$	AE-95/BA-85/Nuclepore/Mitex/Durapore
$(S_3)_{AC}$	TE-30/RC-59/PN-20

$(S_1)_{DCM}$ TCM/HT/GA-8/Nuclepore/Celotate/Versapore

$(S_2)_{DCM}$ ST-68/BA-85/MF-Millipore/AE-95

$(S_3)_{DCM}$ TEBO/Rc-59/PN-20/Mitex

$(S_1)_{METH}$ Versapore/HT/TCM/PN-20

$(S_2)_{METH}$ AE-95/Nuclepore

$(S_3)_{METH}$ GA-8/TE-30/ST-68/RE-59/BA-85/MF-Millipore/ Mitex/Celotate/Durapore

$(S_1)_{ETH}$ Versapore/HT-200/TCM-200

$(S_2)_{ETH}$ None

$(S_3)_{ETH}$ All except $(S_1)_{ETH}$

$(S_1)_{AA}$ TCM-200/GA-8/ST-68/MF-Millipore/Versapore/HT-200

$(S_2)_{AA}$ Celotate/Nuclepore/BA-85/AE-95

$(S_3)_{AA}$ TE-30/RC-59/PN-20/Mitex

$(S_1)_{EG}$ None

$(S_2)_{EG}$ None

$(S_3)_{EG}$ All

Where S_1 complete dissolution

S_2 partial dissolution

S_3 nonsoluble

The treatment factors were:

(a) Dielectric constant

(b) Dipole moment

(c) Vapor pressure

(d) Surface tension

Each factor has six levels corresponding to six chemicals used in the experiment. The values corresponding to these treatment levels are listed in Table 7.6 in increasing order.

Experimental observations (i.e., dv/dt) for all treatment levels applied to all experimental units are listed in Tables 7.7 - 7.10. In each table the column entries represent either the pore size groups (1-7) or the solubility groups (1-3). The row entries represent a contaminant characteristic (dielectric constnat, dipole moment, vapor pressure, and surface tension). Each entry (XY) in the table is the average dv/dt value for all membranes with pore size X exposed to organic having characteristic Y. An entry p_4a_5 in Table 7.7a for example is the average dv/dt for all membranes having pore size equal to 0.45 μm (group p_4) exposed to the organic having dielectric constant of 33.62 (a_5) and so on.

The largest entry indicates that the corresponding membranes and organic are compatible and thus can be used in contaminant detection. Using Table 7.7.a as an example the largest dv/dt value of 49.8 corresponds to membranes with pore size p_6 and methanol as the contaminant, indicating that specific membranes with pore size 0.8 μm (group p_6) are suitable in ambient methanol detection.

The summation of columns reflects the overall performance of a given pore size or solubility group of membranes with respect to all contaminants. Summation of rows reflect the detectability of an organic with a spectrum of membrane pore sizes or solubility. As before the larger the value of dv/dt the better the chances for detection.

Table 7.6. Factorial arrangement of sample sets.

Factor Level	Dielectric Constant	Dipole Moment Debys		Vapor Pressure mm Hg		Surface Tension Dyne/cm	
a_1 AA	6.1	b_1 METH	1.68	c_1 E.G.	1	D_1 ETH	22.3
a_2 DCM	10.6	b_2 ETH	1.69	c_2 AA	11.8	D_2 METH	22.6
a_3 AC	20.7	b_3 AA	1.74	c_3 ETH	66	D_3 AC	23.7
a_4 ETH	24.3	b_4 DCM	2.06	c_4 METH	96	D_4 DCM	26.5
a_5 METH	33.62	b_5 AC	2.90	c_5 AC	185	D_5 AA	27.8
a_6 EG	38.66	b_6 EG	2.28	c_6 DCM	400	D_6 E.G.	47.7

Where

a: Dielectric constant
b: Dipole moment
c: Vapor pressure
d: Surface tension

Table 7.7.a

Pore Size and Dielectric Constant

p_1a_1	p_2a_1	p_3a_1	p_4a_1	p_5a_1	p_6a_1	p_7a_1
p_1a_2	p_2a_2	p_3a_2	p_4a_2	p_5a_2	p_6a_2	p_7a_2
p_{1a3}	p_2a_3	p_3a_3	p_4a_3	p_5a_3	p_6a_3	p_7a_3
p_1a_4	p_2a_4	p_3a_4	p_4a_4	p_5a_4	p_6a_4	p_7a_4
p_1a_5	p_2a_5	p_3a_5	p_4a_5	p_5a_5	p_6a_5	p_7a_5
p_1a_6	p_2a_6	p_3a_6	p_4a_6	p_5a_6	p_6a_6	p_7a_6

P_ia_i

	p_1	p_2	p_3	p_4	p_5	p_6	p_7	Σ
AA	0.08	9.71	-0.1	0.6	7.2	45.8	1.09	64.38
DCM	-0.7	39.6	43.4	16.9	-0.8	51.0	10.6	160
AC	-0.07	35.67	26.3	34.3	2.34	49.6	16.3	164.4
ETH	-0.11	19.66	0.02	9.86	8.6	45.4	0.33	83.76
METH	5.5	30.90	19.2	22.7	23.6	49.8	15.9	167.6
EG	-0.75	0.512	-0.4	-0.303	1.8	2.2	0.31	4.04
Σ	4.75	135.54	88.82	84.36	40.97	241.6	44.22	

Table 7.7.b

Solubility and Dielectric Constant

			S_ia_i			Σ
S_1a_1	S_2a_1	S_3a_1	16.77	2.134	0.478	19.382
S_1a_2	S_2a_2	S_3a_2	32.09	26.2	6.75	65.05
S_1a_3	S_2a_3	S_3a_3	39.73	12.16	11.68	63.57
S_1a_4	S_2a_4	S_3a_4	43.38	0	11.67	55.05
S_1a_5	S_2a_5	S_3a_5	44.20	14.8	10.61	64.61
S_1a_6	S_2a_6	S_3a_6	0	0	0.163	0.163
		Σ	176.17	55.3	41.32	

Table 7.8.a

Pore Size and Dipole Moment

p_1b_1	p_2b_1	p_3b_1	p_4b_1	p_5b_1	p_6b_1	p_7b_1
p_1b_2	P_2b_2	p_3b_2	p_4b_2	p_5b_2	p_6b_2	p_7b_2
p_{1b3}	p_2b_3	p_3b_3	p_4b_3	p_5b_3	p_6b_3	p_7b_3
p_1b_4	p_2b_4	p_3b_4	p_4b_4	p_5b_4	p_6b_4	p_7b_4
p_1b_5	p_2b_5	p_3b_5	p_4b_5	p_5b_5	p_6b_5	p_7b_5
p_1b_6	p_2b_6	p_3b_6	p_4b_6	p_5b_6	p_6b_6	p_7b_6

P_ib_i

METH	5.5	30.90	19.2	22.7	23.6	49.8	15.9	167.6
ETH	-0.11	19.66	0.02	9.88	8.6	45.4	0.33	83.76
AA	0.08	9.71	-0.1	0.6	7.2	45.8	1.09	64.38
DCM	-0.7	39.6	43.4	16.9	-0.8	51.0	10.6	160
AC	-0.07	35.67	26.3	34.3	2.34	49.6	16.3	164.4
EG	-0.75	0.512	-0.4	-0.303	1.8	2.2	0.31	4.04
Σ	4.75	135.54	88.82	84.36	40.97	241.6	44.22	

Table 7.8.b

Solubility and Dipole Moment

				S_ib_i		Σ
S_1b_1	S_2b_1	S_3b_1	44.2	14.8	10.61	69.61
S_1b_2	S_2b_2	S_3b_2	43.38	0	11.67	55.05
S_1b_3	S_2b_3	S_3b_3	16.77	2.13	0.48	19.382
S_1b_4	S_2b_4	S_3b_4	32.09	26.2	6.75	65.09
S_1b_5	S_2b_5	S_3b_5	39.73	12.16	11.68	63.57
S_1b_6	S_2b_6	S_3b_6	0	0	0.163	0.163
		Σ	176.17	55.3	41.32	

Table 7.9.a

Pore Size and Vapor Pressure

p_1c_1	p_2c_1	p_3c_1	p_4c_1	p_5c_1	p_6c_1	p_7c_1	
p_1c_2	p_2c_2	p_3c_2	p_4c_2	p_5c_2	p_6c_2	p_7c_2	
p_{1c3}	p_2c_3	p_3c_3	p_4c_3	p_5c_3	p_6c_3	p_7c_3	
p_1c_4	p_2c_4	p_3c_4	p_4c_4	p_5c_4	p_6c_4	p_7c_4	
p_1c_5	p_2c_5	p_3c_5	p_4c_5	p_5c_5	p_6c_5	p_7c_5	
p_1c_6	p_2c_6	p_3c_6	p_4c_6	p_5c_6	p_6c_6	p_7c_6	

				P_ic_i			Σ
EG	-0.75	0.512	-0.4	-0.303	1.8	2.2	0.31	4.04
AA	0.08	9.71	0.01	0.6	7.2	45.8	1.09	64.38
ETH	-0.11	19.66	0.02	9.88	8.6	45.4	0.33	83.76
METH	5.5	30.90	19.2	22.7	23.6	49.8	15.9	167.6
AC	-0.07	35.67	26.3	34.3	2.34	49.6	16.3	164.4
DCM	-0.7	39.6	43.4	16.9	-0.8	51.0	10.6	160
Σ	4.75	135.54	88.82	84.36	40.97	241.6	44.22	

Table 7.9.b

Solubility and Vapor Pressure

				S_ic_i		
S_1c_1	S_2c_1	S_3c_1	0	0	0.163	0.163
S_1c_2	S_2c_2	S_3c_2	16.77	2.134	0.478	19.382
S_1c_3	S_2c_3	S_3c_3	43.38	0	11.66	55.05
S_1c_4	S_2c_4	S_3c_4	44.2	14.8	10.61	69.61
S_1c_5	S_2c_5	S_3c_5	39.73	12.16	11.68	63.57
S_1c_6	S_2c_6	S_3c_6	32.09	26.2	6.75	65.05
			176.17	55.3	41.32	

Table 7.10.a

Pore Size and Surface Tension

p_1d_1	p_2d_1	p_3d_1	p_4d_1	p_5d_1	p_6d_1	p_7d_1	
p_1d_2	p_2d_2	p_3d_2	p_4d_2	p_5d_2	p_6d_2	p_7d_2	
p_{1d3}	p_2d_3	p_3d_3	p_4d_3	p_5d_3	p_6d_3	p_7d_3	
p_1d_4	p_2d_4	p_3d_4	p_4d_4	p_5d_4	p_6d_4	p_7d_4	
p_1d_5	p_2d_5	p_3d_5	p_4d_5	p_5d_5	p_6d_5	p_7d_5	
p_1d_6	p_2d_6	p_3d_6	p_4d_6	p_5d_6	p_6d_6	p_7d_6	
			P_id_i				Σ
ETH	-0.11	19.66	0.02	9.86	8.6	45.4	0.3	83.76
METH	5.5	30.90	19.2	22.7	23.6	49.8	15.9	167.6
AC	-0.07	35.67	26.3	34.3	2.34	49.6	16.3	164.44
DCM	-0.71	39.6	43.4	16.9	-0.8	51.0	10.6	160
AA	0.08	9.71	0.01	0.6	7.2	45.8	1.09	64.38
EG	-0.075	0.512	-0.4	-0.303	1.8	2.2	0.31	4.04
Σ	4.75	135.54	88.82	84.36	40.97	241.6	44.22	

Table 7.10.b

Solubility and Surface Tension

				S_id_i		Σ
S_1d_1	S_2d_1	S_3d_1	43.38	0	11.66	55.05
S_1d_2	S_2d_2	S_3d_2	44.2	14.8	10.61	69.61
S_1d_3	S_2d_3	S_3d_3	39.73	12.16	11.68	63.57
S_1d_4	S_2d_4	S_3d_4	32.09	26.2	6.75	65.05
S_1d_5	S_2d_5	S_3d_5	16.77	2.134	0.478	19.382
S_1d_6	S_2d_6	S_3d_6	0	0	0.163	0.163
		Σ	176.17	55.3	41.32	

7.5 REGRESSION ANALYSIS

Examination of data in sections 7.1-7.4 indicates the time rate of change of output voltage to be affected by factors including: vapor pressure, dipole moment, dielectric constant, surface tension, and concentration of the organic chemical, and also solubility and pore size of the membrane. Experimental data were further examined to address the contribution of each influencing factor to the output level. The results of such schemes then may be used to develop a predictor model where EOC response can be estimated once the membrane and organic chemical properties are known.

The statement above provides a proper background for using a multivariate rgression of analysis (Gnanadesikan, 1977; Chatterjee and Price, 1977).

In formally selecting a regression model for correlating some or all of the above variables with the time rate of output voltage, there are two extreme possibilities for erroneous conclusions: (1) choosing too many variables, and (2) choosing too few variables.

In choosing too many variables, one can find a situation in which there is more correlation among the independent variables than there is between the independent and dependent variables (multicolinearity). Selecting too few variables results in a biased model with inflated residual mean squares and low correlation coefficients. In this study the stepwise regression method was used for selection of variables. The stepwise algorithm combines forward selection and backward elimination to either add or eliminate a single regressor (independent variable). The independent variable is eliminated if its removal would cause small increases in the value of regression coefficient (R^2 = regression sum

of square). The same procedure is repeated for all variables. The algorithm stops when all variables are examined for inclusion in the model and are either incorporated or rejected. For the purpose of this study a statistical analysis software (micro stat) was used to generate regression equations for dv/dt and a number of independent variables (see 7.5.I and 7.5.II).

7.5.I AMBIENT TESTING

In analysing the experimental observations of ambient testing phase of this study, initially, a multilinear model $Y = X_o + X_i X_i$ was selected where

i = number of independent variables

X_i = value of independent variable i or some variations thereof, to include powers of X_i, Log X_i, ln X_i, etc.

Y = dv/dt = time rate of output voltage

i was selected as to include

X_1 = vapor pressure

X_2 = dielectric constant

X_3 = dipole moment

X_4 = surface tension

X_5 = solubility of the membrane

The original multilinear regression model was:

$$Y = \alpha_o + \alpha_1 X_1 + \alpha_2 X_2 + \alpha_3 X_4 + \alpha_5 X_5$$

Subsequent variations to this model were also used to examine possible improvements in the value of regression coefficient (R^2). These variations included:

a) Multilinear loglinear regression model

$$Y = \alpha_o + \alpha_1 \log X_1 + \alpha_2 X_2 + \alpha_3 X_3 + \alpha_4 X_4 + \alpha_5 X_5$$

b) Log-exponential regression model

$$Y = \alpha_o + \alpha_1 \log X_1 + \alpha_2 X_2 + \alpha_3 X_3 + \alpha_4 X_4 + \alpha_5 e^{X5}$$

c) Loglinear regression model

$$Y_i = \alpha_o + \alpha_i \log X_i, \quad i = 1 \text{ to } 5$$

Table 7.11 represents the results of linear and nonlinear regression analysis. The confidence level used in these calculations was 90%, F value to accept or reject a hypothesis 3 and a stepwise regression model was used to arrive at the solution.

Results of regression equations indicate the time rate of change of voltage for inert membranes (such as teflon and TE-30) to have no correlation with independent variables listed, regardless of whether multilinear, log linear, or exponential correlations were used.

In the multiple linear analysis individual membranes response seems to be unaffected by different variables (i.e., the regression coefficient of the variable is zero). In the log linear model, membranes were grouped according to their polymer composition and were subjected to regression analysis. The correlation coefficients were very high. For the same model the correlation coefficient for individual membranes nuclepore 1 and 8 were low (R^2=0.76) compared to the rest of the data sets. In attempting to correlate the output from all experiments with a set of independent variables the coefficient of regression was very low (0.11→0.25, see Table 7.11.d). This is due to a high degree of response variation among membranes and should not be expected to attain an R^2 value close to unity.

Table 7.11.a

Membrane	R^2	Multilinear Regression Equation for Ambient Testing
Nuclepore 1.0	0.91	$dv/dt = -200.8 - .113\,x_1 + 2.26\,x_2 + 205\,x_3 + 695\,x_5$
Nuclepore 8.0	0.90	$dv/dt = -173.3 - 0.1\,x_1 + 2.15\,x_2 + 1.6\,x_3 + 6.8\,x_5$
MF-Millipore	0.95	$dv/dt = -28.07 + 0.8\,x_1 + 0.52\,x_2 + 0.57\,x_4 + 5.15\,x_5$
Mitex	0.9	$dv/dt = 0.97 + 0.05x_1 + 0.27\,x_2 - 0.51\,x_3 - 0.48\,x_5$
Celotate	0.99	$dv/dt = 8.76 - 0.48\,x_2 - 0.3\,x_3 - 0.1\,x_4 - 1.28\,x_5$
Durapore	0.99	$dv/dt = -34.4 + 0.11\,x_2 + 29.1\,x_3 - 0.63\,x_4 - 2.58\,x_5$
PN 20	No Correlation	$dv/dt =$
ST-68	0.985	$dv/dt = -1.17 + 0.007x_1 + 0.203\,x_2 - 3.8\,x_3 + 2.19\,x_5$
AE-91	0.998	$dv/dt = 8.98 - 0.813x_1 + 0.85\,x_2 + 32.9\,x_3 - 2.45\,x_4$
AE-95	0.986	$dv/dt = -21.3 + 0.45\,x_2 + 5.8\,x_3 - 0.43\,x_4 + 10.54\,x_5$
Teflon	No Correlation	
TE-30	No Correlation	
HT-200	0.98	$dv/dt = 5.7 - 0.08\,x_1 + 0.39\,x_2 - 21.08x_3 + 40.65\,x_5$
All	0.25	$dv/dt = 6.58 + 0.0073x_1 + 0.46\,x_2 - 0.6\,x_3 - 0.62\,x_4 + 6.09\,x_5$

Table 7.11.b

Membrane	R^2	Log Linear Regression Equation for Ambient Testing
Versapore 200	0.98	$dv/dt = -37.4 - 41.2 \log x_1 + 3.5\,x_2 - 3.1\,x_4 + 49\,x_5$
Versapore 800	.999	$dv/dt = 1.164 + 14.34 \log x_1 + 1.13\,x_2 + 8.4\,x_3 - 1.33\,x_4$
AE-95	0.985	$dv/dt = -21.3 + .45\,x_2 + 5.8\,x_3 - .43\,x_4 + 10.5\,x_5$
AE-91	0.82	$dv/dt = 71.71 - 11.41 \log x_1 + 32.8\,x_3 - 2.86\,x_4 - 12.82x_5$
ST-68	0.94	$dv/dt = -4.64 + 0.95 \log x_1 + 0.3\,x_2 - 4.46\,x_3 + 3.21\,x_5$
Durapore	0.99	$dv/dt = -84.36 + 14.4 \log x_1 - 0.51\,x_2 + 33.8\,x_3 + 8.7\,x_5$
Celotate	0.99	$dv/dt = 8.76 - 0.5\,x_2 - 0.3\,x_3 - .1\,x_4 - 1.3\,x_5$
Mitex	0.97	$dv/dt = -9.46 + 3.5 \log x_1 - 7.98\,x_3 + 0.44\,x_4 + 7.08\,x_5$
MF-Millipore	0.97	$dv/dt = 164.93 + 24.5 \log x_1 + 0.69\,x_2 + 2.67\,x_3 + 4.65\,x_4$
Nuclepore 8	0.76	$dv/dt = -41 - 19.5 \log x_1 + 1.7\,x_2 - 0.61\,x_3 + 1.95\,x_4$
Nuclepore 1	0.76	$dv/dt = -46.7 - 23.3 \log x_1 + 1.77\,x_2 - 0.57\,x_3 + 2.5\,x_4$
Nuclepore 8&1	0.98	$dv/dt = 212.2 - 0.05 \log x_1 + 2.64\,x_2 + 2.45\,x_3 + 9.1\,x_4 - 2.75\,x_5$
HT, TCM, GA	0.96	$dv/dt = 28.9 + 0.035 \log x_1 + 7.34\,x_3 - 1.1\,x_4 + 1.55\,x_5$
Versapore 1&8	0.98	$dv/dt = -132.28 - .11 \log x_1 + 2.72\,x_2 - 0.29\,x_4 + 41.3\,x_5$

Where

x_1 = Vapor pressure

x_2 = Dielectric constant

x_3 = Dipole moment

x_4 = Surface tension

x_5 = Solubility

Table 7.11.c

Membrane	R^2	Exponential Regression Equation
Nuclepore 1&8	0.98	$dv/dt = -215.13 - 10.4 \ln x_1 + 2.68 x_2 + 2.1 x_3 + 8.3 x_4 - 2.6 e^{x_5}$
Millipore	0.97	$dv/dt = -164.9 + 24.5 \ln x_1 + 0.69 x_2 + 2.67 x_3 + 4.65 x_4$
Mitex	0.966	$dv/dt = -6.5 + 3.5 \ln x_1 - 7.98 x_3 + .44 x_4 + 1.52 e^{x_5}$
Celotate	0.99	$dv/dt = 7.88 - 0.05 x_2 - 0.3 x_3 - 1.01 x_4 - .15 e^{x_5}$
Durapore	0.99	$dv/dt = -78.4 + 14.4 \ln x_1 - 0.05 x_2 + 33.8 x_3 + 1 e^{x_5}$
PN-20		No Correlation
ST-68	0.87	$dv/dt = -6.74 + 3.3 \ln x_1 - 2.5 x_3 + 0.26 x_4 + .02 e^{x_5}$
AE-91	0.82	$dv/dt = 66.35 - 11.4 \ln x_1 + 32.8 x_3 - 2.8 x_4 - 2.7 e^{x_5}$
AE-95	0.98	$dv/dt = -16.9 + 0.45 x_2 - 5.8 x_3 - 0.43 x_4 + 2.26 e^{x_5}$
Teflon, TE-30		No Correlation
HT-200	0.999	$dv/dt = 1.164 + 14.3 \ln x_1 + 1.13 x_2 + 8.4 x_3 - 1.33 x_4$
TCM	0.999	$dv/dt = 58.8 - 41.8 \ln x_1 + 3.4 x_2 - 4.26 x_4 + 4.15 e^{x_5}$
GA-8	0.97	$dv/dt = 0.54 - 1.05 \ln x_1 + 4.5 x_3 - .35 x_4 + .31 e^{x_5}$
HT, TCM, GA	0.58	$dv/dt = 14.55 + 2.7 \ln x_1 + .82 x_2 + 4.2 x_3 - 1.28 x_4 + 0.59 e^{x_5}$
All	0.24	$dv/dt = 0.77 + 3.93 \ln x_1 + .4 x_2 - .35 x_3 + 0.37 x_4 + 0.59 e^{x_5}$

Table 7.11.d

Membrane	R^2	Log Linear Regression Equation
All	0.11	$dv/dt = -1.19 + 6.92 \log x_5$
All	0.04	$dv/dt = 19.93 - 0.36 \log x_4$
All	0.01	$dv/dt = 11.06 - 0.22 \log x_3$
All	0.004	$dv/dt = 7.95 + 0.09 \log x_2$
All	0.18	$dv/dt = -2.41 + 7.81 \log x_1$
All	0.25	$dv/dt = -4.57 + 3.6 \log x_1 + 0.41 x_2 - 0.33 x_3 - 0.35 x_4 + 5.7 x_5$

Where

x_1 = Vapor pressure
x_2 = Dielectric constant
x_3 = Dipole moment
x_4 = Surface tension
x_5 = Solubility

7.5.II LABORATORY SOIL TESTING

The same procedure as in ambient testing regression analysis was used to arrive at the regression equation for soil samples.

The independent variables in this case included

x_1 = vapor pressure

x_2 = solubility

x_3 = permeability to chemical permeant

x_4 = residence time or time of initial response

x_5 = concentration of the permeant

C/EOC response correlations with combined effects of vapor pressure, solubility, permeability to the organic permeant, time of residence (time of initial response), and concentration of the permeant were very good; with R^2 of 0.93 for clay and 0.99 for silt soils in a multiple linear model (Table 7.11.e). The dv/dt correlations with individual independent variables, however, were low, indicating that the output followed more than one variable in each test.

In regression equations (Tables 7.11 a-e) each coefficient represents the relative contribution of the corresponding independent variable to the dv/dt. A large α_i value indicates that x_i has a strong influence on dv/dt (i.e., EOC or C/EOC output). Negative α_i values indicate that the independent variable x_i has a retardant affect on dv/dt. The regression coefficient R^2 gives an indication of appropriateness of the equation. An R^2 value close to 1 indicates good correlation between the dependent and independent variables. $\alpha_i=0$ is an indication that variable x_i does not correlate with the EOC output.

Table 7.11 may be used to (a) check the magnitude of influence of a specific factor on EOC response, or (b) if the characteristics of the

Table 7.11.e
Correlation for Soil Testing

Membrane	R^2	Multilinear Regression Equation
Silt	0.99	$dv/dt = -3.02 + 0.012\ x_1 + 0.11\ x_2 + 0.55\ x_3 - 7.9\ x_4 + 0.18\ x_5$
	0.53	$dv/dt = 1.42 + 0.397\ x_3 - 39.3\ x_4 + 0.026\ x_5$
	0.11	$dv/dt = 1.48 + 0.02\ x_5$
	0.31	$dv/dt = 4.59 - 36.0\ x_4$
	0.2	$dv/dt = -6.8 + 1.33\ x_3$
Kaolinite	0.93	$dv/dt = 1.28 + 0.007x_1 - .36\ x_2 - .41\ x_3 + 0.035\ x4 + 0.009\ x_5$
	0.25	$dv/dt = 7.03 \quad 8.38\ x_4 + 0.009\ x_5$
	0.11	$dv/dt = .36 + 8.7 \times 10^{-4}\ x_1$
	0.59	$dv/dt = 0.045 - 0.142\ x_3 + 0.186\ x_4 + 0.085\ x_5$
	0.59	$dv/dt = 0.7 + .18\ x_4 + .008\ x_5$
	0.1	$dv/dt = 0.211 + 14.7\ x_4$
	0.43	$dv/dt = 0.24 + 0.08\ x_5$

Where

x_1 = Vapor pressure
x_2 = Solubility
x_3 = Permeability to the chemical
x_4 = Residence time (time of initial response of odor cone)
x_5 = Concentration

membrane and the contaminant organic are known then the regression equation corresponding to the specific membrane can be used to predict the dv/dt range within a confidence interval.

CHAPTER 8

CONCLUSIONS, RESULTS AND RECOMMENDATIONS

8.1 CONCLUSIONS

The findings of this study may be categorized in three broad categories as theoretical, empirical, and implied.

8.1.I THEORETICAL

Theoretical: This study determined that the contribution of physical adsorption in olfactometric detection is minimal. The theories based on chemisorption, however, are most suitable in explaining the EOC operation in detection of contaminants.

8.1.II EMPIRICAL CONCLUSIONS

Empirical conclusions are direct reflections of experimental data in absence of data reduction-manipulation. They include:

a. Each chemical and membrane combination has a unique signature output signal which is different from any other. This property may be used in qualitative differentiation of the organic chemical contaminants.

b. Some membrane polymers react with, and are responsible to presence of a specific contaminant only. Such membranes can be utilized in selective contaminant detection.

c. Application of sudden external pressure produces a short lived, well dissipated output signal which can be clearly distinguished from the normal response of the odor cone. Sustained pressure, however, results in consistently stronger output signal than those without pressure application.

d. EOC responds to application of an ionic field by exhibiting abnormally high peaks voltage values with very fast dissipation of the generated output.

e. EOC and C/EOC are capable of quantitative concentration differentiation. EOC also gives indication of presence of a guest contaminant when detection of another (host) contaminant is already in progress.

f. C/EOC is capable of contaminant detection in both ambient and saturated conditions. Under saturated conditions the inlet to C/EOC is protected against fluid intrusion by using vapor porous hydrophobic Gore-Tex nonwoven membranes. Due to lower volatilization of organics in the fluids (as compared to that in air), the time rate of output voltage in saturated conditions is lower than those for ambient testing.

g. C/EOC can be used for either continuous or intermittent (multiple) contaminant monitoring. In the second case, it may be necessary to decontaminate (purge with freon) before reuse.

8.1.III IMPLIED CONCLUSIONS

Implied conclusions are based on empirical data, available theory and data-reduction-manipulation schemes. Under this category it may be stated that:

a. There is good correlation (i.e., high confidence limits and R^2 values close to 1) between the time rate of change of voltage output and vapor pressure (x_1), dielectric constant (x_2), dipole moment (x_3), surface tension (x_4), and solubility factor (x_5) for ambient testing in both linear and nonlinear models. The correlstion equation may be expressed as:

$$dv/dt = x_0 + \alpha_1 x_1 + \alpha_2 x_2 + \alpha_3 x_3 + \alpha_4 x_4 + \alpha_5 x_5 + E$$

$$dv/dt = x_0 + \alpha_1 \text{ Log } x_1 + \alpha_2 x_2 + \alpha_3 x_3 + \alpha_4 x_4 + \alpha_5 x_5 + E$$

or

$$dv/dt = x_0 + \alpha_1 \ln x_1 + \alpha_2 x_2 + \alpha_3 x_3 + \alpha_4 x_4 + \alpha_5 e^{x5} + E$$

dv/dt for soils correlates with vapor pressure (x_1), solubility factor (x_2), soil permeability to the organic permeant (x_3), time of initial response (x_4), and concentration of the permeant (x_5) as

$$dv/dt = x_0 + \alpha_1 x_1 + \alpha_2 x_2 + \alpha_3 x_3 + \alpha_4 x_4 + \alpha_5 x_5 + E$$

The α_i's in each case relate to the contribution of x_i to the value of dv/dt. Higher α_i values indicate that dv/dt is strongly affected by x_i.

b. A quantitative relation between temperature and time rate of voltage of EOC cannot be inferred from the experiment. Temperature variations, however, lead to output voltage instability at lower temperatures. Slight response fluctuation due to temperature falls within the precision margin or the odor cone and need not be calibrated for.

c. pH of the effluent does not correlate well with the time rate of change of voltage indicating EOC output to be independent of pH of the soil environment.

d. EOC system characteristics are: full scale 11 volts, precision = up to 98% and sensitivity of 10 ppm.

8.2 FUTURE RESEARCH RECOMMENDATIONS

This research program was undertaken as a pilot study exploring, in a limited way, virgin grounds. It has established some trends and has

also created a multitude of questions which need well researched answers. The following list is the what if or suggested future research list:

1. Effects of variation in the size and coating material of capacitor plate on the accuracy and sensitivity of the EOC. The current size is 1 cm diameter copper plate.
2. Development of a multisensor (as opposed to the current single sensor) EOC. This may consist of placing the sensor around the perimeter of the cone as shown in Figure 8.1.

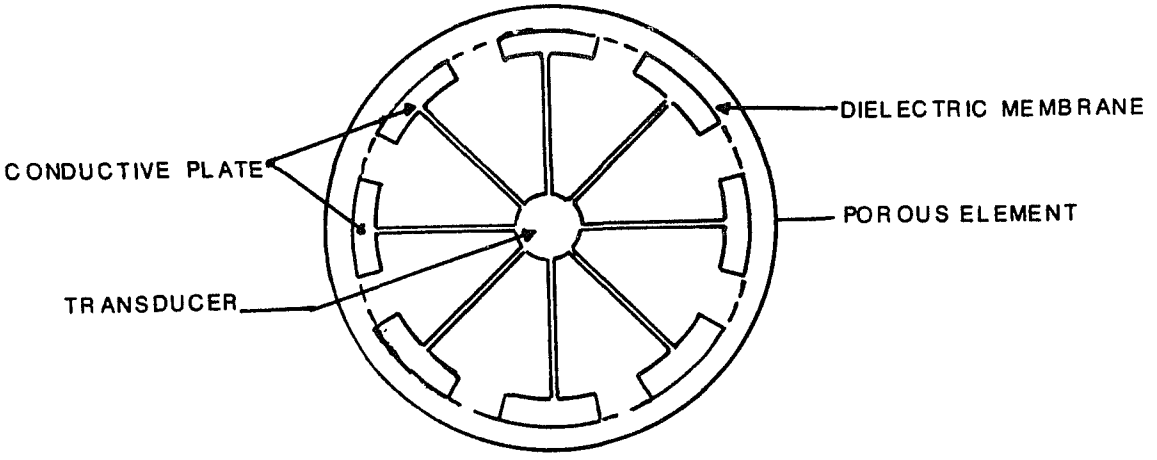

Figure 8.1. Multisensor Odor Cone

This device then may be used in selective detection of different organics simultaneously. The interference study between different sensors is a topic of well deserved attention.

3. A theoretical study to relate heat of mixing or solvation or adsorption of polymer to the output voltage. The results of such a study are essential for accuracy calibration of the EOC.
4. Feasibility of membrane impregnation with a desired trace element for detection of metals, heavy organic and low vapor pressure contaminants.

5. Effect of contaminants in organic soils since organic soils themselves are odorous. The combined odor detection will be of particular interest.
6. Introducing the EOC into the electro-piezo cone penetrometer and conducting field tests for contaminant detection.
7. The effects of interaction between soils and organics on the output, if such interactions are odor-producing.
8. Experimental verification of structural changes in membrane fabric after exposure to contaminants.

BIBLIOGRAPHY

Acar, V.B., Hamidan, A., Field, S.D. and Scott, L. 1983. Organic Leachate Effects on Hydraulic Conductivity of Compacted Kaolinite. ASTM, Special technical publication on impermeable barriers on soils and rocks, pp. 171-187.

Adamson, A.W. 1967. Physical Chemistry of Surfaces. Interscience publishers, pp. 565-641.

Ali, E. and Moore, C. 1981. Improved Techniques for Flow of Liquid Through Landfill. Land disposal of hazardous waste, EPA, 600/19-81-002b, pp. 1-28.

Anderson, D., Brown, K.W., and Green, J. 1982. Effect of Organic Fluids on the Permeability of Clay Soil Liners. Land Disposal of Hazardous Waste. EPA, 600/19-82-002. Pp. 179-190.

Andreoti, T., Tiefenberg, M., and Totsteron, D. 1967. J. Gen. Physiology (50), pp. 2527-2534.

Atkins, P.W. 1976. A Textbook of Physical Chemistry. John Wiley, N.Y., N.Y., 1008 pp.

Bachmat and Bear, J. 1964. The General Equation of Hydrodynamic Dispersion in Homogeneous Isotropic, Porous Mediums. In J. of Geophysical Research, Vol. 69, No. 12, pp. 2561-2567.

Baker, L.E. 1977. Effects of Dispersion and Dead-End Pore Volume in Miscible Flooding. Soci. of Petroleum Engineering J. (Vol. 17), pp. 219-227.

Beddow, J.K. and Meloy, T. 1980. Testing and Characterization of Power and Fine Particles. Heyden & Sons, Ltd., London, 195 pp.

Billmeyer, F.W. 1976. Textbook of Physical Chemistry. John Wiley, New York, N.Y., 240 pp.

Bishop, A.W. and Henkel, D.J. 1962. Measurement of Soil Properties in the Triaxial Test. Edward Arnold Publishers, Ltd. 228 pp.

Bottcher, C.J. and Bodrewijk, P. 1978. Theory of Dielectric Polarization. Elsevier, N.Y., N.Y., 562 pp.

Braunauer, S., Copeland, L.E., and Kautso, D.L. 1976. The Langmuir and BET Theories. In The Solid Gas Interface, E.A. Flood (editor). Marcel Dekker, Inc., New York, pp. 286-313.

Brown, K.W. and Donelly, K.C. 1981. The development of laboratory and field studies to determine the fate of mutogenic compounds from land applied hazardous waste. EPA 600/9-81-002b.

Brown, K.W., Thomas, J.C., and Green, J.W. 1984. Permeability of Compacted Soils to Solvent Mixtures and Petroleum Products. EPA, 10th Symps., pp. 124-134.

Brown, K.W. and Anderson, D. 1982. Effects of Organic Chemicals on Clay Liners Permeability, EPA, 600/9-82-002, pp. 179-190.

Bresler, E. and Dagan, G. 1983. Unsaturated Flow in Spatially Variable Fields. 2. Application of Water Flow Models to Various Fields. Water Resources Research, Vol. 19, No. 2, pp. 421-428.

Bruer, M.M. and Robinson, D. 1969. Dielectric Diffusion, a New Cross Phenomenon. Nature, Vol. 221, pp. 1024-1028.

Burnes, G., et al. 1973. Some Physico-Chemical Interactions of Paraquet with Soil Organic Material and Model Compound. Weed Research, Vol. 13, pp. 71-86.

Burrell, H. 1976. Solubility Parameter Values. In Polymer Handbook, Vol. 4, pp. 337-359.

Cameron, D.R. and Klute. 1977. Convective-Dispersion Solute Transport with a Combined Equilibrium and Kinetic Absorption Model. Water Resources Research, Vol. 13, No. 1, pp. 183-188.

Coats, K.H. and Smith, B.O. 1964. Dead-end pore volume and dispersion in porous media. Soci. of Petroleum Eng. J., Vol. 4, pp. 73-84.

Conway, B.E. 1967. Some Thermodynamic and Kinetic Factors in Sorption on the Solid Gas Interface. A. Flood, editor. Marcel Dekker, Inc., N.Y., pp. 691-726.

Crowell, A.D. 1967. Surface Forces and the Solid-Gas Interface. In The Solid-Gas Interface, E.A. Flood, editor. Marcel Dekker, Inc., New York, pp. 175-193.

Dagan, G. and Bresler, E. 1983. Unsaturated Flow in Spatially Variable Fields. 1. Derivation of Model of Infiltration and Redistribution. Water Resources Research, Vol. 19, No. 2, pp. 413-420.

Daniel, D. 1984. Effect of Hydraulic Gradient and Method of Testing on the Hydraulic Conductivity of Compacted Clays to Water and Methanol. 19th EPA Symposium on Hazardous Waste, pp. 138-144.

Daniel, D.E., Trutwein, S.J., Baynton, S.T., and Foreman, D.E. 1984. Permeability Testing with Flexible Wall Permeameters. ASTM Geotechnical Testing Journal, Vol. 7, No. 3, pp. 7-39.

Dash, J.D. 1975. Films on Solid Surfaces. Academic Press, Inc., N.Y., N.Y., pp. 59-103.

Dean, H.A. 1963. A Mathematical Model for Dispersion in the Direction of Flow in Porous Media. Soci. of Petroleum Engineering, J. (Vol. 3), pp. 49-42.

DeBore, J.H. 1953. The Dynamic Character of Absorption. Oxford University Press, London, pp. 1-87.

DeBore, J.H. 1950. Advances in Colloid Science. Interscience Publications, New York, N.Y., 286 pp.

Debye. 1954. Collected papers. Interscience Publishers, New York, N.Y. 700 pp.

Dewalle, F.B. and Chain, E.S.K. 1981. Detection of Trace Organics in Well Water Near a Solid Waste Landfill. American Water Works Association Journal, pp. 206-211.

Doner, H.E. and Mortland, M.M. 1969. Benzene Complexes with Copper II Montmorolonite. Science (1969), Vol. 116, pp. 1406-1407.

Dragun, J. and Helling, C.S. 1982. Soil and Clay Catalyzed Reactions Physico-Chemical and Structural Relationship of Organic Chemicals Undergoing Free Radical Oxidation. Land Disposal of Hazardous Waste. EPA, 600/19-82-002, pp. 106-121.

Dubois, P.H. 1957. Multivariate Correlational Analysis. Harper and Brothers, Publishers, New York, 202 pp.

Dunn, J. and Mitchell, J.K. 1984. Fluid Conductivity Testing of Fire-Graved Soils. Journal of Geotechnical Engineering, Vol. 110, No. 11., pp. 1648-1662.

Ehlrich, G.G., Gorelitz, D.F., Godsy, E.M., and Hult, M.F. 1982. Degradation of Phenolic Contaminants in Ground Water by Anaerobic Bacteria at Louis Park, Minnesota. Ground Water, Vol. 20, No. 6, pp. 703-710.

Elias, A. 1976. Polymerization of organic systems. Gordon and Breach, London, 330 pp.

Elrich, D.E. and French, L.K. 1966. Miscible Displacement Patterns on Disturbed and Undisturbed Soil Cores. Soil Science Society Association, Vol. 30, pp. 216-227.

Elliot, I.F. and Stevenson, F.J. 1977. Soils for Management of Organic Waste and Waste Water. S.S.S.A., A.S.A., C.S.A., Madison, Wisconsin, 314 pp.

Emrich, G.H. and Buch, W.W. 1981. Top Sealing to Minimize Leachate Generation. Land Disposal of Hazardous Waste. EPA, 600/19-81-002b. pp. 291-297.

Feda, J. 1982. Mechanics of Particular Materials, The Principal. Elsewier Scientific Publishing Company, New York, N.Y., 440 pp.

Foreman, D.E. and Daniel, E.D. 1986. Permeation of Compacted Clay With Organic Chemicals. Journal of Geotechnical Engineering, ASCE, Vol. 112, No. 7, pp. 669-681.

Freund, R.J. and Minton, P.D. 1979. Regression Methods: A Tool for Data Analysis. Marcel Dekker, New York, 346 pp.

Frolhich, H. 1949. Theory of Dielectrics, Dielectric Constant and Dielectric Losses. Clarenson, Oxford, 261 pp.

Fuller, et al. 1981. Behavior of Cd, Ni, Zn in Single and Mixed Combinations in Landfill Leachates. Land Disposal of Hazardous Waste. EPA, 600/19-81-002b, pp. 18-28.

Fuller. 1982. Methods for Conducting Soil Column Tests to Predict Pollutant Migration. Land Disposal of Hazardous Waste. EPA, 600/9-82-002, pp. 87-105.

Garret, B.C., et al. 1981. Development of Solid Waste Leaching Procedure and Manual. Land Disposal of Hazardous Waste. EPA, 600/9-81-002b, pp. 9-17.

Gillham, F.W. and Cherry, J.A. 1982. Contaminant Migration in Saturated Unconsolidated Geologic Deposit. Geological Society of America, Special Paper 189, pp. 31-62.

Gnandadesikan, R. 1977. Methods for statistical data analysis of multivariate observations. John Wiley and Sons, New York, N.Y. 311 pp.

Gomer, R. 1961. Field Emission and Field Ionization. Harvard University Press, Cambridge, Mass., pp. 16-85.

Green, N.J., Lee, G.F., Jones, R.A., and Palit, T. 1983. Interaction of clay soils with water and organic solvents: implication for the disposal of hazardous waste. Environ. Sci. Technol., Vol. 17, pp. 278-282.

Gregg, S.J. and Sing, K.S.W. 1982. Absorption, Surface Area and Porority. Academic Press, New York, N.Y., 209 pp.

Goring, C.A.I. and Hamaker, J.W., editors. 1972. Organic Chemicals in Soil Environment. Vol. 1, Marcel Dekker, 368 pp.

Gunst, F.R. and Mason, L.R. 1980. Regression Analysis and Its Application - A Data Oriented Approach. Marcel Dekker, Inc., New York, 402 pp.

Gupta, S.P. and GreenKorn, R.A. 1973. Dispersion During Flow in Porous Media with Linear Absorption. Water Resources Research, Vol. 9, No. 5, pp. 1357-1368.

Gurney, R. 1953. Ionic Processes in Solution. McGraw-Hill, New York, N.Y., 275 pp.

Hamidon, Abu Bakar. 1984. The effect of organic leachate on hydraulic conductivity of compacted clay. M.S. Thesis presented to Faculty of Civil Engineering, Louisiana State University, 182 pp.

Hilderbrand and Scott. 1949. The Solubility of Non-Electrolytes. Rainhold Publishing Corp., New York, N.Y., pp. 162-188.

Irani, F.R. and Callis, C.F. 1963. Particle Size: Measurement, Interpretation and Application. John Wiley and Sons, Inc., N.Y., 165 pp.

James, R.V. and Rubin, J. 1972. Accounting for Apparent Induced Dispersion in Analysis of Miscible Displacement Experiments. Water Resources Research, Vol. 8, No. 1-3, pp. 717-721.

Jaycock, M.J. and Parfitt, G.D. 1981. Chemistry of Interface. Ellis Harward Limited, Chichester, England. 279 pp.

Jones, F.B. 1953. Instrument Technology. Butterworth scientific publication, pp. 112-186.

Kemper, W.D. 1960. Water and Ion Movement as Influenced by the Electrostatic Charge and Diffuse Layers of Cations Associated with Clay Mineral Surfaces. Soil Sci. Soc. of America. Proceedings, Vol. 24, pp. 10-18.

Kennard, L.H. 1938. Kinetic Theory of Gases. McGraw-Hill, New York, N.Y., pp. 175-198.

Kiang, Y.H. and Metry, A.A. 1982. Hazardous Waste Processing Technology. Ann Arbor Science, 549 pp.

King, P.H. and McCarty, P.L. 1968. A Chromatographic Model for Predicting Pesticide Migration in Soil. Soil Science (106), pp. 112-124.

Kundsen, M. 1946. The Kinetic Theory of Gases. Methven, London, 168 pp.

Ladlie, J.S., et al. 1976. Effects of Soil pH on Microbial Degradation Absorption and Mobility of Metribenzene. Weed Research, Vol. 16, pp. 132-141.

Lamb, T.W. 1958. Compacted clay: structure and engineering behavior. J. Soil Mechanics & Foundation Division, Transactions, Vol. 125, Parts 1 & 2, pp. 682-707.

Lambert, S.M., et al. 1965. Movement and Sorption of Chemicals Applied to Soils. Weeds Vol. 13, pp. 1056-1064.

Lapidus, Amudson. 1952. Mathematics of Absorption Beds. J. Physical-Chemistry, Vol. 56, pp. 984-988.

Law, J.P. and Kunze, G.W. 1966. Reaction of Surfactants with Montmorolonite; Absorption Mechanisms. Soc. Soil Science of America. Vol. 30, pp. 118-127.

Lee, K.L. and Morrison, R.A. 1970. Strength of Anisotropically Consolidated Compacted Clay. J. Soil Mechanics and Foundation Design, ASCE, SM6, pp. 2025-2043.

Low, J. and Johnson, T.C. 1960. Use of Back Pressure to Increase Degree of Saturation of Triaxial Test Specimens. Research Conference on Shear Strength of Cohesive Soils, ASCE, Boulder, Colorado, pp. 819-836.

Lowell, S. 1979. Introduction to Powder Surface Area. John Wiley and Sons, Inc., New York, N.Y., 234 pp.

McIntosh, R. 1976. The Dielectric Constant and the Solid-Gas Interface. The Solid-Gas Interface, A.E. Flood, editor. Marcel Dekker, Inc., N.Y., N.Y., pp. 515-641.

Michael, A.S., and Lin, C.S. 1954. The permeability of kaolinite. Industrial and Engineering Chemistry, Vol. 46, pp. 1239-1246.

Miller, C.W. and Benson, L.V. 1983. Simulation of Solute Transport in a Chemically Reactive Heterogeneous System. Model Development and Application. Water Resources Research, Vol. 19, No. 2, pp. 381-391.

Mitchell, J.K. 1976. Soil behavior. John Wiley and Sons, New York, N.Y., pp. 18-329.

Mitchell, J.K., Hooper, D.R., and Campanella, R.G. 1965. Permeability of Compacted Clay. Journal of Soil Mechanics and Foundation Design, ASCE, Vol. 9, No. SM4, Proc. Paper 4392, pp. 41-65.

Moore, C.A. and Mitchell. 1974. Electromagnetic Forces and Soil Strength. Geotechnique 24, No. 4, pp. 627-640.

Moore, W.J. 1956. Physical Chemistry. Prentice Hall, Engelwood Cliff, N.J., 977 pp.

Morrill, L.G., and Mahitun, B.C. 1982. Organic compounds in soils, sorption, and degradation. Ann Arbor Science, Mich., 326 pp.

Morrison, R. 1984. Instrumentation Fundamentals and Applications. John Wiley and Sons, 483 pp.

Morawetz, H., editor. 1975. Solubility Parameters in Macromolecular in Solution, Vol. 21 of High Polymer Series. John Wiley and Sons, pp. IV-337 - IV-359.

Nielsen, D.R. and Biggar, J.M. 1962. Miscible Displacement. Soil Science Society Proceedings (62), pp. 216-221.

Olson, R.E. and Daniel, D.E. 1979. Measurement of Hydraulic Conductivity of Fine-Grained Soils. ASTM STP 746. T.F. Zimmer and C.O. Riggs, Editors, pp. 18-64.

Overcash, M.R., editor. 1981. Decomposition of Organic Compounds in Soil. Ann Arbor Science, Ann Arbor, Mich., 455 pp.

Parsegian, A. 1969. Energy of an Ion Crossing a Low Dielectric Membrane Solution to Four Relevant Electrostatic Problems. Nature, Vol. 22, pp. 844-848.

Perkins, T.K. and Johnston, O.C. 1963. A Review of Diffusion and Dispersion in Porous Media. Soci. of Petroleum of Engineering, J., Vol. 3, pp. 70-84.

Perry and Chilton. 1973. Chemical Engineering Handbook. McGraw-Hill, New York, N.Y., pp. 16.12-16.18.

Petere, W.R., Snultz, W.R., and Duff, P.W., B.M. 1982. Electrical Resistivity Technique for Locating Liner Leaches. Land Disposal of Hazardous Waste. EPA, 600/9-82-002, pp. 250-265.

Pettyjohn, W.A. 1981. Prediction of Leachate Plume Migration. Land Disposal of Hazardous Waste. EPA, 600/9-81-002b, pp. 71-84.

Ponec, V., Knoz, Z., and Cerny, S. 1974. Adsorption on Solids. Butterworths, London, 693 pp.

Rose, D.A. 1973. Some Aspects of the Hydrodynamic of Solute in Porous Material. In J. of Soil Science, Vol. 24, pp. 284-292.

Scheidegger, A.E. 1954. Statistical Hydrodynamics in Porous Media. J. of Applied Physics, Vol. 25, No. 8, pp. 994-1001.

Seber, C.A. 1977. Linear Regression Analysis. John Wiley, New York, N.Y., 465 pp.

Selim, H.M. and Mansell, R.S. 1976. Analytical Solution of Equation for Transport of Reactive Solute Through Soils. Water Resource Research (76), pp. 528-532.

Smyth, C.P. 1955. Dielectric Behavior and Structure. McGraw-Hill, New York, N.Y., 441 pp.

Sridharan, A. and Rao, V. 1973. Mechanism Controlling Volume Charge of Saturated Clays and the Role of the Effective Stress Concept. Geotechnique 23, pp. 359-382.

Tompkins, F.C. 1967. Surface Potentials and the Solid-Gas Interface. In Solid Gas Interface. A. Flood, editor. Marcel Dekker, Inc., New York, N.Y., pp. 765-785.

Tanyolac, N.N. 1969. Modern Theories of Odor and Olfaction and Objective Olfactometry. In Proceeding of the Ninth International Congress, Mexico, pp. 195-198.

Tanyolac, N.N. 1968. Electron-Odorcell and Theories of Odor. Proceeding of NATO Summer School at Robert College Research Center, pp. 537-561.

Tumay, M.T. 1985. Field calibration of electric cone penetrometer in soft soil, executive summary. Louisiana Transportation Research Center, 37 pp.

Tumay, M.T., Boggess, R.L., and Acar, Y. 1981. Subsurface Investigation with Piezo-Cone Penetrometer. Proceedings of ASCE Session on Cone Penetration Testing and Experience. St. Louis, MO/October, 1981, pp. 325-342.

Van Genvchten, M.T. and Wierenga, P.J. 1976. Mass Transfer Studies in Sorbing Porous Media. I. Analytical Solutions. Soil Science Soci. of America (76), pp. 473.

Van Olphen. 1963. An Introduction to Clay Colloidal Chemistry. John Wiley and Sons, New York, N.Y., 318 pp.

Van Vlack, L.H. 1980. Elements of Materials Science and Engineering. Addison-Merly Publishing Company, pp. 234-276.

Van Vlack, L.H. 1970. Material Science for Engineering. Addison-Merly Publishing Company, Chapter 13, pp. 249-274.

Waller, M.J. and Davis, J.I. 1982. Assessment of Techniques to Detect Landfill Liner Failings. Land Disposal of Hazardous Waste. EPA, 600/9-82-002b, pp. 239-249.

Wissa, A. 1969. Pore Pressure Measurement in Saturated Stiff Soils. JSMFD, ASCE, Vol. 9, No. SM4, pp. 1063-1073.

Young, D.M., Crowell, A.D. 1962. Physical Absorption of Gases. Butterworth, London, pp. 116-124.

Young, R.A., et al. 1975. Industrial Odor Technology Assessment. Ann Arbor Science, Ann Arbor, Mich., pp. 98-118.

Young, R.N. and Warkentin, B.R. 1966. Introduction to Soil Behavior. Macmillan Book Company, New York, N.Y., pp. 31-72.

Zimmie, T.F. 1981. Geotechnical Testing Consideration in the Determination of Laboratory Permeability for Hazardous Waste Disposal Site. ASTM, STP, 760. Hazardous Solid Water Testing, First Conference, pp. 293-320.

APPENDIX A

THE INSTRUMENT

INTRODUCTION

The odor-cone (C/EOC) is a newly designed instrument. Design and operation of the EOC components instrument was covered in Chapter 2. This appendix defines instrument characteristics such as range, sensitivity, precision, selectivity, hysteresis, and time lag of response. Since the amount input to the EOC is not quantifically known, a value for the accuracy of the instrument cannot be established yet.

FULL SCALE

The full scale of EOC is a function of the resistors and the capacitors used in its circuit. The present design has a full range of 11 volts with a shifting zero point on the scale that can be adjusted such that the range is ±5.5 volts.

SELECTIVITY

There are about 2000 distinct odors in the environment. The identification of each one of these odors does not seem to be a practical task at this stage of EOC development. The device however should be able to indicate the sudden presence or sudden disappearance of an odor when it is in the process of monitoring a different odorant molecule. For this purpose, the membrane used in the EOC must be responsive to all detectable odors and that the intruding odor must have adequate signal-triggering strength when it comes within the olfactory reach of the EOC to generate a signal.

Experiments have indicated that EOC is selective in the detection of one contaminant chemical from among a host of contaminants if the membrane used in the EOC is exclusively reactive with a desired contaminant or if it is nonreactive with all but one of the contaminants present. An example of such selective response behavior is provided in Figure A.1, in which EOC with a Durapore membrane is exposed to six different chemical contaminants and only registers a response to acetone. Such a response is useful when searching for a specific chemical contaminant.

EOC is also selective in the identification of contaminants by producing a signature signal for each contaminant, which is unique for any contaminant membrane combination that might produce a detectable level of response. This is demonstrated in Figure A.2.

In a laboratory experiment, EOC was exposed to a flask containing 5 cc of acetone. Dichloromethane was added to this flask in 1, 5, 10, and 25 cc portions and the output for all cases was recorded. Figure A.3 shows the test results. It indicates that the addition of dichloromethane to the acetone flask was reflected in the EOC output as an increase and a gradual transformation of the output curve from that characteristic of the acetone to a curve characteristic of the dichloromethane.

In another experiment, freon was introduced to a flask containing acetone which was being monitored by EOC. The result was a complete reversal of the response pattern, which is indicative of the arrival of freon.

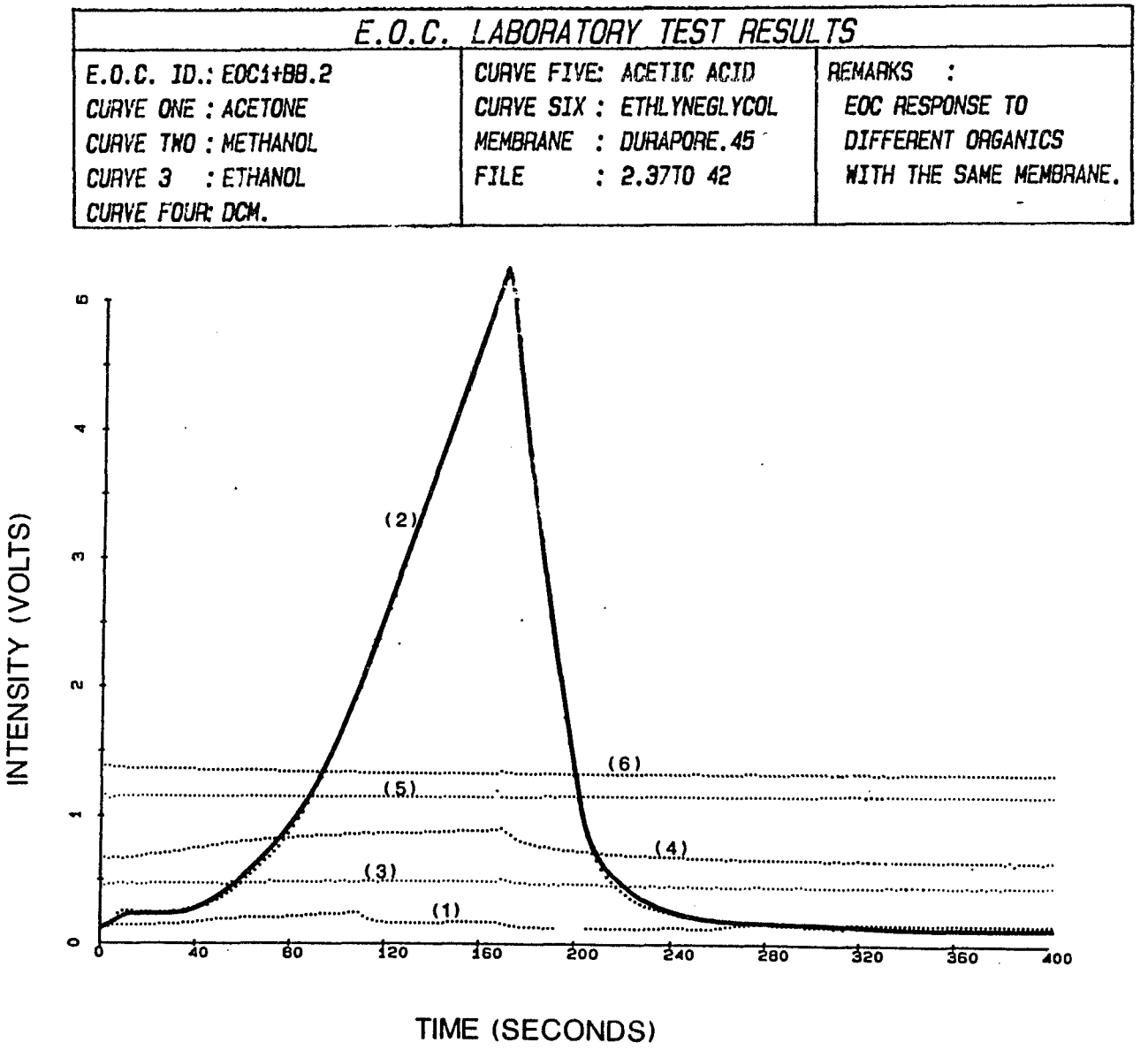

Figure A-1. Selectivity of durapore membrane in detection of acetone.

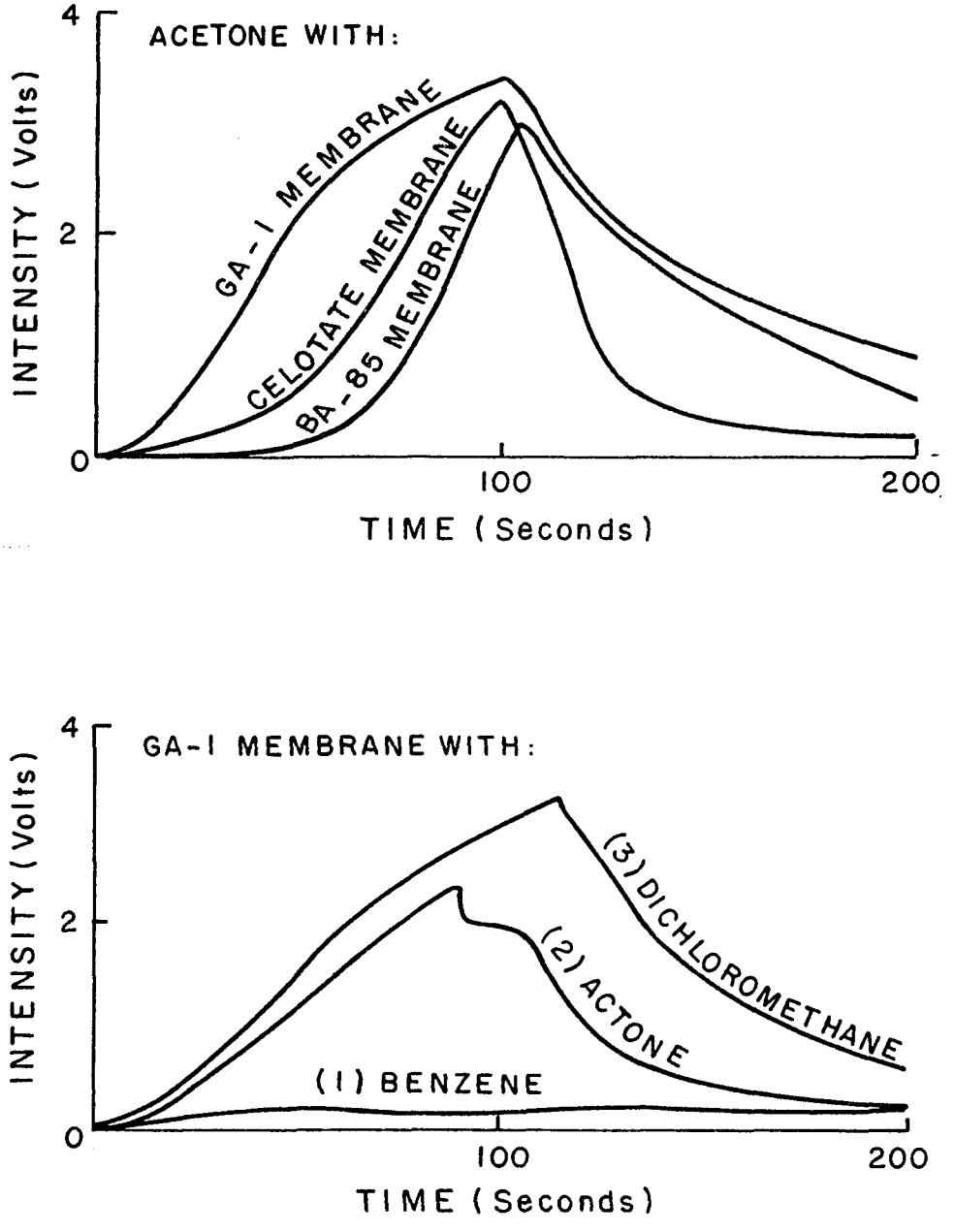

Figure A-2. EOC selectivity with respect to (a) the contaminant, (b) the membrane.

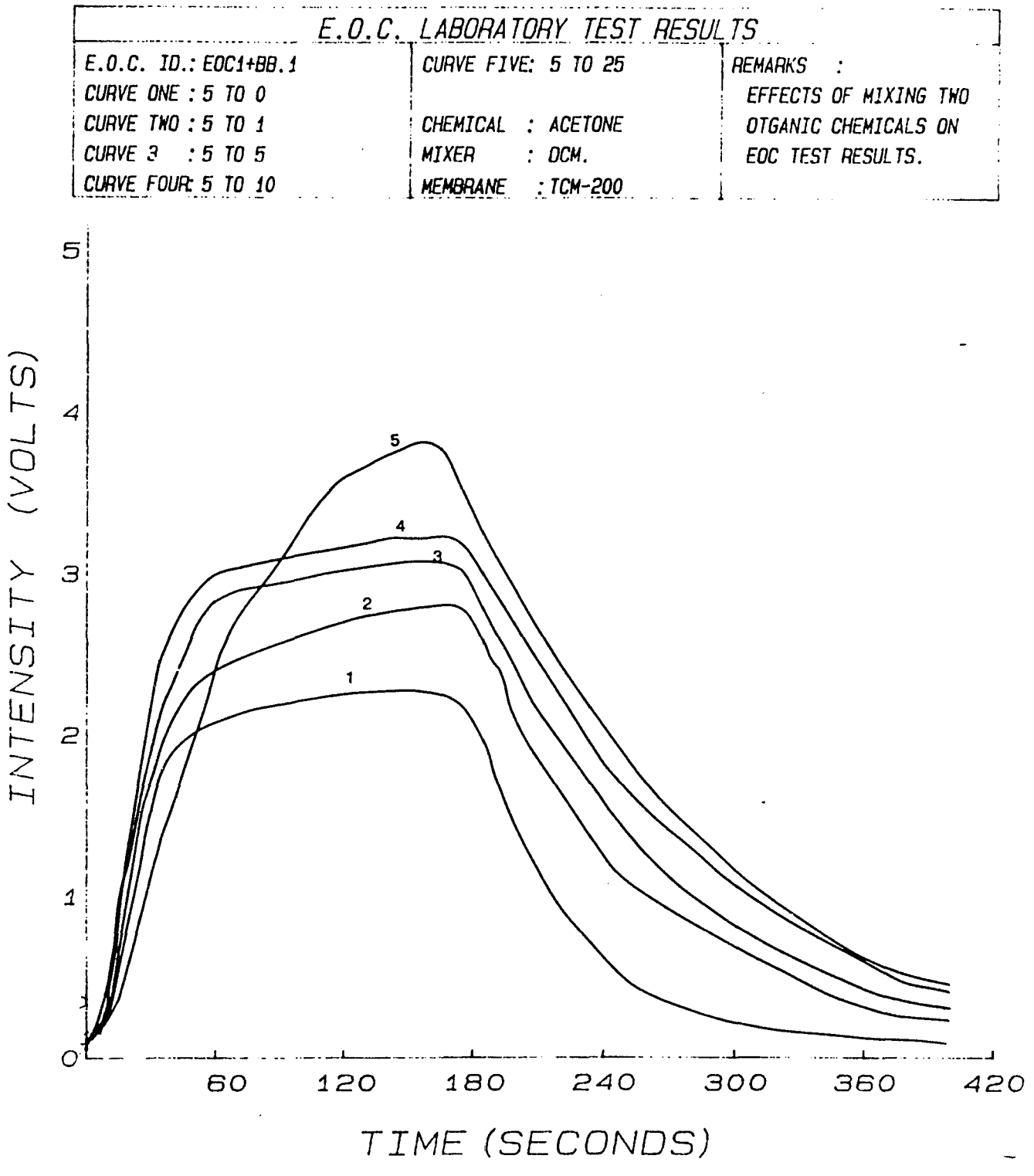

Figure A-3. EOC selectivity in adsorption of mixtures.

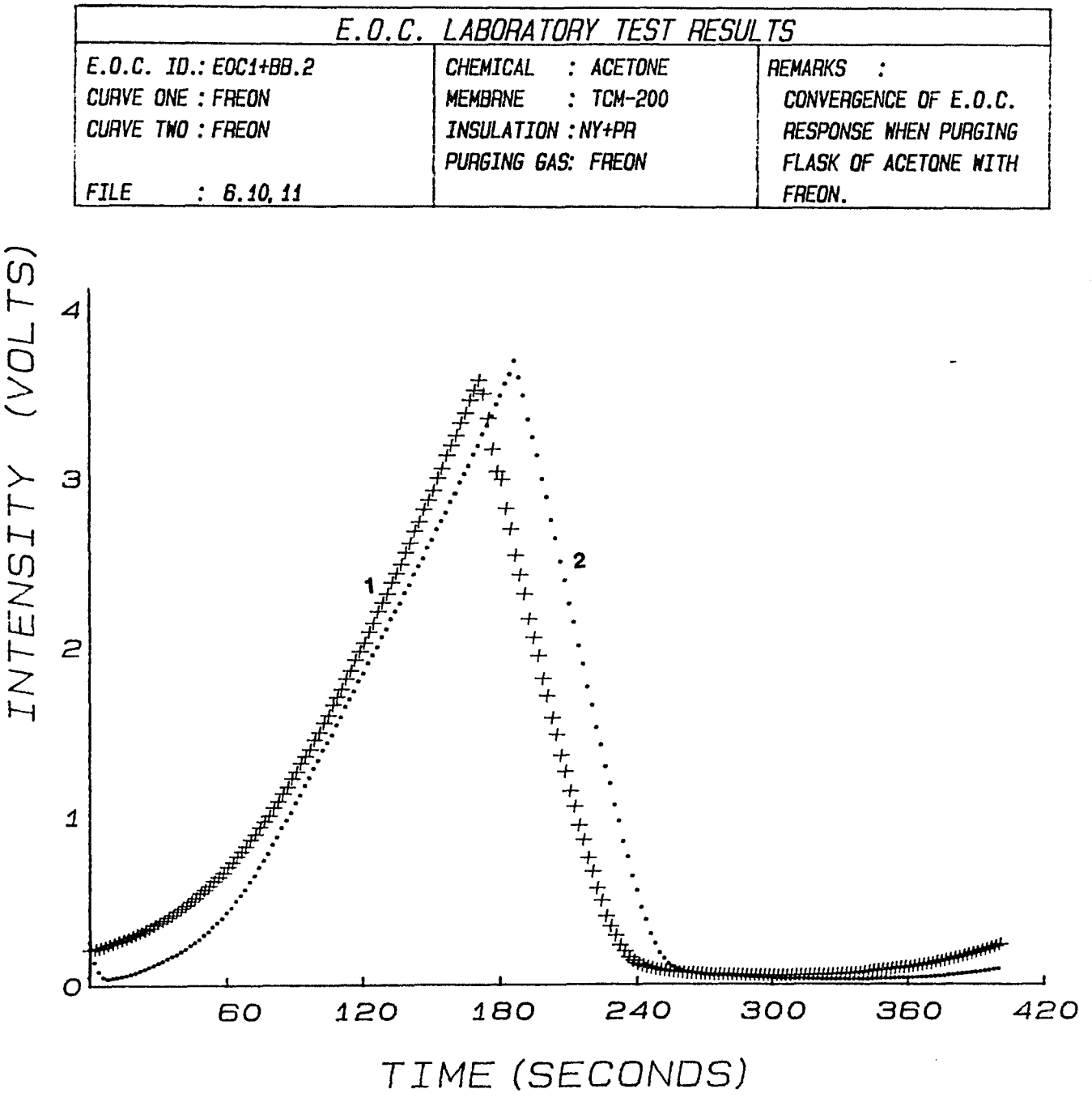

Figure A-4. EOC response to incoming decontaminants (Freon-12).

SENSITIVITY

The sensitivity of an instrument may be measured by the minimum amount of contaminant which can produce a detectable signal. This characteristic of the EOC may be different for different contaminants and it depends on the scale of the instrument, the strength of the background noise or interference, the capacitance value, the voltage gain, leakage, orifice size, membrane type, and the type of contaminant monitored.

In the laboratory assessment of sensitivity of the EOC, the instrument was placed in a 1000 ml jar, the top of which was sealed with a stopper or parafin film to prevent the contaminant molecules from escaping. After the steady state output was established at zero, contaminant was injected through the top of the jar in .01 cc increments and the response was monitored for one minute. If no detectable changes in the output voltage were detected, additional contaminant was added to the jar until a detectable response was generated.

Test results are presented in Figures A.5 and A.6. They indicate a resolution sensitivity of .4% and a threshold sensitivity of 10 ppm for formaldehyde, 10 ppm for trichlorethylene, and less than 10 ppm for pcp.

PRECISION

The precision of a device is measured by the agreement of the readings among themselves or reproducibility. A high degree of reproducibility means that the instrument has no drift, i.e., the calibration of the instrument does not gradually shift over a period of time.

EOC was exposed to the same concentration of an organic chemical. In repeated testing under the same conditions, the results (Figures A.7 a&b) indicate a precision of up to 98%.

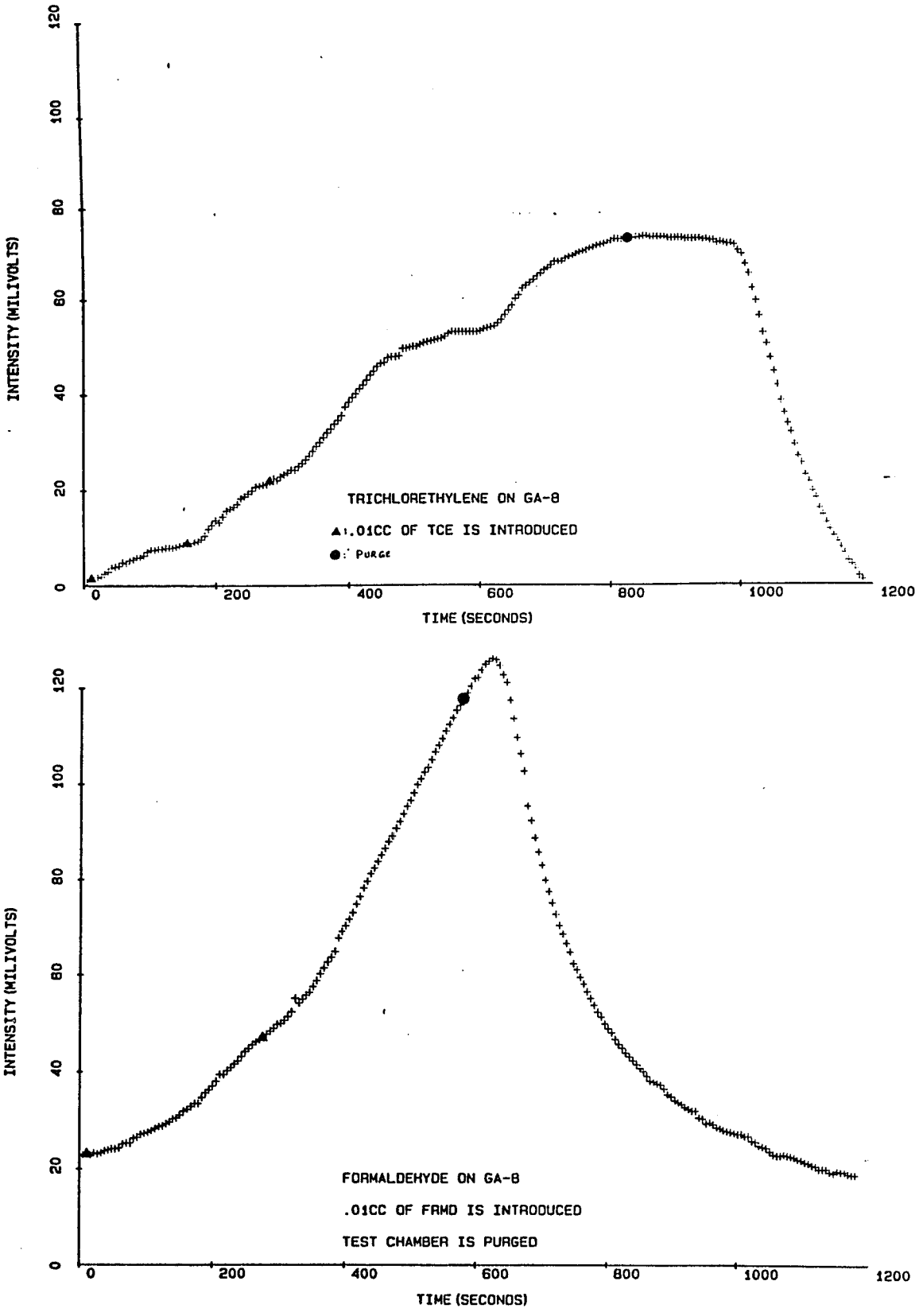

Figure A.5. Sensitivity limit of EOC to a) formaldehyde and b) trichlorethylene.

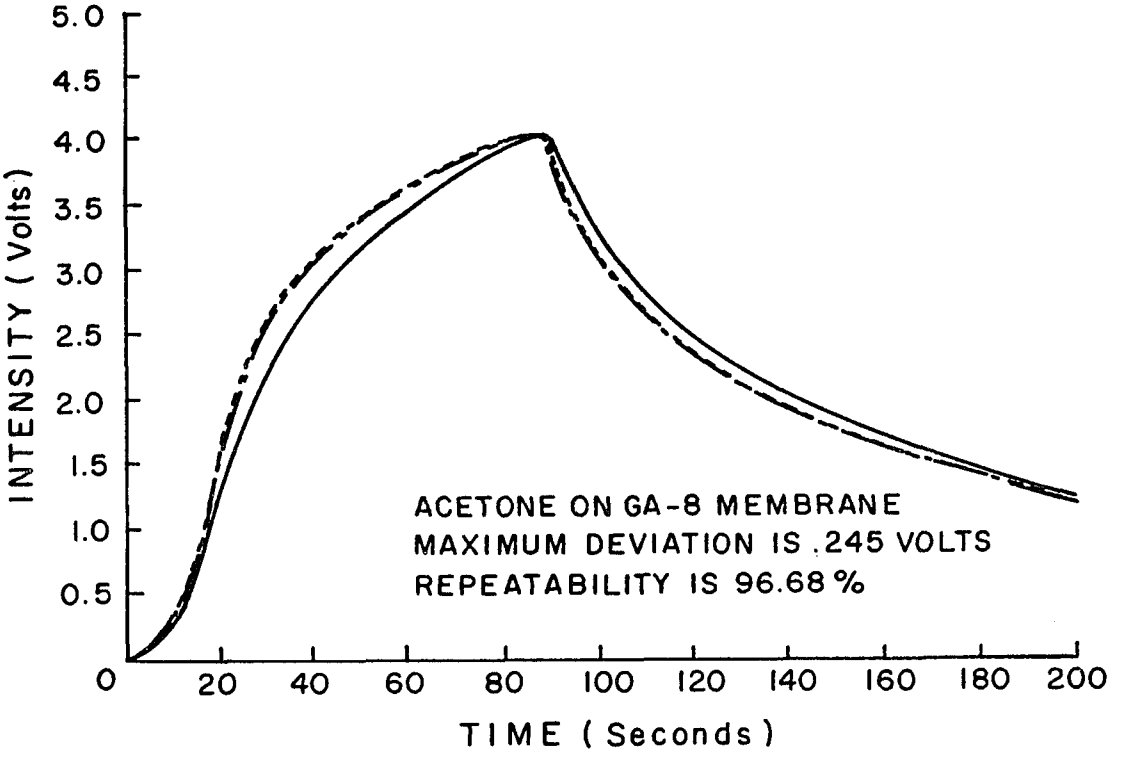

Figure A.6. Precision testing of EOC.

ADSORPTION HYSTERESIS

A process is said to exhibit hyteresis if, when the direction of change of an independent variable x is reversed, a dependent variable y fails to retrace the value through which it passed in the forward process (see Figure A.7). The dependent variable "lags behind" in its attempt to follow the changes in the independent variable.

One should not be concerned in this account with the possible behavior in which the dependent variable drifts steadily.

When experiments are carried out very slowly, the loop may degenerate into a line, and hysteresis may disappear. Time-dependent hysteresis is

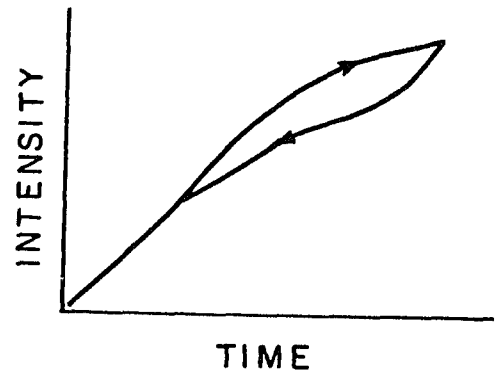

Figure A.7. Adsorption hysteresis

caused by the relaxation phenomenon and it does not enter the picture of permanent hysteresis.

EOC hysteresis is demonstrated by the difference between rates of adsorption and desorption.

Considering adsorption of a vapor on the membrane surface of EOC, the discrepancies of the adsorption-desorption processes are caused partially by differences in the mechanism of filling and emptying pores of specific shape and size, and irreversibility of some of interactions of membrane with the chemical. The two theories most widely used to explain the origin of this hysteresis are the open theory and ink-bottle theory.

In the open theory, pores are assumed to take the shape of regular capillaries open at both ends and never cross one another. Pores are filled up through increases in the gas phase pressure, which causes a multimolecular adsorbate layer to form a cylindrical condensate meniscus along the pore circumference.

The relative pressure value at which the entire pore is filled at once is determined by the radius of the meniscus along the pore circumference. In contrast to this, a condensate-filled pore is emptied on

decreasing the relative pressure by evaporation of the condensate from hemispherical menisci at the capillary ends. The pressure value at which a pore is emptied is therefore determined by the radius of the spherical meniscus. Since this radius is precisely one half of the meniscus radius along the pore circumference, the adsorption branch has to be located to the left of the desorption branch.

The ink-bottle theory assumes that pores take the shape of cavities with one or several narrow inlet necks. With rising relative pressure, the bottle-shaped pores are filled without delay, depending on the radius of curvature of the menisci.

However, the pores are emptied only when the relative pressure decreases to a value that permits the condensate to evaporate from the menisci in the narrow necks.

Pores of diameter greater than about 500-100 A° are too large to be filled by volume capillary condensation; they are in this sense equivalent to a flat surface.

In EOC operation one is not concerned with desorption and output voltage measurements are made, for the most part, unidirectionally. Consequently, the hysteresis phenomenon does not limit the reliability of the EOC.

CELL OPENING

Generally speaking, the pressure drops from P at the inlet of the EOC to P_o at the membrane surface). This pressure drop is related to the inlet diameter, d, as $(P-P_o)\alpha\frac{1}{d}$. The larger the diameter of the opening, the smaller the pressure drop, and consequently, the higher the number of available molecules in the olfactory reach of EOC.

Another factor of importance is the path of migration of odor molecules. The longer and more cumbersome the path, the longer the time lag of initial response.

This fact can be used to enhance the detection limit when the odo-cell is placed in the piezo cone-penetrometer (PCPT) by providing a larger exposure inlet to the olfactory region inside the cone. This, however, may reduce the intruding vapor pressure and inversely affect the EOC exposure levels and thus the output levels.

Test results (Figure A.8) with different openings for the tip of the odo-cell indicate that the magnitude of the output voltage decreases with the decreasing size of the opening. No precise calibrations are made for changes in the magnitude of output voltage vs. the size of the opening.

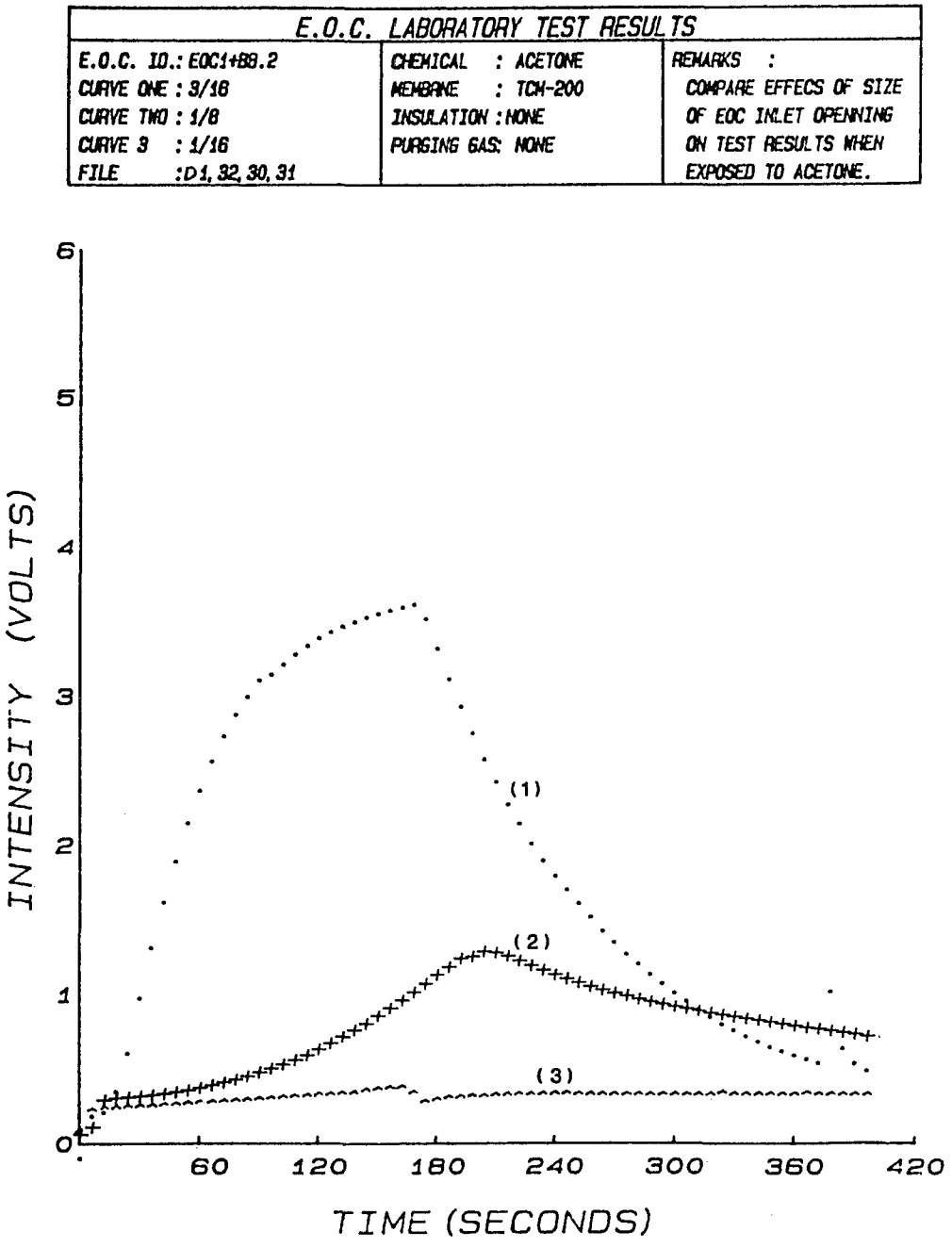

Figure A-8. Effects of different EOC inlet sizes on EOC response.

APPENDIX B

TEST SET-UP AND TESTING PROCEDURE

TEST SET-UP

A schematic diagram of the test set-up used in this study is presented in Figure B.1. Due to the unconventional equipment used in this experiment, all components had to be designed and fabricated to meet the specific requirements of the experiment. The objective was to build laboratory models to simulate contaminant migration through the soil media penetrated by the C/EOC and then attempt to detect or verify the presence of organic permeant in such models when water in the pores is replaced by such organic laden permeants.

The test set-up, in many respects, resembles an apparatus for measuring hydraulic conductivity of organic permeants in fine grained soils. A review of literature reveals numerous approaches with respect to design and operation of such permeameters, with provisions provided for hazardous waste permeation. Modified versions of triaxial cells, shear box and compaction molds are among some of the set-ups used by researchers of this field. Choices of permeameters, however, basically are limited to fixed wall or flexible wall permeameters.

In spite of reported identical values of hydraulic conductivity of identically compacted samples to water in both rigid and flexible wall permeameters, it is reasonable and substantiated in literature to state that in a rigid wall permeameter the possibility and the potential for side leakage along the wall is always present. Such leakage will produce side channels. The pressure head at the top of these channels will gradually drop with increasing velocity, consequently altering the boundary conditions from zero flux to a nonzero flux.

The problem of side leakage is further complicated by sample shrinkage brought about by fabric changes caused by replacing water with organics of lower dielectric constant (Mitchle, 1976).

Yet another factor of concern is the "wall effect." Near the permeameter walls there will be packing irregularities, and zones of high porosity may extend several particle diameters from the container walls. Packing irregularities of this type will have an effect on both longitudinal and transverse dispersion and considerations for this effect are included as β in the dispersion equation (equation 3.18)

$$K_t = D_o/F\phi + 0.0157\ V\delta dp\beta_t$$

It should be noted that in rigid wall permeameters, continuous contact between soil and boundary is not of high significance, if there are enough discontinuous contact points to prevent a fingering fluid path (channel) formation.

In light of above mentioned factors use of rigid wall permeameters was not adopted in this study. Strict coherence to this point, however, became partially impossible as will be explained later.

Flexible wall permeameters provides following advantages.

a. Freedom to vary effective stress by changing the cell pressure and back pressure whenever desired
b. Effectively reducing and possibly eliminating side leakage
c. Freedom to monitor volume changes (outflow data) during testing

To avoid contamination of and possible damage to the saturation lines and connections, all such components were selected from chemical resistant teflon. Mariotte bottles were used as reservoirs for the

organic permeants. Pressures were centrally regulated through an E1E cycle pressure generator. The list of components used in the experiment and pertinent figures follow:

1. E.L.E. pressure distributor and 3way pressure gauge
2,3,4. Actuator valves for lines connected to saturated line, chamber pressure line, chamber fluid reservoir line and outflow line
5. Supplement nitrogen tank gauge with fine divisions
6. Freon tank valve
7. Nitrogen gas tank
8. Freon12 container
9. Saturation water reservoir (triaxial cell, Geonor)
10. Chamber fluid reservoir (triaxial cell, Geonor)
11. Organic chemical reservoir (Mariotte bottle)
12. Chamber pressure line
13. Saturation water reservoir pressure line
14. Chamber fluid reservoir pressure line
15. Organic chemical reservoir pressure line
16. Freon-12 supply line
17. Saturation line
18. Chamber fluid line
19. Bottom platten saturation or drainage line
20. Base plate
21. Top plate
22. Plexyglass chamber
23. Annular soil sample
24. Perforated cylinder
25. One piece top platten

26. C/EOC
27. HP85 Computer
28. HP data acquisition unit
29. HP Disc drive
30. HP 8 Pen plotter

A more detailed description of a single cell set-up is presented in Figure B-2. Components of the cell are presented in plates B-1 thru B-3.

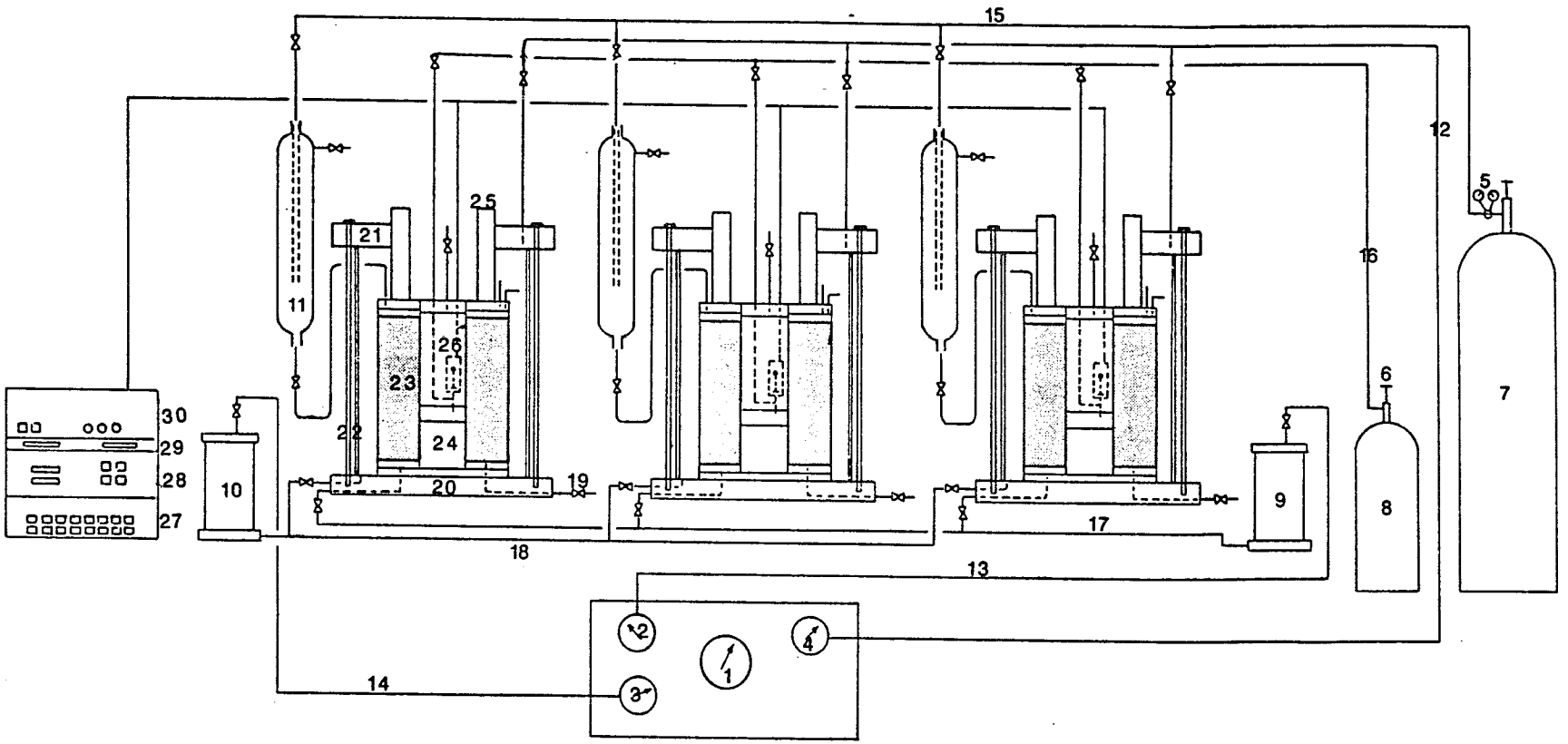

Figure B-1. Laboratory test set-up used in this study.

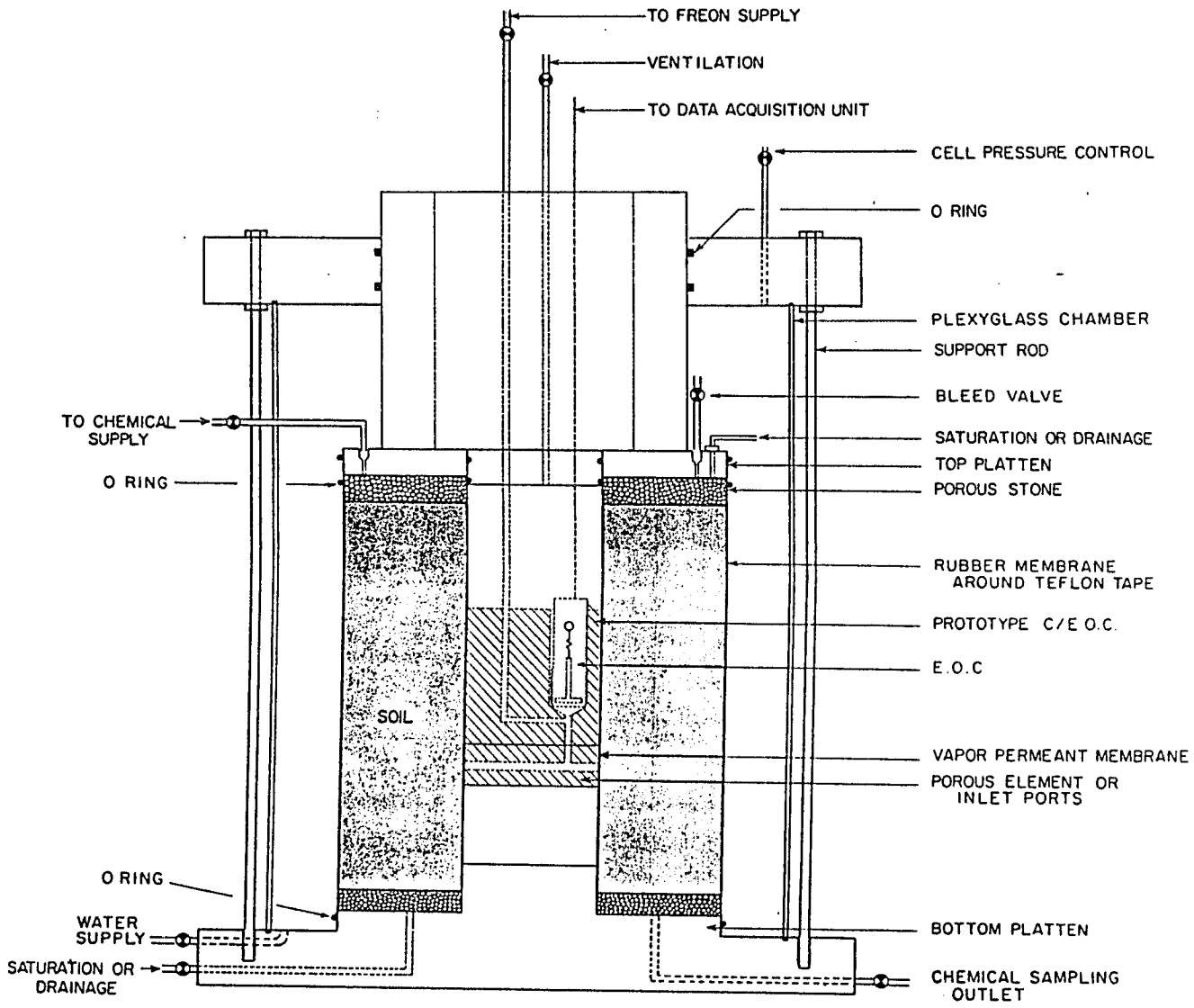

Figure B-2. Single cell details.

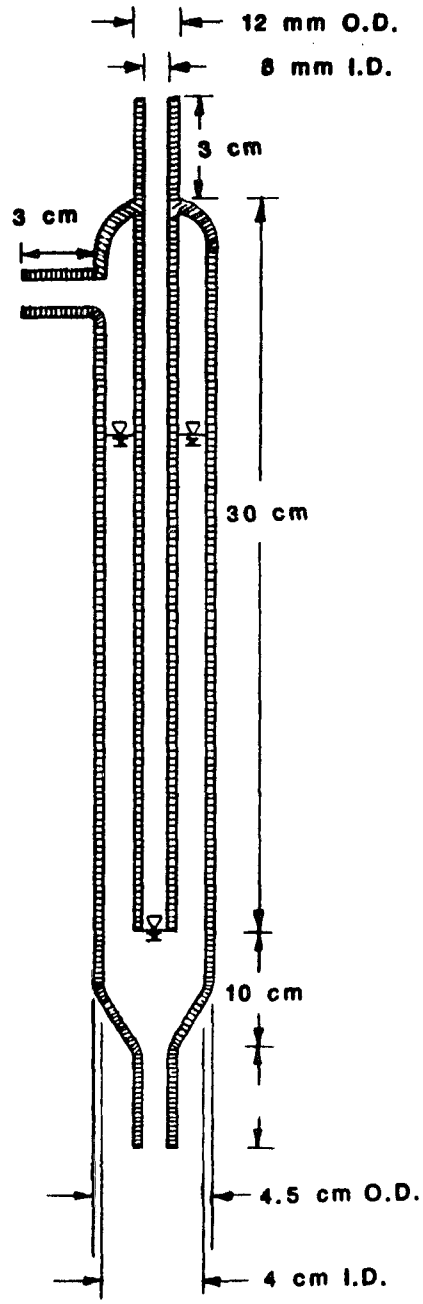

Figure B.3. Mariotte bottle.

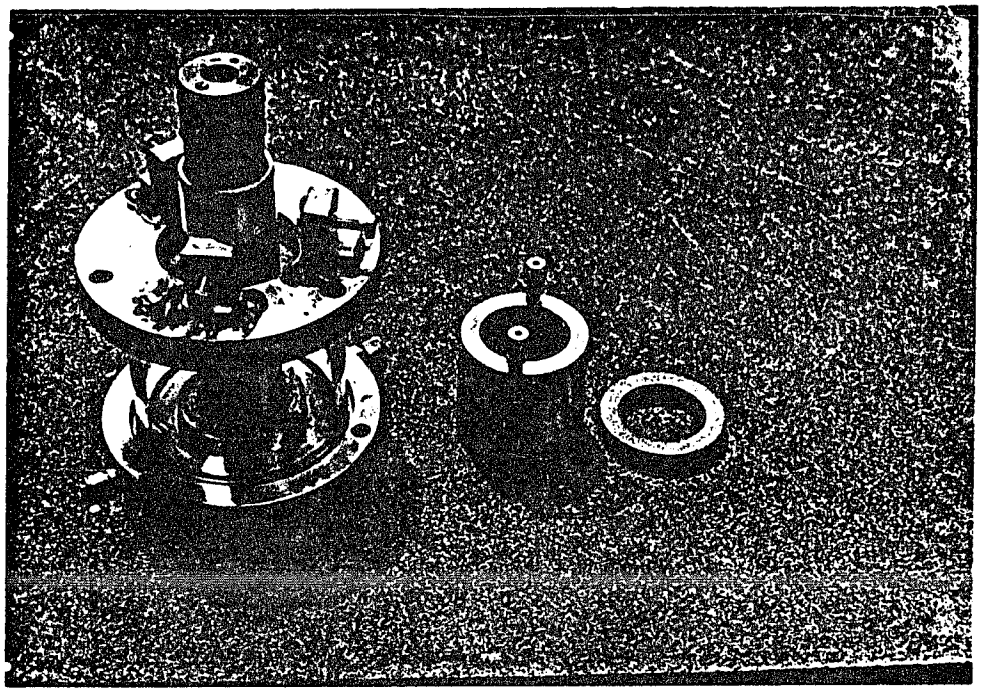

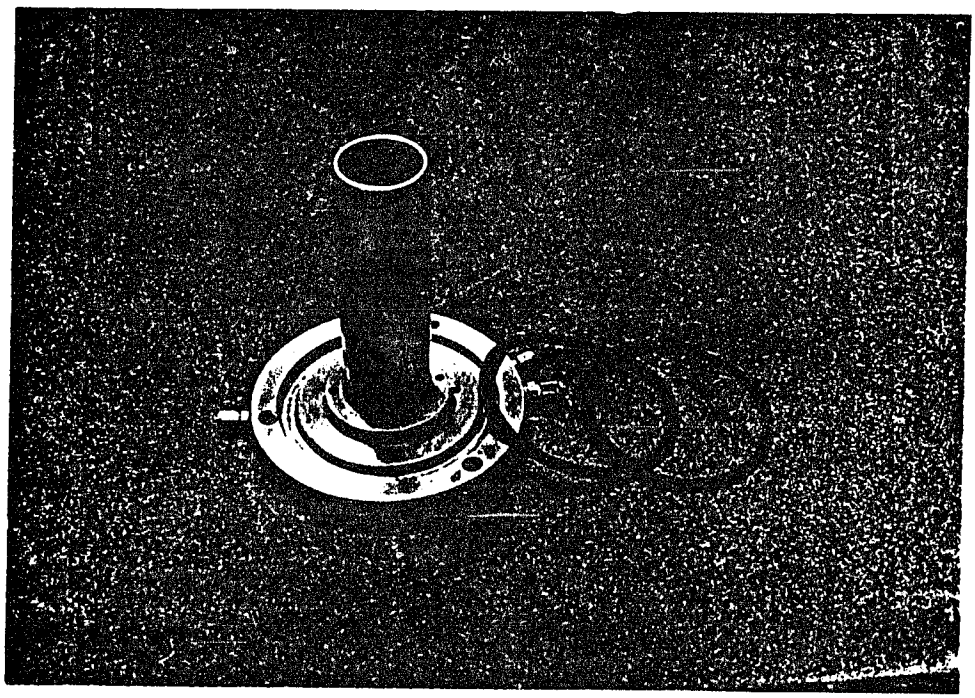

Figure B-4. Special triaxial set-up for soil testing (a) combined set-up, (b) base platten.

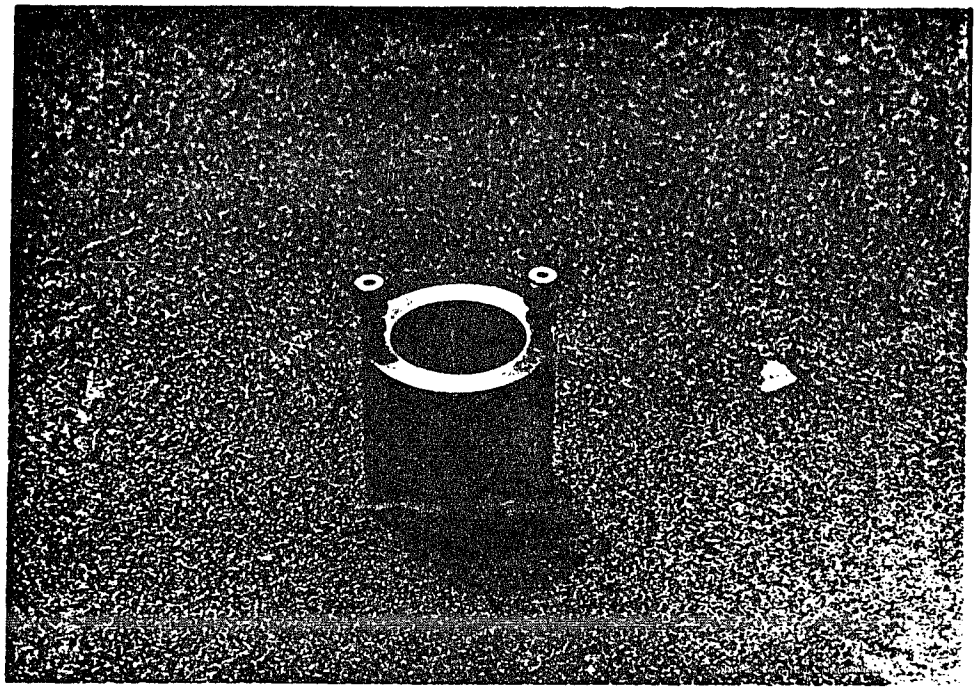

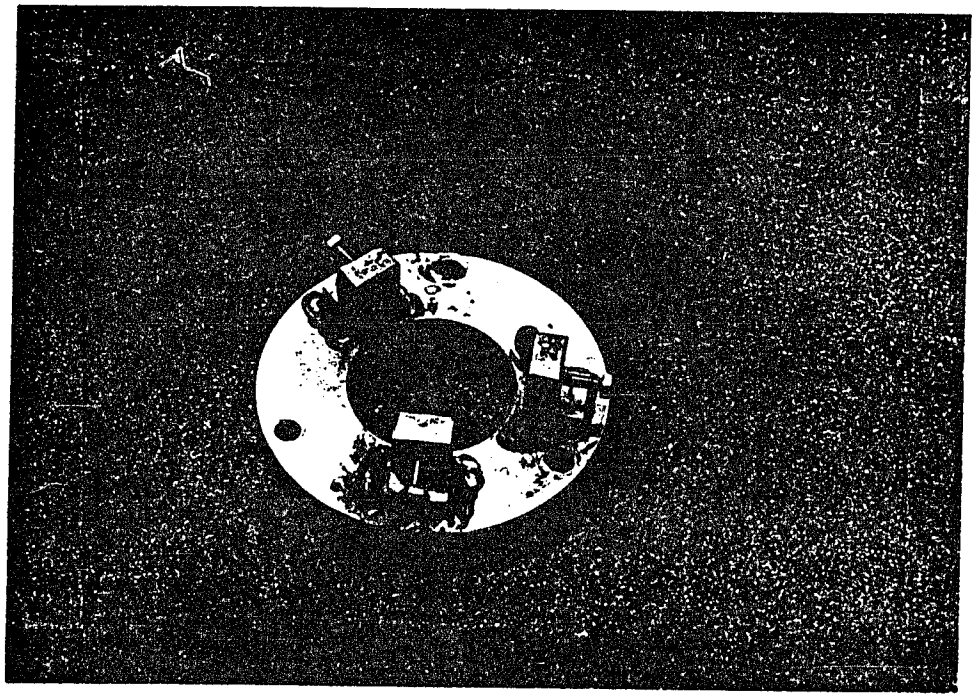

Figure B-5. Special triaxial set-up component (a) top platten, (b) base platten.

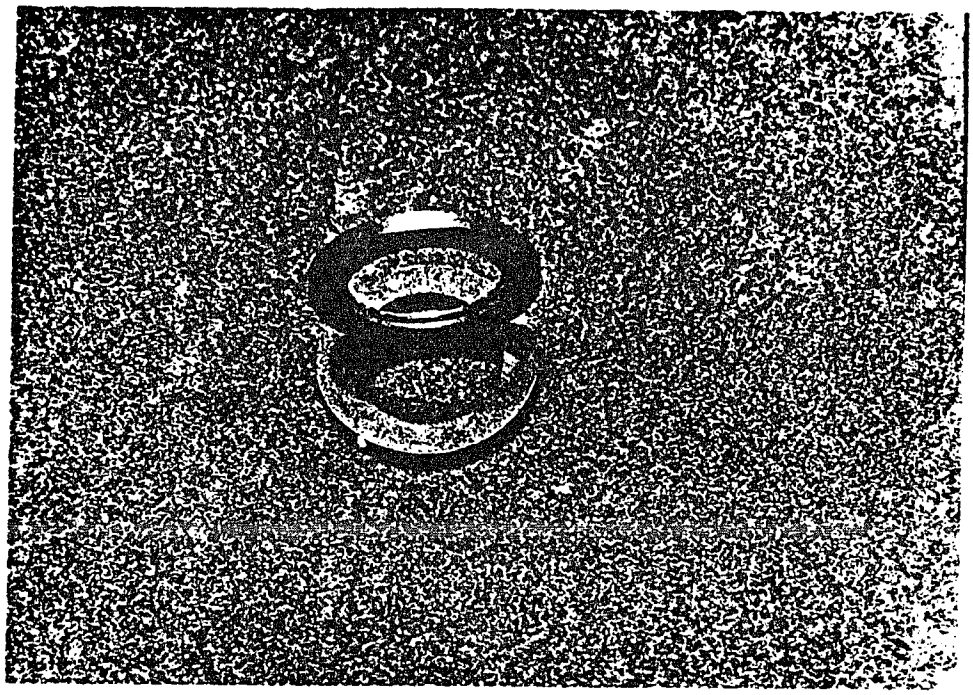

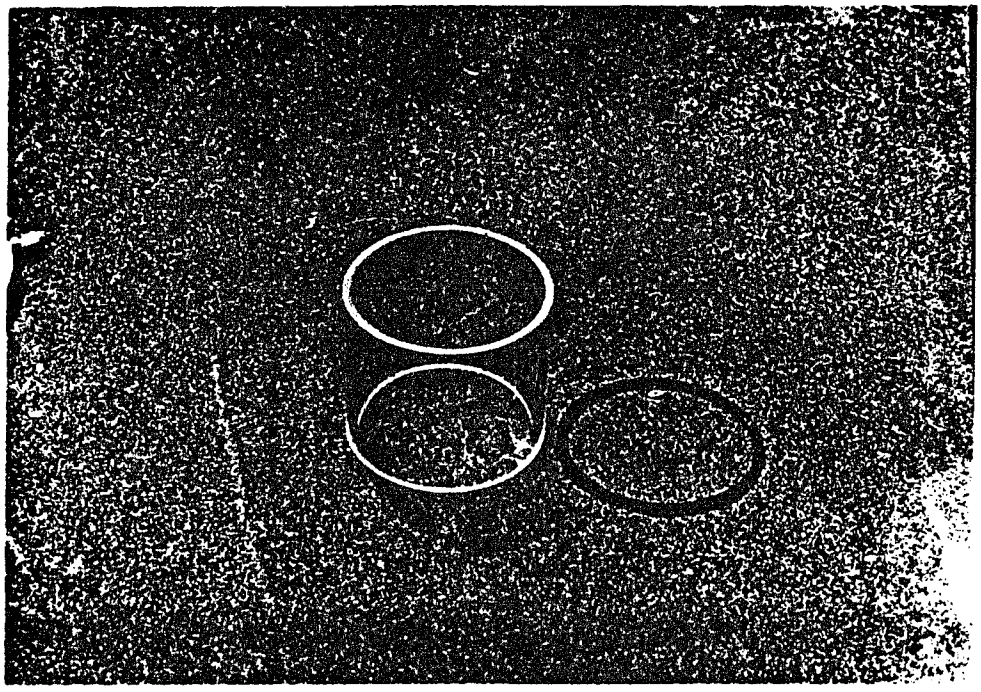

Figure B-6. (a) porous stone, (b) plexy glass chamber.

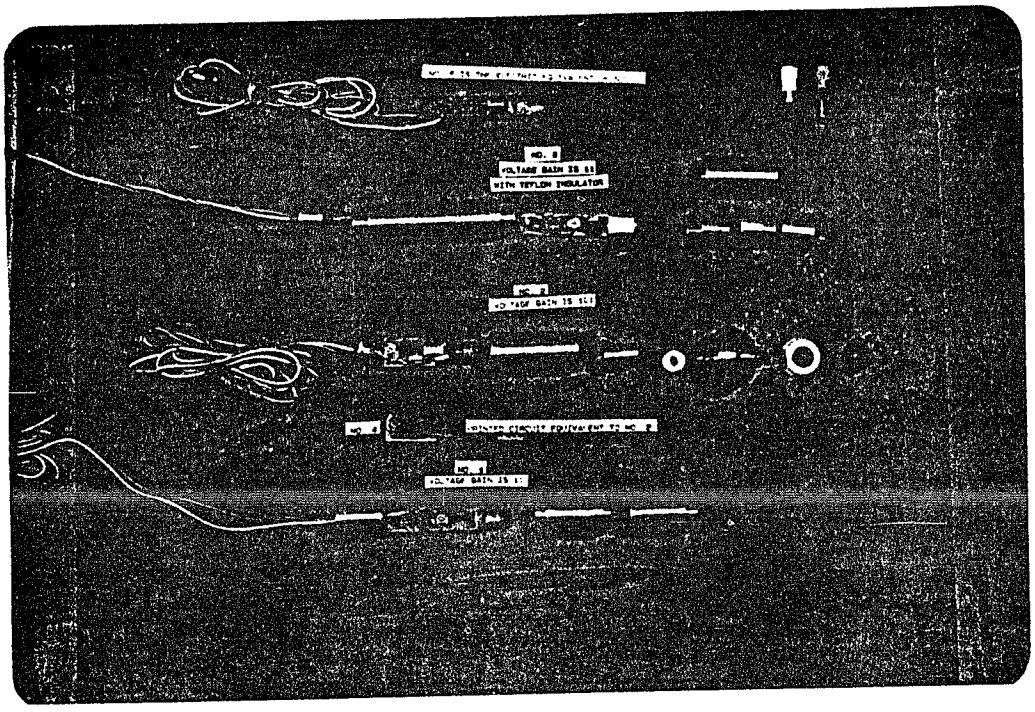

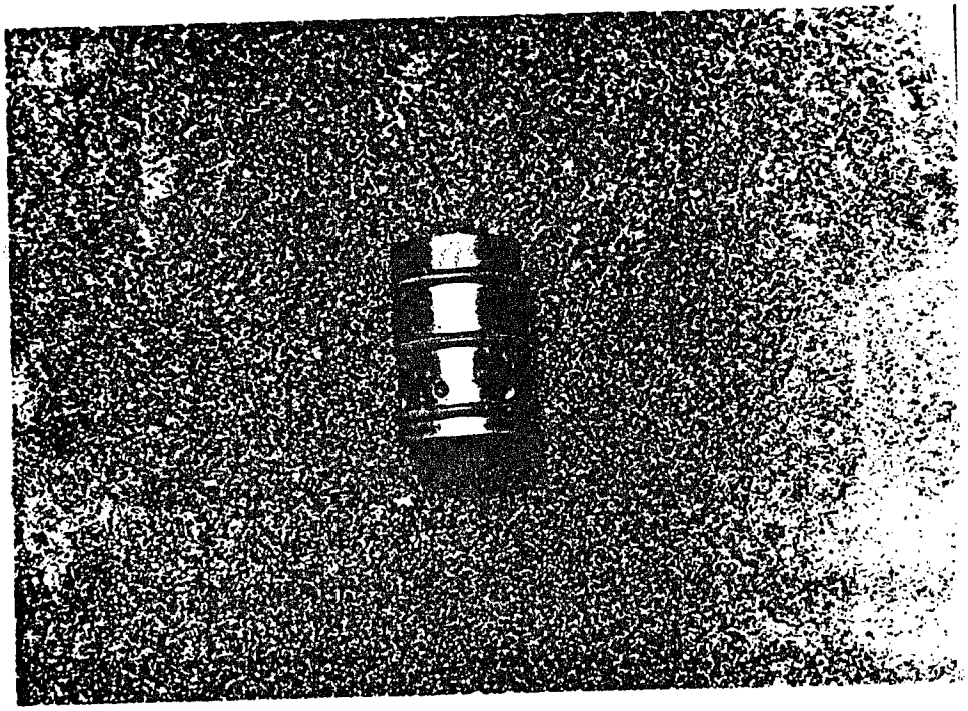

Figure B-7. (a) EOC, (b) C/EOC housing in triaxial set-up.

TESTING PROCEDURE

1. Soil sample is prepared for compaction in the following manner
   a. A preweighed amount of kaolinite is placed in a mechanical drum mixer and water is added to it at small proportions (about 50cc each time) every 20 minutes at low speed of rotation.
   b. At about 25% water content where smearing (i.e., shear disaggregation) on the walls of the mixer may take place water is sprayed on the clay manually up to optimum moisture content of about 31%.
   c. Clay from step 1.b is placed in the polyetelene bags. These bags are left in the humidity room to cure (achieve uniform water content). Now clay is ready for use in the testing.
2. The hollow cylinder is covered with epoxy and then with soil to provide a rough surface (wait for epoxy to dry).
3. Gore-tex membrane was secured by a waterproof chemical resistant epoxy around the perforated section of the cylinder. This was done to avoid the intrusion of liquids to the EOC circuitry and short-circuiting the odor cone. This membrane under moderate pressure allows the passage of vapor molecules but restricts any fluid flow.
4. The saturated bottom porous stone was placed on the bottom platten and the filter paper was placed on it.
5. The inside of the split compaction mold was entirely coated with high-vacuum silicone grease to provide a smooth surface that was flush with the rubber membrane and also to minimize frictional interference with the annular hammer.

6. The rubber membrane was checked for microholes and secured on the compaction mold by o-ring seals.
7. The mold was set on the base plate around the cylinder and the vacuum was applied.
8. Clay was poured around the cylinder to form an annulus between the mold and the cylinder. The soil was compacted at three layers about 2 cm each, with the special compactor, designed and fabricated for this test. The soil surface was scarified between each compaction to void laying and discontinuous stratification.
9. Filter paper and porous stone were placed on top of the sample.
10. The vacuum was stopped, the mold dismantled and removed.
11. The membrane was rolled down and a layer of teflon tape was wrapped around the sample to protect the latex membrane from chemical attack, slacking, and to diffusion through the membrane.
    When samples are wrapped in teflon tape, the tape has some rigidity and does not conform to the irregular sides of specimen as well as the compactive membrane alone. Testing by Daniel et al. (1984), however, showed little difference in hydraulic conductivity and minor changes in sample height and the cross-sectional area between tests performed with or without teflon tape when using water as permeant.
12. The laytex membrane was rolled back and secured around the top platten by two o-rings. The excess portion was rolled back down.
13. The plexiglass chamber was set on the seal inside the groove on the bottom plate. The top platten was placed on top of the plexiglass chamber and secured by bolts and nuts to the lower plate.

14. The screw set on the aluminum angles on the top plate were secured against the upper portion of the top platten. This was done to prevent the top platten from popping out when pressure was applied to the chamber.
15. The chamber was filled with water.
16. The C/EOC is placed inside the cylinder on the top platten.
17. a. Saturation line is connected to the water reservoir.
    b. Chambers are filled with water from the reservoir.
    c. Confining pressure is applied to the chamber through chamber pressure line at the top of the chamber.
    d. The drainage line is connected to mariotte bottle; this will allow application of a constant head type of pressure and also makes monitoring of volume change during saturation possible.
    e. The mariotte bottle is in turn connected to the nitrogen pressure tank which acts as the pressure source for it.
18. Back pressure reservoir is filled with de-aired water and is properly connected to the saturation line and pressure supply.
19. A confining pressure is applied to the chamber fluid, followed by applying back pressure (about 10 psi less than chamber pressure) to the reservoir and opening the valves from the reservoir to the saturation lines.
20. Chamber pressure and back pressure are increased in a stepwise fashion [similar to that of Lee and Morrison (1970)] and checks are made for B values. Once B values close to 1 are chived the saturation is stopped.
21. a. The valves to saturation line are closed

b. Mariotte bottles are filled with desired dilution of the organic permeant (10%, 25%, 50%).

c. The lower drainage line is opened.

d. The chamber pressure is reduced to the desired effective pressure.

e. Organics in the meriotte bottle (chemical reservoir) are subjected to a pressure head smaller than confining pressure by 10 psi.

f. The valves from the bottom of the mariotte bottle to the top platten connection lines are opened.

22. The C/EOC is connected to the data acquisition unit andoutput is monitored.

23. A program is executed to automatically scan, time and record the response of C/EOC as the organics move within the soil sample.

24. Once a significant output for the C/EOC is observed, data is taken more frequently.

25. Upon saturation of C/EOC membrane or about 60,000 seconds after the onset or significant output terminate the test.

26. Purge and decontaminate the C/EOC by Freon-12 and repeat steps 22-25 to check for repetibility of the results.

APPENDIX C

THERMODYNAMICS OF ADSORPTION

An important amount of information about the adsorption process is revealed by isotherms which are plots of surface coverage vs. pressure at constant temperature for a specific adsorbate and adsorbent. Theoretical expressions exist for either monolayer or multilayer adsorption.

For the derivation of monolayer adsorption isotherms, different approaches such as statistical thermodynamic approaches, classical kinetic derivation, and thermodynamic derivation are employed. The applicability of each approach is determined by several factors; among them:

(a) Whether adsorption is localized (adsorption sites are separated from each other by a barrier high enough to bind the adsorbed particles firmly to the crystal lattice of the adsorbate for the majority of the time they spend on the surface) or nonlocalized

(b) Whether the sites are statistically identical

(c) Whether there are surface nonhomogenuities

(d) Whether there exist molecular interactions between adsorbate and adsorbent.

The most often used isotherm for single layer adsorption is Langmuir's adsorption, applicable to monolayer physical adsorption of gases below their critical temperature and with no capillary condensation.

The model is based on the kinetic theory of gases. It considers that since surface forces have a short range, only those molecules

striking a bare surface can be adsorbed, and others will be elastically reflected into the gas phase.

Thus, the rate of adsorption may be expressed as:

$$\frac{-dN_g}{dt} = \frac{dN}{dt} = R_{ads} - R_{des} = k_a(T)\ f(\theta_t)\ P - k_j\ (T)\ g(\theta_t) \qquad (C.1)$$

where Ng = Number of molecules in the gas phase

N = Number of molecules which have entered the adsorbed phase

$f(\theta_t), g(\theta_t)$ = The probability of a site or group of sites suitable for adsorption or desorption being available at time T.

$k(T)$ = A constant including Stoicheiometric factors (i.e., the number of adsorption sites)

And the rate of adsorption per unit area of the surface is

$$R_{ads} = x_o\ (1 - \Theta)\ N \qquad (C.2)$$

where x_o = (inelastic collision)/(Total collision)

Θ = covered fraction of the surface

If q is the energy evolved when a molecule is adsorbed, the only molecules that will be able to adsorb are those that acquire an energy quantity equal to or greater than q. Thus, the rate of adsorption per unit area, R_{des}, becomes:

$$R_{des} = k_o\ e^{-q/kT} = V\Theta \qquad (C.3)$$

k_o = constant

V = adsorbed volume

T = temperature (°k)

$$\Theta = \alpha_o N / k_o e^{-q/kT} - \alpha_o N \qquad (C.4)$$

at equilibrium $R_{ads} = R_{des}$

for $$N = P/\sqrt{2\pi\ mkT} \qquad (C.5)$$

P = Equilibrium pressure

m = Mass of a molecule

k = Boltzmann's constant

N = Number of molecules which collide with unit surface area per unit time

And $$b = (xe^{q/kT})/K_o\sqrt{2\pi\ mkT}$$

then $$\theta = bP/(1 + bP) \qquad (C.6)$$

P = pressure

Furthermore, if there is no lateral interaction between adsorbed molecules, then b is a constant, and if the free energy of adsorption (q) does not change with θ then $x_o = 1$.

θ in equation (25) can also be expressed as $\theta = V/V_m$ (C.7)

then $$V = V_m bP(1 + bP) \qquad (C.8)$$

which at low pressure becomes $V = V_m bq$ (C.9)

which is Henry's Law, where V_m = volume of A monolayer

Experimentation shows that relatively few of the vapor adsorption isotherms obey Langmuir's equation, and there is evidence that more than one layer of adsorbed molecules can exist on the surface of the adsorbate. In adsorption over a single layer (i.e., multilayer adsorption) the most widely accepted isotherm is that named after Branuer-Emmett-Teller, or BET.

Generally the rate of adsorption is affected and thus limited by:

1. The rate of mass transfer of the gas to the adsorbent surface (convection and external diffusion)

2. The rate of mass transfer within pores in the adsorbent (internal diffusion)
3. The rate of transfer of heat liberated by the adsorption process from the captured molecule to the adsorbent
4. The surface migration rate, which always is, the rate of activated migration of the adsorbed particles for adsorption
5. The rate of the surface process, requiring for example that an activation energy be supplied
6. The possibility that adsorption may change into a volume reaction (multilayer adsorption)

Desorption: A molecule will desorb when it receives an amount of energy greater than the required minimum, E_{des}, in a direction perpendicular to the surface. When a molecule undergoes a number (V_{des}) of attempts to desorb within a time, dt, the fraction of attempts in which it achieves an energy greater than E_{des} is given by Boltzman's factor as exp $(-E_{des}/k_BT)$, consequently a molecule will desorb within the time τ expressed as:

$$\tau = \frac{1}{V_{des}} [\exp (E_{des}/k_Bt)] \qquad (C.10)$$

where k_B is Boltzman's constant

DIFFERENCES BETWEEN PHYSICAL ADSORPTION ISOTHERMS AND CHEMISORPTION ISOTHERMS

Chemisorption isotherms differ from physical adsorption curves for several reasons.

1. Variable heat of adsorption caused by:
   a. Surface heterogeneities resulting in site energy distribution

b. Adsorbate-adsorbent interactions consisting of:

I. Short-range repulsion, affecting the nearest molecules only (Coulomb repulsion), resulting in distortion of the surface bond from the direction of normal to the surface.

II. Long-range (dipole field repulsion): If adsorption bond formation polarizes the adsorbate, or strongly orients an existing dipole, then the adsorbate film will consist of similarly aligned dipoles that will have a mutual electrostatic repulsion.

2. Effect of site and adsorbate coordination number: in chemisorption a situation may arise in which a molecule occupies or blocks the occupancy of a second adjacent site. This means that each molecule effectively requires two adjacent sites. Here the adsorption is localized, and even though the adsorbed film might be mobile (in the presence of small activation energy), the adsorbed molecules are not mobile.

3. Adsorption thermodynamics: The measured differential heats of adsorption are much different from calorimetric values and may not represent an equilibrium adsorption.

BET ISOTHERM

A BET isotherm applies in the range of 0.7-1.3 layers (relative pressure of 0.005-0.35). At low pressures the extent of adsorption predicted by the BET theory is usually less than experimental values, because the surface usually contains sites of higher heats of adsorption than those which are occupied at monolayer surface coverage. At higher

pressures, when the number of layers rises rapidly according to the BET theory, theoretical data deviate from experimental data.

Basic assumption of BET: Molecules of vapors can be adsorbed on top of already adsorbed molecules, but each separate adsorbed layer obeys a Langmuir equation.

Derivation of two-parameter BET: Let $S_0, S_1, S_2, S_3 \ldots, S_i$ represent the surface covered by 0,1,2,3...,i layers of adsorbed molecules. At equilibrium the rate of condensation of the $i - 1^{th}$ surface must equal the rate of evaporation from i^{th} layer, i.e.,

$$a_i P S_{i-1} = b_i S_i e^{-E_i/RT} \qquad (C.10)$$

a & b are constants and E_i is the heat of adsorption in the i^{th} layer. R is the universal gas constant and T is temperature. Now the total surface of the adsorbent is given by $A = -S_i$ (C.11)

and the total volume of the adsorbent is given by

$$V = V_o - S_i \qquad (C.12)$$

where V_o is the volume of vapor adsorbed on 2 cm^2 of surface when it is covered by a complete monolayer.

Then

$$(V/V_m) = (V/AV_o) = (iS_{i=o\to i})/(S_{i=o\to i}) \qquad (C.13)$$

Assuming that the evaporation-condensation properties of the molecules in the second and higher layers are similar to those in the liquid state, we have:

$$E_2 = E_3 = \text{----} = E_i = E_L = \text{Heat of liquefaction} \qquad (C.14)$$

$$\frac{b2}{a_2} = \frac{b3}{a_3} = \text{----} = \frac{bi}{a_i} = g = \text{constant} \qquad (C.15)$$

$$S_1 = YS_o = \text{----} = y = (a_1/b_1)Pe^{Ei/RT} \qquad (C.16)$$

$$S_2 = XS_1 \ , \ x = (P/g)eE_L/RT \qquad (C.17)$$

or $$x = P/P_o (AT\ V = \infty)$$

then $$S_i = c\, x^i s_o, \quad c = y/x \tag{C.18}$$

and $$(V/V_m) = cx/(1 - x)(1 - x + cx) \tag{C.19}$$

or

with $$c = \text{Exp}\ (\Delta F_L^o + \Delta_L^o)/RT. \tag{C.20}$$

where ΔF_I^o = Standard Gibb's free energy of adsorption of vapor on the bare surface

ΔF_L^o = Standard Gibb's free energy of condensation of the vapor.

In equation (32) and (33) the value of parameter c determines the shape of the adsorption isotherm. There are basically five types of vapor adsorption isotherms as shown in Figure C.1 (Perry and Chilton, 1973).

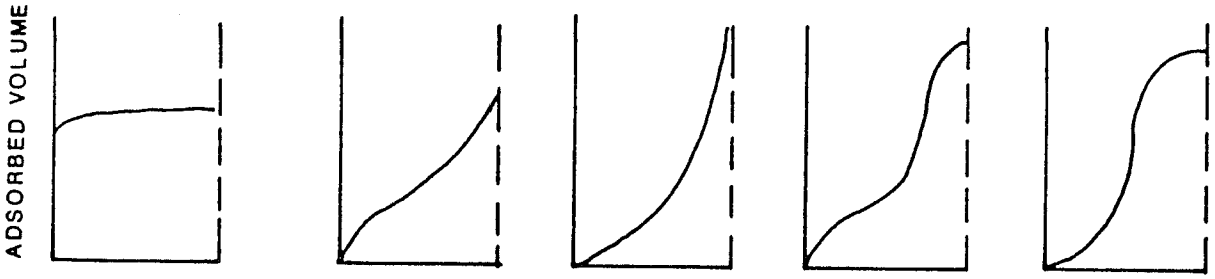

Langmuir Type Monolayer | Mono and Multilayer Adsorption | Mono and Multilayer Plus Capillary Condensation

Figure C-1. Vapor adsorption isotherms.

If the adsorption takes place in the pores of an adsorbent membrane, then at saturation, only a finite number of layers, N, can be built up on the surface and equation C.13 becomes:

$$(V/V_m) = cx\ (1 - X^n)/(1 - x)(1 - x + cx) \qquad (C.21)$$

This is BET's three-parameter equation (Braunauer et al., 1976; Braunauer, 1938; Braunauer, 1935).

ENERGETIC QUANTITIES RESULTING FROM ADSORPTION AND DESORPTION

1. Work function (surface potential): The surface potential, x, may be expressed in terms of total dipole moment per unit area, M_t, according to $x = 4\pi M_t$. When δ molecules of a gas are adsorbed at a surface, they are polarized by the field gradient to give δ dipoles per unit area aligned perpendicularly to the surface. The adsorbed layer therefore constitutes a double layer of charge density, δe, separated by a distance, d. If the dipole moment of the adsorbed molecule is independent of coverage, then the dipole sheet corresponds to a capacitor, the potential difference between its plates being proportional to the number of adsorbed molecules per unit area. The dipole moment per adsorbed species, M_t, is then ed, Where e is the energy of the molecule and d is the separation distance.

According to electrostatics, there is no external field emanating from a perfect double layer; consequently, the work function is increased by $4\pi M_t$, when the adsorbed layer has its negative pole outward or is reduced by the same amount when the sign of the dipole is reversed (Tompkin, 1976).

The surface potential change effected by adsorption is equal in magnitude but opposite in sign to the change in the work function.

If the membrane surface contains micropores which are no more than a few molecular diameters in width, the potential field from neighboring walls will overlap and the interaction energy of the solid with the vapor

molecule will be enhanced by a factor of Q/Q^*, where Q^* is the interaction potential of a molecule with a freely exposed surface and Q is the interaction potential of an adsorbed molecule.

The surface potential in turn causes changes in the interfacial tension between γ, the odor and membrane according to Gibb's equation

$$d\gamma = \Gamma\ RT\ \ln a \qquad (C.22)$$

Γ = surface access, R = gas constant, T = 299^{oK} Vibrational
a = vibrational activity of the molecule

Specifically 1 dyn/cm reduction in interfacial tension is equal to a decrease in the surface potential of one erg per square centimeter.

2. The heat of adsorption is the total energy liberated (or consumed) during adsorption (or desorption) processes. This is usually measured by a calorimeter. Upon adsorption the potential energy of a molecule decreases to the level of the equilibrium minimum u_o (Greg and Sing, 1967; Dash, 1975). If in adsorption of n_s moles of a gas, a total amount of heat $Q_{int} = n_s u_o$ is liberated then the quantity dQ_{int}/dn_s is called the differential heat of adsorption, Q. It is fully defined if conditions of adsorption are fully defined, in terms of temperature, volume, pressure, molecular weight and availability of adsorption components. Differential heat of adsorption remains constant through the range of adsorption, provided that the surface is homogeneous and is free from mutual interaction between adjacent molecules. In the case of mobile adsorption on a homogeneous surface the differential heat of adsorption depends in a linear manner on the degree of surface coverage.

Different kinds of heats of adsorption are distinguished by the variable which is kept constant in the course of adsorption. In the case of isothermal constant volume adsorption, for example, when n_s moles are

transferred from the gas to the adsorbed phase, the total integral heat of adsorption is

$$Q_{int} = E_g - E_s = N_s \, (E_{g/n} - E_{s/n}) \qquad (C.23)$$

and the differential heat of adsorption is:

$$Q_{diff} = (\partial Q_{int} / \partial \, n_s) \qquad (C.24)$$

where $E_{g/n}$ = molar energy of gaseous phase

$E_{s/n}$ = molar energy of adsorbed phase

N_s = moles of gaseous phase molecules that are transferred to adsorbed phase.

VITA

Mohammad Mohammadi was born on March 2, 1956, in Bodjnord, Iran. His early education was at Hemmat High School. He attended University of Texas at Austin (1976-1978). Mr. Mohammadi earned his Bachelor of Science in Civil Engineering from University of North Carolina at Charlotte (1980).

He received his Master of Science in Mathematics from Texas A & I University in 1982.

Mr. Mohammadi began his study at Louisiana State University in January 1982 and is presently a candidate for the degree of Doctor of Philosophy in Civil Engineering (Geotechnical Division).

DOCTORAL EXAMINATION AND DISSERTATION REPORT

Candidate: Mohammad MOHAMMADI

Major Field: Civil Engineering (Geotechnical)

Title of Dissertation: Olfactometric In-Situ Soil Exploration-
Development of the Electro-Odo-Cone

Approved:

Mehmet T. Tumay
Major Professor and Chairman

Dean of the Graduate School

EXAMINING COMMITTEE:

Ara Arman

Ray E. Ferrell

Joseph N. Suhayda

Neal W. Stoltzfus

Dipak Roy

Date of Examination:

November 18, 1986